Universidade do Porto

Faculdade de Engenharia

FEUP

Methodologies for the Participation of an Electric Vehicles' Aggregator in the Electricity Markets

Ricardo Jorge Gomes de Sousa Bento Bessa

Thesis submitted to the Faculty of Engineering of University of Porto in partial fulfillment of the requirements for the degree of Doctor of Philosophy

Thesis Supervisor
Professor Manuel António Cerqueira da Costa Matos
Full Professor at the Department of Electrical and Computer Engineering
Faculty of Engineering, University of Porto

April 2013

”As we walked along the flatblock marina, I was calm on the outside, but thinking all the time - Now it was to be Georgie the general, saying what we should do and what not to do, and Dim as his mindless greeding bulldog. But suddenly, I viddied that thinking was for the gloopy ones, and that the oomny ones use like, inspiration and what Bog sends. Now it was lovely music that came into my aid. There was a window open with the stereo on, and I viddied right at once what to do.”

Alex, *Clockwork Orange*, 1971

Acknowledgments

The support of exceptional researchers, colleagues, friends and family was essential to conclude this work. Here, I will express a public word of appreciation and acknowledge their role in this thesis.

This thesis was supervised by Professor Manuel Matos, Full Professor at the Faculty of Engineering of the University of Porto (FEUP), to who I am grateful for accepting this supervision. Professor Manuel Matos was much more than a supervisor, it was a true professor. His guidance and advices allowed me to improve my scientific and personal competences, which ultimately changed my viewpoints in different subjects.

The opportunity to work with Professors Peças Lopes and Vladimiro Miranda was also very rewarding at different levels, and their teachings and enthusiasm influenced this thesis. I am truly grateful to Professor Cláudio Monteiro since, on an early stage of my career, trusted in me to work with him in different research projects. His friendship and advices were crucial to follow this path and this thesis is also a result of his conviction in my capacities.

My former professors from the Faculty of Economics of the University of Porto, in particular Professor João Gama, were responsible for making me think "out-of-the-box" and open to multidisciplinary research.

In 2006, when I went to work at INESC Porto, the high quality of the human resources created the perfect conditions to evolve at the scientific level. For me, it was a luck and a pleasure to have true scientists as examples, such as Carlos Moreira, Luis Seca, André Madureira, Jorge Pereira and Ricardo Ferreira. They were an inspiration to this thesis, and their support a valuable help. The opportunity to work with João Sousa and his friendship was essential for my integration at INESC Porto and important for improving my programming skills. Furthermore, the research work and the vision of Joel Soares and Pedro Almeida about the electric vehicles topic, as well as their friendship and valuable discussions, was an important contribution to this thesis. The help of Leonardo Bremermann was an essential support to combine the work of the ANEMOS.plus project with this PhD thesis. The friendship and sense of humour during critical (and non-critical) situations of Bernardo Silva were very gratifying during these years. Finally, I cannot forget Célia Couto, Paula Castro and Rute Ferreira since their work made my life much more easier during the PhD period.

At a personal level, I must dedicate a few paragraphs to acknowledge a group of persons that made this work a reality.

First, thanks to my parents. It is not fair to work hard during their life in order to give a better

life to their children, and see both leave their home to graduate in another city. This thesis and all my research work during these almost four years, is dedicated to them, for their effort, for their support and for their love. To my sister Ana Rita, most of the time I was away and unavailable, but she also played an important role. To my grandmother, who I know is very proud of her grandson.

I also have a very good group of friends. I cannot mention all their names here because the number of pages of this thesis would increase exponentially. I particularly acknowledge Vanessa and António Pina, Joaquim Matos, Pedro Correia and Lourenço Moura since their friendship, their words and advices in specific moments of my life were essential to complete this path. The "mavericks" Pedro Costa and Tiago Azevedo were also essential to maintain the equilibrium between the forces.

Finally, words are not enough to described the role and importance of my beloved Ana Pinto. Her support and love during these years were the light during darkest times, the absolute trust in my capacities was the fuel of this work, and her words were full of music and hope. Definitely, this is also her thesis!

This work was supported by Fundação para a Ciência e a Tecnologia (FCT) de Portugal, under PhD grant SFRH/BD/33738/2009 and by INESC TEC - Science and Technology.

Abstract

The Electric Vehicle (EV) is one element that contributes to a sustainable transport sector since it helps reducing greenhouse gas (GHG) emissions and oil-dependency. It also establishes a connection between the transport and electric power sectors. In order to promote a sustainable development, different stakeholders from the electric power sector are seeking an increase of Renewable Energy Sources for Electricity (RES-E), complemented by a smart grid infrastructure that enables a more active participation of the demand-side in the power system operation.

The EV charging, if uncontrolled and during peak hours, could result in technical problems at the distribution network level (e.g., branches congestion). However, direct-control of the EV charging using the smart grid technology increases the demand-side flexibility which mitigates the technical problems and supports the integration of RES-E (e.g., by offering reserve services). The existing electricity market rules do not allow bids from small loads and, in order to decrease the communication requirements between the system operators and EV, a market agent called aggregator can serve as an intermediary between a group of vehicle owners, electricity market, transmission and distribution system operators. Computational algorithms are needed to make the smart grid architecture feasible.

Within this context, this PhD thesis explores the concept of an EV aggregator and contributes with a set of computational tools that enable its active participation in the electricity market, in particular the provision of secondary and balancing reserve services.

Firstly, a framework with optimization/forecasting models covering the majority of the electricity market sessions is defined. Then, day-ahead optimization models, based on forecasts for the market prices and EV variables, are formulated to determine the bids for the electrical energy, secondary and balancing reserve market sessions. Operational management algorithms, using information from the plugged-in EV and the accepted bids, are proposed to coordinate EV charging during the operating day and comply with the market commitments (e.g., avoid reserve shortage). The optimization models are evaluated in a test case with synthetic EV time series and data from the Iberian electricity market.

The main contributions from this PhD thesis are: (a) day-ahead optimization models for electrical energy, secondary and balancing reserve bids; (b) operational management algorithms that coordinate the EV individual charging and allow the provision of reserve without compromising power system reliability; (c) estimation of the forecast errors impact on the aggregator's total cost and reserve shortage magnitude.

Resumo

O veículo elétrico (VE) é um elemento de uma solução global para o desenvolvimento sustentável do sector dos transportes, uma vez que permite reduzir as emissões de gases de efeito de estufa e dependência do petróleo. Estabelece uma ligação com o sector elétrico, no qual diferentes agentes procuram, em conjunto com o conceito de rede inteligente, aumentar a contribuição de fontes de energia renovável para produção de eletricidade, promovendo um desenvolvimento sustentável.

A integração de VE, com carregamento não-controlado, pode provocar problemas técnicos na rede elétrica de distribuição. No entanto, o controlo do carregamento com base numa infraestrutura de comunicação bidirecional mitiga problemas técnicos e auxilia a integração de geração de base renovável. De forma a reduzir os requisitos de comunicação para controlo do carregamento, e dado que as atuais regras do mercado de eletricidade não permitem a participação individual de pequenas cargas, é introduzido um novo agente de mercado chamado agregador de VE. Este agente serve de intermediário entre um grupo de VE, mercado de eletricidade, operadores da rede de transporte e distribuição.

Neste contexto, esta tese de doutoramento explora o conceito de agregador e contribui com um conjunto de algoritmos computacionais que permitem uma participação ativa do agregador no mercado de eletricidade, em particular no fornecimento de reserva secundária e de balanço.

Numa primeira fase, é definida uma arquitetura que inclui modelos de previsão e otimização para cada sessão do mercado. Em seguida, são formulados modelos de otimização, baseados em previsões para o dia seguinte dos preços de mercado e consumo dos VE, com o objetivo de otimizar as ofertas de energia elétrica e reserva. São igualmente propostos algoritmos operacionais para coordenar o carregamento dos VE de forma a satisfazer os compromissos do mercado elétrico durante o próprio dia e com base em informação de VE estacionados para carregamento. Os modelos de otimização são testados num caso de estudo construído com dados sintéticos do consumo de VE e dados reais do mercado Ibérico de eletricidade.

As principais contribuições desta tese são: (a) modelos de otimização para o dia seguinte das propostas de compra de energia elétrica e venda de reserva secundária e de balanço; (b) algoritmos operacionais que coordenam o carregamento individual dos VE, e permitem ao agregador fornecer reserva sem comprometer a fiabilidade do sistema elétrico; (c) estimação do impacto dos erros de previsão no custo total do agregador e na magnitude das situações com reserva não-fornecida.

Contents

List of Figures

List of Tables

List of Acronyms and Symbols

Acronyms

AC	Alternate Current
ACE	Area Control Error
AGC	Automatic Generation Control
AIC	Akaike Information Criterion
AMI	Advanced Metering Infrastructure
BETTA	British Electricity Trading and Transmission Arrangements
BMS	Battery Management System
BPA	Bonneville Power Administration
CAISO	California Independent System Operator
CAMC	Central Autonomous Management Controller
CAU	Central Aggregation Unit
CD	Control Device
CPM	Charging Point Manager
CSP	Curtailment Service Providers
CVC	Clusters of Vehicle Controllers
DBIAS	Deviations Bias
DC	Direct Current
DLC	Direct Load Control
DMS	Distribution Management System
DR	Demand Response

DSO	Distribution System Operator
EDA	Estimation Distribution Algorithm
ENTSO-E	European Network of Transmission System Operators for Electricity
ERCOT	Electric Reliability Council of Texas
ERGO	Electric Recharge Grid Operator
ESP	Energy Service Providers
EV	Electric Vehicle
EVC	External Vehicle Charger
EVM	Electric Vehicle Meter
EVSE	Electric Vehicle Supply Equipment
FAN	Field Area Network
GHG	Greenhouse Gas
GLM	Generalized Linear Model
HAN	Home Area Network
HSL	High Sustained Limit
ICT	Information and Communications Technology
IEC	International Electrotechnical Commission
IP	Internet Protocol
ISO	ISO New England
ISO	Independent System Operator
LMP	Locational Marginal Price
LOLE	Loss of Load Expectation
LSL	Low Sustained Limit
MAE	Mean Absolute Error
MAPD	Mean Absolute Percentage value of the Deviations
MAPE	Mean Absolute Percentage Error
MG	MicroGrid
MGAU	MicroGrid Aggregation Unit
MGCC	MicroGrid Central Controller

MISO	Midwest ISO
MMG	MultiMicroGrid
NERC	North American Electric Reliability Corporation
NYISO	New York ISO
OC	On-board Computer
OPF	Optimal Power Flow
OVC	On-board Vehicle Charger
PBIAS	Percentage Bias
pCRPS	Percentage of Constant Reserve Power Shortage
pICRPS	Percentage of Intervals with Constant Reserve Power Shortage
pIRNS	Percentage of Intervals with Reserve Not Supplied
PJM	Pennsylvania-New Jersey-Maryland Interconnection
PLC	Power Line Communication
POP	Preferred Operating Point
pRNS	Percentage of Reserve Not Supplied
pRPS	Percentage of Reserve Power Shortage
RES-E	Renewable Energy Sources for Electricity
RNS	Reserve Not Supplied
RTO	Regional Transmission Organization
SAE	Society of Automotive Engineers
SEI	Solid Electrolyte Interphase
SoC	State of Charge
TCP	Transmission Control Protocol
TSO	Transmission System Operator
UCTE	Union for the Co-ordination of Transmission of Electricity
V2G	Vehicle-to-Grid

V2V	Vehicle-to-Vehicle
VC	Vehicle Controller

List of symbols

μ	Ratio between upward and downward secondary reserve power.
α_t	Factor that relates the maximum charging power with the percentage of satisfied charging requirement.
β	Coefficient of the linear relation between the maximum charging power and the percentage of satisfied charging requirement.
Δ_k^{down}	Variable for adjusting the initial downward reserve bids in time interval k.
Δt	Time step (length of the time interval) of time interval t.
Δ_k^{up}	Variable for adjusting the initial upward reserve bids in time interval k.
D_t	Seasonal index that takes a different value for each day of the week.
E_t^{base}	Baseline for the upward balancing reserve in time interval t.
E_t^{bid}	Accepted energy bid in the day-ahead market for time interval t.
E_t^{cons}	Consumed electrical energy in time interval t.
E_k^{DA}	Initial plan from the day-ahead optimization.
E_t^{down*}	Dispatched downward balancing reserve in time interval t.
ε_t	Unobservable error term (or disturbance).
E_t	Optimized electrical energy for time interval t.
$E_{t,j}$	Optimized electrical energy for charging the jth EV in time interval t.

$E^{*}_{t,j}$	Electrical energy consumed by the jth EV in time interval t.
E^{up*}_{t}	Dispatched upward balancing reserve in time interval t
g	Smoothing spline.
H	Set of time intervals from the optimization horizon.
$\hat{H}^{plug}_{j}[i]$	ith forecasted availability (or plugged-in) period of the jth EV.
$H^{plug}_{j}[i]$	ith availability (or plugged-in) period of the jth EV.
h_t	Seasonal index that takes a different value for each hour of the day.
I^{Export}_{t}	Cross-border exported electrical energy during time interval t.
I^{Import}_{t}	Cross-border imported electrical energy during time interval t.
L_j	Number of availability periods of the jth EV.
l	Maximum order of lagged variables.
λ^{down}_{t}	Number of equivalent minutes of dispatched downward secondary reserve in interval t.
λ^{up}_{t}	Number of equivalent minutes of dispatched upward secondary reserve in interval t.
φ	Convex loss function.
M_t	Total number of EV plugged-in at time interval t.
Φ	Costs associated to reserve shortage.
ϕ	Regression model's coefficients.
π^{-}_{t}	Negative imbalance unit cost of time interval t.
π^{+}_{t}	Positive imbalance unit cost of time interval t.
$\hat{P}^{max}_{t}$	Forecasted total maximum charging power in time interval t.

$\bar{P}_{t_0}^{\max}$	Maximum, constant and feasible charging power of the EV fleet in time interval t_0.
$\bar{P}_{t_0}^{\min}$	Minimum, constant and feasible charging power of the EV fleet in time interval t_0.
P_j^{max}	Maximum charging power of the j$^{\text{th}}$ EV.
$P_{t,j}^{down}$	Downward secondary reserve power of the j$^{\text{th}}$ EV for time interval t.
$P_{t,j}^{up}$	Upward secondary reserve power of the j$^{\text{th}}$ EV for time interval t.
$p_t^{shortage}$	Price for negative imbalances of time interval t.
$p_t^{surplus}$	Price for positive imbalances of time interval t.
Ψ	Costs associated to deviations between actual charging and accepted bids.
$\hat{p}_t$	Day-ahead energy price forecast for time interval t.
P'_{t_0}	Operating point (or actual preferred operating point).
$P'^{down}_{t_0}$	Available downward secondary reserve power.
$P'^{up}_{t_0}$	Available upward secondary reserve power.
$\hat{p}_t^{cap}$	Forecasted capacity price of secondary reserve.
$\hat{p}_t^{down}$	Forecasted price for dispatched downward reserve.
$\bar{P}_t^{down}$	Downward secondary reserve power that can be sustained during interval t.
$\bar{P}_t^{up}$	Upward secondary reserve power that can be sustained during interval t.
p_t	Day-ahead energy price for time interval t.
$\hat{p}_t^{up}$	Forecasted price for dispatched upward reserve.
$\bar{P}_{t_0}^{upper}$	Upper power limit that guarantees full availability of downward reserve power in time interval t_0.
$\bar{P}_{t_0}^{lower}$	Lower power limit that guarantees full availability of upward reserve power in time interval t_0.
γ	Penalization coefficient for secondary reserve capacity shortage.

ρ	Penalization coefficient for reserve not supplied (electrical energy).
$\hat{R}_{j,i}$	Forecasted charging requirement for the ith availability period of the jth EV.
RNS_t^{down}	Downward reserve not supplied in time interval t.
RNS_t^{up}	Upward reserve not supplied in time interval t.
$\hat{R}_t$	Forecasted total charging requirement for time interval t.
$R_{t_0,j,i}$	Residual charging requirement for the ith availability period of the jth EV at beginning of time instant t_0.
$\hat{R}_t^D$	Forecasted total charging requirement distribution for time interval t.
T	Time interval of the last plugged-in EV to depart.
t	Time interval.
t_0	First time interval.
τ_t^+	Binary variable for the upward balancing downward reserve direction.
τ_t^-	Binary variable for the upward balancing upward reserve direction.
t_{final}	Last time interval of the availability period.
$t_{initial}$	First time interval of the availability period.
v_k	Slack variable.
wp_t	Forecasted wind power penetration level.
y	Response variable from a regression model.
y_{t-j}	jth lag of the response variable y.

Chapter 1

Introduction

1.1 General Context and Motivation

Sustainable development is as much an economic necessity as it is an environmental and social obligation. This term was introduced, in 1987, by the Brundtland Commission report as the "development that meets the needs of the present without compromising the ability of future generations to meet their own needs" [1]. This concept provides guidelines for strategic decision-making for planning human activities using a holistic approach that includes environmental, social and economic long-term goals. The electric power and transport sectors are following these fundamental guidelines to construct their sustainable paths.

The sustainable path of the electric power system is mainly characterized by the following actions [2][3]: increase energy efficiency in generation, transmission and distribution of electrical energy; high quality and security of supply; promotion of energy efficiency and saving measures in final costumers combined with smart meters deployment; increase the share of Renewable Energy Sources for Electricity (RES-E). The main goals/outcomes are greenhouse gas (GHG) emissions reduction, primary energy dependency reduction, social and economic development of regions/country (e.g., lower electricity prices, contribution from the RES-E sector to increase employment rate).

In the transport sector, the term *sustainable transport* can be defined as "transportation that does not endanger public health or ecosystems and meets mobility needs consistent with (a) use of renewable resources at below their rates of regeneration and (b) use of non-renewable resources at below the rates of development of renewable substitutes." [4].

In the European Union (EU), the GHG emissions from the transport sector increased around

36% since 1990, which degraded the environmental quality [5]. This sector, because of its oil-dependency, is responsible for around a quarter of EU GHG emissions, and the road transport represents about one-fifth of the EU's CO_2 total emissions[1]. Moreover, concerns such as the dependency on oil supply [6] and a foreseen "end of cheap oil" during this century [7] have motivated a wide range of policy and technological measures for the transport sector.

The European Commission (EC), in order to promote the use of energy from renewable resources, approved the Directive 2009/28/EC [8] that sets a mandatory target of 20% share of energy from renewable sources in the Community's gross final consumption of energy by 2020 and a mandatory 10% minimum target of energy from renewable sources in the transport sector. The target for the transport sector should be pursued with a mix between different technological solutions (e.g., hybrid and battery electric vehicles, biofuels, hydrogen) [9] and policies (e.g., including the transport sector in the EU Emissions Trading System, behavior change programs, standards for fuel quality) [10]. The EC strategy consists in supporting the market development of alternative fuels and investment in their infrastructure [9].

The Electric Vehicle (EV) is one element that helps to decarbonize the transport sector and decrease its oil-dependency [11][12]. There are three main types of EV [13]: battery, hybrid and fuel cell. The hybrid EV combines an internal combustion engine with batteries and electric motor. The hybrid EV is divided into two groups: conventional vehicles that, for instance, charge the battery using regenerative braking that converts the vehicle's kinetic energy into electrical energy; vehicles capable of plugging-in with the electric system to charge and discharge the batteries. The fuel cell EV uses hydrogen to generate electricity that can be used for driving or stored in batteries and can plug-in for discharging stored electrical energy.

Presently, plug-in EV are a niche in the global market. In [14], it is forecasted a decrease to a third of conventional combustion vehicles sales by 2030, and an increase of the hybrid EV (full hybrids 22%, mild hybrids 34%), including 8% of plug-in EV sales. The hydrogen fuel cell EV are only foreseen to be fully commercialized around 2025, but this might be an optimistic prediction since this technology stills in a R&D phase [15].

According to a report from the International Energy Agency (IEA), EV can contribute to reducing the world's CO_2 emissions of the transport sector in 2050 to 30% below the levels in 2005, considering an annual sale of around 50 million light-duty EV and 50 million of plug-in hybrid EV per year [16].
Figure 1.1 depicts the final energy savings of the European transport sector in two scenarios characterized by different forecasts for the number of plug-in hybrid and battery EV until 2050 [17]. In the ambitious scenario, the battery EV only show large-scale market integration

[1] Source: http://ec.europa.eu/clima/policies/transport/index_en.htm (accessed in December 2012).

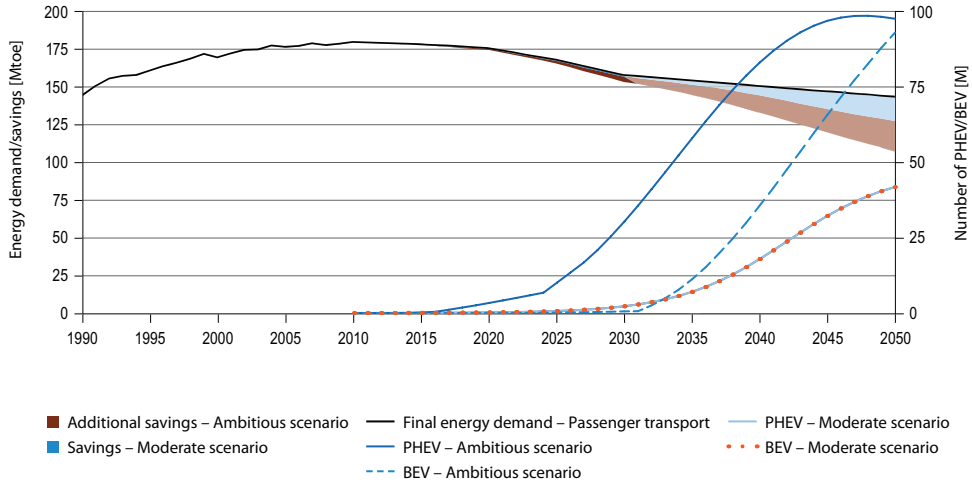

Figure 1.1: *Final energy savings of the European transport sector and forecasted number of electric vehicles [17].*

after 2035, while the hybrid EV start in 2020. In the moderate scenario, both battery and hybrid EV start their market deployment after 2030. The final energy savings are 16 Mtoe (11% reduction compared to baseline scenario) in the moderate scenario and 36 Mtoe (25% reduction) in the ambitious scenario.

The deployment of EV technology establishes a connection between the transport and electric power sectors. In fact, this EV deployment can contribute to a sustainable development of the electric power system, but their positive effect depends on two aspects: (a) the impact on GHG emissions varies with several factors, such as the power system generation portfolio, season of the year (e.g., availability of hydropower resources) and geographical location of EV charging; (b) the EV charging strategy, in particular whether it is controllable or not, impacts the power system operation.

Regarding the first aspect, as mentioned in [18], EV are not "zero-emission vehicles", since they can be charged with RES-E, but also with coal and gas-fired power plants (and even with nuclear). In coal-based power systems and without technological solutions for carbon capture and storage, the EV can result in GHG emissions comparable (or even higher) to the ones from classical combustion vehicles [19].

Figure 1.2 depicts the life cycle GHG emissions from a set of vehicles (hybrid EV, plug-in hybrid EV with 30, 60 and 90 km of range, classical combustion vehicle) as a function of the life cycle GHG intensity of the power system [20]. The small slope in the combustion vehicle and hybrid EV is related to the electricity used for vehicle manufacturing. For the plug-in EV, this picture indicates that with a low carbon generation portfolio the GHG emissions of

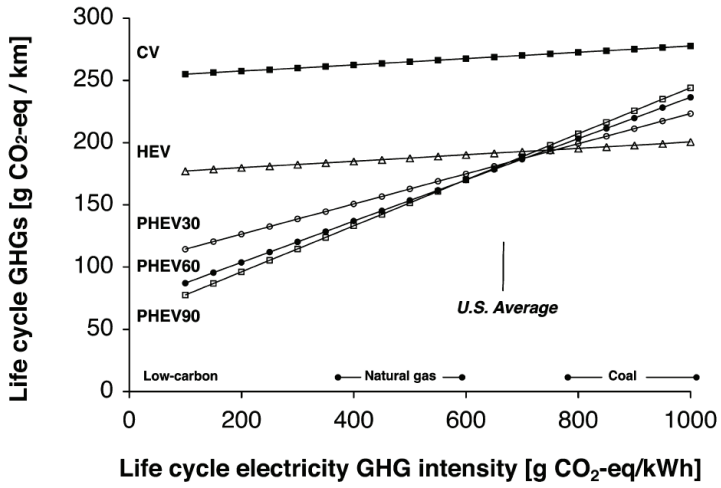

Figure 1.2: *Life cycle GHG emissions from vehicles shown as a function of the life cycle GHG intensity of electricity generation [20].*

plug-in hybrid EV are lower compared to a hybrid EV, but for coal-based power systems the emissions are higher than the ones for hybrid EV.

Therefore, the development and investment in EV should be complemented with decarbonization policies for the electric power system, such as investment in RES-E, more flexible resources in the supply and demand-side, and participation of distributed generation in ancillary services.

The second aspect, and which is related to this PhD thesis, is that, even in countries with a high penetration of RES-E, if the EV are charged during peak hours, peak power units with intensive GHG emissions are likely to be dispatched, which undermines the benefits from EV. This is likely to happen if the EV charging is uncontrollable, e.g. the EV starts charging when the drivers plug-in at home after returning from work. This uncontrollable charging can increase the GHG emissions [21] and create technical problems in the distribution network [22] (e.g., branches congestion and voltage limits violation).

Therefore, in order to take full advantage of the EV benefits to the system and avoid technical problems, it is essential to directly control and coordinate the charging process of each EV. For instance, a coordinated strategy of EV charging can help to decrease the power losses and branch congestions, as well as to improve voltage profiles [23]. Moreover, direct control also enables the provision of ancillary services (e.g., reserves) from the EV [24].

The backbone that enables EV charging control is a smart grid infrastructure [25], which provides additional capabilities for the observability and controllability of the distribution network level, and is strongly supported by the Information and Communications Technology (ICT) and the Advanced Metering Infrastructure (AMI). This enables new features, such as

a two-way communication infrastructure, which creates conditions for demand response and dispatch.

The massive deployment of the EV and necessary interaction with the power system operators of transmission and distribution networks can be supported by an agent responsible for aggregating EV and managing their charging process within the smart grid paradigm [26]. This agent is called aggregator and it is an enabler of the EV integration in the electricity market and power system operation. From the system operators' viewpoint, the EV aggregator is part of a hierarchical control architecture and coordinates the EV charging in response to the system operators' signals, which decreases their communication requirements [23]. From the EV owners' viewpoint, the aggregator uses their available flexibility to purchase electrical energy at low price and sells ancillary services in the electricity markets, which ultimately lead to a retailing tariff reduction.

The combination of a smart grid infrastructure, direct control of EV charging and aggregators entails the following benefits that cover economic, environmental and social aspects:

- with the electric power sector unbundling, the economic signals and incentives for future investments in generation capacity generally come from the electricity market prices. With the increasing penetration of RES-E, the market prices are showing a declining tendency (in some cases are even negative [27]), which decreases the incentives to build additional and more flexible generation capacity to handle RES-E variability and uncertainty, and can put offline secondary and tertiary reserve resources when needed. Nevertheless, countries with a significant penetration of EV can use this existing flexible demand-side resource and postpone the need to create financial instruments (e.g., capacity markets or tariffs) that encourage investments in flexible generation capacity. This also postpones investments in flexible conventional power plants;

- it creates conditions for integrating high penetration of RES-E, since it contributes to avoiding curtailment of RES-E during valley hours, and its flexibility and fast response capability support the system in handling variability and uncertainty of RES-E (e.g., through the provision of reserve services);

- shifting EV load to valley hours allows conventional power plants to run at a higher load factor, improving their efficiency and reducing GHG emissions;

- compared to a situation with uncontrolled EV charging, controllable charging reduces the peak load and decreases the need to invest in additional conventional peak power plants;

- it introduces new competition in the ancillary services market, reduces the amount of

reserve power used from conventional power plants, and contributes to a more active participation from the demand-side in these services;

- it encourages competition and innovation in the electricity retail market. For instance, electricity retailers might expand their products, such as adopting a retailing tariff closer to the wholesale market price, and create financial incentives for inducing a more flexible and price-responsive behavior of the loads. In this case, the consumer benefits from a decrease in the final cost of electricity and is encouraged to make behavioral changes.

These benefits and various features of sustainable development can only be activated with an adequate coordination between EV aggregators and system operators within the smart grid infrastructure. This coordination requires interdisciplinary computational models (from operations research, statistics, data mining, etc.) that support the EV aggregator activity and its integration in the power system. This interdisciplinary framework is called *computational sustainability* [28], and is defined as "new computational models, methods, and tools to help balance environmental, economic and societal needs for sustainable future" [29].

Related to this context and considering the potential benefits from EV aggregators for the power system, this PhD thesis aims to contribute with a set of computational tools that support the participation of plug-in hybrid and battery EV in the electricity market, enabling the provision of secondary and balancing reserve services from this agent and ultimately supporting an increasing penetration of RES-E. The goal is to have demand-side treated equally with the supply-side and provide similar services (e.g., secondary and balancing reserve) without compromising power system reliability.

This research work was driven by the following research question:

> *Which decision-aid methods are required by an EV aggregator to participate in the electricity market and perform economical and technical management of its portfolio?*

Even with the possibility of collecting a large amount of information, there are information gaps and also inherent uncertainties such as the drivers' behavior and electricity market prices. Therefore, this activity requires a chain of computational models divided into three phases: forecast, day-ahead optimization and operational management. The forecasting phase provides the inputs of the day-ahead optimization that determines the "optimal" bids for the electricity market. An operational management algorithm is used, during the operating day, to coordinate the EV charging and comply with the market commitments; the actual charging decisions of the EV fleet result from this operational phase.

These algorithms take into account the current power system design, which includes a liberal-

ized electricity market environment, and minimize the aggregator's wholesale cost. Therefore, EV charging follows economic signals given by the electricity market, but from a demand-side perspective that results in some benefits to the power system. For instance, moving EV charging from high prices (i.e., peak hours) to low prices (i.e., valley hours) periods increases the efficiency of conventional generators that operate with low load factor during valley hours. During valley hours, the occurrence of situations with RES-E surplus (in particular wind power) might be frequent and the EV charging contributes to the decrease wind power curtailment.

Furthermore, EV aggregators with suitable management procedures, such as the operational management algorithms proposed in this PhD thesis, help decrease forecast errors associated to EV charging, since one objective consists in minimizing imbalance costs. An EV aggregator that operates its EV fleet charging in response to reserve prices (i.e., cheap charging as downward reserve and income from selling upward reserve) uses its flexibility to handle imbalances from other market agents (e.g., wind farms), and since it can offer bids at a very low marginal price, it also helps decrease the system operational costs (which are included in the consumers' final tariff).

Finally, by discussing the role of an EV aggregator, the framework to support its participation in the electricity market and necessary computational tools for enabling its operation, we are moving the discussion from the supply to the demand-side. The discussion is about finding solutions in the demand-side that support the increasing share of electrical energy from RES-E, and developing appropriate computational tools that enable the integration of RES-E from the electrical power system in the transport sector.

1.2 Objectives of the Thesis

The work presented in this thesis involves the development of new computational tools for supporting the EV aggregator participation in electricity markets. The main objectives are:

- to define a model for the EV aggregator that includes a framework with the necessary computational algorithms for each market session, available information and communication flows and commercial relations with stakeholders;
- to formulate optimization problems, which use forecasts as input, to support the EV aggregator in defining the "optimal" and robust bids for the energy, secondary and balancing reserve market sessions and without considering the vehicle-to-grid (V2G) concept;

- to formulate operational management algorithms that coordinate the EV individual charging in order to minimize imbalance costs due to deviations between accepted bids and actual charging, and avoid reserve shortage situations;
- to study the sources and effects of uncertainties in the optimization results. The optimization results should provide information about the impact of forecast errors in the total wholesale cost and reserve shortage magnitude;
- to refine our current understanding of the electricity market rules to accommodate this new market agent. Although this is not a main objective, the optimization models results should lead to a set of suggestions for adjusting the current electricity market protocols in order to better accommodate EV.

1.3 Structure of the Thesis

The work developed within the scope of this PhD thesis is organized into seven chapters (including the present one).

The current **chapter 1** presents the general context and motivation to this PhD thesis, defines the problem under research and its main objectives.

Chapter 2 is a literature review about the integration of EV in the power system and electricity market, covering technical and economic perspectives, as well as optimization algorithms for supporting the EV aggregator participation in the electricity market. Relevant background for this topic, such as power system reserves and electricity markets, is also presented.

The aggregator model (e.g., architecture, economic, physical and information flows), and a framework for the electricity market sessions with corresponding optimization/forecasting algorithms are described in **chapter 3**.

The following three chapters propose optimization problems covering different electricity market sessions, illustrated with the same test case composed of synthetic EV time series and market data from the Iberian electricity market. Each chapter has its own results section.

The participation of the EV aggregator solely in the day-ahead electrical energy market is addressed in **chapter 4**. Two alternative optimization approaches, *global* (uses forecasts for aggregated EV variables) and *divided* (uses forecasts for EV variables of each vehicle), are described and compared. An operational management algorithm that coordinates the EV individual charging in order to minimize imbalance costs is also described and evaluated. The

impact of forecast errors in the total wholesale cost is estimated.

Chapter 5 formulates a day-ahead optimization problem for energy and secondary reserve bids and an operational management algorithm that coordinates EV charging in order to minimize differences between contracted and realized values of energy and secondary reserve.

Chapter 6 covers the participation of an EV aggregator in a reserve intended to solve energy imbalances between scheduled and realized values for the system, generally resulting from renewable generation forecast errors. A day-ahead optimization problem is formulated for the electrical energy and balancing reserve bids, and two operational management algorithms, one for day-ahead bids and another for hour-ahead bids, are proposed for this balancing reserve.

Chapters **5-6** also estimate the impact of forecast errors in the total cost and reserve shortage magnitude.

The main document ends with **chapter 7**, where the main contributions, findings and topics for future work are described.

Three appendices complement the main document.

Appendix A presents statistical analyses of the synthetic EV time series and market data used in the test case. **Appendix B** presents the forecast error analyses of the EV and market prices time series. **Appendix C** describes two heuristic operational management algorithms from the state-of-the-art and that were enhanced by Lima [30]. These two algorithms are compared with the operational algorithm proposed in chapter 4.

1.4 List of Publications

International Journals

- (Chapter 2) R.J. Bessa and Manuel A. Matos, "Economic and technical management of an electric vehicles aggregation agent: a literature survey," *European Transactions on Electrical Power*, vol. 22, no. 3, pp. 334-350, Apr. 2012.
- (Chapter 4) R.J. Bessa and M.A. Matos "Global against divided optimization for the participation of an EV aggregator in the day-ahead electricity market. Part I: theory," *Electric Power Systems Research*, vol. 95, pp. 309-318, Feb. 2013.
- (Chapter 4) R.J. Bessa and M.A. Matos "Global against divided optimization for the

participation of an EV aggregator in the day-ahead electricity market. Part II: numerical analysis," *Electric Power Systems Research*, vol. 95, pp. 319-329, Feb. 2013.

- (Chapter 5) R.J. Bessa, Manuel A. Matos, F.J. Soares, and J.A. Peças Lopes, "Optimized bidding of a EV aggregation agent in the electricity market," *IEEE Transactions on Smart Grid*, vol. 3, no. 1, pp.443-452, Mar. 2012.

- (Chapter 5) R.J. Bessa and M.A. Matos, "Optimization algorithms for an EV aggregator selling secondary reserve in the electricity market," paper under review in *Electric Power Systems Research*, 2013.

- (Chapter 6) R.J. Bessa and M.A. Matos, "Optimization models for EV aggregator participation in a manual reserve market," *IEEE Transactions on Power Systems*, in press, 2013. (doi: 10.1109/TPWRS.2012.2233222)

International Conferences

- (Chapter 3) R.J. Bessa and M.A. Matos, "The role of an aggregator agent for EV in the electricity market," in *Proceedings of MedPower 2010*, Agia Napa, Cyprus, 7-10 Nov. 2010.

- (Chapter 4) R.J. Bessa, N. Lima, and M.A. Matos, "Operational management algorithms for an EV aggregator," in *Proceedings of MedPower 2012*, Cagliari, Italy, 1-3 Oct. 2012.

- (Chapter 5) R.J. Bessa, F.J. Soares, J.A. Peças Lopes,and M.A. Matos, "Models for the EV aggregation agent business," in *Proceedings of IEEE PowerTech 2011*, Trondheim, Norway, 19-23 June 2011.

- (Chapters 4-6) R.J. Bessa and M.A. Matos, "Forecasting issues for managing a portfolio of electric vehicles under a smart grid paradigm," in *Proceedings of the Third IEEE PES Innovative Smart Grid Technologies (ISGT 2012)*, Berlin, Germany, 14-17 Oct. 2012.

National Conferences

- (Chapter 4) R.J. Bessa and M.A. Matos, "Two alternative approaches for modelling a portfolio of electric vehicles," *1st PhD. Students Conference in Electrical and Computer Engineering*, Faculty of Engineering, University of Porto, Portugal, 28-29 Jun. 2012.

- (Chapter 5) R.J. Bessa and M.A. Matos, "Alguns problemas de optimização para um agente agregador de veículos eléctricos. Optimization problems for an EV aggregation agent," presentation in the 15° *Congresso Nacional da Associação Portuguesa de Investigação Operacional*, Coimbra, Portugal, 18-20 Apr. 2011.

Chapter 2

Background and State of the Art

Abstract

This chapter presents a literature review about the integration of EV in the power system and electricity market, from technical and economic perspectives and with particular emphasis on the role of an EV aggregator. Moreover, optimization algorithms for supporting the EV aggregator participation in the electrical energy and ancillary services market are reviewed. Relevant background for this topic, such as power systems reserves and electricity markets, is also presented.

2.1 Introduction

Primarily, the EV[1] is an additional electric load in the power system, characterized by a significant temporal uncertainty of its consumption value. However, in a Smart Grid environment, it is possible to control the EV charging or even inject power from the EV batteries into the electrical network [called Vehicle-to-Grid (V2G)].

The present state of the art in the topic of EV is mainly devoted to study the integration of EV in the electrical network and power system operations. Different authors are studying the EV integration, exploring scenarios where EV are additional loads, but also scenarios where EV are controllable loads that could include or not the V2G capability. Generally, the outcome of this research is that new management procedures, with a strong link to the Smart Grid paradigm, allow a massive integration of EV and mitigate impacts on voltage profiles, power losses and branch congestions. It is not an objective of this chapter to present a detailed

[1] In this thesis the acronym EV means plug-in battery or plug-in hybrid vehicles if nothing more is added.

review on this topic, thus only the relevant results are briefly presented in section 2.3.

The literature review will be mainly focused in two research directions. The first one is related to the economic and technical value of EV in the electricity market (section 2.4). The aggregation of EV was found to be technically attractive and economically valuable and, in general, to favor the deployment of EV, if a good business model is adopted. Thus, business models for an EV aggregator are also reviewed.
The second one, in section 2.6, is related to optimization algorithms developed to support the participation of an EV aggregator in the electricity market.

This chapter also presents the relevant background for this topic (section 2.2), which contains a description of the power system reserves, electricity market and demand-side integration.

2.2 Background

2.2.1 Power System Reserves

Reserve Definitions

In each time instant, the Transmission System Operator (TSO)[2] is responsible for managing the load-generation mismatch in the power system. A positive imbalance (generation greater than load) will increase the system frequency above its nominal value (50 or 60 Hz), and a negative imbalance (load greater than generation) will decrease the system frequency. This leads to the need of an upward and downward reserve capacity composed of loads and generation units able to respond to frequency disturbances. The upward reserve consists of generation units (or loads) online or offline able to, in a short period, increase their generation levels (or decrease their consumption levels). The downward reserve consists of online generation units able to decrease their generation levels or loads able to start consuming (or increase consumption) in a short period. The nomenclature and technical characteristics of reserve categories are different across several countries, even inside the same interconnected system [32].

The classical reserve categories, depicted in Figure 2.1, are defined by the European Network

[2] In the USA a different nomenclature is used: Independent System Operator (ISO) and Regional Transmission Organization (RTO). Both have the same functions of the TSO in Europe, but the main difference is that the ISO usually operates only within a single USA state, while the RTO operates over large interstate areas. A detailed comparison between TSO, ISO and RTO can be found in [31].

of Transmission System Operators for Electricity (ENTSO-E) Operational Handbook as:

- *primary control reserve*: "joint action of all interconnected TSO, primary control stabilizes the system frequency at a stationary value after a disturbance or incident in the time-frame of seconds, but without restoring the system frequency and the power exchanges to their reference values. The time for starting the action is a few seconds after the incident, the deployment time for 50% or less of the total primary control reserve is at most 15 seconds and from 50% to 100% the maximum deployment time rises linearly to 30 seconds. Primary control power must be delivered until the power deviation is completely offset by the secondary/tertiary control reserve of the control area in which the power deviation has occurred." [33];

- *secondary control reserve*: "is used to keep or restore the system frequency to its set-point value of 50 Hz and the power interchanges with adjacent control areas to their programmed scheduled values, thus ensuring that the full reserve of primary control power activated will be made available again." [34]. "Secondary control makes use of a centralized and continuous Automatic Generation Control (AGC), modifying the active power set points / adjustments of generation sets/controllable load in the time-frame of 30 seconds (at the latest) up to typically 15 minutes (at the latest) after an incident" [33];

- *tertiary control reserve*: "is usually activated manually by the TSO in case of observed or expected sustained activation of secondary control. It is primarily used to free up the secondary reserve in a balanced system situation, but it is also activated as a supplement to secondary reserve after larger incidents. Schedule activated tertiary control reserve is activated with relation to the predefined timeframe of exchange schedules, e.g. 15 minutes" [33].

The Nordic countries (forming the Nordel network) are not connected to the Union for the Co-ordination of Transmission of Electricity (UCTE) interconnected network (with the exception of West Denmark) and their reserve nomenclature is different [35]. Nevertheless, in technical terms the use of the reserves is rather similar.

The primary reserve is divided into *normal* and *disturbances automatic frequency controlled reserve*, and secondary reserve is called *load frequency control*. Other types of reserves are required for full restoration of imbalances. These reserves are mostly manually activated and used to restore the balance after deviations (e.g., forecast errors) during the operating hour and to relieve the frequency controlled reserves. The activation time of these reserves is less than 15 minutes.

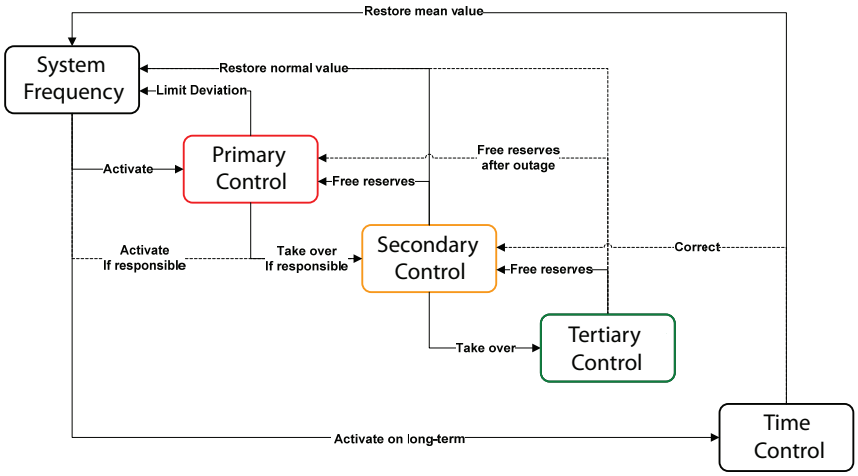

Figure 2.1: *Frequency control scheme and actions of the ENTSO-E operational handbook [33].*

The nomenclature of ENTSO-E is presently being revised in the "Draft Network Code on Load-Frequency Control and Reserves" [36] that is under public consultation. Primary reserve will be named *frequency containment reserve*, secondary reserve named *frequency restoration reserve* and tertiary reserve named *replacement reserve*. Nevertheless, the definitions are rather the same.

In the USA, the reserve nomenclature and categories are also different across the North American Electric Reliability Corporation (NERC) jurisdiction. Nevertheless, the three control types of the ENTSO-E definitions can also be found [37]. The primary frequency control is frequently called *primary frequency response* and the secondary control is often referred to as *regulation reserve* [38]. The tertiary control is often referred to as *ramping* or *load-following* reserve [37].

The difference between the USA and Europe is that *contingency reserves* are explicitly defined in North America while they are not in Europe [39]. Contingency reserves are mainly considered for handling forced outages of conventional generation. Kirby [40] presents a reserve description, depicted in Figure 2.2, that is reasonably consistent across North America. The primary, regulation and load following reserve are included in the group of reserves for normal conditions (i.e., compensates for the variability and uncertainty of load), while the reserves for contingency conditions are: *spinning*, *non-spinning* and *replacement* (or *supplemental*) *reserve*.

Spinning reserve is defined as "online generation, synchronized to the grid, that can increase output immediately in response to a major generator or transmission outage and can reach full output within 10 min". Non-spinning reserve is the "same as spinning reserve, but need not respond immediately; resources can be offline but still must be capable of reaching full output within the required 10 min". The replacement reserve "is used to restore spinning and

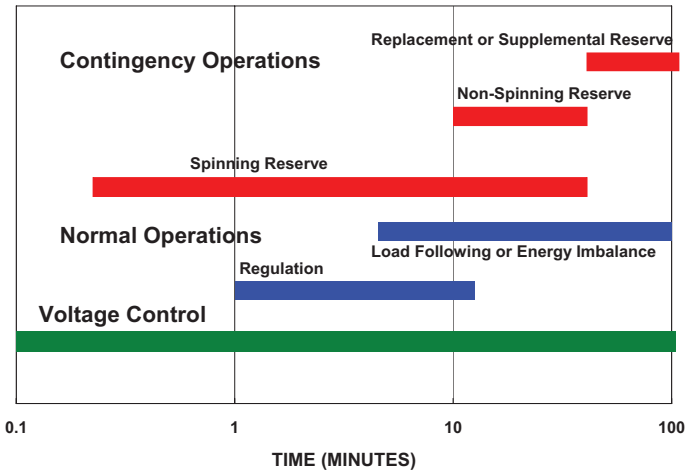

Figure 2.2: *Response time and duration of different reserve categories in the USA [40].*

non-spinning reserves to their pre-contingency status; it must have a 30-60 minutes response time.".

Redefinition of the Reserve Nomenclature

For countries with high penetration of RES-E (mainly wind and solar), Holttinen et al. [41] revised the reserve nomenclature: *non-event* (normal operation) for variability and forecast errors inside the scheduling period; *fast-event* (contingency operation) for unplanned outage of a generator or cross-border transmission line; *slow-event* for net-load ramps and forecast errors that can occur in longer time-scales (from ten minutes to hours). The authors argue that RES-E based generation does not change faster enough to be a contingency event and the impact in secondary reserve is lower (c.f., [42][43]) than the impact on tertiary reserve (both reserves are included in the *non-event* category). High penetrations of RES-E based generation will introduce *slow-events* characterized by high generation ramps and forecast errors.

In the time-scale of tertiary reserve, several countries have already created a reserve category for *slow-events*. For instance, the Spanish power system has a *deviations reserve* that is only activated for load-generation deviations above 300 MWh [44]. In Denmark, the *manual reserve* is used to handle forecast errors. The Hydro-Quebec power system includes an *energy balancing reserve* for handling forecast errors [43]. In the USA, it is under discussion the creation of a *ramping reserve* [45].
Conversely, in Portugal, the tertiary reserve[3] is used to compensate forecast errors [47]. Elec-

[3] In fact, in Portugal tertiary reserve is called *reserva de regulação* [46], but this term is not used because its English translation is regulation reserve, which could create confusion with a reserve category in U.S.A. that has the same name but a different function.

tric Reliability Council of Texas (ERCOT) uses the non-spinning reserve for handling wind power forecast errors [48].

In this thesis, the reserve is divided into the following categories according to its main functions:

- *frequency reserves*: classical reserve categories (i.e., primary, secondary and tertiary frequency control) that are procured by the TSO/ISO for handling frequency excursion problems;
- *balancing reserve*: active power manually requested by the TSO/ISO to handle forecast errors and ramp up/down events related to RES-E generation. This reserve is slower than frequency reserve and the TSO will procure this type of reserve for handling positive and negative imbalances of the market schedule.

2.2.2 Electricity Markets

Figure 2.3 depicts the general structure of an electricity market, which will be reviewed in this section.

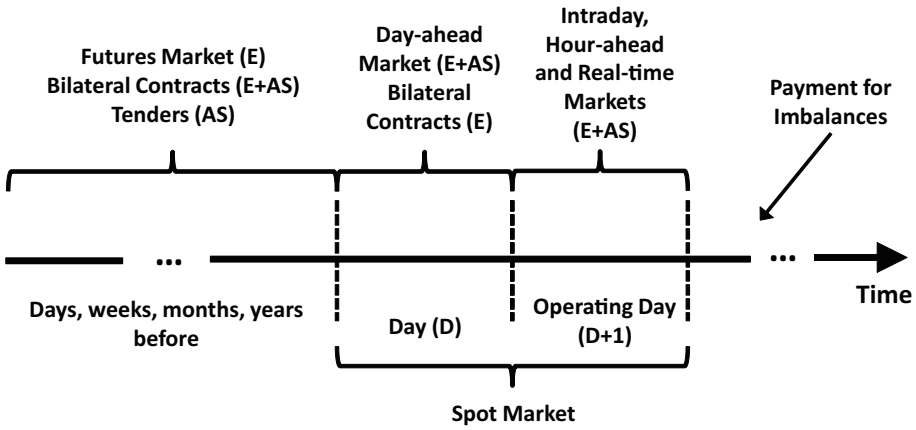

Figure 2.3: *Structure of the electricity market (E: Electrical energy; AS: Ancillary services).*

The electricity market can be divided into two different types [49]: the *spot market*, where the electrical energy and ancillary services[4] are traded for immediate physical delivery, and the *futures market*, where the delivery is at a later date and normally does not involve physical delivery. The *futures market* is normally used for risk hedging [50]. In this section, emphasis is given to the *spot market*.

[4] Ancillary services are functions separated from the electrical energy market, which are used to support reliability and power quality of the power system. One example is the power system reserves.

Coexisting with the electricity market, there are also bilateral contracts that the market agents are free to trade. These contracts are normally used to guarantee a certain amount of electrical energy for the demand-side, or to guarantee a certain profit for the supply-side, or used as a risk hedging mechanism.

Typical European Spot Markets

A typical European electricity market can be operated by the TSO or by a pool operator. The pool operator establishes relations with generators, distribution companies, retailers, eligible consumers and the TSO. The pool operator or TSO runs a centralized market-clearing algorithm.

The *spot market* can be divided into two main categories: electrical energy and ancillary services. The electrical energy market is divided in day-ahead and intraday (or hour-ahead) sessions.

The day-ahead electrical energy market is a double-side auction where the supply-side (i.e., agents with generation units) submits bids (i.e., minimum price they want to receive and quantity) that are ordered by ascending price and cumulative quantity (named supply curve) and the demand-side (i.e., agents with loads) submits bids (maximum price they want to pay and quantity) that are ordered by descending price (named demand curve). The point of intersection of these two curves is the market-clearing price, which is a uniform price since all the market agents pay/sell the electrical energy at this price value. An alternative auction, which is uncommon to find in electrical energy markets, is called pay-as-bid price auction. In the pay-as-bid system, the supply-side sells the cleared quantity at the offered bid's price (the same is valid for the demand-side).

The market gate closure[5] is normally before noon. The market agents may present buy and sell hourly bids that cover all 24 hours (or 48 half-hours in some markets) of the next day (or operating day). Different types of bids are possible: a price independent bid for all hours regardless of the price level, with only a price cap and floor; a price dependent hourly bid for all hours where a stepwise curve is submitted (i.e., different quantities for different prices); complex bids that can include inter-temporal constraints of the generation units (e.g., ramp constraints) or minimum revenue requirement (e.g., start up and down costs).

After the market-clearing, the TSO performs constraints management (i.e., solves network congestion and voltage limits violation). The procedure to solve technical constraints modifies

[5] Time instant when participants cannot modify their bids any-more.

the day-ahead schedule and determines which selling and buying offers should be added or removed from the initial daily program of operation. In electricity markets with more than one control area and in case of congestions between interconnected areas, the market is separated into lower/higher price areas.

There are a few countries without a day-ahead energy market. One example is the British Electricity Trading and Transmission Arrangements (BETTA), which moved from a pool trading to a free bilateral trading operating on a rolling half-hourly basis and one hour-ahead of actual supply (gate-closure is one hour before) [51].

Intraday markets are conceptually analogous to day-ahead energy markets and the main difference is the gate closure. Essentially, it follows the day-ahead session, and works as an adjustment market close to the operating hour. In these cases, with additional and/or more accurate information, the market agent can correct the accepted bids from the day-ahead market or from previous intraday sessions.

Two structures of intraday markets can be found:

- continuous trading that takes place after the day-ahead market and with a gate closure of one hour before physical delivery. One example is the Elbas session from NordPool [52];
- fixed number of sessions at pre-defined periods and for the remaining hours of the operating period. One example is the Iberian electricity market, which has six intraday market sessions [53].

The majority of these intraday markets are non-mandatory and present a low liquidity [52][54].

The ancillary services are divided in reserve services and other services (e.g., voltage control, black start). The mechanisms for procuring reserve differ from country to country and from category to category. In general, the TSO is responsible for procuring these services and different mechanisms can be used: mandatory and non-remunerated; monthly or yearly tenders; bilateral contracts; electricity market (i.e., on a daily basis) [55].

For example, in the Nordic countries, the automatic frequency controlled reserves are acquired by TSO using different types of contracts with generators [35]. In Germany, there is a competitive tendering for primary and secondary control reserve that takes place every six months and is organized by the TSO for its control area [56]. The primary reserve is traded only with a capacity price bid, while secondary reserve is traded with a price for available and dispatched capacity. In other countries, such as Portugal and Spain, primary reserve is mandatory and non-remunerated [55]. In France, the secondary reserve is procured with bi-

lateral contracts between TSO and generators with a pay-as-bid-price for both net energy and capacity [55].

The secondary reserve can also be procured with day-ahead auctions in the electricity market. For example, in Portugal and Spain, there is a market pool for secondary reserve [53]. The agents present capacity bids (quantity in MW and price in €/MW), and the amount of reserve contracted to each unit is settled at the marginal price of the secondary reserve market. The dispatched reserve price (price in €/MWh) is defined by the price that results from the tertiary reserve market. In Portugal, the TSO defines a ratio between upward and downward reserve capacity [57][58]. Another country with a day-ahead market for secondary reserve is Italy [59], but with a pay-as-bid-price system and mandatory participation.

Tertiary reserve is contracted for the next day or during the operating day [54]. For example, in NordPool the manual reserve is purchased in the *regulating power market*, with a gate closure of 45 minutes before the operating hour. The bids presented by the market agents (called production and load balancing responsible) are placed in priority order according to the price and the TSO uses this list as far as possible to handle imbalances due to forecast errors [35].

The tertiary reserve bids in Portugal and Spain are presented for the next day (at 23h00) to the TSO and the market agents can continuously update and modify these bids until one hour (in Portugal) and 45 minutes (in Spain) before the operating hour. The TSO, has for each hour, a list of bids, which are used when it is necessary (i.e., can be called 15 minutes before and during the operating hour) to handle forecast errors and/or replace secondary reserve [54]. There is only a single price for dispatched reserve power and maximum duration is usually one hour. In Spain, there is also a deviations reserve market that takes place between intraday sessions and the agents can present bids one hour before the time horizon of the corresponding balancing market session [58].

In Germany, upward and downward tertiary reserve (or *minute reserve*) is procured on a daily basis after the energy market for six four-hour time slots of the next day [60]. Tertiary reserve is traded with two prices, one for available capacity and another for dispatched power. In Italy, there are five balancing market sessions with pre-defined opening and gate closure times where reserve services are procured for solving imbalances and congestions [59]. The participation is mandatory and with a pay-as-bid price.

Other type of ancillary services, such as voltage control, are normally mandatory and non-remunerated, or remunerated with bilateral contracts [55].

Imbalance prices (or financial penalizations), for both positive and negative deviations from

schedule, result from the use of reserves for solving imbalances, and these prices reflect the costs incurred by the TSO for delivering electrical energy in real-time [61].

For example, in Portugal, the imbalance prices are tariffs related to the costs of contracting and using reserves (secondary and tertiary), while in the NordPool, the imbalance prices are the clearing price of the regulating power market (i.e., manual reserve). Two possibilities exist for imbalance prices: single (or symmetrical) price and double (or asymmetrical) price for negative and positive deviations. Some countries like Germany and the Netherlands have a single imbalance price, while others, like Portugal and Denmark, have a double price [54]. In most cases, deviations opposite to the total system deviation are not penalized (i.e., they are valued at the electrical energy price from the last day-ahead or intraday market session).

USA Spot Markets

The USA markets have two fundamental differences to the European markets. First, the price is calculated for every node [called Locational Marginal Price (LMP)] of the transmission network [62]. The LMP reflects the cost of generation in specific nodes. For instance, when there is transmission congestion, the generation with lower cost cannot supply the loads in certain locations and, in this case more expensive generation is scheduled to meet these loads and the LMP is higher in those nodes.

The second difference is the market-clearing mechanism. Ellison et al. [63] identified three different clearing mechanisms:

- *integrated joint-optimization*: prices and schedule of energy and reserves are determined simultaneously by an optimization problem with a single objective function and a set of constraints. The ISO with this mechanism are Midwest ISO (MISO), New York ISO (NYISO), California Independent System Operator (CAISO) and ERCOT.

- *coupled joint-optimization*: separated optimization for energy and reserves, but both optimization problems have coupled constraints (e.g., the energy optimization contains inequality constraints related to reserve requirements). The Pennsylvania-New Jersey-Maryland Interconnection (PJM) uses this mechanism.

- *decoupled optimization*: separated optimization of energy and reserve without coupled constraints (i.e., similar to the European markets). The ISO New England (ISO) uses this mechanism.

There is also a real-time market in the USA which performs functions similar to the intra-day markets in Europe. The gate closure of this market varies widely across ISO, ranging

between 30 and 75 minutes before the operating hour. Financial penalties are considered for imbalanced energy from the day-ahead or real-time schedule [64].

In the real-time market, the agents can present reserve bids, but in cases, such as the NYISO [65] and CAISO [62], the majority of the reserve is procured in the day-ahead market.

2.2.3 Demand-side Active Participation

One of the goals of the Smart Grid paradigm is to enable the transmission of direct control or price signals to reduce consumptions during peak hours or emergency situations [66]. This is achieved by integrating Information and Communications Technology (ICT) [e.g., Advanced Metering Infrastructure (AMI)] and advanced control technologies into the power system. With the availability of bidirectional communication, distributed sensors (e.g., phasor measurement units), advanced data mining and optimization techniques, a proactive participation of the demand-side in the electricity market is feasible and expected.

Europe

Torriti et al. [67] presented an overview of the Demand Response (DR) programs in Europe. According to the authors, this mainly consists of long-term contracts or programs to promote the DR participation of large industrial consumers, through interruptible tariffs and time-of-use tariffs. For example, in Spain, Portugal and Italy the DR mainly consists of interruptible contracts for large consumers which receive curtailment signals from the TSO some time in advance. For small consumers the only incentive is a time-of-use tariff.

However, this is changing in Europe, in particular with the deployment of the Smart Grid paradigm [25]. For example, in [68] it is mentioned that the TSO of Norway (Statnett) is developing action plans for acquiring 260 MW of DR through both tendering and market bidding, mainly focused on medium-size end-users and independent aggregators.

The TSO of Denmark (presently Energinet.dk), in order to promote the participation of small loads in the regulation power market, published a proposal in 2010 for the following years which outlines two methods [69]:

- participation in the regulation power market under the current rules and to overcome the minimum bid size constraint (10 MW) it will be allowed to aggregate assets on the demand-side;

- self-regulation: the price of the regulation power market[6] will be published during the operating hour (in opposition to one hour after the operating hour) and in this model the small loads units will have the chance to self-regulate in accordance to this price. This service can be divided into two types: (a) the balance responsible has direct control over some loads (e.g., heat-pumps, electric boilers); (b) the balance responsible defines the electricity tariff according to the regulation price (and its business model) and the end-user reacts to the tariff value.

Finally, in Germany, the Federal Network Agency defined new conditions for the primary and secondary reserve tenders [70]. The goal was to enable access from small generators, loads and storage. For primary reserve, the main changes were: reducing the tender horizon from one month in advance to one week; reducing the minimum bid from 5 MW to 1 MW; the possibility to aggregate resources. For secondary reserve, the changes were similar, but minimum bid was reduced from 10 MW to 5 MW.

USA

In the USA, there is an increasing share of DR programs and integration in the electricity market. Kirby et al. [71] present an overview of the current situation. The experience of having loads supplying ancillary services is limited to the markets of ERCOT, MISO, PJM, NYISO and some pilot projects in ISO-NE, Bonneville Power Administration (BPA) and CAISO. In PJM, around 250 MW of spinning reserve is from demand-resources and half of the spinning reserve in ERCOT comes from loads. Similarly to Europe, almost all loads are industrial or large consumers. MISO uses loads for regulation reserve; PJM and BPA also have pilot projects with loads supplying primary reserve. Interruptible loads (based on low frequency threshold or ISO signal) participate in contingency reserves in ERCOT, MISO, PJM and NYISO.

In the restructured market of ERCOT, the role of demand was enhanced and a set of DR types were created [72]. One of these types was LaaR (*load acting as a resource*). The idea of LaaR is to have loads directly competing with generators to provide several ancillary services (e.g., non-spinning reserve) procured in the day-ahead market. In 2008, the level of participation in LaaR was around 1300 MW, but this available capacity consists of large and medium industrial and commercial facilities.

Another example is the PJM market, which allows the participation of Curtailment Service Providers (CSP) that aggregate demand resources to reduce load [73][74]. The CSP can participate in PJM Economic Load Response market that enables demand resources to reduce

[6] Latest activated regulation power unit.

consumption in response to energy, spinning reserve and/or day-ahead supplemental reserve prices, or follow a PJM regulation signal to reduce or increase load. The participation of loads in the spinning reserve market increased during the last years and, presently, loads provide 17% of this reserve (mainly industrial consumers). There is no participation of loads in the regulation reserve market.

The participation of residential loads in the DR programs is minimal and it only exists at pilot projects level [71]. One example is the Demand Response Reserves Pilot Project from ISO-NE for single or aggregated load resources providing a service similar to the forward reserve market in ISO-NE [75]. The program was primarily designed to supermarkets, big-box retailers and aggregators of residential air-conditioning with direct control, until a maximum load reduction of 5 MW.

Reserve Shortage in DR Programs

The authors of [40] and [71] mentioned the fact that forecasting the load participation in ancillary services might be a difficult task. Several factors (e.g., nature of the load, control algorithms, aggregation size) could make difficult to deliver the contracted energy. Therefore, it is important to develop mechanisms that mitigate this problem.

Some TSO/ISO already have penalty terms for situations with reserve capacity shortage. For example, ISO-NE has two penalty terms for the forward reserve market[7] [75]: *failure-to-reserve penalty* that is imposed when the available reserve capacity in that hour is less than the capacity contracted in the market; *failure-to-activate* is imposed when a resource failed to activate or reduce load when requested to do so by the ISO within 10 or 30 minutes. Between 2008 and 2010, the *failure-to-activate* term was very low, compared to the *failure-to-reserve penalty*, which ranged between 3% and 4% of the forward reserve payment [76].

PJM and CAISO have recently introduced a pay-for-performance compensation for resources providing regulation reserve[8]. PJM uses three components [77]: *accuracy score* is the correlation between control signal and regulating unit's response; *delay score* is the time delay between control signal and point of highest correlation from the *accuracy score*; *precision score* is a function of the difference in the energy provided versus the energy requested by the regulation signal.

[7] The forward reserve market has seasonal auctions (summer and winter) and comprises obligations of 10-min non-spinning reserve and 30-min operating reserve.

[8] http://info.a123systems.com/blog/bid/133226/New-California-ISO-Frequency-Regulation-Rules-Favorable-to-Grid-Energy-Storage (accessed in March 2013)

These three components make a *performance score* that is included in the clearing process. Poor performing resources will appear more costly and thus less desirable. For instance, a 20 MW resource with a 0.25 performance score would appear as costly as an 80 MW resource with a 1.00 performance score. The NYISO also has a factor (between 0 and 1) related to the regulation service performance (i.e., capability of following the AGC signal) [78].
In Portugal, there is also a penalization term for situations with secondary reserve capacity shortage [57].

2.3 Integration of EV into the Power System

2.3.1 Early Studies

The first studies about economic and technical problems resulting from the massive integration of EV in the power system were mainly characterized by the following aspects:

- EV were merely additional loads for charging batteries [79][80];
- two alternative charging strategies were used for assessing the EV impact: (a) charging begins when the drivers park the EV; (b) a time-of-the-day pricing induces the driver to charge the EV in periods when the electricity price is lower (e.g., low-load periods) [79][81];
- the distribution network was not included in the studies [79][80][82].

Two important conclusions were relevant for future studies. First, a considerable improvement is needed in residential areas of the distribution network if early planning is not conducted and the installation of control devices for controlling time and power of EV charging is recommended [79]. Second, the impact of EV should be studied at the substation level, mainly because EV load is not uniformly distributed in the distribution network and residential areas are expected to have a high EV consumption [82].

2.3.2 Recent Studies

Recently, with the possibility of bidirectional communication and load control from the Smart Grid paradigm [83], the EV integration studies have been revised and the following aspects introduced:

- EV is an active resource, either by exploring the possibility of bidirectional power injec-

tions (V2G) or by exploring the possibility of controlling the EV charging;

- detailed studies are conducted at the distribution network level, in order to assess the impact of different EV penetration levels in the network losses, congestion and voltage profiles.

The first point refers to the V2G concept, which was introduced in 1997 by Kempton and Letendre [84]. Under this concept, the electrical network could receive power from a plugged-in EV and, in this case, the charger is bidirectional (able to deliver power to the grid and to charge the battery).

Brooks and Thesen [85] claim that, even without V2G, EV with controllable unidirectional charging might also provide (or sell) reserve services. The authors described the concept of Preferred Operating Point (POP), from what the EV provides upward and downward regulation, similar to the operating point of conventional generators for spinning reserve. The difference between the POP of the conventional units and the EV is that the conventional units have a positive POP (e.g., dispatched generation level) while for the EV it could be zero or negative (i.e., load is treated as negative generation). The capacity of the regulation services is only linked to the deviation capacity from the POP. Figure 2.4 depicts the example of one EV consuming 7 kW (i.e., the value of POP) with a maximum charging power of 14 kW, which means that it can provide 7 kW of upward regulation until it reaches the "zero load" situation and 7 kW of downward regulation.
Using this POP approach, the EV is capable of reducing or increasing consumption under a dispatch control signal.

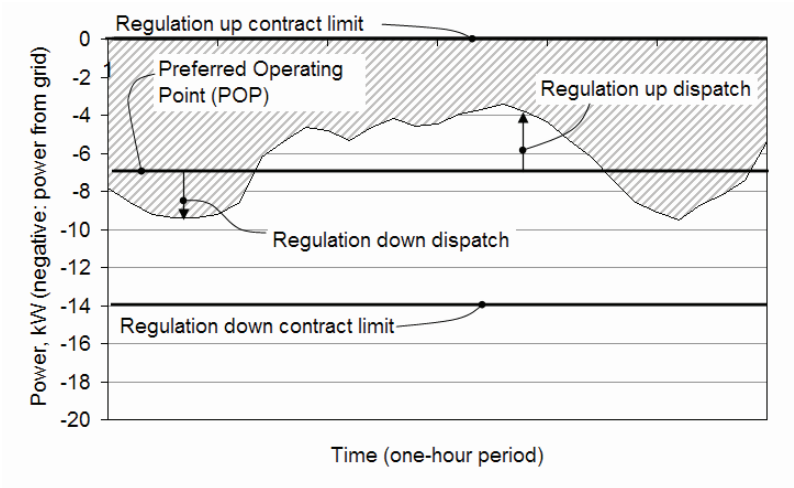

Figure 2.4: *Illustrative example of an EV providing regulation up and down with a POP value of -7kW (i.e., 7 kW of load). The shaded area represents the energy delivered to the vehicle by the grid over the one-hour period [85].*

The V2G or the POP modes enable the provision of power system reserves. Still, the EV is an electric load and the possibility of controlling its charging rate and schedule (which is frequently called smart charging) offers benefits compared to a situation where the EV is an uncontrollable load. Two alternative modes for controlling the EV charging (or power injection in V2G) are envisioned: (a) direct control of the charging rate; (b) indirect control using a price signal to induce a certain behavior in the EV charging. The majority of the studies in the literature explore the direct control mode.

Impact on the Distribution Network

Several authors have studied the impact of EV in the distribution network, including smart charging strategies[9] with V2G or unidirectional controllable load.

Fernández et al. [86] describe an assessment methodology to evaluate the impact of different EV penetration levels on the distribution network investments (e.g., LV lines, MV/LV transformers) and energy losses. The results for three different scenarios of EV penetration (35%, 51% and 62%) are presented for peak and off-peak hours. The possibility of V2G is included and also a smart charging strategy to avoid EV charging simultaneously during peak hours. The authors concluded the following:

- for a scenario with 62% of EV, the integration of EV increases the investment levels up to 19% in a residential urban area and up to 3% in an industrial and residential area;
- the use of a smart charging strategy during peak hours decreases the need for network reinforcements: the investment in the urban area is up to 5% and in the industrial and residential area is up to 1%;
- when moving EV charging from peak to off-peak hours the investment needed at peak hours decreases between 5% and 35%. Nevertheless, additional investment can be needed for accommodating this additional off-peak load;
- if the majority of EV charge during off-peak hours, the electrical energy losses increase up to 40% (scenario with 62% of EV and residential urban areas) compared to the reference case without EV, while in peak hours the increase is only 13%.

This study was devoted to a planning phase [i.e., *ex-ante* evaluation of Distribution System Operator (DSO) investments] considering economic and technical aspects. A different ap-

[9] In general terms, smart charging consists in controlling the EV charging process to avoid violations of physical constraints of the distribution network [23].

proach, more focused in studying the impact of EV at the operational level, is presented by Lopes et al. [23]. Steady-state simulations were conducted on a typical semi-urban 15 kV distribution network to analyze the EV impact on branch power flow limits and voltage profiles. The authors concluded the following:

- with uncontrollable charging[10], only a maximum EV penetration of 10% is tolerable; above this limit, branch congestion and excessive voltage drops start to occur;
- a dual tariff policy[11] allows a maximum penetration of 14%. The main problem with this strategy is that it concentrates most of the EV charging around hour 23h00 which induces a large decrease in the voltage values;
- a smart charging strategy, where the DSO controls the EV charging in order to avoid problems such as branch congestion, allows a maximum penetration of 52%;
- the voltage's lower limit, in this specific case-study, was the limiting factor of the EV integration. However, in a network with the load concentrated in specific points, such as a residential urban area, the branch limits might be the limiting factor.

These steady-state simulations are further extended and enhanced in [22]. The author describes a stochastic method combining power flow calculations and Monte Carlo simulation for evaluating EV impact on the distribution network. The analysis of four different distribution networks (three MV networks and one LV) showed that the impacts of EV are influenced by several factors, such as EV integration level, EV driver's behavior, mobility patterns, technical characteristics of the network and charging strategies.
The author also describes an operational procedure to be used by a DSO to resolve congestion and voltage violations caused by EV charging in the distribution network. The process defines EV charging decrease/increase set-points to be used as corrective and preventive actions during emergency situations.

In order to assess the impact of battery EV in the residential distribution network, Clement-Nyns et al. [87] use an optimization problem that minimizes power losses and voltage deviations. The following conclusions were obtained:

- with uncontrollable charging, an increase in the number of EV leads to a significant increase in the power losses and voltage deviations, e.g. for a scenario with a 30% penetration level, the power losses are 6% of the total power if EV fleet charge between 18h00 and 21h00 and 2.2% if charge between 21h00 and 6h00;

[10] No charging control and the charging starts immediately when the EV plugs-in.
[11] Higher tariff at peak hours, compared to off-peak hours.

- with smart charging (i.e., solving the optimization algorithm) the power losses decrease for all charging periods and penetration scenarios. The difference is more significant in the voltage deviations since the maximum voltage deviation is well below 10%;

Impact on the Generation System

Hartmann and Ozdemir [88] evaluated the impact of two different charging strategies (uncontrollable charging and grid stabilization storage using V2G) on the daily fluctuations of the German power system. The uncontrollable charging increases the daily fluctuations 1.5% with 1 million of EV and 92% with 42 million of EV, compared to scenarios without EV. When the EV uses V2G, a reduction of 16% is achieved. A third charging strategy, driven by profit maximization using V2G, was also tested. According to the authors, because of the similarity between price and load peaks, the fluctuations are also reduced by around 12%.

Bremermann et al. [89] present a probabilistic method that embeds a homogeneous Poisson process for modeling EV driving behavior in a sequential Monte Carlo simulation. The methodology is used to evaluate the generation capacity reserve (or static reserve) and operating reserve adequacy from a long-term perspective. Three charging strategies were analyzed: uncontrollable charging, dual-tariff charging and smart charging[12].

For a modified IEEE-RTS 96 system and for static reserve, the results are the following: uncontrollable charging increases the Loss of Load Expectation (LOLE) from 1.45 hrs/year (no EV in the system) to 2.8 hrs/year (in a scenario with 100,000 EV), while the dual-tariff gives a LOLE of 1.5 hrs/year for the same scenario. In the operating reserve evaluation, the results are the following: uncontrollable charging increases LOLE from 3.87 hrs/year (no EV in the system) to 5.77 hrs/year (in a scenario with 100,000 EV); dual-tariff charging increases the LOLE to 9.54 hrs/year in the same scenario since it introduces a new peak in off-peak hours; with smart charging, the LOLE from the dual-tariff strategy decreases to 3.79 hrs/year, which is lower than the base case with no EV.

Impact on Power System Emissions

A changing in the generation system (e.g., units start-up, load factor, and wind power curtailment) also impacts its Greenhouse Gas (GHG) emissions. Goransson et al. [21] studied the integration of plug-in hybrid EV in a wind-thermal power system (25% wind power and 75% thermal generation) based on western Denmark. The results show that EV can reduce the CO_2

[12] In this work, smart charging consists in postponing EV charging during off-peak hours with loss of load events.

emissions of the power system if the EV charging follows one of these two strategies: (a) EV charging is controlled and takes place when it is more favorable from the system perspective; (b) the power system is free to charge and discharge EV in V2G mode. The average emissions reduction with strategy (a), compared to a system without EV, was around 3% for a scenario with 20% share of EV in the total load, and 4.7% for strategy (b) in the same scenario.
This improvement is mainly due to a reduction in the start-up of thermal units and an increase in system's ability to manage short-term variations. A uncontrollable charging strategy increases the CO_2 emissions around 3.1% in a scenario with 20% share of EV in the total load. The two previously mentioned strategies also decrease the wind power curtailment levels, which entails a reduction in the emissions between 0.5-0.7 kg/MWh.

Sioshansi and Denholm [90] used a unit commitment model based on the one used by the ERCOT to simulate the power system operation with different EV penetration levels (from 1% to 15%). The authors found that, as the EV penetration increases, a strategy that controls directly the EV charging for minimizing operational costs achieves a reduction in nitrogen oxides (NOx) emissions during ozone season and a slightly increase in CO_2 and sulfur dioxide ($S0_2$) emissions. The load shift from less efficient to more efficient generation units results in this NOx decrease.
The use of V2G reduces the CO_2, NOx and SO_2 emissions. This reduction with V2G is mainly due to the provision of spinning reserves by the EV since they reduce the need to keep natural gas-fired plants online to provide this service.
Note that these simulations were conducted for year 2005 in Texas, with installed wind power around 2.4% of total capacity.

Schill [91] found out that for the German generation mix in 2009, EV integration would not increase the feed-in of wind power since the situations with wind power curtailment are occasional in this system. Furthermore, the additional load from EV will increase the utilization of low-cost and emission-intensive generation in Germany, such as lignite-based generation.
It is important to stress that the authors only conducted simulations in a two weeks period and assuming perfect forecasts for wind power. A larger period and the inclusion of forecast errors might have changed the conclusions.

As final a remark, the impact of EV in GHG emissions cannot be generalized for every power system since it depends on its specific characteristics, such as the mix of generation technologies or the amount of renewable-based generation surplus.

Impact on the Power System Dynamic Behavior

Lopes et al. [23] conducted dynamic simulations to assess potential benefits of the EV integration. The authors propose an electronic interface control based on droop control for primary frequency control in both emergency and islanding operation modes of microgrids[13]. The V2G mode and direct control are included.
The authors present the following main results:

- adapting the EV charging (i.e., battery charge and discharge rates) under frequency excursions is an efficient procedure in reducing the total required storage capacity in the microgrid;
- in a larger isolated system (e.g., an island), with the participation of EV in frequency control, the frequency drops only to 49.65 Hz (instead of 49.40 Hz in a scenario without EV in frequency control). This is achieved by reducing EV consumption from 401 kW to 141 kW during frequency drop.

The dynamic simulations were also extended and enhanced in [93], where in addition to primary control, the provision of secondary frequency control is also addressed. For the island of Flores (Azores), the author showed that the provision of frequency control from EV reduces the frequency oscillation band of the system, with a small effort for EV in terms of consumed energy and, under high penetration of wind power, the dynamic behavior is better than a scenario where EV are uncontrollable loads.

Regarding the possibility of participating in secondary frequency control, the results show that EV can improve the performance [i.e., higher reduction in the Area Control Error (ACE)] of this service in interconnected systems, allowing a reduction of the conventional reserves (i.e., EV is a reserve resource) and facilitating an increase in the RES-E penetration.

Impact on the Electricity Market

Schill [91] describes a complete market simulation algorithm based on the game theoretic Cournot model [94] to assess the impact (prices and social welfare) of one million of EV on the German electricity market.
Uncontrollable charging creates an evening peak in the electricity price because of the addi-

[13] A microgrid "comprises an LV distributed system with small modular generation technologies, storage devices and controllable loads, being operated connected to the main power network or islanded, in a controlled coordinated way" [92].

tional load, while controllable charging (direct control) increases slightly the off-peak prices compared to a baseline scenario without EV. When V2G mode is considered, the price difference is smoother when compared to controllable charging.

The authors also evaluated changes in producer profits (i.e., amount received by sellers minus cost to sellers) and consumer surplus (i.e., value to buyers minus amount paid by buyers). The uncontrollable charging increases the producer profits and decreases the consumer surplus. Controllable charging has the same effect, but with a much lower magnitude. When V2G is used for price arbitrage (i.e., take advantage of a price differences between hours), it produces a different effect since the price smoothing decreases producer profits and increases consumer surplus substantially (i.e., consumers benefit from lower peak prices). Note that the battery degradation costs were not included in these calculations. When degradation costs are included, the results with V2G are close to the case with controllable load.

2.4 Economic and Technical Issues of EV in the Electricity Market

2.4.1 Peak and Base Power

Kempton and Letendre [84] studied the economic value of three types of battery EV (differing in battery type, battery cost and potential output) as peak power resource, using V2G. The authors compared EV supplying peak power with an existing utility program [i.e., residential Direct Load Control (DLC)]. The EV solution offers the same investment cost but five times or more the peak support capability of the DLC program.

The authors also compute the annual cost to the EV owners from giving the utility access to their batteries and, the annual value of the EV peak power capacity to the utility. The results showed that peak power supply can be cost-effective for the utility as well as for the EV owner.

The approach described in [84] was used by Kempton and Kubo [95] to evaluate the economic potential of EV for the Kanto region of Japan. The authors concluded that a decline in battery costs, a small change in utility purchase rates, and changes in the regulation policy (e.g incentives for large-batteries) will make EV attractive to sell peak power in Japan.

Kempton et al. [96] computed the economic potential of having EV of different types (battery, fuel cell and plug-in hybrid) selling peak power in three years of the California's electricity market and the cost to the EV owner for providing the power.

The cost of electricity injected into the electrical network was estimated and found too high to be competitive for base load power, e.g. the Honda EV has a cost of $0.446/kWh while the

base load power price is around $0.1/kWh. The fuel cell EV shows the highest potential profit for selling peak power.

The authors computed the cost of providing power to the network and found that:

- in battery EV, the cost of battery degradation was more important than the cost of recharging electricity;
- in fuel cell EV, the cost of hydrogen fuel and the capital cost for additional V2G interface devices are the main factors;
- in plug-in hybrid EV, the V2G cost depends on the fuel cost and on the investment in V2G equipment.

In general, the results show that the peak power market, when compared to the ancillary services market, is less promising, since peak power price was never high enough. Similar conclusions were obtained by Kempton and Tomic [97], Williams and Kurani [98].

Peterson et al. [99] analyzed the net income that an EV owner gets from discharging the battery at high prices during peak hours for using at home and charging during low-price hours. The results for historical price data from Boston, Rochester and Philadelphia, and for a vehicle with a 16 kWh battery, suggest that the incentives are not sufficient to motivate this kind of practices by an EV owner. The maximum annual profit with perfect price forecasts and without battery degradation is between $142-249 in the three cities; with battery degradation included, the profit decreases to between $12-118 and in the case with naive price forecasts it is between $6-72.

In a companion paper, Peterson et al. [100] analyzed the battery degradation of a Li-ion battery cell. The statistical analysis shows that the battery capacity loss that results from using the EV battery in V2G mode is approximately half the capacity loss resulting from rapid cycling while driving. An important result was that several thousand driving/V2G days incur substantially less than 10% capacity loss regardless of the amount of V2G support used.

Hartmann and Ozdemir [88] conducted economic analysis about the revenue of EV participating in V2G mode in the European Energy Exchange market (Germany, EEX). The strategy consists in selling a share of stored electrical energy in the market. The following conclusions are relevant to understand the potential value of V2G compared to a diesel vehicle:

- an EV without V2G must drive at least around 10,000 km in one year to compensate the higher investment cost compared to a diesel vehicle. With V2G and a high battery cost (434 €/kWh) the yearly distance is above 45,000 km, while with low battery cost

(217 €/kWh) the yearly distance is above 20,000 km;

- the battery degradation has an important impact on the economic performance, in particular when a high share of battery is used for V2G, since it demands an early battery replacement. Moreover, if a share of the battery used for V2G is above 20%, the degradation costs also result in a higher cost per km for the EV. compared to a diesel vehicle. The inclusion of this cost might offset the revenue from the V2G.

2.4.2 Ancillary Services

According to Hawkins [101] and Andersson et al. [102], the following characteristics of EV make them attractive for ancillary services: fast response, distributed location, possibility of automatic regulation response and can provide downward reserve in a cost effective manner.

As weaknesses, the following characteristics were identified [102]: the capacity and period for supplying reserve is limited by the battery size and by the connection wires power; the uncertainty associated to the drivers behavior affects the reserve reliability; upward reserve with V2G has a high cost and implies energy losses in charging and discharging. As it will be discussed in section 2.4.4, an EV aggregator helps solving these weaknesses.

Kempton et al. [96] computed the economic value of EV with V2G for three years of the California's spinning and secondary reserve markets. In these two reserves, the EV is paid for dispatched (in $/MWh) and available (in $/MW) capacity prices.

According to the authors, for the capacity payment, the maximum power of the connection wires is an important limiting factor. This is also the limiting factor for the energy payment of secondary reserve, mainly because this reserve is only dispatched in periods between 4 seconds and 1 minute. In the spinning reserve, the limiting factor is the storage capacity since this reserve type can be dispatched for periods between 10 minutes and 1 hour and a low storage capacity decreases the ability of an EV to provide this service for several minutes continuously.

For the spinning reserve market, most of the EV analyzed by the authors could deliver this service with a positive net income. The battery EV can provide the service at an average net income from tens of dollars to $700, for the fuel cell EV it ranges between tens of dollars to $2000 and insensitive to fuel prices, while the hybrid EV in motor-generation can provide a net income around $2000.

For the secondary reserve, fuel cell and hybrid vehicles (in motor-generation mode) only provide upward regulation. The results show that battery EV is particularly promising for this

service, with a net income between $8442 and $3162 for the lead-acid battery. This is because the EV would be injecting and absorbing power under real-time commands from the system operator and over an extended period of time and the net total energy becomes approximately zero [26]. Therefore, battery EV could perform regulation function indefinitely with a much lower deep of discharge, with battery charging power fluctuating around its POP. This avoids capacity issues related to battery state-of-charge and promotes less battery degradation, thus decreasing the battery degradation cost. However, with V2G, the degradation and replacement costs of the battery are still the most important share in the service cost.

The fuel cell and hybrid EV did not provide a positive net income. Only in one year, a positive income was obtained; on average, the fuel cell EV with on-board hydrogen achieves a net income ranging from -$2984 to $811 while for the hybrid EV it is of -$759.

Kempton and Tomic [97] and Williams and Kurani [98] obtained similar conclusions.

Kempton et al. [103] tested a single battery EV with V2G operating under real-time dispatched by PJM. The test shows that the power response of the EV (dashed line) tracks the AGC signal (grey line) very closely, as depicted in Figure 2.5. The battery State of Charge (SoC), in black, varies between 60% and 70% in two hours (from 12h30 to 14h30) and, after 13h45, the SoC decreases because more upward secondary reserve was requested. The energy is stored and injected during the provision of secondary reserve.

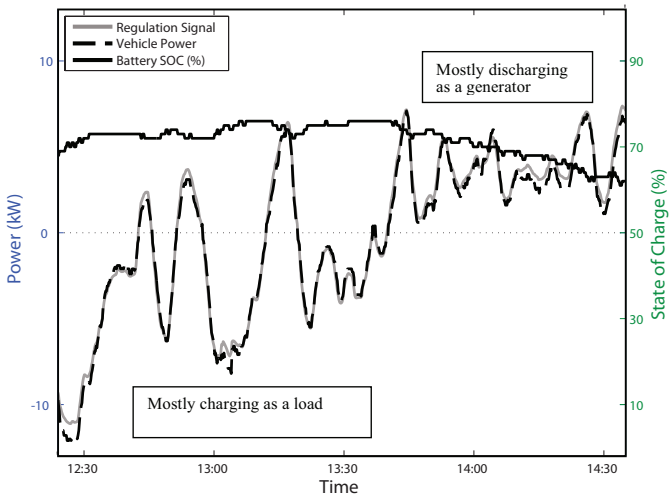

Figure 2.5: *A test on providing two hours of secondary reserve [103].*

2.4.3 Storage and RES-E

Kempton and Tomic [104] presented storage and backup power of EV as an important mechanism to accommodate high penetration of RES-E and handle forecast errors. The main conclusions from the authors are: storage from battery and hybrid in battery mode is more adequate for the most frequent and low electrical energy shortfalls of wind power, while the backup from fuel cell and hybrid in motor-generator mode is more adequate for less frequent and high shortfall of wind power.

Markel et al. [105] discussed several indirect control schemes based on grid communication of real time load, price and RES-E generation. One of these charging schemes consists in charging EV exclusively with RES-E at a fast rate when there is a high penetration of renewable energy and at a slow rate in periods with lower penetration. The authors show that EV can reduce the wind farm 10 minutes ramp rates by 5%, which means that smart charging can help reducing RES-E generation ramps.

Ekman [106] studied different EV charging strategies in order to estimate the effect of EV on the balance between generation and load under high penetration of wind power generation. A smart charging strategy leads to a reduction of the maximum excess wind power generation by 800 MW and improves the balance between wind power generation and load. The V2G mode will not reduce the need for additional power capacity but it can be important for balancing management.

Kiviluoma and Meibom [107] describe a model that optimizes long-term investments for switching from conventional generation to wind power by combining heat storages, wind power and EV. The authors concluded that dedicated electricity storage is not economically viable to accommodate wind power forecast errors, and the flexibility introduced by heat storage and EV with V2G could be more economical. The results show that the accepted increase in wind power was much larger with the heat storage measures than with plug-in EV; heat storage measures offer a larger flexibility while the EV are more limited.

2.4.4 EV Aggregation Agent

Concept and Role

The set of services that EV can provide were reviewed in the preceding sections from economic and technical viewpoints. However, the current market rules do not allow the participation of loads and generators with power capacity of few kilowatts [108]. Furthermore, it would

be very demanding to have a DSO or TSO directly controlling and receiving information from thousands of EV.

The solution suggested by different authors is an aggregation agent for EV. This concept was introduced in 2001 by Kempton et al. [96]. The aggregator serves as an intermediary between the vehicle owner, electrical utilities or the electricity market. The aim of the aggregator is to represent a large power capacity (at least 1 MW) that can be sold in the electricity market or by a contract established with an electrical utility.

A similar aggregation agent concept was introduced by Brooks [109]. According to the author, the interaction between the aggregator and the EV owners shall be performed considering the fundamental principle that the highest priority of an EV is transportation. Therefore, an operation where the drivers communicate their driving needs to the aggregator and the aggregator manages all this information is proposed. With all the driving profiles, the aggregator creates a "virtual power plant" where the number of vehicles expected to be plugged at any given time of the day is known, along with how much electrical energy is expected to be available in the battery and required for charging. The main advantage is that the total power and available electrical energy in each hour would be forecasted with less uncertainty in contrast with a single vehicle.

The similar aggregator concept is mentioned by Kempton and Tomic [97], Guille and Gross [110], and Quinn et al. [111].

Lopes et al. [23] described an architecture, depicted in Figure 2.6, where the EV is included in the MicroGrid (MG) and MultiMicroGrid (MMG) concepts. The authors describe a hierarchical control scheme: the Distribution Management System (DMS) communicates with a Central Autonomous Management Controller (CAMC) that is installed at MV/HV substation level and is responsible for managing a large amount of EV plugged with the network; CAMC controls under abnormal system operation (e.g., grid operating near its technical limits, islanded operation) the Clusters of Vehicle Controllers (CVC), which represent EV fleet charging and charging stations and communicates with the MicroGrid Central Controller (MGCC); the MGCC sends set-points to the corresponding Vehicle Controller (VC) (that is the charging/discharging process of batteries) under abnormal system operation, related to charging rates, adjustment of operation droops (for primary frequency control).
Under normal system operation, this hierarchical architecture encompasses an aggregator that acts as an intermediary between the EV owners and the electricity market. The aggregator is composed by two sub-entities with hierarchical dependence: Central Aggregation Unit (CAU) and the MicroGrid Aggregation Unit (MGAU). The CAU is physically connected to the MV/HV substations and the MGAU links the EV (through a VC) to the CAU. An aggregator may have several CAU and each CAU will communicate with several MGAU.

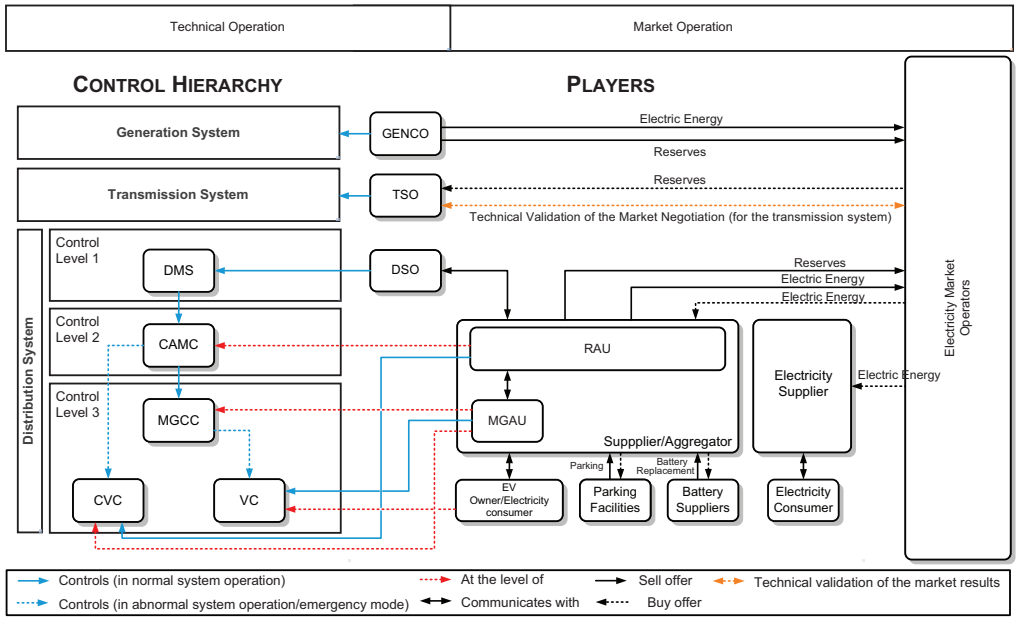

Figure 2.6: *Technical management and market operation framework for EV integration into electric power systems [23].*

In this framework, the DSO makes an *ex-ante* validation of the EV aggregator bids and during the operating day, the aggregator can respond to signals from the DSO under abnormal operating conditions or, in last resort, the DSO sends direct control signals to the EV.

Economic and Technical Issues

Brooks [109] evaluated the feasibility and practicality of having EV providing the secondary reserve. The test was performed in a Volkswagen Beetle converted to electric propulsion with an 18 kWh battery with V2G and dispatched remotely by wireless communication. An aggregator function with direct control was developed to serve as the intermediary between the system operator and multiple vehicles.
The economic value of this service beats the battery wear cost under almost all operating conditions. The cost of battery is between 20% and 60% of the annual potential revenue. Moreover, the battery capacity increased around 13% during the test, but according to the authors the only consistent conclusion is that no harm was done to the battery pack during the test.

Almeida et al. [112] modified the traditional AGC in order to make possible the EV response to changes in system frequency and schedule power flows in interconnection lines. The studies were conducted for an equivalent of the Portuguese power system, including interconnections with Spain. The scenario considers 1.5 million EV, corresponding to 30% of the entire Por-

tuguese light vehicles fleet. The EV were modeled as an aggregated controllable load that provides secondary reserve by reducing its load until reaching zero consumption; the V2G mode was not tested in this work.
For an off-peak scenario with high availability of hydro and wind resources, it was simulated a short-circuit which resulted in the loss of approximately 1100 MW of wind power generation. Under these conditions, the results show that the AGC response with EV participation is faster than with EV as non-controllable loads. Without EV, the total reserve levels considered in the study would be insufficient to recover the scheduled interconnection value, while this is possible with the additional reserve provided by the EV. Moreover, when EV participate in AGC, there is a faster reduction in the value of line loading after the disturbance and the ACE assumes values near zero after 10 minutes.

Tomic and Kempton [113] analyzed, in a period of four years of the New York ISO market, the net revenue of two real fleets (100 Th!nk City and 252 Toyota RAV4) with battery EV that provide secondary reserve. Upward and downward secondary reserve of the first fleet was found to be profitable in all years (with the exception of 2001), but the authors found that it was more lucrative for this fleet to provide only downward reserve (the EV operates just as a grid-controllable load). For the second fleet, the upward and downward reserve was found to be very lucrative in the New York ISO. Nevertheless, there is also profit if the aggregator supplies only downward reserve. According to the authors, when providing downward reserve, the battery SoC at the instant of starting to provide reserve limits this service.

The analysis was extended to three additional electricity markets: ERCOT, PJM, CAISO. The results show that the first fleet could provide secondary reserve with profit in these three markets (in the previous one the market value of ancillary services is lower), and the second fleet presents high profits in most of the markets. For these three markets, the authors also concluded that, although with lower profit, the provision of only downward reserve is interesting.

Quinn et al. [111] compared the situation with a direct communication between the TSO/ISO and the EV owner and, the situation with an intermediate communication between an aggregator and the TSO/ISO. The results show that the reserve power in the direct architecture is less available during large portions of the day, while the aggregator availability is almost 100%. The direct architecture is less reliable (measured with the forced derated hours ratio) than the aggregator, mainly because the direct scheme relies totally on the uncontrolled behavior of EV owners. The aggregator scheme can control the reliability through the contracted fleet size, the contract power, or both.

These authors, in addition to analyzing the viewpoint of the system operator, consider the angle of EV drivers measured by the robustness of the return on their investment in hardware

and vehicles. Both architectures have positive net present value with profits of $7643-7943 for the direct communication and $3268-3568 for the aggregator. The results show that the aggregator architecture limits the amount of initial investment that an EV driver can payback and also the gross profit (but still with a positive net present value) and, therefore, from the EV driver viewpoint, the direct architecture is more attractive.

Some assumptions in the paper can explain the economic difference between the two architectures. First, the EV, in the direct communication architecture, is always paid for being available (capacity payment) and it is always dispatched (energy payment); in reality, however, in some hours, the EV may not be assigned to provide the service nor dispatched. Second, it is assumed that the aggregator increases the fleet size in order to guarantee a reliability standard and this limits the profit obtained by the particular EV, when compared with a single EV without this requirement.

Andersson et al. [102] simulated the behavior of 500 individual plug-in hybrids with V2G as providers in the primary, secondary and tertiary reserves of Germany and Sweden. The results for both countries showed the following:

- none of the Swedish reserve markets are profitable. In Germany, it is possible to generate profit on all three reserve markets (30-80 € per EV and month) because the available and dispatched reserve capacity prices are higher than in Sweden (where reserve power is delivered by hydropower plants);
- the German secondary reserve market is the most attractive because of its high capacity payments and the EV were often activated for downward reserve (which means cheap charging). A comparison between the profit from selling upward and downward reserve, showed that downward regulation will always be interesting because it means charging at a lower cost. Conversely, upward reserve is financially more "risky" because the battery degradation cost is the main factor that affects the results.

Schill [91] using a market simulation tool evaluated the participation of an EV aggregator in the German electricity market, considering V2G and direct control. The aggregator is either a price-taker or an agent with strategic bidding (i.e., forecasts the market reactions to its bids). The results show that if battery degradation costs are considered, the interest of using V2G for price arbitrage decreases. For instance, for 10 €/MWh of degradation cost, only half of the battery is used for arbitrage, while above 50 €/MWh the battery storage capacity is not used. This is more critical for an aggregator with strategic bidding since, in order to mitigate the price smoothing effect, it utilizes less storage capacity than a price-taker.

Dallinger et al. [114] investigate the impacts of driving behavior of a battery EV fleet on the

value of V2G for secondary reserve. A *dynamic* approach for analyzing the impact of mobility stochastic behavior (with Monte Carlo simulation) is compared with a *static* approach (with average daily values as in Kempton et al. [96] and Kempton and Tomic [97]). The *dynamic* approach presented a 40% reduction in the available power for reserve compared to the *static* approach. This shows that it is absolutely indispensable to consider the dynamic behavior of EV, otherwise the economic results may be misleading. The authors also showed that a large EV fleet could compensate the stochastic behavior of the individual drivers.

From the economic analysis with both *static* and *dynamic* approaches, the authors concluded that downward secondary control is the most profitable service for an aggregator in the German electricity market for the year 2008.

2.4.5 Business Models for the Aggregator

This section reviews business models for an EV aggregator with direct control over the EV charging process, including V2G in some cases. Note that if all the EV are uncontrollable loads, the aggregator is a typical electricity retailer that is responsible for buying electrical energy in the market, to satisfy the consumption requirements of its clients.

Different Prospects for the Aggregator Model

Kempton and Tomic [104] described three different business models for the aggregator and EV with V2G.

In the first model, the aggregator manages time availability of the fleet used for transportation and sells services directly to the system operator or to the electricity market. The fleet is parked in a single location and connected to a single network point, e.g. corporation's fleet.

The second model consists in using power from dispersed vehicles but with a business partnership with an electricity retailer company. In this case, the aggregator buys electrical energy from hundreds or thousands of vehicles with V2G and sells services in the electricity market. The aggregator does not have any control over the individual vehicles, but can provide financial incentives so that they stay plugged-in when possible.

In the third model, instead of an electricity retailing company, the aggregator could be a company from a different business area. The aggregator could be a battery manufacturer that offers free replacement batteries in exchange for some of the profit from selling energy to the grid, or a cell phone network that may provide communications functions and other services

similar to the ones used for cell phones, or an Energy Service Company (ESCO).

For Brooks [109], the aggregator communicates and makes transactions directly with the grid operator and then shares the value created with the connected vehicles. The commercial interaction with the vehicles' owners can be done through direct payments, subsidized leases, or ownership and/or warranty of the vehicle battery pack by the aggregator.

Gomez et al. [115] propose different business models and discuss regulatory issues for residential, public (in the streets) and private charging (e.g., fast-charging stations) points:

- *residential charging*: (a) a classical electricity retailer supplies the electricity, with time-of-use tariffs, for EV charging, which can be billed separated from domestic electricity consumption; (b) an aggregator buys energy from a retailer or participates in the market, sells this energy to EV drivers and optimizes charging power and period in order to maximize its profit;

- *public street charging*: an aggregator is responsible for buying and selling electricity for EV charging and pays a regulated fee for using the charging infrastructure owned by the DSO;

- *private charging point*: a Charging Point Manager (CPM) owns the charging infrastructure, buys electricity from a retailer (or aggregator) and provides charging services to EV drivers, or, in alternative, the CPM can participate directly in the market.

The authors suggest that the EV owners could have a supply contract with the aggregator, which would be valid in different charging points. This means a separation of the retailing activity from the ownership of the charging stations.

Battery-centered Business Models

Kempton et al. [96] describe a business model where the aggregator provides free replacement batteries and possible free charging or cheap charging, in exchange for being able to use the vehicle stored energy. The advantage of this model is that the aggregator is the only entity responsible for technically managing the batteries (e.g. deep of discharge, cycling) and for the replacement.

Guille and Gross [110] described a business model called "package deal", to attract and preserve EV owners with proper incentives. Figure 2.7 presents an overview of this proposed business model. The aggregator will interact with the ISO/RTO, Energy Service Providers (ESP), battery suppliers and parking facilities. The dotted/dashed arrows represent money

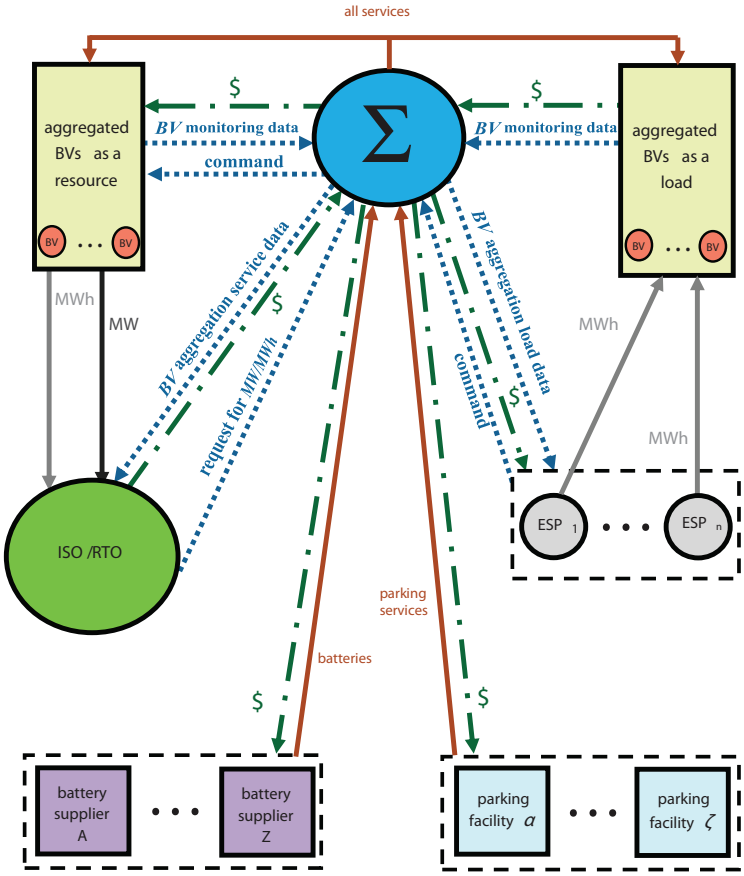

Figure 2.7: *"Package deal" business model [110].*

flows, the dotted arrows are the communication flows, the full lines connected to the aggregator represent the extra services provided by the aggregator to EV and the full lines marked with MWh and MW are energy related services.

The aggregator provides preferential rates for the acquisition of batteries (or additional battery warranty), maintenance and discount rates for charging the EV. In exchange, the EV owner is constrained to plug the vehicle at the times determined in the contract. The incentive for long-term contracts is higher than for short-term commitments. If an EV owner fails to meet the contract, it is penalized by losing all discounts and/or battery maintenance, or, in the limit, the contract is canceled. Rewards are also considered for "well behaved" EV owners.
The aggregator can use its large purchase power to negotiate better prices and conditions (e.g., extended warranty) with battery manufacturers and parking lot owners and offer these services as part of the "package deal". This model is appealing for an EV owner because it offers lower charging rates and the owner is no longer concerned about battery degradation. This will decrease the investment and operational costs of the EV with V2G.

"Real-world" Examples

Presently, business models for EV are being implemented in several countries. Andersen et al. [116] analyze the business model of Better Place, which is investing in several countries such as Denmark, Israel and the USA. The core business consists in creating an Electric Recharge Grid Operator (ERGO), which has the following basic elements: charging points grid with a smart-metering infrastructure that communicates with its users and manages the charging process of each vehicle; partnership with vehicle, batteries and hardware manufacturers; separation of battery ownership from car ownership by offering several kinds of leasing deals for batteries or even for vehicles. In addition to charging points, battery replacement stations for trips above 160 km are also considered.

The idea is to operate the battery leasing as a cell phone communication business. The EV owner pays for the energy he uses to travel kilometers, in analogy to the payment per minute in communications. Different leasing schemes can be arranged for the batteries, e.g. paying for using the battery during a predefined number of kilometers. This model does not explore the V2G concept.

In Portugal, the industrial and scientific network MOBI.E[14] is implementing a charging network accessible to all users. Each user has a card that provides access to the charging points and may liberally select a retailer for electrical mobility. In this model, the aggregator is a typical electricity retailer and the EV are uncontrollable loads. This retailer was also included in the Portuguese legislation for the EV sector [117]. A similar retailer is also envisioned in the Spanish legislation [118].

More advanced aggregators, able to sell services to the grid (with V2G, for example) are also emerging as start-up companies from universities. One example is Nuvve[15], a spin-off company from the University of Delaware, that is proprietor of different patents such as "Aggregation server for grid-integrated vehicles" [119] and "Electric vehicle equipment for grid-integrated vehicles" [120]. The company provides a complete V2G solution that includes hardware and software, aiming at aggregating EV and participating in ancillary services markets.

Detailed information about its business model and participation in the electricity market is not available. The only detail about their model is that they are giving an incentive to EV owners to plug-in as often as possible. This company is also expanding its business to Denmark[16].

[14] www.mobie.pt (accessed in November 2012)
[15] www.nuvve.com (accessed in November 2012)
[16] http://green.autoblog.com/2011/06/27/denmark-to-test-nuvve-vehicle-to-grid-technology/ (Nov. 2012)

Another company is Fleet Energy Company [121], a spin-off from Burt Fleet Services. This company is an aggregator and project developer for electrification of medium and heavy-duty fleet vehicles to be used in ancillary services.

2.4.6 EV and Market Rules

In order to accommodate EV (as flexible loads) some changes in the current electricity market rules are necessary. Andersson et al. [102] compared the current and ideal market design in Germany and Sweden to accommodate EV. The conclusions were the following:

- electricity markets with prices for available and dispatched reserve capacity are desired. For an EV, it is appealing to have a payment for being ready to provide downward secondary reserve and then charge at a cheap price;
- the period in the contract for supplying reserve should be short (e.g., 30 minutes, one hour);
- in order to avoid high forecast errors, EV need a short time-period (e.g., one hour) between gate closure and operating hour in the different market sessions;
- it is necessary to reduce the minimum bid size to values lower than 1 MW.

Hay et al. [122] discussed the introduction of EV in the NordPool regulating power market and concluded that changes are needed in the current market rules. Firstly, real-time measurements are required, which can be costly to fulfill in a fleet with thousands of EV. Secondly, the minimum bid is 10 MW which avoids individual participation of EV and requires the aggregation of thousands of EV to meet this value.

Søndergren et al. [69] discussed a set of possible modifications in the electricity market for possible branch's overload in the distribution network:

- LMP for the distribution network. This means joint market-clearing of demand and generation bids and network constraints management. However, including the distribution network in this process might be prohibitive;
- market for grid capacity where the DSO is the seller, operating in parallel with the energy market. This can take place after the day-ahead energy market. This solution might also suffer from the same problems of the previous point;
- local adjustment markets in the distribution network to solve congestions. This solution might suffer from low market liquidity or market agents with market power;

- prior to the energy market, the DSO publishes network capacity limitations to all agents, and the energy trading is performed within these constraints;

- the DSO imposes, for the following day, a grid tariff (called dynamic tariff) for each time interval and node, and the agents bid into the market taking into account the tariff value (total price = energy price + dynamic tariff). In areas with congestions, the EV will get an incentive for not consuming in that interval. Nevertheless, it might be difficult to set a price sufficiently high to avoid congestion situations and, during the operating day, the network conditions may change and additional congestions could occur.

Some of these solutions (in particular the first three) require significant changes of the current electricity market, while the last three only require minor changes.

2.4.7 Summary and Remarks

Table 2.1 summarizes the type of vehicles that are more suitable for each market session. This shows that some EV types are more suitable (both in technical and economic terms) for some market services: fuel cell EV showed the highest potential for selling peak power, battery EV presented a higher potential for the secondary reserve market, battery and hybrid EV are also attractive for the spinning reserve market. Fuel cell can only provide upward secondary reserve due to technical limitations.

The analyses of Table 2.1 were conducted from a single vehicle perspective. The introduction of an aggregation agent might change some of these conclusions. For instance, an aggregator can solve the limitation of the storage capacity in battery EV and overcome the main drawback to provide peak power.
Nevertheless, even with an aggregator, the market prices play an important role in the economic value. For instance, peak power is only profitable to an aggregator if the price difference between peak and off-peak hours offsets the battery degradation costs.

Table 2.1: *Economic value of different types of EV in the electricity market (inspired by [123]). ++: very suitable; +: suitable; (blank) not suitable; (*) limited by storage*

	Electricity Market Opportunities (Sell Bids)		
EV Type	Peak Power	Spinning Reserve	Secondary Reserve
Battery	(*)	++	++
Plug-in Hybrid	(*)	++	+
Fuel Cells	+		

The reserve services can be supplied with V2G or by defining a POP (i.e., no bidirectional power injection). The POP approach entails several advantages over V2G: it does not require additional capital costs with V2G equipment; it reduces the costs with battery degradation; it implies lower losses in the charger and battery. Note that in the long-term, V2G could be more profitable than this approach. However, the present high battery cost and the uncertainty around the impact of battery degradation cost make V2G only attractive for driving distances above 45,000 km per year and price arbitrage between peak and off-peak hours is not economically attractive. Moreover, the provision of reserve services with V2G is highly dependent on the market prices (available and dispatched reserve capacity price) and battery degradation costs.
Socio-technical aspects, such as costumer acceptance, historical aversion to technology and stakeholders influence, can create barriers in a transition to V2G [124]. Another psychological barrier is that EV owners might not feel comfortable in having a third-party extracting power from their batteries. Furthermore, there are legal and regulatory impediments to V2G, such as warranty problems related to increased battery wear caused by repeated cycling [125].

The main disadvantage of the POP approach is that it does not use the full potential of EV battery and provides less reserve capacity than a V2G approach. For instance, the upward reserve capacity is limited by the flexibility of each EV in postponing its charging, and the downward reserve capacity is limited by the initial state-of-charge (SoC) of the battery. Nevertheless, providing only downward reserve is economically attractive since it means cheap charging.
Although there are already business models for aggregators exploring V2G, it seems that the POP approach will be the first step for an active participation of EV in ancillary services markets and then a full transition to V2G is expected when economic and technical issues are resolved.

Finally, the economic calculations reviewed in this section ignore the fact that it is necessary to forecast the EV consumption and the market prices. Forecast errors in the EV consumption could be translated into financial penalizations because of the deviations between bids and actual values and forecast errors in the market prices could be translated into opportunity losses (e.g., missing an hour for selling power at a high price). Therefore, in future developments it is necessary to include this information in long-term economic analysis, similarly to what was done in [126] for sizing different storage technologies under wind power uncertainty.

2.5 Smart Grid and Standardization

The International Electrotechnical Commission (IEC) standard 61851-1 defines four different charging modes [127]:

- mode 1: “connection of the EV to the Alternate Current (AC) supply network utilizing standardized socket-outlets at the supply side, single-phase or three-phase, and utilizing phase(s), neutral and protective earth conductors”;

- mode 2: “connection of the EV to the AC supply network utilizing standardized socket-outlets, single-phase or three-phase, and utilizing phase(s), neutral, and protective earth conductors together with a control pilot conductor between the EV and the plug or in-cable control box”;

- mode 3: “direct connection of the EV to the AC supply network utilizing dedicated EV supply equipment where the control pilot conductor extends to equipment permanently connected to the AC supply”;

- mode 4: “the indirect connection of the EV to the AC supply network utilizing an off-board charger where the control pilot conductor extends to equipment permanently connected to the AC supply”.

The active load management option is only feasible in charge mode 3 [128], and it requires an Electric Vehicle Supply Equipment (EVSE)[17]. Several associations, such as EURELECTRIC and ORGALIME, recommend shifting over time to mode 3, since it is the preferred solution in all types of locations and allows charge management within the Smart Grid context [130][131]. Manufacturers of charging equipment are also adopting this charging mode [132][133]. Modes 1 and 2 are considered to be transitional solutions.

Standardization is also being conducted for chargers and associated cables, normally divided into three/four charging levels. Bending et al. [134] presented the following categorization:

- *single-phase AC charging*: normally used for household charging and provides low power levels compared to the battery capacity. This is normally called level 1 charging and the typical power is around 3 kW (it takes 12 hours to charge a 35 kWh battery). Furthermore, in dedicated charging installations, it is also possible to find higher power levels for this charging type. This refers to level 2 charging with a typical power around 10-20 kW (it takes 2-4 hours to charge a 35 kWh battery);

- *three-phase AC charging*: requires access to a three-phase power supply and can provide higher charging power levels than single-phase charging. This could be used in level

[17] The EVSE is divided into three components: *supply device* that supplies electrical power and provides shock protection (located on-board for normal charging); *power cord*, which is a cable that carries electrical current and communications signals from the *supply* to the *connector*; *connector*, which connects the EVSE to the charging sockets on the EV [129].

3 charging (or fast charging) with charge power around 40 kW (it takes less than 45 minutes to charge a 35 kWh battery);

- *Direct Current (DC) charging*: requires a dedicated off-board charger and can also be used in fast charging stations (level 3).

The number of standards for the EVSE that allow these levels is large and varies from region to region [134]. For example, Society of Automotive Engineers (SAE) J1772 allows two charging levels, one of 1.9 kW (level 1) and another one of 19 kW (level 2); the Mennekes solution offers charging power ranging between 3 kW and 43 kW. Note that these standards and charging levels define the maximum EV charging rate.

Tuttle and Baldick [135] divided the EV technology development into four generations:

- *first generation*: the majority of the EV only includes unidirectional power flow and an on-board interface to define the charging window;

- *second generation*: the communications of the EV will be enhanced with Power Line Communication (PLC) capability between EV and EVSE, ZigBee™ wireless communication protocol between smart meter and EVSE and also a cell phone network or wireless communications between the EV and Home Area Network (HAN)[18]. This enhanced communication infrastructure will allow the interaction with aggregators through price or direct control signals, as well as the participation in the ancillary services market. More than three to four years are necessary to create this generation;

- *third generation*: the V2G mode is included in the EV. Nevertheless, it is only used in three applications: supply power to an isolated load; backup generator in a household; support a larger isolated facility (e.g., mobile hospital). In this first approach to V2G, there is a very little interaction with the network. The timeframe for this technology is five years after EV manufacturers conducted detailed tests about battery durability and costs;

- *fourth generation*: full interaction of EV with V2G and the network, and participation in the electricity market. This scenario is likely to take more than eight to ten years.

Communications technologies are the backbone of the Smart Grid and EV charging infrastructure. There is a large set of wireless communication protocols for implementing bidirectional communications, such as HomePlug™, ZigBee™ and cellular network [136]. These tech-

[18] Communication infrastructure, implemented in the costumer domain, which deals with the flow between EV and smart meters.

nologies are not yet proven to work for EV applications and there is a lack of industry-wide codes and standards for EV-network interaction.

According to Gungor et al. [137], two communication infrastructures can be distinguished: HAN and Field Area Network (FAN), being the later the communication infrastructure of the power system network (i.e., between the smart meter and the network control center). It is suggested that for the HAN, PLC and wireless communications (e.g., ZigBee^{TM}, 6LowPAN, Z-wave) can be used, while for FAN the recommendation is cellular and internet-based communication.

The joint work of the International Organization for Standardization and IEC for standardization of the EV communication interface was focused on the communication interface between EV and EVSE, in particular the message structure and patterns defined in the ISO/IEC 15118 standard and on the standard IEC 61850 for enabling a homogeneous interaction between EV and the aggregator [138].

These standards are also being tested in the EDISON project [139]. Figure 2.8 depicts the aggregator framework of the project and corresponding standards. The standard IEC 61850 supplies the necessary components to describe and send relevant data between EVSE and aggregator, while standard IEC 61851 is for the physical connection and charging of an EV. Another possibility is the ISO/IEC 15118, which deals with both physical interconnection and high-level communication protocol.

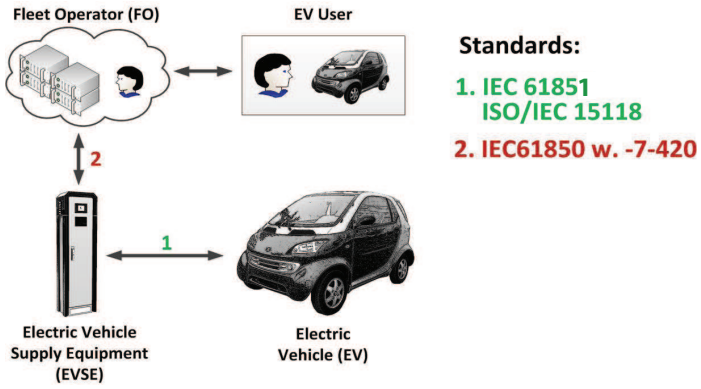

Figure 2.8: *Standards used in the EDISON project [139].*

A large set of standards have already been developed for the EV charging infrastructure [136]. For example, the SAE J2293 establishes the requirements for EV and the off-board EVSE, the SAE J2847 provides requirements and specifications on the necessary communication between EV and the network, SAE J2894 defines recommendations for power quality in the charging equipment.

2.6 Algorithms for Supporting the EV Aggregator Business

Several authors developed algorithms for optimizing EV charging, but their objective function was exclusively oriented to reduce distribution network losses or voltage deviations [140][141]. This type of formulation does not embrace the participation in the electricity market nor any cost minimization of the EV charging.

Under the current regulatory framework and without incentives for minimizing losses and voltage deviations, the main goal of an aggregator is to minimize the costs with EV charging by using optimization and forecasting techniques. Therefore, this section only reviews algorithms developed for meeting this goal. Two types of optimization algorithms are reviewed: 1) algorithms that do not include network constraints in their formulation; 2) algorithms that include these constraints together with a cost/profit minimization/maximization.

2.6.1 Optimization Algorithms without Network Constraints

Participation in the Electrical Energy Market

Kristoffersen et al. [142] developed a model to define the optimal charging plan of an EV aggregator participating in the NordPool day-ahead energy market. The objective function is the minimization of the total cost (fuel, electricity and battery wear). The strategy consists in charging at a lower price while limiting fuel consumption and in selling power, if profitable, using V2G. The problem is limited by several constraints, such as the electrical energy balance of the battery and technical limitations of the battery. The k-means clustering algorithm was used to assign a driving pattern to each EV.

The model is deterministic and assumes perfect forecast for all the variables involved in the problem. The results show that the optimal strategy charges the EV mostly during the night, when prices are lower. However, when the penetration of EV increases, prices during the night also increase, which decreases the incentive to store and sell electrical energy (i.e., difference between peak and off-peak prices). When EV penetration grows, the economic opportunity to sell electrical energy decreases.

Bashash et al. [143] present a multi-objective formulation for optimizing the charging of a hybrid EV fleet, and extends a method previously published [144] for a single hybrid EV. The objective functions are the minimization of the total cost (fuel and electricity prices) and battery degradation for each driving cycle. Battery degradation is evaluated using an electrochemistry-based model that simulates Solid Electrolyte Interphase (SEI) growth, which

is responsible for battery health degradation during energy storage and cycling. Both objective functions are conflicting because, according to the authors, a high SoC (in particular when subjected to a high charging rate) corresponds to a high SEI growth and, conversely, a high SoC, prior to departure, reduces the total cost since electricity is cheaper than fuel.

The multi-objective problem is solved with NSGA-II [145] and the result is a Pareto front. The preferred solution is determined with a trade-off analysis. The results for an aggregator (decision-maker) that gives more importance to the total cost compared to another decision-maker showed that the EV charge more electricity from the grid. The authors also concluded that the possibility of charging at work reduces the average energy cost between 1% and 19% and does not significantly affect battery degradation. This happens because charging at work allows the EV to reduce the amount of electricity charged at home before the first trip, which reduces battery degradation.

Sánchez-Martin et al. [146] describe an optimization problem for an aggregator with direct control over EV charging in parking areas and participating in the energy market. The objective function minimizes the cost of charging EV. Three EV operating modes are considered: controllable load (i.e., shifting charging to cheap hours), V2G and Vehicle-to-Vehicle (V2V), which consists in exchanges between EV interconnected in the same parking area. The problem is solved with mixed integer linear programming since binary variables are used to indicate whether the EV is charging or discharging. The authors consider the possibility of EV departing without being completed charged because of constraints in the network and a penalization term is included in the objective function to minimize this situation.
Furthermore, the model also includes the negative impact of the depth of discharge limit in battery lifecycle. A constraint is included for not allowing discharging a battery when its SoC is lower than a specific value (set to 70% in the paper).

The results for a fleet with 50 EV (80% hybrid and 20% full electric) show that the use of V2G and V2V is much lower compared to the EV charging in cheap prices hours. Thus, the cost reduction is mainly because charging takes place during cheap hours. Compared to an uncontrolled charging strategy, the proposed algorithm achieves a cost reduction of 38.5%. Sensitivity analysis, modifying the depth of discharge level, increases the V2G and V2V use, but with the current battery technology this is prohibitive.

Sundstrom and Binding [147] addressed the problem of optimizing EV charging in the presence of forecast errors. The authors identified two variables that are essential for the optimization process and which can be forecasted or transmitted by the driver for the next day: minimum energy needed to drive during the next trip; time of departure of the next trip. It is assumed that this information could be inaccurate and that the aggregator must be conservative in the charging (i.e., buy more energy in order to avoid not satisfying the minimum

energy needed). A service margin approach is proposed, where the forecasted minimum energy needed is incremented and the time of departure of the next trip is anticipated, both according to a safety margin. These safety margins are included in a linear optimization problem. The authors do not present results of the methodology.

The following limitations can be identified in the method:

- the use of safety margins might not be the minimum cost solution since, to avoid energy shortage, the aggregator could pay a high penalization cost associated to energy surplus;
- this method deals with the forecast error associated to each EV and does not take advantage of coordinating EV charging to decrease forecast errors;
- it is also necessary to forecast the arrival time instant, which requires the adoption of a safety margin. The introduction of this third variable can increase the complexity when computing the safety margins.

Participation in the Energy and Secondary Reserve Market

Most of the approaches reviewed in this section use the V2G mode for selling secondary (or regulation) reserve in the electricity market.

Rotering and Ilic [148] describe an optimization model for an optimal controller that can be installed in an EV. Two algorithms based on classical dynamic programming are proposed. The first optimizes the charging rates and periods for minimizing the cost. The second aims to generate profits from selling secondary reserve using V2G in the secondary reserve market. Constraints caused by vehicle utilization and technical limitations are included in the algorithms, which use as input the following information: forecast of the market price, maximum available power for regulation up and down, and power required for the next driving cycle. Both algorithms assume perfect forecasts for the input reserve and EV variables.

Han et al. [149] propose a dynamic programming for selling secondary reserve with V2G in the electricity market. The authors identified three control variables for the aggregator: charging sequence, duration and rate. However, if the EV driver defines a single point for the target SoC (and not a range), the problem of calculating the charging duration is solved. Moreover, a proof is provided saying that the charging control should be on or off at the maximum charging rate to maximize the revenue. Therefore, the dynamic programming problem determines the charging sequence (i.e., time intervals when EV charges at maximum power).

Perfect forecasts are assumed for all the input variables. Furthermore, it is assumed that the EV, under dispatch via AGC, would be injecting and absorbing power and the net total energy becomes approximately zero after short periods of time. This assumption cannot be generalized to all the power systems since the traditional AGC signal can request secondary reserve in one direction during a long period of time and the net total energy is different from zero in each market time interval [150].

Escudero-Garzas et al. [151] describe a set of optimization algorithms for a fair allocation of power for secondary reserve (with V2G) among the EV, controlled by an aggregator that participates with bids in the electricity market. A fair allocation is focused on avoiding situations such as having EV with low SoC supplying upward secondary reserve and reaching the minimum level, or EV with high SoC supplying downward reserve and reaching the maximum level. The following optimization algorithms are proposed:

- *state-dependent utility*: allocates power to EV, according to their available battery (i.e., power is proportionally allocated according to the previous SoC);
- *charging dynamics optimization*: maximizes the difference between the SoC at present time and the SoC at the previous regulation period;
- *water-filling algorithm*: explores similarities between this problem and the power allocation problem for parallel channels in communications [152];
- *variance minimization*: minimizes the SoC variance with respect to the mean SoC of the EV.

These four algorithms maximize the aggregator profit, but also seek a fair allocation of the reserve among the EV fleet. The results for the New York ISO market and for a fleet with 1500 EV showed that the *water-filling* approach almost achieves perfect fairness and the *variance minimization* method also presents an interesting performance. The *state-dependent utility* approach provides the lowest variance of profit per vehicle and the *charging dynamics optimization* achieves the highest profit at a reasonable performance in fairness.

The main limitation of this algorithm is that perfect forecasts are assumed for the price and EV variables.

Sortomme and El-Sharkawi [153] explore the use of a POP for selling secondary reserve in the market. The authors describe and compare two types of methods for selecting the initial POP: heuristic and optimization algorithms. The heuristic algorithms are the price-based and load-based algorithms described in [105] and a third one is based on the maximum regulation participation. These three algorithms set the initial POP and three additional constraints

define the final POP and regulation up and down capacities. According to the authors, these three charging strategies lead to suboptimal solutions. Hence, optimal analogues for the three heuristic strategies are described. The load-based charging includes an additional constraint preventing excessive load during peak hours. However, this constraint does not avoid congestion and voltage violations in the distribution network.

Results for a fleet of 10,000 EV show that the maximum regulation algorithm guarantees the maximum profit to the aggregator.

In this work, the possibility of coordinating the EV charging for internally balancing the forecast errors is not considered. In fact, the authors use perfect forecasts for all the input variables. It is important to stress that forecast errors in these variables could lead to situations with reserve shortage.

In [154], the same authors enhanced these algorithms to include bids simultaneously to the secondary and spinning reserve markets. The process of dispatching the EV for both reserves is sequential. First, the aggregator optimizes the secondary reserve bids and, then, the resulting power is used to calculate the spinning reserve bid.

Compared to the previous methods from the authors, two additional modifications are introduced:

- the optimization problem considers the complete day and a binary variable indicating if the EV is plugged-in or not is used to control the maximum charging power. Note that perfect forecast is used for this variable;
- the formulation takes into account unplanned departures by EV owners and includes a constraint based on the probability of departure for compensating this loss of capacity; this constraint "forces" the aggregator to under schedule capacity and then over dispatch when the EV departs.

The same authors, in [155], propose a linear optimization algorithm for optimizing the bids (i.e., maximize aggregator's profit) in the energy, secondary and spinning reserve markets, including the possibility of V2G. The income comes from selling energy, secondary and spinning reserve and costs are considered for battery degradation and purchasing energy. The dispatch for upward secondary or spinning reserve can be a reduction in the POP, or an increase in the discharging power, or a combination of both. The same is valid for the downward reserve. As in the previous paper, the process of dispatching secondary and spinning reserve is sequential, but considering the capability of discharging energy.

This formulation also takes into account unplanned departures by EV owners. However, vari-

ables such as the arrival time instant, the energy required for charging EV and the percentage of used reserve power are assumed to be known. Therefore, even with this constraint, this method suffers from the limitations of the authors' former methods. The role of forecasting errors might be more critical in this method because situations where the aggregator supplies secondary reserve at the expense of the spinning reserve can occur.

In [154], a comparison is presented between the algorithm that optimizes the energy and secondary reserve bids using the POP approach (described in [153]) and the algorithm that uses V2G. The results for ERCOT and for a fleet of 10,000 EV showed the following: the use of V2G achieves a higher profit for different battery degradation costs, mainly because only with POP there is no income from selling energy and V2G provides more reserve capacity to the system (i.e., more income from available reserve capacity); the average price of electricity for the EV owners is 0.01$/kWh with V2G and 0.025$/kWh with POP. Note that the results do not include any investment in hardware for V2G or forecast errors impact.

Wu et al. [156] propose a game-theoretic model to supply secondary reserve with a decentralized control of EV with V2G. In this framework, a software agent that represents the interests of the EV owner is installed in each EV and chooses if the EV charges, discharges or remains in standby for maximizing its own payoff function.

An aggregator is responsible for setting a pricing policy (i.e., indicating how much it pays for EV participation) that promotes the EV participation in the secondary reserve market. The aggregator might not be able to supply the full reserve quantity contracted by the TSO/ISO since some EV may not enroll with the service. Thus, it is assumed that the aggregator has a backup battery bank in its portfolio.

The benchmark case is a centralized approach where the aggregator minimizes the use of battery bank. The goal of the decentralized control is to reach a Nash equilibrium[19] such that it is the optimal solution of the centralized control.

The results show that the proposed decentralized algorithm achieves a performance comparable to a centralized algorithm and the battery bank is almost unused. The main limitations of this algorithm are:

- the authors do not consider the fact that the aggregator needs to inform the TSO/ISO of how much regulation capacity is available for the next day and this introduces forecast errors that affect the reserve reliability and would require an intensive use of the battery bank;

[19] "Is a vector of all players' strategies such that no player has an incentive to deviate unilaterally."

- the Nash equilibrium is defined for each hour independently and this might affect the multi-period performance of the method. The authors give the following example: in one particular time interval, the optimal solution consists in having five out of ten EV discharging their batteries, but since the problem is solved only for one time interval it does not matter which five EV discharge. However, different selections of the five EV may affect the performance in subsequent time intervals.

Han et al. [157] address the problem where an EV aggregator makes a contract with a TSO/ISO for providing secondary reserve using V2G mode. The aggregator should specify explicitly in the contract the amount of contracted power capacity (CPC) prior to delivering this service (this is also valid for secondary reserve market bids). The authors present a probabilistic model for modeling the achievable power capacity (APC) of an EV aggregator and for providing the CPC that gives the maximum profit. The EV are clustered into different groups characterized by their plug-in probability and power capacity. For each group, the APC probability is derived from a binomial distribution, which is then approximated by a Gaussian distribution. The total APC is computed by summing the Gaussian distributions of each group. Based on the probability distribution of the APC, profit functions (representing the aggregator's revenue) for four different financial penalization schemes are derived.

The main limitation of the method is that the calculated APC may be very optimistic because of two reasons. First, the clustering approach is an approximation and EV may change from one cluster to another as the hour changes (i.e., power capacity changes with the hour). Second, the APC is dynamic and proportional to the charging strategy of each EV. Therefore, it must be updated as the charging of each EV evolves (as discussed by Dallinger et al. [114]). This makes the method only suitable for markets where the aggregator can update its bids in the short-term (e.g., hourly updates).

Pantos [158] describes a stochastic linear optimization problem for computing bids for the energy and secondary reserve market using the V2G mode. The model takes as input probabilistic information from several variables:

- a clustering technique is applied to historical driving behavior (i.e., energy needs for driving). The driving patterns are considered as stochastic scenarios and the fleets as a scenario subset from the clustering technique. In case of new EV without historical data, a Monte Carlo simulation is used;

- the remaining variables (e.g., energy needs in the market, energy needs for secondary reserve, prices of energy and secondary reserve) are modeled by their statistical central moments (mean and variance).

The stochastic problem is solved with the point estimate method (based on [159]) which defines a set of input data points at which the output variables are deterministically evaluated. The author also proposes a method to calculate the final energy price (i.e., retail tariff), which uses the value-at-risk based on the charging cost and profit from selling ancillary services.

This method has the following limitations:

- the serial dependency of the variables and forecast errors is neglected when modeling stochastic variables;
- the proposed model merges EV with similar driving pattern and an average profile is assigned to EV from the same cluster. This reduces the computational complexity, but at the same time it is an imperfect representation of the information which introduces additional uncertainty into the problem (as discussed by Dallinger et al. [114]);
- there is no joint coordination of EV during an operational phase where it is necessary to coordinate EV charging for complying with the market commitments. In fact, the formulation should be a two-stage stochastic optimization, with a "wait-and-see" phase where decisions depend on which of the scenarios is realized.

Operational Management Algorithms

During the operating day (close to real-time), the aggregator needs to manage the EV charging to ensure that the drivers' requirements are satisfied. These operational algorithms can be divided into two groups: (a) algorithms that manage the EV charging under time-of-use tariffs or real-time price; (b) algorithms that minimize the difference between the actual charging and a given signal (e.g., accepted bids in the electricity market).

The algorithms from the first group are reviewed in the following paragraphs.

Cao et al. [160] described a method for controlling the EV charging in response to a time-of-use price. The EV aggregator defines the charging periods according to the maximum charging power and expected ending time defined by the EV driver. A heuristic algorithm was developed for minimizing the charging cost considering the relation between the maximum charging power and the battery SoC. This approach resulted in a reduction of the charging cost and a better distribution of the load between peak and off-peak periods compared to uncontrolled charging.

Su and Chow [161] describe an optimization algorithm for managing a large number of EV charging in municipal charging stations. The objective function is the maximization of the

average SoC at the next time interval. The average SoC is obtained by weighting the SoC considering the rated battery capacity, the remaining time for charging and the price difference between real-time price and the price that a specific EV owner is willing to pay. This weighting scheme defines a priority list for EV, according to these three criteria. The optimization problem is solved with Estimation Distribution Algorithm (EDA) [162]. The aim of the paper was to compare the EDA algorithm with a genetic algorithm, an equal priority algorithm and a heuristic algorithm [163]. The results show that the EDA presents a higher optimization performance, since it improved the fitness value between 8 % and 22% compared to the other methods.

Amoroso and Cappuccino [164] also propose two heuristic methods for charging electric vehicles close to real-time. In both methods, the EV are ordered by decreasing priority, where the priority function is defined by the user's satisfaction[20] and the aggregator's profit[21]. After defining the priority order, the first algorithm charges each EV at the maximum rate of the battery, while the second algorithm divides uniformly the required energy for charging over the entire available plugged-in period.

The main limitation of these two heuristic methods is that the EV charging is defined only considering the current time interval and, since forecasts are not used, these algorithms are only suitable for real-time markets or for distributing the purchased energy by the plugged-in EV.

The following two algorithms are from the second group.

Wu et al. [165] describe a heuristic algorithm for determining the time intervals of the day-ahead market and in bilateral contracts where the aggregator should purchase energy for EV charging. The objective is to minimize the cost of purchasing electrical energy. The time intervals are ranked according to their price and are associated with the purchased energy until the maximum charging power is reached.

The algorithm is based on price and on EV load forecast and there is the possibility of having deviations between the day-ahead bids and the actual charging. Thus, a second heuristic algorithm is proposed for mitigating these deviations during the operating day. This algorithm distributes by each EV the purchased electricity following the prices ranking used in the day-ahead algorithm (i.e., all the plugged-in EV charge first in the time slot with the lowest day-ahead price) and with minimum deviation as possible. The algorithm dynamically updates the list of EV and corresponding information (i.e., energy requirement and expected departure

[20] Energy required to complete charging process divided by available time before departure.

[21] Combination of the electricity price paid by the user and penalty that the aggregator must pay if all the required energy is not supplied to the user.

time) and the decisions are made for each arriving EV.

This operational algorithm suffers from the following limitations:

- it is not an optimization algorithm and this could lead to suboptimal solutions because using the same price ranking of the day-ahead algorithm does not guarantee a solution with minimum deviation;
- it does not include the possibility of having the total EV charging greater than the day-ahead accepted bid. This may occur in hours where the purchased electricity was insufficient to meet the driver's energy requirement;
- it does not consider the imbalance prices, which might be different for positive and negative deviations.

Bashash and Fathy [166] describe a modeling and control framework for EV charging in the presence of renewable generation. First, the authors describe a state-space transport-based partial differential equation (inspired in [167]) that represents the charging dynamics of an EV fleet controlled by an aggregator and considering V2G.

Then, the developed state-space model is integrated in a robust sliding mode control algorithm (inspired in [168]). The goal of this algorithm is to minimize the error between desired signal (i.e., renewable energy generation) and the EV charging. The results showed that the proposed control algorithm is able to track the renewable energy generation and minimize the ACE.

The methodology described in this paper is oriented to a situation where the system operator controls EV charging to handle generation variability. However, although not mentioned by the authors, the controller can be adapted to minimize the deviation between accepted bids and actual charging levels. The main limitation of this method is that the space-state model does not take into consideration forecasts for the EV variables or economic considerations, such as minimizing charging cost or selling reserve services.

2.6.2 Network Constrained Optimization Algorithms

Galus and Andersson [169] propose a modeling approach for EV, with an integration scheme modeled by an energy hub agent and an EV aggregator. The authors describe a demand management scheme for the aggregator, based on mechanism design theory [170]. The aggregator tries to recharge all EV plugged in its control area while maximizing their total utility in each time step. The EV are modeled to increase their value of energy individually over time,

as they try to reach their individual objectives and respect the technical constraints. Reactive and proactive behavior is incorporated and electricity prices are also incorporated in the model. Perfect forecasts are used for the input variables.

Sundstrom and Binding [171] presented an optimization problem for minimizing the cost of charging EV constrained by the distribution network branch limits. The objective is to determine the charging schedule that minimizes the charging costs, respects the electrical energy requirements for the next trips and respects the distribution network capacity. The optimization problem is formulated as a linear program, which is solved iteratively for complying with the maximum tolerable load in each node of the network. The method showed a significant reduction of network's overloading, compared to unconstrained charging. Nevertheless, the authors also show that the proposed algorithm is computationally demanding.

The importance of having a forecasting module to estimate how much electrical energy (duration of the connection event and minimum required SoC) has to be delivered to the EV was identified for future work, together with the need to investigate the impact of forecasting errors in the optimization system.

O'Connell et al. [172] present the concept of day-ahead dynamic distribution network tariffs, which is similar to the concept of LMP and reflects congestion costs of the network. The method for calculating the tariffs is as follows: the DSO uses day-ahead forecasts for the price and EV load as input in a DC Optimal Power Flow (OPF) that computes LMP. The LMP are decomposed into three components: marginal cost of generation, losses and congestion. The marginal congestion cost defines the tariff value. Note that to avoid complex and computational demanding calculations, the process is sequential and the congestions are handled separated from the energy market-clearing. In this stepwise approach, the DSO communicates to the EV aggregators the congestion tariffs before bidding in the day-ahead energy market and the aggregator makes its optimization, minimizing the sum of the forecast energy price plus dynamic tariff.

This approach is different from the previous ones because the dynamic tariffs scheme is decoupled from the optimization model (i.e., network constraints are not explicitly included in the optimization model). Therefore, the algorithms from section 2.6.1 could be used in this approach and the only necessary modification is to include an additional price in the objective function.

This approach has two main barriers: a) calculating LMP, including the distribution network, seems to be a challenge from the computational side and some simplifications, such as using a DC model, might be necessary; b) the DSO will need to use forecasts for the generation and load and this might lead to suboptimal solutions and, during real-time operation, some

congestion problems can still occur.

2.6.3 Forecasting EV Variables

An EV aggregator participates in the electricity market under the same rules as generators and other load retailers. This means that it must make an estimative of the EV consumption for the next day and hours in order to use optimization algorithms such as the ones described in the previous sections.

The current literature is scarce in terms of forecasting algorithms for supporting the optimization algorithms of the EV aggregator. It is more common to find algorithms for modeling the EV driving pattern and consumption [173][174], which are more suitable for planning studies.

Forecasting methods for optimizing the aggregator's bids should consider the following aspects:

- a time-series approach modeling the serial dependency of the variable should be adopted, because average (or typical) profiles are just a coarse estimative for the variables;
- if the aggregator has direct control over the EV charging (i.e., dispatchable DR), this means that the classical approach of forecasting the load in each time interval cannot be strictly followed because the aggregator is forecasting a variable that it controls at the same time;
- if the EV consumption is responsive to a price signal (i.e., voluntary DR), it is necessary to forecast, based on historical data, the impact of the price signal on the EV consumption.

For the dispatchable DR paradigm, two recent works can be found in the literature.

Aabrandt et al. [175] describe an exponential smoothing model to forecast the plugged-in intervals. A formula is also given for calculating the variance associated to the prediction. The energy needed for this next trip is not forecasted by the model.

Sundstrom et al. [176] describe a trip forecasting algorithm, based on a semi-Markov model (according to [177]). The aim of the algorithm is to forecast the charging periods (instead of driving periods) and the following variables are forecasted: energy consumed during the trip; waiting time before disconnection; duration after disconnecting before connecting again; location of the vehicle during connection event. This forecasting method was evaluated in

three months GPS data of one vehicle (not an EV) and the results showed 84% of correctly predicted locations and 4 hours error in the waiting time. These results are for one step-ahead forecast.

Currently, in the literature, there are no methods to forecast EV load consumption under a voluntary DR paradigm. However, methods for other type of loads can be found [178][179] and, in the future, these methods can be adapted to include EV.

2.6.4 Battery Model for Optimization Algorithms

Sundstrom and Binding [180] compared two different battery models, linear and quadratic approximation, used by an aggregator with the goal of minimizing the charging costs when participating in the energy market. This quantifies the level of detail necessary to include the battery in the optimization problems.

In the linear approximation, the internal power P_{int} is assumed to be equal to the external power $P_{int} = P_{ext}$, which means that all the internal losses in the battery are neglected. The aim of the quadratic approximation is to represent the non-linear relation between external and internal power, $P_{ext} = f(P_{int})$, using a second-order Taylor series expansion. This approximation attempts to capture a non-linear relation between charging power and rate of change of the battery SoC.

The comparison results showed that the difference between the two models is minor, indicating that a linear approximation is sufficient. According to the authors, the losses in the battery increase with the charging power, thus for lower charging power (e.g., 3.5 kW) the impact is not significant. Furthermore, although using perfect forecasts for all the variables, the authors state that forecast errors are likely to have a significantly larger impact than the battery model.

Furthermore, concerning this topic, Wu et al. [165] observed the following: “optimal battery charging follows a varying power profile. However, it has been found that modeling this profile in detail does not affect the simulation results significantly”. Marra et al. [181] modeled the demand profiles generated by EV charging and showed that the charging power of 3.7 kW only drops when the battery SoC is above 95%.

2.6.5 Final Remarks

During the last three years, numerous authors developed algorithms for supporting the aggregator participation in the electricity market. These algorithms were not restricted to the V2G concept and some authors explored the concept of using the EV as a controllable load (POP approach) for supplying secondary reserve. The main limitation of most of these works is the assumption that perfect knowledge is available about the EV variables. In fact, it is necessary to forecast these variables and account for the forecast errors in the algorithms. Otherwise, it may be unmanageable to comply with the market commitments, such as providing reserve. Moreover, the algorithms only consider the possibility of managing the EV charging individually and do not explore the possibility of computing bids based on the total values of the EV variables.

The operational management algorithms from the literature are mainly focused on controlling the EV charging, according to a time-of-use tariff or a real-time price. However, when the aggregator participates in day-ahead or intraday sessions it is necessary an operational management algorithm for coordinating EV charging, in order to avoid penalizations due to deviations from the accepted bids. In fact, one of the aggregator's goals is to coordinate all EV to meet service commitments contracted by the ISO/TSO with acceptable quality while also satisfying requirements of the EV drivers.

All the bidding optimization algorithms from the literature only address the participation in the secondary (or regulation) reserve market. The participation in tertiary and balancing reserve markets is not addressed. Moreover, the algorithms for secondary reserve either assume that the EV under dispatch via AGC would have a net total energy approximately zero (i.e., upward regulation offsets downward regulation) or neglect the fact that the secondary reserve capacity may not be fully mobilized in each hour.

Finally, although the idea of constrained optimization (discussed in section 2.6.2) sounds interesting, it should be noted that the branches' overload would differ with the charging profiles of other EV (not associated to the same aggregator). Hence, it seems more appropriated to create new market rules and develop new management algorithms to address the risk of congestion in distribution networks.

The following chapters of this thesis describe original optimization algorithms covering the electrical energy, secondary and balancing reserve markets. These algorithms take as input forecasts for the EV and market variables and operational management algorithms are proposed for minimizing the imbalance costs and guarantee an acceptable reliability when supplying reserve.

Chapter 3

EV Aggregator Model and Framework

Abstract

This chapter describes different aspects of the aggregator model, such as: architecture and stakeholders role; interactions between the different agents; economic, physical and information flows. A framework with the electricity market sessions and optimization/forecasting algorithms to support the EV participation is described.

3.1 Architecture

The EV aggregator's architecture defines the technical interactions with the electricity market, EV owners, DSO and TSO. Andersen et al. [182] defined three architectures for EV market integration, discriminated according to stakeholders and mechanisms used to influence the EV behavior: *centralized control*, *partly centralized* and *fully distributed*. This nomenclature and definitions may produce ambiguous interpretations. Therefore, new definitions are proposed here:

- *standard retailer*: the aggregator is a standard electricity retailer for electrical mobility. It may indirectly influence the EV charging by setting the typical time-of-use electricity tariffs. The charging monitoring is only for billing purposes;
- *indirect control*: the aggregator sends price signals to each EV for indirect control and the EV driver is an independent decision-maker. Intelligent negotiation software parameterized with the driver's preferences (decision-maker) is installed on-board and controls the EV charging in response to the price signal. The price signal can be the real-time price, the forecasted market price, or any specific value to get a certain behavior from

the EV (e.g., obtain consumption reduction to offer as upward reserve);

- *hierarchical direct control*: the aggregator directly controls the charging of each EV, receives signals requesting consumption increase/decrease from the DSO and TSO and distributes these signals by the fleet of plugged-in EV. For example, the aggregator may receive signals from the DSO to reduce consumption in one node of the distribution network to avoid technical problems (e.g., overloads, voltage limits violation) and the aggregator takes appropriate control actions to meet the DSO request;

- *autonomous*: the EV behaves as an autonomous and intelligent agent that can interface directly with the DSO/TSO and/or electricity market.

In the *standard retailer* architecture, the aggregator does not have any control over the EV charging and it is a simple electricity retailer. Thus, the provision of ancillary services or load curtailment in case of technical problems in the distribution network is not possible. Due to its simplicity, this architecture will be adopted in an early phase of EV integration.

The provision of ancillary services is possible with the *indirect control* [69][156]. However, it is necessary to define a correct pricing scheme to enroll EV in ancillary services provision and forecast the available reserve capacity. Moreover, since the aggregator does not have direct control over the charging process, it may be difficult to provide ancillary services (such as secondary reserve) with the reliability and availability standards demanded by the TSO. This architecture was adopted in the e-mobility Berlin pilot project, where decision-making algorithms that negotiate with the aggregator were installed in the EV [182].

Regarding the *autonomous* architecture, the current electricity market rules typically set a minimum bid size around megawatts (e.g., in Germany is 5 MW for secondary reserve), which leaves aside bids from individual EV. Moreover, this approach also suffers from two disadvantages: a) for secondary reserve it requires that the AGC sends signals to each individual EV and managing all this information exchange may be prohibitive in terms of communication requirements; b) the load forecast for a single EV could have high forecast errors for the next day and the EV owner could incur in high financial penalizations because of deviation from the contracted levels. Because of this second disadvantage, the EV can become averse to offering reserve services and the TSO averse to buying reserve from the EV.

The aggregator overcomes these disadvantages since it is an intermediary between EV driver and the TSO/DSO in terms of communications, and coordinates EV individual charging to mitigate deviations from scheduled values. The *hierarchical direct control* allows the provision of ancillary services to the TSO and supports the DSO in managing the distribution network with a high penetration of EV and postpones reinforcements of the distribution network. This

architecture has been adopted in several National and International projects, such as the European project MERGE [183], the Danish Edison project [184], the Portuguese project REiVE[1] (*Redes Eléctricas Inteligentes com Veículos Eléctricos*) and Google Energy [24]. Note that ancillary services such as primary frequency control and primary voltage control are automatic and local, therefore they do not require any *hierarchical direct control* or *indirect control*.

The architecture developed in this thesis follows the *hierarchical direct control*, illustrated in Figure 3.1 and described in the following paragraphs and subsections.

The owners of plug-in EV, seeking the lowest electricity tariff, establish a contract with an aggregator. The aggregator is an electricity retailer and represents the EV drivers in the electricity market (e.g., purchases electrical energy for EV charging). The retailing activity is only for electrical mobility, which allows separate pricing of electricity for this purpose and the inclusion of taxes from the government.

Two different groups of clients are foreseen for the EV aggregator:

- *inflexible EV load*: a client who does not allow the aggregator to control the charging process. For this client, the aggregator is only an electricity provider;
- *flexible EV load*: a client who allows the aggregator to control the charging process (bidirectional communication), which means that its preferences (i.e., final SoC and departure time instant) must be satisfied, but presents a degree of freedom regarding when this load can be supplied.

The interaction with these clients will be described in section 3.1.1.

The aggregator can present the following bids in the electricity market:

- *buying bid in the energy market*: the aggregator purchases electrical energy for charging the EV at the lowest price. The sellers are generators;
- *selling bid in the energy market*: if V2G is available, the aggregator can offer electrical energy in the electricity market in hours with high prices. The buyers are other electricity retailers;
- *selling bid in the ancillary services market*: the aggregator offers reserve services and the buyers are the TSO and DSO.

[1] http://reive.inescporto.pt/en (accessed in December 2012)

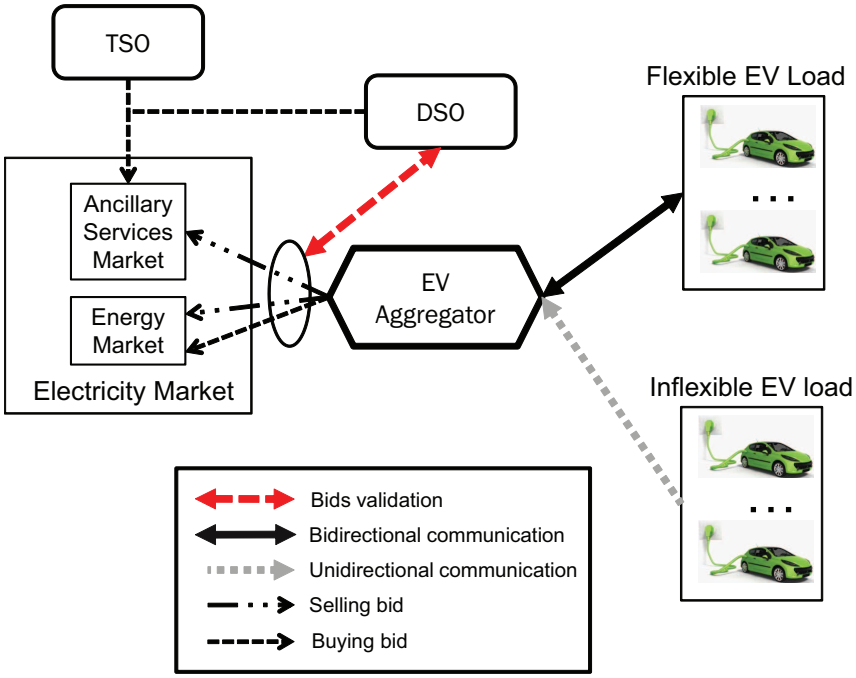

Figure 3.1: *EV aggregator architecture.*

The DSO makes an *ex-ante* technical validation of the aggregator's bids. The TSO purchases reserve services from the aggregator for load-generation balancing. The relation between aggregator and TSO/DSO is described in section 3.1.2.

The V2G mode is not considered in this thesis and reserve services are provided using the POP approach. This choice was mainly driven by the uncertainty that arises from battery wear issues and other technical problems related to V2G. The V2G is a viable option, but only for the long-term. Therefore, the goal in this thesis was to explore a solution with less technological challenges, which only requires bidirectional communication and variable control of the charging rate.

3.1.1 Interaction with EV Owner and Charging Point Manager

The EV driver can connect for charging in different types of locations [133]:

- home and office for long parking periods. The recommended charging is single-phase AC with charge power around 3 kW (it takes between 6-8 hours to complete charging). This is called normal charging;

- car parking, shopping center and public street for parking periods between 1 and 2 hours. The recommended charging is single-phase AC with 7 kW (it takes 3-4 hours to full charge), or three-phase AC with 10 kW (it takes 2-3 hours to full charge). This is

called normal public (or semi-public) charging;

- fast-charging stations for professional use (e.g., taxi, bus) or for long driving distances (located in highways). The charging can be performed with three-phase AC and charge power up to 43 kW (20-30 minutes to full charge), or with DC connection and charge power up to 50 kW. This is called fast-charging.

Public and Fast-charging Stations

The public, semi-public and fast-charging points are owned and operated by a CPM, which is independent from the aggregator. The aggregator establishes contracts with several CPM which give to the EV driver mobility and freedom to use different charging points, but remaining with the same aggregator. The owner of public charging points could be the DSO.

Figure 3.2a depicts the components of a DC fast-charging station that allow the interaction between CPM, aggregator and EV owner.

The EVSE in DC fast-charging points includes an External Vehicle Charger (EVC) that converts AC to DC (supplied by a three-phase circuit), power cord, connectors and an Electric Vehicle Meter (EVM) for billing purposes. The EV has an On-board Computer (OC) that displays the SoC evolution and allows the EV driver to define its preferences for the charging process. There is also a Battery Management System (BMS) that manages output, charging and discharging, monitors its state and provides critical safeguards to protect the battery from damage.

Figure 3.2b depicts the components of a public (or semi-public) and fast-charging AC point. This figure illustrates two alternative solutions: normal charging with single-phase AC and fast-charging with three-phase AC. The difference to Figure 3.2a is an On-board Vehicle Charger (OVC) designed to charge from 3 to 43 kW [133], instead of an EVC.

In this thesis, it is assumed that the EV are inflexible loads when connected to the charging points (a) and (b) of Figure 3.2. This is a plausible scenario since a driver, connected to a fast-charging station, is only interested in having the EV plugged-in for a few minutes.
Bidirectional communication with the aggregator would be possible in public and semi-public charging points. However, the EV in shopping centers and public stress is only parked, on average, during two hours and this does not give too much flexibility to control EV charging and justify the investment cost in an advanced EVSE with bidirectional communication.

For these inflexible EV, the aggregator only estimates, for each hour, the quantity of energy that is necessary to purchase in the market for meeting their charging demand. The interaction

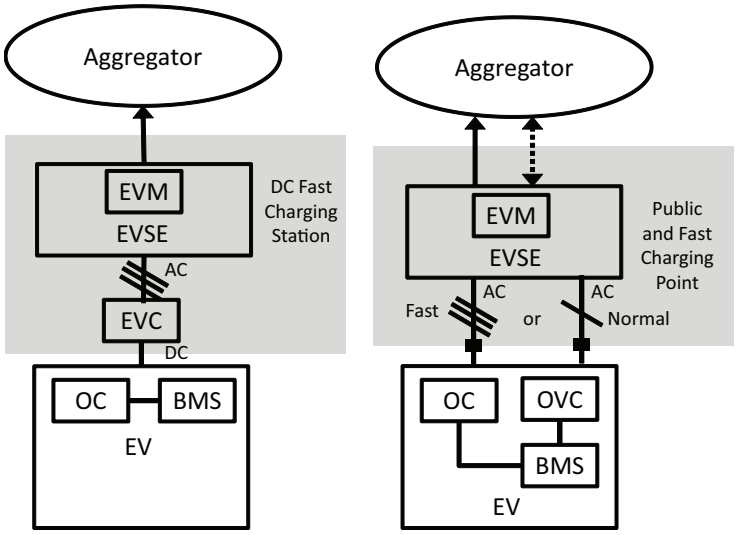

(a) *DC fast-charging station.* **(b)** *Public and fast-charging AC point.*

Figure 3.2: *Components of public and fast charging stations for Aggregator-EV-CPM interaction. EVSE: EV Supply Equipment; EVM: EV Meter; EVC: External Vehicle Charger, OC: On-board Computer; BMS: Battery Management System.*

is unidirectional and just for billing purposes and can be described as follows: the EV driver parks for charging, uses an ID card associated to his aggregator and defines the target SoC (on the OC) for the charging process; the EV starts charging after the validation task; after charging completion, the metered data is sent by the EVSE to the aggregator.

Home and Work Charging Points

The flexible EV are connected at home, office or residential car parking (in a garage or a street close to buildings). Surveys about drivers behavior and preferences indicate that charging at home during the night and at office is the natural behavior of plug-in EV drivers [185][134]. The expected charging power for these points is around 3 kW [130] and it is expected that the DSO will set a limit in the contracted power, similar to what is done for household consumers. This power limit is also likely to be found in private company parking lots; otherwise, a significant upgrade of the company electrical installation would be required.

An EV driver can also choose to be inflexible in these charging points.

Figure 3.3 depicts the components of a residential or office charging point with bidirectional communication for flexible EV. The EVSE is owned by the EV driver or by his company, but

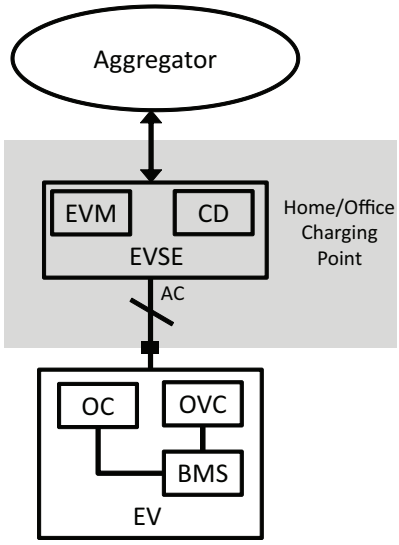

Figure 3.3: *Components of a residential or office charging station. EVSE: EV Supply Equipment; EVM: EV Meter; CD: Control Device; OVC: On-board Vehicle Charger; OC: On-board Computer; BMS: Battery Management Systems.*

the aggregator is responsible (at least partially) for installing and supporting the costs of the EVM and Control Device (CD). The EVM and CD together can also be called "energy box" for EV. The vehicle charger is located inside the EV and the CD is installed outside the EV since it allows the communication protocol between aggregator and EVSE to be different from the protocol between EVSE and OVC.

There are different protocols for the communication infrastructure (see section 2.5 of chapter 2) between the elements of Figure 3.3. One possible solution is to adopt standard IEC 61851 for the EVSE-EV communication and standard IEC 61850 that defines protocols for Transmission Control Protocol (TCP)/Internet Protocol (IP) networks and enables aggregator-EVSE communications [139]. It is assumed that the aggregator does not use the smart meters infrastructure owned by the DSO[2].

The bidirectional interaction between aggregator and EV can be described as follows: the EV driver parks for charging at home or at office (in this case the driver uses an ID card), defines in the OC the target SoC and expected departure time instant; the aggregator controls the charging process respecting the preferences of the EV driver; the metered data is collected in real-time by the aggregator via EVSE. If the EV driver fails to communicate his preferences, a default profile defined in the contract with the aggregator is used (e.g., target SoC of 100%, departure in 8 hours).

For the flexible EV, the aggregator optimizes the quantity of purchased energy in the electricity

[2] Otherwise, the aggregator pays a tariff to the DSO for using its communication infrastructure.

market and corresponding period in order to decrease its wholesale cost. Moreover, it can also offer reserve services to minimize the cost. The aggregator controls the EV charging process to meet accepted bids, but it does not have any control over the individual EV driving behavior. The driver preferences must still be respected and are the main priority. The EV driver is free to arrive for charging and depart before charging completion. The benefit to the EV driver is a cheap electricity retailing tariff (topic discussed in section 3.1.4). The driver will use public and fast-charging stations as complementary services.

3.1.2 Interaction with TSO and DSO

TSO

The TSO is a buyer of frequency and balancing reserves and the EV aggregator is a potential provider. The benefit, for the TSO, from buying reserve from the EV aggregator is access to cheap (compared to coal and gas-fired power plants) and fast reserve and the possibility of using a flexible resource already available in the system instead of conventional generators with intensive GHG emissions. The active participation of the demand-side increases the sufficiency and efficiency of the secondary and balancing reserve markets.

In the frequency reserves category, only primary and secondary reserves are automatic. Tertiary reserve is manual. Here, it is assumed that primary reserve is mandatory and non-remunerated. Thus, the only automatic reserve that is purchased in the market is secondary reserve and the aggregator is a potential provider.

The aggregator distributes the control signals from the AGC by each plugged-in EV and coordinates the EV individual charging to increase the secondary reserve reliability. The TSO remunerates this service with a price for dispatched reserve (in €/MWh) and another for available reserve capacity (in €/MW).

The tertiary and balancing reserves are manually activated. The EV aggregator can supply tertiary reserve, but here more emphasis is given to the balancing reserve.

The aggregator distributes the requested amount of balancing reserve by the plugged-in EV and coordinates their charging to ensure an acceptable reliability level. It is remunerated with a price for dispatched reserve[3].

In order to supply secondary and balancing reserve, the EV charger should be able to operate

[3] In general, this reserve is only paid by delivered energy (or dispatched reserve power), but in order to stimulate investments in flexible resources (demand and supply-side) some countries may introduce a capacity price.

at values different from zero and maximum charge power. Presently, with charging mode 3 it is possible to have a variable charge rate.

Since balancing reserve handles "slower" events (e.g., hourly deviation from schedule) compared to secondary reserve, the charge rate variation is expected to be slower during the mobilization period. On the contrary, secondary reserve will take more use of a fast variable rate to handle random variations in shorter time-scales.

In terms of timing requirements, the standard IEC61851 defines a maximum of 15 seconds for modifying the available current level [127]. This maximum time complies with the minimum mobilization time of secondary reserve (generally 30 seconds) and tests conducted on an EV show an acceptable capability in following AGC signals [103].
As an alternative, the aggregator can combine on/off charging signals within the fleet in order to provide ramp up/down response.

DSO

There are different and alternative mechanisms for the aggregator/DSO coordination in order to solve technical problems in the distribution network (reviewed in section 2.4.6 from chapter 2). Here it is proposed a possible procedure for handling technical problems at the distribution network level, but this thesis does not develop algorithms to solve this problem.

The proposed procedure assumes that the DSO purchases upward and downward power from the aggregator in an *adjustment market* in order to solve potential technical problems at the distribution network level. The bids in this *adjustment market* can be shared with the balancing reserve market. This means that the aggregator can submit the same bid in both markets, but a technical coordination between DSO and TSO is necessary to avoid that the use of the adjustment power by the DSO counteracts the load-generation balancing task of the TSO. Presently, this market does not exist, but it is similar to what is done in most electricity markets for solving congestions in the transmission network.

The aggregator/DSO interaction is as follows:

1. the DSO makes an *ex-ante* validation of the aggregator's energy and reserve bids (as proposed by Lopes et al. [23])[4] and determines load reduction/increase quantities and location to solve technical problems using, for instance, a heuristic method (such as [186][22]);

[4] The level of detail associated to the distribution network is an open-issue and depends on the available information about the network topology.

2. the EV aggregators submit bids in the balancing reserve and adjustment markets;

3. with the output of points 1 and 2, the DSO checks if the available upward and downward adjustment bids, associated to a distribution network node, are sufficient to solve the technical problems. If not, the DSO determines additional and mandatory adjustment bids for a specific hour and node;

4. this validation exercise is conducted for each market session (e.g., day-ahead, intraday and hour-ahead) and the DSO uses the adjustment bids when it is necessary;

5. during the operating hour, the DSO sends signals to the aggregator requesting the purchased adjustment power. In case of emergency operation, the DSO, using its own communication infrastructure, can send compulsory signals to stop the charging of flexible and inflexible EV, but only in last resort.

Note that this is just one possible solution, for which new management procedures are needed, but it requires minimum changes in the current electricity market. This approach separates the technical constraints management of the distribution network from the bidding optimization phase.

The benefits to the DSO is the possibility of using upward and downward adjustment power from EV to solve technical problems and investment deferral in the distribution network [86]. The cost incurred by the DSO from using this service gives economic signal for additional investments in the distribution network. If this cost is higher than the investment cost in new or upgraded lines and equipment, the decision should be network reinforcement.

In this procedure, it is necessary to develop regulatory rules to avoid windfall profits and unfair situations for the aggregators. One case of windfall profits that suitable regulation rules should avoid is an EV that purchases a high quantity of electrical energy for a node connected to branches with frequent congestions and, then, obtains a high income from selling consumption reduction in that node.
For instance, the zonal market in ERCOT system involuntarily created an incentive for wind farms owners to overestimate wind power generation in order to receive a curtailment payment for solving network congestions [187]. This allowed a payment even in situations where the wind resource was insufficient to meet the scheduled quantity.

3.1.3 Information Flows

The required data from the EV is collected using the communication infrastructure between aggregator, EVSE and EV. The goal is to respect confidential information and avoid using data

that could raise ethical issues and refusal from the drivers. Therefore, data such as historical and future EV driving routes or real-time location of the EV is not used or collected. In fact, data is only collected when the EV is plugged-in for charging and only from its electrical consumption.

The communication infrastructure should be able to enroll and register the EV with its aggregator when it connects for charging and transmit static and dynamic information from the EV to the aggregator and vice-versa. It should be reliable (i.e., response time) enough to supply ancillary services such as secondary reserve.

The static information is the following:

- EV type, e.g. hybrid, battery, fuel cell;
- ID of the EV and charging point;
- power capacity of the EVSE (kW);
- battery capacity (kWh);
- target SoC (in %) and expected departure time instant defined by the driver;
- charging characteristics, e.g. the EV is only able to switch charging on or off, or there is a maximum ramp rate in charging power (in %/sec).

Figure 3.4 depicts the dynamic information flows between aggregator, DSO/TSO and EV driver. The dynamic information consists of the following:

- EV status (binary variable - connected or not);
- signals from the TSO and DSO;
- charging rate in each time instant (kW) and the integral gives the consumed electrical energy;
- battery SoC in each time instant.

It would be very demanding to have a DSO or TSO directly controlling and receiving information from thousands of EV. Therefore, the communications flow should be bidirectional: upstream information from the EV to the aggregator and from the aggregator to the TSO/DSO; downstream information from the TSO/DSO to the aggregator and from the aggregator to the EV [188].

More specifically, the aggregator receives control (or request) signals for secondary and bal-

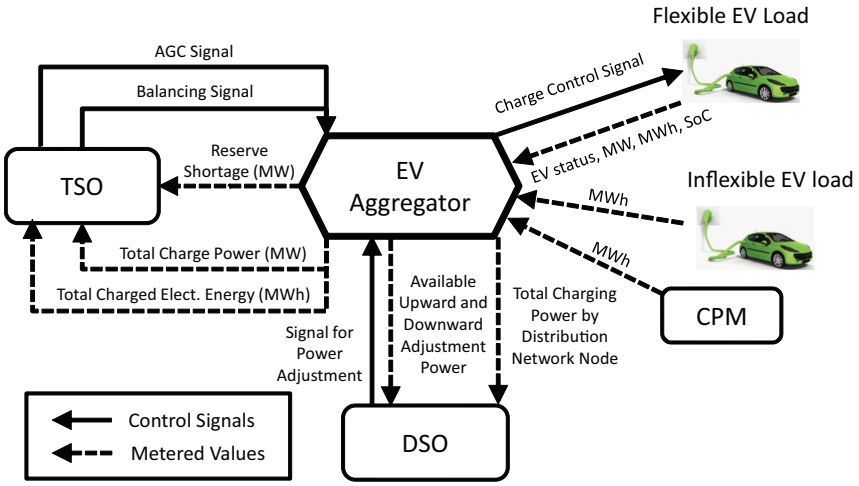

Figure 3.4: *Information flows between aggregator, DSO/TSO, EV and CPM.*

ancing reserve from the TSO and distributes these signals by the plugged-in flexible EV. The EVSE, from the flexible EV, sends real-time measures of dynamic information to the aggregator and, then, the aggregator sends total values of power and energy to the TSO/DSO in real-time. Furthermore, using the information collected from the EVSE, the aggregator estimates the potential shortage in reserve capacity and transmits this information to the TSO. The DSO sends a signal requesting the use of adjustment power to solve branches' overloads and voltage problems and the aggregators informs the DSO about the total charging power in each network node and also the available upward and downward adjustment power in each node.
The aggregators only receive metered values of energy from inflexible EV connected to home and office charging points and also from EV charging in public and fast charging stations owned by the CPM.

It is assumed that real-time measurements are required by the TSO for secondary and balancing reserve provision. Nevertheless, the TSO could waive this requirement (in particular for balancing reserve) and request only time interval measurements (e.g., 10 minutes) to the aggregator.

3.1.4 Economic and Physical Flows

The economic and physical flows between aggregator, DSO/TSO and EV owner are depicted in Figure 3.5. This business relation must create value (but not necessarily monetary value) among all involved stakeholders. The product is the EV charging controllability and flexibility, which is contracted by the aggregator to the driver, and sold to the DSO and TSO in the electricity market.

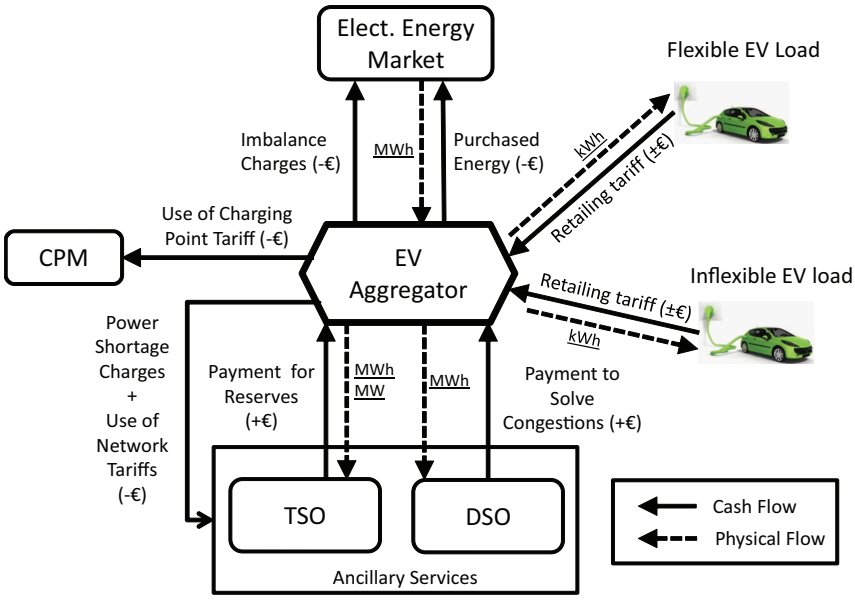

Figure 3.5: *Economic and physical flows between aggregator, DSO/TSO and EV driver.*

The aggregator has costs related to the electrical energy purchased in the market and imbalance penalties if the consumed energy is different from the accepted bid. If participating in the reserve markets, the aggregator receives a capacity payment, from the TSO, for having available secondary reserve capacity and a payment for supplying secondary and balancing reserves. The aggregator also receives an energy payment if the DSO uses the adjustment power bids. In both cases, if the aggregator is unable to supply all the requested reserve or adjustment power it incurs in financial penalties for power shortage. The penalties are only applied to the aggregator and not to each individual EV.

The aggregator pays tariffs to the DSO and TSO for the transmission and distribution network use and in some countries (like Portugal) there is also a tariff (paid to the TSO) related to the global use (or management) of the system.

An important part of the aggregator's business model is the definition of the retailing tariffs for EV drivers. These tariffs depend on the business model and should be established by considering a trade-off between expected profit per EV and capacity of attracting new clients. For instance, the aggregator can reduce the retailing tariff for each EV (or its markup) and, with a good marketing campaign, increases the number of EV under contract, which results in an increase of the total profit. The calculation of the tariffs' value is not addressed in this thesis, but here some considerations are made about their structure and objectives.

For public, semi-public and fast-charging points, the retailing tariff paid by the driver to the aggregator includes two components: consumed electricity and charging installations use. The aggregator pays to CPM for using its charging point, and the tariff paid by the clients

includes a markup related to the aggregator profit's margin (from the retailer activity). The aggregator must define *a priori* the retailing tariff.

Since in these charging points the aggregator does not control the charging process, the tariff should be higher than the one for flexible EV connected to home and office charging points.

In home and office charging points, the contract between aggregator and EV owners establishes that the client may choose to be flexible or inflexible. The inflexible EV client pays a tariff similar to the public and fast charging points but without the cost associated to the charging installation use.

The flexible client offers controllability and flexibility to the aggregator and gets in exchange a lower retailing tariff. For the EV owner, it is irrelevant if the offered controllability is used for supplying reserve or just for charging during low-price hours. The EV owner sells flexibility, which the aggregator uses for minimizing its wholesale costs. The value of flexibility depends on the aggregator model (e.g., marketing, management processes, optimization algorithms) and, thus, it should be the aggregator to define *a priori* its value.

There are a large number of conceivable tariffs for flexible EV. One possibility is to adapt the classical time-of-use tariff that differentiates by price different periods of the day and introduce a variable term to remunerate flexibility. In this case, the tariff should include the following incentives: plug-in in specific periods of the day (e.g., off-peak hours, hours with high reserve price), during the maximum possible time and with low ratio between required energy and charging period length[5].
The remuneration by flexibility should be transparent and clear to the EV driver. For example, the on-board computer of the EV could inform the driver about the tariff value that corresponds to the different combinations of the expected departure hour and target SoC, also considering the period of the day (i.e., peak or off-peak period).

As mentioned before, the EV driver is free to leave before the defined departure time instant, but two penalizations are foreseen: a) the target SoC may not be reached because of early departure (but this was a decision taken by the driver); b) a penalty is added to the tariff for not complying with the transmitted information. To avoid these penalizations, the EV driver can be very conservative when defining the expected departure, but, in this case, it would decrease its flexibility and get a higher tariff. This scheme creates incentives to avoid early departure or very conservative definitions of the expected departure time instant and promotes a high level of commitment from the driver.

[5] An EV that requires 10 kWh to meet its target SoC with an expected departure after 5 hours is less flexible than an EV that requires the same quantity but with a departure only after 10 hours.

There is no lower limit for the retailing tariff, depending on the aggregator's business model and reserve prices, the value could be zero or even negative (i.e., the aggregator pays to the EV driver).

The contract between aggregator and EV establishes that the aggregator must meet the target SoC defined by the clients, otherwise penalties (e.g., financial payments, termination of the contract) are envisioned if quality of service standards are not satisfied. In exchange for an additional discount in the tariff, the EV driver may allow some flexibility (i.e., a tolerance band) around the target SoC.

3.2 Management Processes

The management processes of an EV aggregator can be divided into five time horizons:

- *long-term (or business model)*: time horizon greater than one year. The aggregator determines which type of EV and clients are necessary to attract, in order to increase the fleet's economic value in some markets. The aggregator defines the retailing price and contract conditions for building its portfolio of EV drivers. Depending on the business model, the aggregator can make or renegotiate contracts with suppliers, such as battery manufacturers or smart grid equipment suppliers. Marketing campaigns are also planned in this phase;

- *mid-term*: time horizon ranging from weeks to months ahead. The aggregator defines the position in several markets (e.g. ancillary services, energy, futures) based on the EV portfolio, predicted market prices, drivers' behavior and EV technical characteristics. This process involves the participation in markets of futures and bilateral contracts, as well as an estimation of which sessions from the spot market are more attractive to the aggregator;

- *short-term*: time horizon up to two days ahead with hourly or half-hourly time steps (depending on market rules). The aggregator participates in day-ahead markets to buy electrical energy and sell ancillary services;

- *very short-term*: time horizon ranging from 1 to 6 hours ahead with hourly and half-hourly time steps. The aggregator participates in intraday markets to adjust the day-ahead bids, reserve markets or in real-time (or hour-ahead) markets;

- *operational (or "almost" real-time)*: the starting point is the *short* or *very short-term* schedule and the aggregator coordinates the EV individual charging to fulfill the market

commitments (and avoid financial penalizations) and EV owners' needs. The aggregator may also respond to signals from the DSO under abnormal operating conditions (such as network operated near its technical limits).

As the time horizon decreases, more information is available since all plugged EV are monitored by the aggregator and it is assumed that the EV drivers communicate their preferences for the charging process (otherwise, a default profile is used).

In this thesis, the *long-term* and *mid-term* management horizons are not addressed. The next section describes the framework defined in this thesis for the *short-term*, *very short-term* and *operational* time horizons.

3.3 Electricity Market Framework and Algorithms

For inflexible EV, an optimization model for the market bids is not necessary. The aggregator only needs to forecast the total consumption in each hour and purchase, in the energy market, the forecasted quantity. This process can be more complex if information about forecast uncertainty is included in the bidding process, following a strategy similar to the wind power bidding in the electricity market [189].

Figure 3.6 depicts the proposed framework of electricity market sessions and optimization (and forecasting) algorithms for flexible EV. This framework covers the majority of electricity markets schemes across the world, it is divided by time horizons and a separation is made between input information and market processes. The grey blocks indicate the algorithms not developed in this thesis.

The developed optimization models have the following characteristics:

- deterministic, but use point forecasts as inputs;
- the aggregator is a "price-taker": the decisions made by the aggregator do not affect the market clearing prices [190]. The problem consists only in determining the quantity to buy/sell in each time interval. The "price-taker" assumption is valid when there is sufficient competition in the market and a single market agent does not have a large quota of the market (i.e., market power). Note that this assumption does not mean that the increasing participation of aggregators in the electricity does not impact the price levels. A change in the market price levels may occur with the increasing number of EV aggregators, but this thesis does not study the future impact of EV in the electricity market prices.

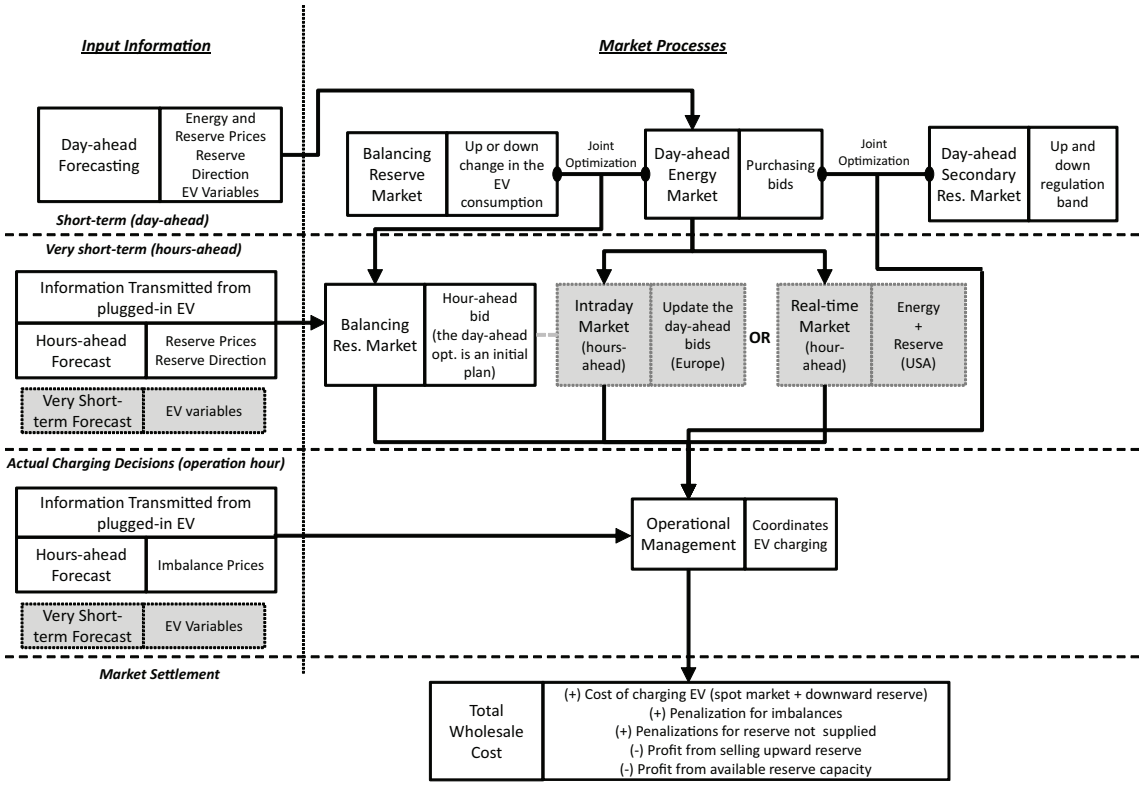

Figure 3.6: *Electricity market framework and algorithms for the EV aggregator.*

3.3.1 Short-term Horizon

The day-ahead (or short-term) optimization processes are intended for energy, secondary reserve and balancing reserve market sessions. The aggregator has different possibilities: (a) optimization of the energy bids; (b) joint optimization of the energy and secondary reserve bids; (c) joint optimization of the energy and balancing reserve bids; (d) joint optimization of energy, secondary and balancing reserve bids. In this thesis, optimization models for problems (a)-(c) are formulated.

The outputs from the day-ahead optimization models are: energy bid for each market time interval; upward and downward balancing reserve capacity bid; upward and downward secondary reserve capacity bid (in MW). Since the aggregator is a "price-taker", it is assumed that the bid price is lower enough to be accepted.

The joint optimization models can be used in sequential markets or in joint markets where energy and reserve bids are cleared together.

This framework assumes that secondary reserve is only contracted in a day-ahead session. This is valid for most European markets with daily secondary reserve markets, like the Iberian and Italian markets. In most of the USA markets it can be contracted in the real-time (or

hour-ahead) market, but as mentioned in section 2.2.2 (chapter 2), the majority of secondary reserve in the USA is contracted in the day-ahead market. A day-ahead session for the balancing reserve market is also considered.

The day-ahead optimization models require forecasts for different variables: energy and reserve prices, balancing reserve direction and EV variables.

Forecasting the balancing reserve direction consists in anticipating if the power system will need upward or downward balancing reserve in each time interval of the next hours and day. Since the secondary reserve handles less predictable events, the optimization model for secondary reserve does not use information about secondary reserve direction.

The load forecasting task is common in problems related to power systems and electricity markets. However, this problem is different because the aggregator controls EV consumption, which means that the approach of forecasting the EV consumption in each time interval (similarly to classical load forecasting problems) cannot be strictly followed. The approach proposed in this thesis is to forecast two EV variables (illustrated in Figure 3.7): charging requirement and availability.

The availability is the time-period where the EV is plugged-in for charging. In the example of Figure 3.7, it is the time period between 21h30 and 8h30. The charging requirement is the total electrical energy needed to get from the initial (i.e., when the EV arrives for charging) to the target SoC defined by the EV driver for the next trip, including the charger efficiency. In Figure 3.7, the charging requirement is the total energy required for getting from a 50% to a 100% SoC, which is 10 kWh, plus the charger's efficiency losses (1.11 kWh). A charging requirement value is always associated to an availability period. The aggregator then distributes this quantity, according to its optimization strategy, by the time intervals of

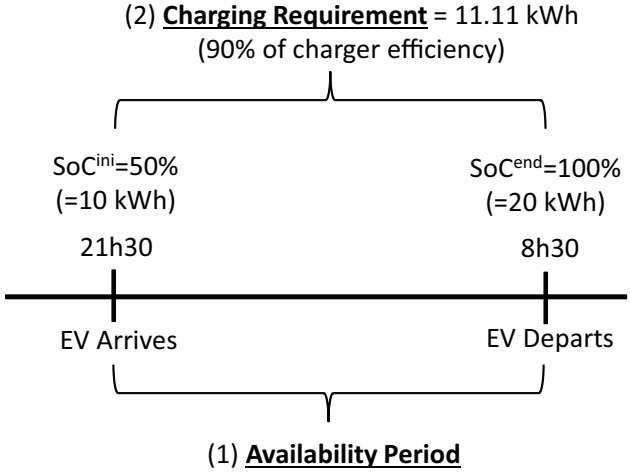

Figure 3.7: *EV variables: charging requirement and availability.*

the corresponding plugged-in period.

Note that this approach does not require personal information, such as driving routes (historical and planned) or the number of travelled kilometers. The metered values of these variables can be computed from the variables described in section 3.1.3 (i.e., EV status and electrical energy consumption) and the historical data is used for fitting forecasting models.

3.3.2 Very Short-term Horizon

The following sessions are included in the very short-term horizon: hour-ahead balancing reserve market; intraday market (typically in Europe); real-time market (typically in the USA).

The participation in the intraday market sessions is not mandatory, but it is foreseen that the aggregator will use these sessions to update day-ahead bids using recent information (e.g. very short-term forecasts, information transmitted by plugged-in EV). The same is valid for the real-time market and, in both cases, the aggregator is mitigating imbalances and corresponding financial penalties. Note that the price difference between real-time (or intraday) and day-ahead price can induce losses and income in case of differences to the day-ahead bid quantity [189].

Two situations are considered for balancing reserve: (a) day-ahead submission of bids that cannot be changed during the operating day; (b) day-ahead bids that can be adjusted or removed 45 minutes before the operating hour in an hour-ahead market for this reserve.

This thesis does not formulates optimization models for the participation in intraday and real-time markets. A bidding optimization model is proposed for the hour-ahead balancing reserve market. It takes as inputs hour-ahead forecasts for the reserve price and direction, as well as information transmitted by plugged-in EV (i.e., target SoC and expected departure time instant). Although not addressed in this thesis, the model can use hour-ahead forecasts for the EV variables.

3.3.3 Operational Management

Since it is not possible to produce perfect forecasts, it is necessary to have an operational management phase were the EV individual charging is coordinated to satisfy the contracted energy and reserve levels (i.e., bids for the short-term and very short-term horizons).

During the operating day, the TSO sends set-points requesting balancing and secondary reserve from the aggregator. Operational management algorithms are developed for the energy

and reserve markets and use information from the plugged-in EV as input. These algorithms may include very short-term forecasts for the EV variables. Forecasts for the imbalance prices due to deviations between purchased energy and actual consumption are also used as input.

3.3.4 Market Settlement

After the operating day, there is a settlement phase where the deviations from the market schedule (both energy and reserve) are determined using metered data for hourly (or half-hourly) periods and priced according to positive and negative imbalance prices. From this process, it results a cost term that is summed to the cost from purchasing electrical energy. The income from providing secondary or balancing reserve is also computed in this phase.

3.4 Final Remarks

This thesis adopts a hierarchical direct control architecture where the aggregator has direct control over the charging process of each EV and receives signals from the TSO/DSO for providing secondary and balancing reserve. This architecture covers three fundamental requirements for EV integration in the electricity market: a) copes with a minimum bid size limit around megawatts; b) reduces the communication requirements between TSO/DSO and EV; c) coordinates the EV individual charging to guarantee an acceptable reliability of the reserve provision and decrease imbalance costs.

In order to enable the aggregator concept and EV integration in the electricity market, it is necessary to develop a suitable business model. Nevertheless, the aggregator business model does not guarantee profitability, but creates the necessary conditions for it. The profit highly depends on the algorithms that an aggregator uses to participate in the electricity market and also on the commercial issues, such as setting the retailing tariffs (problem not addressed in this thesis).

A market framework, divided by different time horizons (with different available information), that covers the majority of the possible spot market sessions was defined. The goal is to design algorithms independently of specific market rules or that could handle different market rules with little adaptation. These algorithms optimize the bids for different market sessions (e.g., energy, secondary and balancing reserve). Furthermore, it is crucial to include forecasts for the input variables of the optimization problem and consider an operational management phase where the aggregator coordinates the EV individual charging in order to supply the contracted energy and reserve power levels.

These optimization models do not conduct long-term economic evaluation of the aggregator business activity, but their performance, measured by a reduction in the wholesale cost, provides the economic basis for setting retailing tariffs that simultaneously attract new clients and guarantee an interesting profit.

Chapter 4

Optimization Models for the Day-ahead Energy Market

Abstract

This chapter addresses the bidding optimization problem faced by the EV aggregator when participating in the day-ahead electrical energy market. Two alternative optimization approaches, *global* and *divided*, are described. The difference is on how information about EV is modeled. The *global* approach uses aggregated values of the EV variables, while the *divided* approach uses individual information from each EV. In any case, an operational management algorithm is required to minimize imbalance costs by mitigating the deviation between purchased energy and actual EV charging during the operating day. A realistic test case is used to study the impact of EV information modeling in the optimization models.

4.1 Introduction

The EV aggregator participates in the day-ahead electrical energy market (or energy market in abbreviated form) with bids for purchasing electrical energy for charging its clients. The optimized decisions related to this market are performed on a daily basis and the bids are not discriminated by EV.

The EV information can be modeled in the optimization model by two alternative approaches (depicted in Figure 4.1):

- *global* approach: the variables related to each EV are aggregated (summed) and the

optimization model determines the "optimal" bids entirely based on summed values of EV availability and charging requirement. EV individual information is not included in the optimization model;

- *divided* approach: the variables related to EV behavior are forecasted for each EV and the optimization model based on this information computes the optimal charging for each EV. The bid is equal to the sum of the optimized individual charging.

Both approaches have the same goal (i.e., solve the same problem), being the difference on how information about the EV is modeled in the optimization phase.

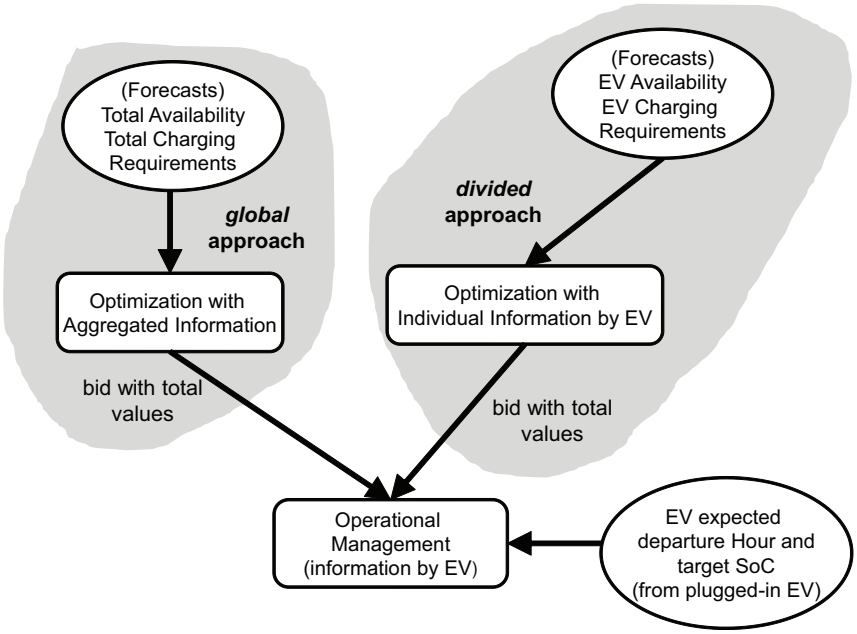

Figure 4.1: *Global and divided approaches for short-term management.*

After the participation in the day-ahead market and during the operating day, the aggregator uses an operational management algorithm to coordinate the EV individual charging in order to minimize imbalance costs (that result from the deviation between accepted bids and actual charging) and satisfy the drivers' charging requirements. This algorithm takes the following inputs: accepted bids from the day-ahead energy market; expected departure time interval, present and target SoC level of the plugged-in EV. This algorithm is discriminated by EV and explores the EV fleet flexibility since it allows different combinations of the individual EV charging to obtain different total values of the actual consumption.

An important part of this model chain consists in forecasting algorithms for the EV variables (i.e., availability period and charging requirement). In order to test the optimization models, statistical forecasting methods are proposed for these variables, which are handled as time series. A comparison with other time series forecasting algorithms is out of this chapter's

scope, since the goal in this thesis is to describe which variables should be forecasted and how it could be done and to assess the impact of information modeling and forecast errors in the optimization phase. Therefore, the forecasting algorithms are instrumental and were developed to enable a comprehensive evaluation of the optimization models.

This chapter is organized as follows: the *global* and *divided* approaches are described in sections 4.2 and 4.3; the operational management algorithm is described in section 4.4; section 4.5 describes the realistic test case used to compare the optimization approaches; sections 4.6-4.8 present a comparison between both approaches; section 4.9 discusses the main results.

4.2 *Global* Approach

4.2.1 Representation of the EV Information

The EV information in the *global* approach is represented by aggregated values of three variables. The first variable is the total maximum charging power, and the aggregated value is the sum of the maximum charging power of each plugged-in EV in a specific time interval. For example, if, in a specific time interval, 10 EV are plugged-in with a maximum charging power of 3 kW, the total maximum available power is 30 kW.

The second variable is the total charging requirement. The charging requirement of each EV is associated to a specific availability to charge (or plug-in) period and it is placed in the last time interval before departure. For example, consider an EV (with battery size 30 kWh) that plugs-in for charging at interval H1 with an initial SoC of 50%, expected to depart in time interval H9 with a target SoC of 100%. The charging requirement of this EV is 16.5 kWh (assuming a charger efficiency of 90%) and this value is placed in time interval H8 to construct the charging requirement time series of each EV. This variable means that 16.5 kWh must be supplied to the EV by the end of time interval H8. The total charging requirement is the sum of the individual time series.

The third variable is the total charging requirement distribution and the only difference is that the charging requirement is placed in all the time intervals of the availability period. For example, for the aforementioned EV, the 16.5 kWh are placed in all the time intervals between H1 and H8. This variable means that in each time interval of the period between H1 and H8 there is one EV that requires 16.5 kWh for reaching its target SoC.

4.2.2 Advantages and Limitations

The main advantage of the *global* approach is that the aggregated values present less variability and a more pronounced periodic behavior. Figure 4.2 depicts a seasonal plot [191] for a one-month time series from a single EV and from the number of plugged-in EV in a fleet with 1500 EV.

The time series are synthetic and generated by the method described in [22][192] (more details about the time series are given in section 4.5.1 where the test case is described and also in appendix A). The plot shows one-month of time series data grouped by the individual seasons (daily pattern) in which the data were observed. Each line in the plot, with 48 half-hours, is one day from the one-month time series; thus, each plot has 31 lines. The time series of one EV is binary and shows a high variability from day-to-day. The aggregated time series does not show a high daily variability and depicts two clear seasonal patterns: one for weekdays where the number of plugged-in EV in residential areas after 10 AM is low, and another for weekend days where the number of plugged-in EV is higher.

Another advantage is that the optimization problem has a low number of decision variables and constraints. The main disadvantage is that this approach does not fully capture the impact of the charging process in the total maximum charging power for each hour. To illustrate this statement, an example with three EV plugged-in during six hours, with maximum charging power of 3 kW, is given in Table 4.1.

The *global* approach uses as input the total maximum charging power. In this example, its value is 9 kW in each hour since the three EV are plugged-in during the six hours period. As the charging progresses in time, this total maximum power must be corrected by discounting the EV with full battery (or almost) but that remain plugged-in.

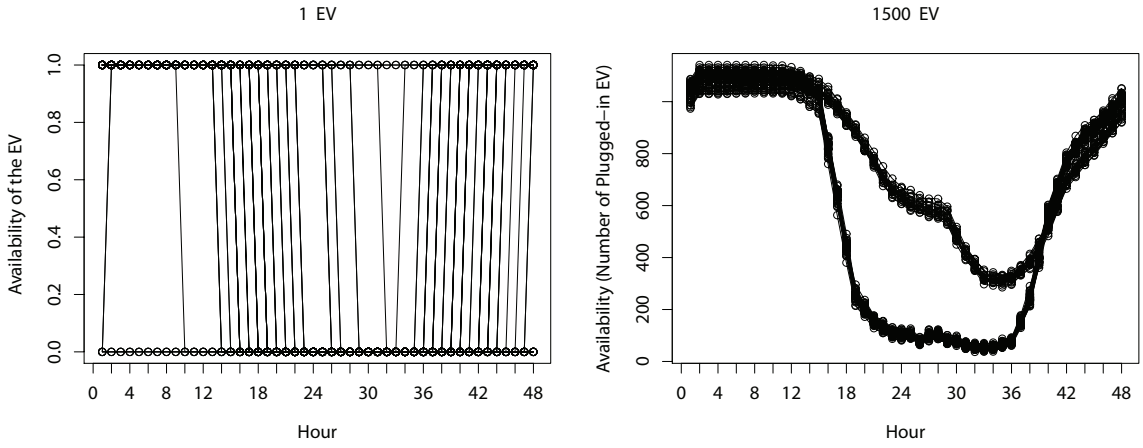

Figure 4.2: *Seasonal plots for EV availability of one and 1500 EV in half-hour time intervals.*

Table 4.1: *Illustrative example of three EV with charging process controlled by the aggregator.*

	H1	H2	H3	H4	H5	H6
Information used in the global approach						
Total (sum of) max charging power [kW]	9	9	9	9	9	9
Individual information from each EV	*Individual charging [kW]*					
EV-1 (needs 18 kWh for SoC = 100%)	3	3	3	3	3	3
EV-2 (needs 5 kWh for SoC = 100%)	3	0	2	0	0	0
EV-3 (needs 7 kWh for SoC = 100%)	3	0	3	1	0	0
Total adjusted max charging power [kW]	9	8	8	4	3	3

By analyzing the individual information, one can see that, in the beginning of hour H2, the total of charging requirement that remains to be satisfied is 21 kWh (30 kWh minus the 9 kWh charged in hour H1) but the maximum charging power is 8 kW instead of 9 kW because EV-2 can only charge additional 2 kWh. In the beginning of hour H4, the total charging requirement that remains to be satisfied is 10 kWh (9 kWh for EV-1 and 1 kWh for EV-3) but the maximum charge is decreased to 4 kW because EV-2 remains plugged-in but it is already full and EV-1 can only charge additional 1 kWh.

However, the *global* approach does not use individual information from each EV and the charging optimization is not performed individually for each EV; instead, it is made for the aggregated values of the EV fleet. If individual information was used (matter discussed in section 4.3), the aggregator would have information about which EV reached the target SoC (i.e., met the charging requirement) and it would not be necessary to calculate the total charging power.

4.2.3 Formulation of the Optimization Problem

The mathematical formulation of the optimization problem is the following:

$$\min \sum_{t \in H} \left(\hat{p}_t \cdot E_t \right) \tag{4.1}$$

subject to:

$$\sum_{j=1}^{t} \left(E_j \right) \geq \sum_{j=1}^{t} \left(\hat{R}_j \right), \quad \forall t \in H \tag{4.2}$$

$$\sum_{j=1}^{t} \left(E_j \right) - \sum_{j=1}^{t} \left(\hat{R}_j \right) \leq \hat{R}_t^D, \quad \forall t \in H \tag{4.3}$$

$$\frac{E_t}{\Delta t} \leq \hat{P}_t^{max} \cdot \left(1 - \alpha_t \right), \quad \forall t \in H \tag{4.4}$$

where E_t is the decision variable (i.e., optimized electrical energy), H a set of time intervals from the optimization horizon (e.g., one day), $\hat{p}_t$ the day-ahead energy price forecast for time interval t (a generic time interval), $\hat{R}_t$ the forecasted total charging requirement, $\hat{R}_t^D$ the forecasted total charging requirement distribution, $\hat{P}_t^{max}$ the forecasted total maximum charging power, α_t a factor that relates the maximum charging power to the percentage of satisfied charging requirement, Δt the time step (i.e., length of the time interval).

If the time step Δt is lower than the market time step (typically one hour), the bid's quantity (E_k^{bid}) is the sum of each E_t contained in the market time interval k. In this case, the market price is the same in each time interval contained in the market time step. Note that this time step should be defined according to the average duration of a trip or lower enough to capture EV that depart and arrive for charging.

The objective function (4.1) consists in minimizing the cost of buying energy E_t in the market for charging the EV fleet. The model has three constraints. The first constraint (4.2) guarantees that, when an EV departs, the energy required for satisfying the charging requirement was purchased in the energy market.

The constraint (4.3) guarantees that energy is only purchased in time intervals where there are sufficient EV plugged-in for charging the corresponding quantity. This constraint is explained with an illustrative example of three EV, presented in Table 4.2.

In this example, EV-1 and EV-2 are connected between H4 and H6 and have charging requirement equal to 9 kWh and 8 kWh correspondingly; EV-3 is plugged-in during six hours and has charging requirement equal to 3 kWh. The maximum charging power is 3 kW. The charging requirement is placed in the last time interval before departure, which is H6 for all EV. The sum of the individual values gives the total charging requirement (R_t). In the charging requirement distribution variable, the values are placed in the time intervals where the EV is plugged-in (e.g., the 9 kWh are placed in hours H4-H6 of EV-1). The sum for each hour is the total charging requirement distribution (R_t^D).

A possible E_t is also illustrated in the table. As shown in Table 4.2, constraint (4.3) limits to zero the energy purchased at H2 and H3 (otherwise the LHS would be greater than the R_t^D), since EV-3 is already charging 3 kWh in H1 (which is the EV charging requirement value) and, in time intervals H2 and H3, there are no additional EV plugged-in for consuming electrical energy. Without (4.3) it would be possible to have $E_t > 0$ at intervals H2 and H3 if these were hours with a price lower than in H4-H6.

The constraint (4.4) guarantees a purchased energy below or equal to the forecasted total maximum charging power ($\hat{P}^{max}$) in time step t. The factor α_t was introduced to adjust the

Table 4.2: *Illustrative example of the charging requirement distribution of three EV.*

	H1	H2	H3	H4	H5	H6
Individual information from each EV	*Charging req. [kWh]*					
EV-1 (needs 9 kWh for SoC = 100%)	0	0	0	0	0	9
EV-2 (needs 8 kWh for SoC = 100%)	0	0	0	0	0	8
EV-3 (needs 3 kWh for SoC = 100%)	0	0	0	0	0	3
	Charging req. dist. [kWh]					
EV-1	0	0	0	9	9	9
EV-2	0	0	0	8	8	8
EV-3	3	3	3	3	3	3
Information used in the global approach						
Total charging requirement [kWh]: $\hat{R}_t$	0	0	0	0	0	20
Total charging requirement dist. [kWh]: $\hat{R}_t^D$	3	3	3	20	20	20
E_t [kWh]	3	0	0	6	6	5
LHS of (4.3): $\sum_{j=1}^{t}\left(E_j\right)-\sum_{j=1}^{t}\left(\hat{R}_j\right)$	3	3	3	9	15	0

maximum charging power as the charging process evolves (problem explained in section 4.2.2 and illustrated by Table 4.1) and it is a linear function of the percentage of satisfied charging requirement[1] at the beginning of period t:

$$\alpha_t = \beta \cdot \left(\frac{\sum_{j=1}^{t-1}\left(E_j - \hat{R}_j\right)}{\hat{R}_t^D} \right), \quad \forall t \in H \tag{4.5}$$

The coefficient β is estimated from historical data (i.e., EV availability, charging requirement) to minimize the deviation between purchased energy and actual total EV charging. The estimation process has two steps: (a) run the *global* optimization model for different values of β; (b) select the β that leads to the lowest deviation. Historical data are available, unless the aggregator is starting its business; in this case, the aggregator should start with a high β value (above 0.5) to be conservative.

It is important to stress that (4.4) mitigates the problem, but it does not solve it totally. The problem can only be solved using information from individual EV, as in the *divided* approach that will be described in section 4.3. Moreover, this equation can also have other shapes, such as a quadratic function.

[1] In the example of Table 4.1, this percentage, in the beginning of interval H4 is given by $(9+5+6)/30 \cdot 100\% = 66.6\%$, and this corresponds to a reduction of 55.5% in the maximum power (from 9 kW to 4 kW).

4.2.4 Forecasting Tasks

It is assumed that the EV driver defines, when plugs-in the EV for charging, the target SoC and the expected departure hour. This information is unknown for the next day. Therefore, in order to use the day-ahead optimization model, the aggregator needs to forecast the following variables: total charging requirement ($\hat{R}_t$), total charging requirement distribution ($\hat{R}_t^D$) and the total maximum charging power ($\hat{P}_t^{max}$). The proposed forecast algorithm consisted in a linear model with lagged variables and covariates and can be written as:

$$y_t = \phi_0 + \phi_1 \cdot y_{t-1} + \phi_2 \cdot y_{t-2} + \cdots + \phi_l \cdot y_{t-l} + h_t + D_t + \varepsilon_t \tag{4.6}$$

where y is the response variable ($\hat{P}_t^{max}$, or $\hat{R}_t$, or $\hat{R}_t^D$), ϕ the model's coefficients, y_{t-j} the j$^{\text{th}}$ lag of the response variable y, l the maximum order of lagged variables, h_t a seasonal index that takes a different value for each hour of the day, D_t a seasonal index that takes a different value for each day of the week and ε_t an unobservable error term (or disturbance).
The model's coefficients can be fitted on historical time series data using the generalized least squares [193] (implemented in function *gls* from R package *nlme* [194]) since the model's residuals were found to be autocorrelated.

If the number of EV drivers under contract with the aggregator changes, the model parameters need to be re-estimated. Recursive least squares with forgetting factor can be used for estimating the coefficients in time varying conditions [195].

This model can also be used to forecast the load of inflexible EV.

To select the lagged variables, the first step is to check, using a unit-roots test [196], whether or not the time series is stationary. Then, the visual analysis of the autocorrelation diagram, together with the Akaike Information Criterion (AIC) [197], is used to select the lagged variables.

Figure 4.3 depicts an illustrative example of a total charging requirement forecast (for 1500 EV) and corresponding realized values from the synthetic time series that will be described in section 4.5.1 (a detailed analysis is also presented in appendix A).
This forecasted variable informs the total charging requirement that must be satisfied by the aggregator until the corresponding time interval. For example, it was forecasted that in the 43$^{\text{rd}}$ time interval there are EV departing totalizing a 1.04 MWh of charging requirement. Time intervals with charging requirement equal to zero (e.g., 30$^{\text{th}}$ time interval) mean that there are no EV departing by the end of this interval. The forecasted charging requirement shows a good fit to the realized value.

For the objective function (4.1), it is necessary to produce forecasts of the day-ahead energy

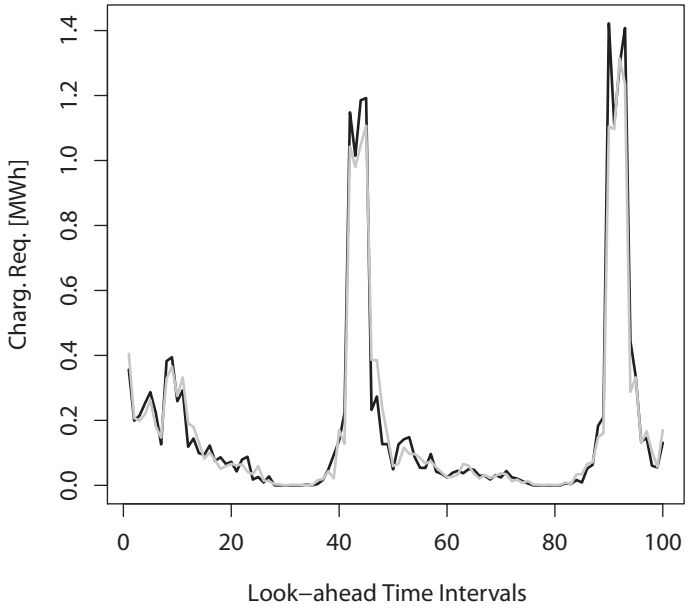

Figure 4.3: *Total charging requirement forecast (grey line) and realized value (black line).*

price. For this purpose, a forecast model, based on additive models theory [198] and with nonlinear relations modeled by smoothing splines, is proposed. The model is a linear predictor involving a sum of smooth functions of covariates and it is written as:

$$\hat{p}_t = \phi_0 + \phi_1 \cdot p_{t-1} + \phi_2 \cdot p_{t-2} + \cdots + \phi_l \cdot p_{t-l} + g\left(wp_t\right) + h_t + D_t + \varepsilon_t \tag{4.7}$$

where g is a smooth function estimated using cubic *basis* splines and wp_t the forecasted wind power penetration level.
The function g is a linear combination of known *basis* functions of the corresponding covariate:

$$g(x) = \sum_{j=1}^{s} \left(b_j(x) \cdot \omega_j\right) \tag{4.8}$$

where $b_j(x)$ is the j^{th} *basis* function for cubic splines, ω the coefficients of the regression model to be estimated with least squares and s the number of *basis* functions. Inserting (4.8) in (4.7) yields a linear regression model. It is necessary to define the number and location of the splines *knots*, which are the points where the sections of cubic polynomial join.
The cubic *basis* splines function can be constructed with function *gam* from R package *mgcv* [199].

For feature selection, the same procedure of the EV variables can be followed. Based on recent price forecasting literature [200] and also in preliminary results, it was decided to include as covariate the forecasted penetration of wind power (i.e., ratio between forecasted totals of load and wind power generation).

Finally, multi-step ahead forecasts are necessary for the optimization problem. For the mod-

els in equations (4.6) and (4.7) there are two alternative multi-step forecasting strategies: *iterated* and *direct* approach [201]. In the *iterated* approach, the one look-ahead time step forecast is computed and used as the "real" value for producing the forecasts for the second look-ahead time step, and the process is repeated iteratively and always using the same model. This approach has two disadvantages: (a) since the measured value is replaced by the forecasted value, the error is propagated through the time steps; (b) the model is fitted only for one-step ahead forecasts.
In the *direct* approach, k models are fitted for each look-ahead time step. The inputs are always the same in each model, while the response variable is the k step-ahead value. This model solves the two disadvantages of the *iterated* approach. Nevertheless, the k models are learned independently which induces a conditional independence and inhibits the modeling of temporal dependence.
Tests in the EV and price time series showed that the *iterated* approach leads to a better performance.

4.3 *Divided* Approach

4.3.1 Representation of the EV Information

In the *divided* approach, EV information is disaggregated by EV and represented by two variables. The first variable is the availability period, which is a binary variable indicating the time intervals where the EV is plugged-in and available for charging. The second variable is the charging requirement of each EV, associated to the specific availability period.

4.3.2 Advantages and Limitations

The *divided* approach uses the individual information from each EV, which prevents the problem of the maximum charging power (described in section 4.2.2), in contrast to the *global* approach.

However, the main disadvantage is that the availability and consumption time series of a single EV present a high variability (c.f., variability of a single EV in the left-hand side of Figure 4.2). This variability is reduced by aggregating the output from the individual optimization in order to submit the market bid, but it remains necessary to study the influence of the individual variability in the final solution. Another disadvantage is the very high dimension of the optimization problem, which may difficult the inclusion of information about uncertainties of the input variables.

4.3.3 Formulation of the Optimization Problem

The basic idea of the *divided* approach is to determine the market bids using individual information from each EV. The mathematical formulation is as follows:

$$\min \sum_{t \in H} \left(\hat{p}_t \cdot \sum_{j=1}^{M_t} \left(E_{t,j} \right) \right) \tag{4.9}$$

subject to:

$$\frac{E_{t,j}}{\Delta t} \leq P_j^{\max}, \quad \forall\, t \in H, \forall j \in \{1, \cdots, M_t\} \tag{4.10}$$

$$\sum_{t \in \hat{H}_j^{plug}[i]} \left(E_{t,j} \right) = \hat{R}_{j,i}, \quad \forall\, j \in \{1, \cdots, M_t\}, \forall i \in \left\{1, \cdots, L_j\right\} \tag{4.11}$$

where $E_{t,j}$ is the decision variable (i.e., optimized energy for charging the j$^{\text{th}}$ EV in time interval t), H a set of time intervals from the optimization horizon, $\hat{p}_t$ the day-ahead energy price forecast for time interval t (a generic time interval), $\hat{R}_{j,i}$ the forecasted charging requirement for the i$^{\text{th}}$ availability period of the j$^{\text{th}}$ EV, P_j^{max} the maximum charging power, $\hat{H}_j^{plug}[i]$ the i$^{\text{th}}$ forecasted availability period (from a set with L_j availability periods) of the j$^{\text{th}}$ EV, M_t the total number of EV plugged-in at time interval t, and Δt the time step. Note that each i$^{\text{th}}$ availability period is a vector of time intervals between t_{inital} and t_{final}, e.g. an EV that stops for charging two times has: $\hat{H}_j^{plug}[i=1] = \left[t_{inital} = 12\text{h}00; t_{final} = 16\text{h}00\right]$ and $\hat{H}_j^{plug}[i=2] = \left[t_{inital} = 18\text{h}00; t_{final} = 22\text{h}00\right]$.

The market bid E_k^{bid} is the sum of $E_{t,j}$ contained in the market time interval k.

The objective function minimizes the total cost of purchased energy. The constraint (4.10) limits the energy purchased for each EV by its maximum charging power. The constraint (4.11) ensures that the energy purchased for each availability period i of the j$^{\text{th}}$ EV matches the forecasted charging requirement for that period.

The optimization problem of equations (4.9)-(4.11) can be solved separately for each EV since there are no joint constraints between EV. Moreover, the optimal solution of this linear programming problem can be obtained with a heuristic method (similar to Wu et al. [165]) that ranks the forecasted energy price and defines the EV charging according to this price merit order.

In the *divided* approach, in addition to the day-ahead energy price, there are two variables that need to be forecasted for each EV: the EV availability period ($\hat{H}^{plug}$) and the charging requirement $\hat{R}_j$. The following section formulates a forecasting methodology for these variables.

4.3.4 Forecasting Tasks

The forecasting algorithm for the EV availability and charging requirement is divided into two phases. First, a binary variable for the EV availability is forecasted. Then, non-parametric bootstrapping is used to forecast the charging requirement associated to the forecasted availability period. This approach is inspired on the work of Willemain et al. [202] for estimating the entire distribution of the sum of the demands for service parts inventories over a fixed lead-time.

For the binary forecasting, the Generalized Linear Model (GLM) theory is used [203]. Compared to the classical linear models, GLM are for non-Gaussian response variables, such as count and binary data. The basic idea is to express linear models for a transformation of the mean value (*link* function) and keep the observations untransformed, which preserves the distributional properties of the observations. The *link* function is any monotone mapping of the mean value space to the real line used to form the linear predictor. The logit function *ln(a/(1-a))* was used.

In this problem, the response variable y is 1 if the EV is plugged-in or 0 otherwise. A natural distributional assumption is the Bernoulli distribution. The quantity modeled by the GLM is the *posterior* probability $p(y = 1|x)$, where x is a set of covariates. Let y_t be the response variable; the GLM for the EV availability can be written as:

$$\begin{gathered} prob\left(y_t = 1|y_{t-1}\cdots y_{t-l}\right) = \\ 1/\left(1+\exp\left(-\left(\phi_0+\phi_1\cdot y_{t-1}+\phi_2\cdot y_{t-2}+\cdots+\phi_l\cdot y_{t-l}\right)\right)\right) \end{gathered} \tag{4.12}$$

where *1/(1+exp(-a))* is the inverse of the *link* function. The model is a binary regression model with lagged values of the response variable and the coefficients can be estimated with the function *bayesglm* from R package *arm* [204].

Multi-step ahead forecasts are necessary for the EV availability. In the *iterated* approach, the forecasting model is fitted for one-step ahead forecasts and, because of this, the probability of having a 0 following a 1 (i.e., EV departing) would be very low for any look-ahead time step. For example, the model's coefficients from fitting (4.12) to a synthetic time series of one EV could be the following:

$$\begin{gathered} prob\left(y_t = 1|y_{t-1}\cdots y_{t-l}\right) = \\ 1/\left(1+\exp\left(-\left(-4.03+6.276\cdot y_{t-1}+0.6689\cdot y_{t-48}+1.05\cdot y_{t-336}\right)\right)\right) \end{gathered} \tag{4.13}$$

where the lags 48 and 336 are for modeling the daily and weekly seasonal pattern (with half-hour time steps).

With the model of (4.13), the *posterior* probability in time interval t of the forecast horizon is equal to 0.98 when $y_{t-1} = y_{t-48} = y_{t-336} = 1$, and equal to 0.9 when $y_{t-1} = 1$ and $y_{t-48} =$

$y_{t-336} = 0$. Moreover, the subsequent look-ahead time steps $t+1, t+2, \ldots$, will always have a *posterior* probability greater or equal to 0.9, even when $y_{t-48} = y_{t-336} = 0$. Therefore, the *direct* approach seems to be more appropriate; however, a modification is necessary to include the two seasonal patterns (daily and weekly). The modified *direct* approach is:

$$prob\left(y_t = 1 | y_{t-1} \cdots y_{t-l}\right) = 1/\left(1 + \exp\left(-\left(\phi_0 + \phi_1 \cdot y_{t-1} + \phi_2 \cdot y_{t-2} + \phi_3 \cdot y_{t-3} + \phi_4 \cdot y_{t-48} + \phi_5 \cdot y_{t-336}\right)\right)\right) \tag{4.14}$$

$$prob\left(y_{t+1} = 1 | y_{t-1} \cdots y_{t-l}\right) = 1/\left(1 + \exp\left(-\left(\phi_0 + \phi_1 \cdot y_{t-1} + \phi_2 \cdot y_{t-2} + \phi_3 \cdot y_{t-3} + \phi_4 \cdot y_{t-47} + \phi_5 \cdot y_{t-335}\right)\right)\right) \tag{4.15}$$

$$prob\left(y_{t+2} = 1 | y_{t-1} \cdots y_{t-l}\right) = 1/\left(1 + \exp\left(-\left(\phi_0 + \phi_1 \cdot y_{t-1} + \phi_2 \cdot y_{t-2} + \phi_3 \cdot y_{t-3} + \phi_4 \cdot y_{t-46} + \phi_5 \cdot y_{t-334}\right)\right)\right) \tag{4.16}$$

$$\ldots$$

where each model is fitted individually for each look-ahead time step. The difference for the standard *direct* approach is that the lagged variables related to the seasonal pattern are not fixed and change with the look-ahead time step.

After producing forecasts for the EV availability periods (i.e., sequence of intervals where $y_t = 1$), the second step is to use non-parametric bootstrapping [205] to estimate the charging requirement in each plugged-in period. The bootstrap samples are taken from an artificial time series created from historical charging values. This artificial time series consists in rearranging the historical charging data by removing the charging dependency from market prices inside each availability period; i.e., each EV starts charging when it plugs-in and until the charging requirement is satisfied. For example, an EV that needs 12 kWh for reaching full SoC will charge at 3 kW during the first 4 hours[2]. With this reorganization, the charging behavior only depends on the number of hours that the EV is plugged-in for charging (and, of course, on the initial and target SoC) and not on the market price.

The bootstrap samples are conditioned to the number of hours the EV is plugged-in. For example, for the first hour the bootstrapping technique resamples from the artificial time series, but only from historical data of consumption during the first hour of the availability period. The same process is followed for the subsequent hours. Summing the bootstrap samples inside each time interval of the availability period gives us the forecast for the charging requirement associated to a specific EV.

The bootstrapping technique is repeated N times and the result is a distribution of the charging requirement. This process is summarized in Algorithm 1, where $\hat{c}_{t+h}$ is a bootstrap sample

[2] This corresponds to the charging behavior of inflexible EV.

from the artificial charging time series for look-ahead time step $t+k$, $\tilde{R}_n$ the charging requirement of the bootstrap sample n, $plug.time_{t+h}$ the plugged-in hour of time interval $t+k$, and *aval.period* the availability period.

Algorithm 1: Forecast the charging requirement of each EV.

Data: Historical consumption data; availability forecast made at time step t for look-ahead time step $t+h$ ($y_{t+h|t}$); time horizon (Th)

Result: Charging requirement forecast for each availability period

while $n \leq N$ **do**

  for $h = 1 : Th$ **do**

    use GLM to forecast $y_{t+h|t}$;

    if $y_{t+h|t} = 1$ **then**

      $\text{plug.time}_{t+h} = \text{plug.time}_{t+h-1} + 1$;

      $\hat{c}_{t+h} = \text{bootstrap sample}|\text{plug.time}_{t+h}$;

    else

      $\text{plug.time}_{t+h} = 0$;

      $\hat{c}_{t+h} = 0$;

    end

  end

  $\tilde{R}_n = \sum_{k \in \tilde{H}_j^{plug}[i]} (\hat{c}_k)$

end

The N bootstrapping samples create the charging requirement distribution, from which the expected value and other statistics can be computed.

Figure 4.4 depicts an illustrative example of forecasted and realized values for the availability of one EV. The realized values are taken from a synthetic time series generated with the algorithm described in [22][192]. The forecasted value is obtained with the forecasting approach described in equations (4.14) and (4.15) for a time horizon of 100 look-ahead time steps.

The availability forecast shows three different situations: in the first period, the forecasted departure instant is before the realized one; in the second period, the forecasted arrival and departure instant do not match with the realized ones; in the last period, the forecasted departure time is after the realized one. These deviations of the availability variable can be called phase errors.

Based on the forecasted periods, the bootstrapping approach estimated a charging requirement of 11.52 kWh for the period between the 1st and 14th intervals (the realized value was 17.03 kWh for a period between the 1st-17th), for the period between the 54th and 67th inter-

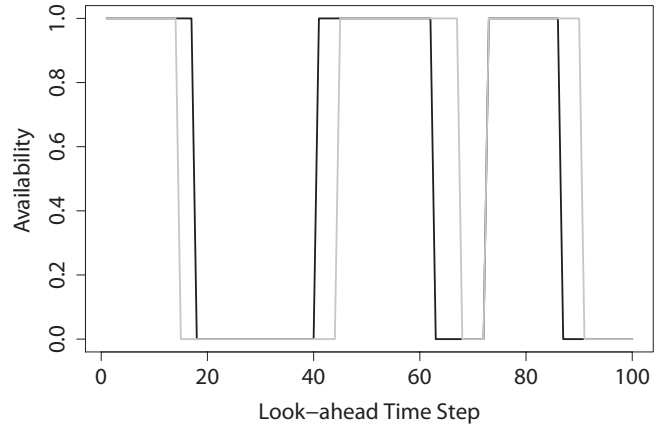

Figure 4.4: *Availability forecast (grey line) and realized value (black line) of one EV.*

vals the estimated charging requirement was 11.36 kWh (the realized value was 11.15 kWh for a period between the 41^{st}- 62^{nd}), and for the period between 73^{rd} and 90^{th} intervals the estimated charging requirement was 10.43 kWh (the realized value was 9.11 kWh for the period 73^{rd}-86^{th}).
The deviation between forecasted and realized charging requirement in the second and third periods is rather low, but in the first period there is an underestimation of the charging requirement. This means that the aggregator, for the first period, will purchase less energy in the day-ahead market than what will be required by the EV during the operating day.

4.4 Operational Management Algorithm

The two previous sections described two alternative day-ahead optimization models. Regardless of the day-ahead bidding optimization approach, an operational management algorithm is necessary to dispatch and combine the charging process of plugged-in EV, in order to minimize the imbalance costs due to deviations between accepted bid and actual charging.

This section describes an operational algorithm that optimizes the charging by EV even if the day-ahead bid results from a *global* optimization approach, which is independent of the algorithm used for the day-ahead bidding.

4.4.1 Formulation of the Optimization Problem

Prior to present the formulation of the operational algorithm, it is necessary to explain the calculation of the total cost from purchasing energy in the market since the definition of imbalance costs is relevant for the objective function.

When the aggregator has surplus of energy in the market bid, it has to sell this extra energy at an imbalance price ($p_t^{surplus}$), in general, below the day-ahead energy price (p_t); if the situation is shortage of energy, it has to pay an imbalance price ($p_t^{shortage}$), in general, above the day-ahead energy price [206]. This corresponds to the following equation for the total cost:

$$TotalCost = \sum_t \left(E_t^{bid} \cdot p_t + \begin{cases} -p_t^{surplus} \cdot \left(E_t^{bid} - E_t^{cons}\right), E_t^{bid} \geq E_t^{cons} \\ p_t^{shortage} \cdot \left(E_t^{cons} - E_t^{bid}\right), E_t^{bid} < E_t^{cons} \end{cases} \right) \tag{4.17}$$

where E_t^{bid} is the accepted energy bid in the day-ahead market for time interval t (the length of this interval is typically one hour and can be different from Δt), p_t is the day-ahead energy price, E_t^{cons} is the consumed electrical energy, $p_t^{surplus}$ is the price for positive imbalances and $p_t^{shortage}$ is the price for negative imbalances.

Equation (4.17) can be formulated to such that the total cost results from the cost of paying the consumed electrical energy at the energy price plus the imbalance costs. Thus, it becomes:

$$TotalCost = \sum_t \left(E_t^{cons} \cdot p_t + \begin{cases} \left(p_t - p_t^{surplus}\right) \cdot \left(E_t^{bid} - E_t^{cons}\right), E_t^{bid} \geq E_t^{cons} \\ \left(p_t^{shortage} - p_t\right) \cdot \left(E_t^{cons} - E_t^{bid}\right), E_t^{bid} < E_t^{cons} \end{cases} \right) \tag{4.18}$$

The first component of (4.18) corresponds to the cost incurred by the aggregator in case of zero deviations (i.e., cost exclusively from purchasing energy). The second component is the surplus or shortage imbalance costs, where the price difference $p_t - p_t^{surplus}$ is the positive imbalance unit cost (π_t^+) and the difference $p_t^{shortage} - p_t$ the negative imbalance unit cost (π_t^-).

The objective function of the operational management algorithm becomes the minimization of the imbalance cost [second part of (4.18)]. Note that the real goal of the aggregator is not to minimize individually the deviations of each EV; instead, it is to minimize the deviations of the aggregated EV fleet, which leads to a different solution. In its mathematical form, the objective function is given by:

$$\min \sum_{k=t_0}^{T} \left(\varphi \left(E_k - \sum_{j=1}^{M_k} \left(E_{k,j}^* \right) \right) \right) \tag{4.19}$$

where the decision variable $E^*_{t,j}$ is the electrical energy to be consumed by the jth EV in time interval t, T is the time interval of the last plugged-in EV to depart, t_0 is the current time interval, E_k is the result (or accepted bid) from a generic day-ahead optimization model, M_k is the number of EV plugged-in during time interval k, φ is the loss function given by

$$\varphi(u) = \begin{cases} u \cdot \hat{\pi}^+_k, u \geq 0 \\ -u \cdot \hat{\pi}^-_k, u < 0 \end{cases} \tag{4.20}$$

The piecewise linear convex function of (4.19) can be represented by:

$$\min \sum_{k=t_0}^{T} \left(\max \left(-u \cdot \hat{\pi}^-_k, u \cdot \hat{\pi}^+_k \right) \right) \tag{4.21}$$

where $u = E_k - \sum_{j=1}^{M_t} \left(E^*_{k,j} \right)$.

For a market with symmetric imbalance prices (i.e., $\pi^+_k = \pi^-_k$), the objective function is the minimization of the deviations absolute value.

This convex objective function can be transformed into an equivalent linear objective function problem by expressing the formulation in its epigraph form [207]. The objective function becomes:

$$\min \sum_{k=t_0}^{T} (v_k) \tag{4.22}$$

$$\left(E_k - \sum_{j=1}^{M_t} \left(E^*_{k,j} \right) \right) \cdot \hat{\pi}^+_k \leq v_k, \quad \forall k \in \{t_0, \cdots, T\} \tag{4.23}$$

$$-\left(E_k - \sum_{j=1}^{M_t} \left(E^*_{k,j} \right) \right) \cdot \hat{\pi}^-_k \leq v_k, \quad \forall k \in \{t_0, \cdots, T\} \tag{4.24}$$

$$v_k \geq 0 \tag{4.25}$$

where t_0 is the first time interval, v_k a positive slack variable that, due to constraints (4.23) and (4.24), can take the following values: zero when there is no imbalance, $u \cdot \hat{\pi}^+_k$ when the imbalance is positive and $u \cdot \hat{\pi}^-_k$ when it is negative. Therefore, minimizing the sum of v_k in (4.22) is analogous to minimizing imbalance costs in (4.21).

The following constraints are also included in the operational algorithm:

$$\frac{E^*_{k,j}}{\Delta t} \leq P^{\max}_{k,j}, \quad \forall j \in \{1, \cdots, M_k\}, \forall k \in H^{plug}_j[i], \forall i \in \{1, \cdots, L_j\} \tag{4.26}$$

$$\sum_{k \in H^{plug}_j[i]} \left(E^*_{k,j} \right) = R_{t_0,j,i}, \quad \forall j \in \{1, \cdots, M_k\}, \forall i \in \{1, \cdots, L_j\} \tag{4.27}$$

where $H_j^{plug}[i]$ is the ith availability period of the jth EV, $R_{t_0,j,i}$ is the residual charging requirement for the ith availability period of the jth EV at the beginning of time instant t_0.

The constraint (4.26) limits the EV charging by its maximum power. The constraint (4.27) enforces the charging requirement communicated by the EV driver.

The Δt of the operational management algorithm must be lower or equal to the one used in the day-ahead *global* or *divided* optimization and enough to capture arrival and departures of EV.

The operational management algorithm uses the realized values of $H_j^{plug}[i]$ and $R_{t_0,j,i}$ from the plugged-in EV. Information from EV that will connect in future time intervals is not used or forecasted [i.e., $i = 1$ in (4.26) and (4.27)]. Nevertheless, the inclusion of this additional information does not require significant changes in the algorithm, but it means an increase of the computational running time[3]. One possibility to improve computational performance is to use parallel computing for the forecasts.

Note that the result from the day-ahead optimization (E_k) is only greater than zero for the market clearing period, and for time intervals outside of this period E_k, π_k^- and π_k^+ are made equal to zero. For instance, in $t_0 = 5^{th}$ hour, k takes values between t_0 and T but there is only energy purchased for the 24 hours period of the market, thus, the E_k is only greater than zero between t_0 and the 24th hour. Nevertheless, the optimization problem is solved for $k > 24^{th}$ hour since it is necessary to satisfy the charging requirement constraint (4.27) of the EV that depart after the 24th hour (i.e., $T > 24^{th}$ hour).

This optimization problem is solved in each time interval with the following sequential process:

1. new information (expected departure time instant and target SoC) from the recently plugged-in EV (i.e., that connected for charging between $t_0 - 1$ and t_0) is included in equation (4.27) of the optimization model;

2. the optimization problem is solved with this new information for a period between t_0 and the maximum departure hour of all the EV (which is updated every t_0); $\hat{\pi}_{t_0}^+$ and $\hat{\pi}_{t_0}^-$ are made equal to a large number (e.g., 1000) in order to force the deviation to be zero at time interval t_0;

3. set points corresponding to the optimal charging levels for time interval t_0 are transmit-

[3] A forecast for each EV takes 0.2 seconds, e.g., a 3 months participation in the electricity market would take additional 180 hours for a fleet with 1500 EV.

ted to the plugged-in EV; only the dispatch for time interval t_0 remains unchanged, the charging levels for the subsequent time intervals can be modified in the next time interval $(t_0 + 1)$. The charging requirement $R_{t_0,j}$ is updated for the next period, $R_{t_0+1,j} = R_{t_0,j} - E^*_{t_0,j}$;

4. this optimization process is repeated for the next time interval, $t_0 + 1$ (go back to step 1).

4.4.2 Forecasting the Imbalance Unit Costs

For the constraints (4.23) and (4.24), it is necessary to forecast the imbalance unit cost. In this thesis, an approach based on additive models is used:

$$\begin{aligned} y_t = \phi_0 + \phi_1 \cdot y_{t-1} + \phi_2 \cdot y_{t-2} + \cdots + \phi_l \cdot y_{t-l} + g\left(wp_t\right) + \\ g\left(I_t^{\text{Import}}\right) + g\left(I_t^{Export}\right) + g\left(p_t\right) + h_t + \varepsilon_t \end{aligned} \tag{4.28}$$

where g is a smooth function estimated using cubic basis splines, p_t the energy price from the day-ahead market, I_t^{Import} and I_t^{Export} the cross-border interconnection exchanges (exported and imported electrical energy) of the bulk power system. The response variable y is the positive $(\hat{\pi}_t^+)$ or negative $(\hat{\pi}_t^-)$ imbalance unit costs.
During the operating day, the energy price, export and import cross-border interconnections exchange are already known since these values result from the day-ahead market clearing.

It is important to stress that this model should be seen as a first approach to the problem and it is a topic for future improvement.

4.5 Test Case Description

This section presents the test case used to compare and evaluate the two alternative optimization approaches. The test case uses real electricity market data, only the EV data is synthetic and tries to mimic a forthcoming situation. Note that the price levels of the electricity market are without the presence of EV, but the goal of this evaluation is not to quantify the impact of EV in the electricity prices but rather to evaluate the robustness and applicability of the optimization models.

4.5.1 EV Synthetic Time Series

To produce time series of the EV availability and consumption, the generation mechanism to create EV synthetic time series described in [22] and [192] was used. The movement of a fleet with 3000 battery EV along one year was simulated using a discrete-time-space Markov chain at each time step of half-hour (which is the average trip duration in Portugal), in accordance with the common traffic patterns in the northern region of Portugal [208]. The statistical post-processing of these traffic patterns is described in [22].

Having the EV movements fully defined, their power consumption was computed. Each EV was initially characterized in terms of battery capacity, energy consumption and battery SoC in the beginning of the simulation. These values were defined according to truncated Gaussian probability density functions. The mean, standard deviation, maximum and minimum values are given in Table 4.3.

The initial battery SoC values were defined as a parameter in the simulation, while the other two variables were gathered from the information made available by 42 different EV manufacturers. The charger efficiency was assumed to be 90% and the battery depth of discharge was 10%.

A specific driver behavior was also assigned initially to each EV. The possible behaviors considered in this paper were obtained from a survey made within the framework of the MERGE project [134]. The results revealed that there are three major types of behavior regarding EV charging, as presented in Table 4.4. Note that drivers of type 0 normally charge at home, while types 1 and 2 charge at home and office (or industrial area).

The simulation methodology assumes that, at every time interval, each EV can be in one of the following states: in movement, parked in a residential area, in an industrial area, in a commercial area or in a fast-charging station. When the state is “in movement”, the energy consumption and the respective reduction in the battery SoC are computed. At each time interval, the EV battery SoC is updated according to the energy spent traveling or according to the energy absorbed from the electrical network.

Table 4.3: *Parameters of the truncated Gaussian probability density function [192].*

	Mean	Std. Dev.	Max.	Min.
Battery capacity [kWh]	24.73	17.19	85.00	5.00
Slow charging rated power [kW]	3.54	1.48	10.00	2.00
Energy consumption [kWh/km]	0.18	0.12	0.85	0.09
Initial battery SoC [%]	75.00	25.00	95.00	25.00

Table 4.4: *Three types of behavior regarding EV charging.*

Type	Behavior	Percentage of the Responses
0	EV charges after the last trip of the day	57%
1	EV always charges when parked	20%
2	EV charges only when it needs[a]	23%

[a] It was defined a battery SoC threshold for charging equal to 40%.

Three charging levels were considered for the simulation: EV "parked in a residential area" and "parked in an industrial area" charge at 3 kW (i.e., home and office charging points), EV "parked in a commercial area" charge at 12 kW (i.e., public and shopping center charging points) and the charging power in fast-charging stations is 40 kW [134].

When an EV is parked, the decision of whether or not plugging it in for charging is made taking into consideration its driver's behavior (see Table 4.4) and its current SoC (only for type 2 drivers). This test case only studies EV parked in residential and industrial areas.

The simulation methodology provides, for a one-year period with half-hour time intervals (Δt=0.5 hr in all the optimization problems), the following time series: the periods where EV are plugged-in and available to charge, the EV power absorbed at each time interval (assuming that the EV starts charging when it plugs-in), the EV battery SoC evolution and the EV traveled distances. These time series are used for fitting the forecasting algorithms (as historical data), producing forecasts with these algorithms and testing the optimization models.
A statistical analysis of the EV synthetic time series can be found in appendix A.

4.5.2 Electricity Market

The case-study follows the data and rules of the Iberian electricity market [53]. For the day-ahead energy market, the market agents may present buy and sell hourly bids that cover all 24 hours of the next day (physical delivery period). The gate closure occurs at the 10h00 hour.

In general, the day-ahead session structure and rules do not change from market to market. Therefore, the *global* and *divided* algorithms can be directly applied to different electricity markets without significant changes.

The total cost is computed with equation (4.18) and for an hourly time step. The imbalance prices ($p_t^{surplus}$ and $p_t^{shortage}$) in the Portuguese control area are related to the tertiary reserve (or *reserva de regulação*) prices. For simplicity and without loss of generality, it is assumed

that both are the same.

The electricity market data of the case-study is from a three year period (2009-2011) of the Iberian electricity market (control area of Portugal) and consists of: electrical energy price of the day-ahead market for Portugal[4]; price of upward and downward tertiary reserve for Portugal[5]; interconnection exchanges between Portugal and Spain (from OMIE website); day-ahead load and wind power forecast for the Iberian Peninsula[6].

A statistical analysis of the market prices data can be found in appendix A.

4.5.3 Participation in the Electricity Market

Figure 4.5 depicts a diagram with the sequence of tasks of the aggregator participation in the Iberian electricity market.

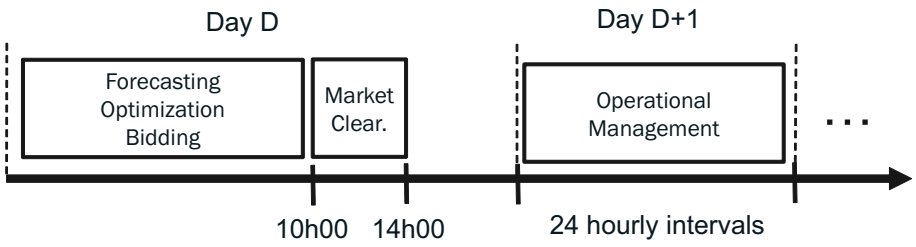

Figure 4.5: *Diagram with the sequence of tasks for participating in the Iberian electricity market.*

Before 10h00 of day D, the aggregator forecasts the market and EV variables for day D+1, computes optimal bids based on these forecasts, and then presents bids in the day-ahead energy market. The market clearing process takes place between the 11h00 and 14h00 of day D. Then, during day D+1, the aggregator manages the EV individual charging to minimize the imbalance costs that result from the deviation between bids (presented in day D) and actual consumption in day D+1.

Figure 4.6 depicts the diagram with the temporal horizons of the forecast and optimization models.

The bidding optimization is performed for the market clearing period (24 hours of day 1), but extended to have 12 additional hours since most of the EV are expected to depart in day 2. Since the gate closure of the day-ahead energy market is 10h00 and Δt=0.5 hr, the aggregator needs to forecast the EV variables for a time horizon of 100 half-hour time intervals

[4] [OMIE - Market Operator of MIBEL] http://www.omie.es/inicio (accessed in December 2012).
[5] [REN market data] http://www.mercado.ren.pt/Paginas/default.aspx, (accessed in December 2012)
[6] [e-sios, REE] http://www.esios.ree.es/web-publica/ (accessed in December 2012).

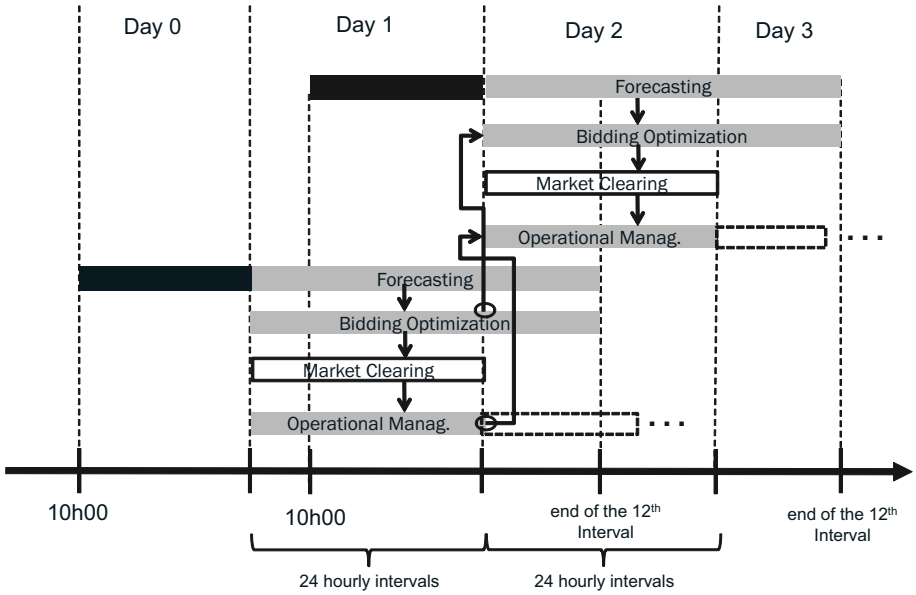

Figure 4.6: *Diagram with the temporal horizons of the forecast and optimization models.*

(i.e. between 10h00 of day 0 and 12h00 of day 2). Only the forecast between the first time interval of day 1 and the 12^{th} time interval of day 2 is an input of the bidding optimization model.

The output of the bidding optimization until the 24^{th} interval of day 1 is one input of the bidding optimization exercise in day 2 (as illustrated by the arrow in Figure 4.6), and this interaction is repeated in each day. This guarantees the temporal continuity of the charging process.

The output of the day-ahead optimization (or the output from the market clearing) is an input of the operational management algorithm. The time horizon of the operational algorithm is variable and equal to the maximum departure hour of all the EV. The output until the 24^{th} interval of day 1 is an input of the subsequent optimization in day 2 (as illustrated by the arrow in Figure 4.6). The market clearing results of the energy market is made available at 14h00 of day 2 and this result is used to extend the period with accepted bids (i.e., where $E_k > 0$) of the operational management algorithm.

In order to assess the advantages and limitations of the optimization approaches for flexible EV, the two bidding approaches will be compared (e.g., quantify the cost decrease with flexible charging) with the situation where all the clients charging at home/office points are inflexible EV loads. In this mode, the charging starts immediately when the EV plugs-in. The aggregator, in this case, is a standard electricity retailer that forecasts the total consumption and offers in the day-ahead energy market a bid equal to the forecasted load for each time interval.

4.5.4 Forecasting Models

Sections 4.2.4 and 4.3.4 describe generic statistical forecasting algorithms for the different input variables. Here, the statistical models specifically used in the test case are described, with particular emphasis on the selected lag terms and covariates.

Aggregated EV Variables

Three different EV variables are required for the *global* approach: total maximum charging power, total charging requirement and charging requirement distribution. Moreover, for the inflexible EV it is also necessary to forecast the total consumption.

The application of a unit-roots test showed that all the four time series are stationary. The analysis of the autocorrelation diagrams for the aggregated variables (which can be found in appendix A) shows a daily (higher peak in lag 48) and weekly (higher peak in lag 336) patterns. Therefore, based on this information and using the AIC as a performance metric, the following model was used to forecast the four variables:

$$y_t = \phi_0 + \phi_1 \cdot y_{t-1} + \phi_2 \cdot y_{t-2} + \phi_3 \cdot y_{t-48} + \phi_4 \cdot y_{t-336} + h_t + D_t \tag{4.29}$$

The analysis of the forecast error can be found in appendix B.

The function *gls* from R package *nlme* [194] was used to estimate the coefficients using generalized least squares. On a laptop computer with an Intel Core i5 CPU M450 @ 2.40 GHz processor and 4 GB of RAM, the execution time for estimating the model's parameters was 106 seconds on average and 0.45 seconds for producing a single forecast with 100 look-ahead time steps.

Individual EV Variables

For each EV, the availability is first forecasted and then non-parametric bootstrapping is used to estimate the charging requirement for each plugged-in period.

The drivers of the three different types described in Table 4.4 exhibit different autocorrelation diagrams for the availability time series (the autocorrelation plots are shown in appendix A). The difference is particularly clear between types 0/1 and type 2. EV drivers of types 0 and 1 have a clear double seasonal pattern (i.e. daily and weekly), while type 2 drivers do not have a seasonal cycle. Thus, because of different autocorrelation patterns, two GLM were

considered:

$$prob\left(y_t = 1 | y_{t-1} \cdots y_{t-l}\right) = \\ 1/\left(1 + \exp\left(-\left(\phi_0 + \phi_1 \cdot y_{t-1} + \phi_2 \cdot y_{t-2} + \phi_3 \cdot y_{t-3} + \phi_4 \cdot y_{t-48} + \phi_5 \cdot y_{t-336}\right)\right)\right) \tag{4.30}$$

for types 0 and 1 drivers, and

$$prob\left(y_t = 1 | y_{t-1} \cdots y_{t-l}\right) = \\ 1/\left(1 + \exp\left(-\left(\phi_0 + \phi_1 \cdot y_{t-1} + \phi_2 \cdot y_{t-2} + \phi_3 \cdot y_{t-3} + \phi_4 \cdot y_{t-4}\right)\right)\right) \tag{4.31}$$

for type 2 drivers. In both cases, y is a binary variable indicating whether or not the EV is plugged-in. The same lagged variables were used for all EV from the same type.

The analysis of the forecast error can be found in appendix B.

The execution time for the charging requirement forecast (including the GLM fitting and availability forecast) was 8.56 seconds for one EV and for a single forecast with 100 look-ahead time steps, while for a single forecast without GLM fitting was 0.2 seconds. The execution times of this forecasting algorithm might be prohibitive if the number of EV is high. For the simulations, the execution time is around 8 hours for 1500 EV during a test period of 3 months. However, this process can be parallelized and an implementation in C or Fortran would increase considerably the computational performance.

Market Prices

The unit-root test showed that the price time series is non-stationary and a differentiation of order 1 is needed [this means replacing y by $\Delta y = y_t - y_{t-1}$ in equation (4.7)]. Moreover, based on the autocorrelation diagram with a daily and weekly seasonal cycle (shown in appendix A) and using the AIC, the following model was used to forecast the day-ahead energy price:

$$\Delta\hat{p}_t = \phi_1 \cdot \Delta p_{t-1} + \phi_2 \cdot \Delta p_{t-2} + \phi_3 \cdot \Delta p_{t-24} + \phi_4 \cdot \Delta p_{t-168} + g\left(wp_t\right) + h_t + D_t \tag{4.32}$$

where $\Delta\hat{p}_t$ is a first-order differentiation $(p_t - p_{t-1})$ of the day-ahead energy price.

The interior knots of the basis splines were placed in each quantile according to 6 degrees of freedom (which attains the lowest AIC). The boundary knots were placed in the extremes of the data.

The following model was used to forecast the negative imbalance unit cost:

$$\Delta\hat{\pi}_t^- = \phi_1 \cdot \Delta\pi_{t-1}^- + \phi_2 \cdot \Delta\pi_{t-2}^- + \phi_3 \cdot \Delta\pi_{t-24}^- + \phi_4 \cdot \Delta\pi_{t-168}^- + g\left(wp_t\right) + g\left(I_t^{\text{Import}}\right) + g\left(p_t\right) + h_t + D_t \tag{4.33}$$

The degree of freedom for the knots is 10.

For the positive imbalance unit cost $\hat{\pi}_t^+$ (i.e. difference between surplus regulation and energy price), the model of equation (4.33) is used, but with I_t^{Import} replaced by I_t^{Export}.

The analysis of the forecast error can be found in appendix B.

4.5.5 Sampling Process for Evaluation

For a robust evaluation of the optimization results, a sampling process based in [209] was adopted for producing random repetitions of a simulation experiment. The objective is to evaluate the optimization results for different market data randomly sampled (but maintaining the temporal sequence) from the three year period. Since the forecasting algorithms require training and evaluation datasets, a fixed length for these two sets was defined: 9 months for the training dataset, 3 months for the evaluation dataset.

Then, a sampling process without replacement is used to draw the first hour of the day, n, from the candidate set. This sample is used to split the three years of data in training (between $n-9$ months and n) and evaluation (between n and $n+3$ months) datasets. The process is repeated 100 times and, for each sample n, the *global* and *divided* optimization models are applied to the evaluation dataset (using the process described in section 4.5.3 for the market participation), and corresponding costs of purchasing electricity (including imbalance costs) are computed. The result, instead of a single value for the total cost, is a distribution with 100 samples.

This sampling process is only used in the electricity market data. Due to a high calculation time (in particular in the *divided* approach), it is not possible to apply this sampling process to the EV data. In order to test the optimization methodologies in different EV data, the synthetic time series for 3000 EV is divided into two groups of 1500 EV: fleets A and B. Moreover, each EV dataset is divided as follows: the first 9 months for fitting the models and the last 3 months for evaluating optimization models and producing forecasts for the EV variables.

A detailed characterization of fleets A and B is given in appendix A, but in summary, fleet A is more flexible and requires less energy for charging (i.e., the EV from fleet B present a lower SoC when they arrive for charging compared to fleet A).

4.6 Comparison Between *Global* and *Divided* Optimization Models

For the *global* approach, it is necessary to set the value of the β parameter, which adjusts $\hat{P}_t^{max}$ linearly as the charging process evolves. Using the complete year of 2010 as a dataset and realized values of all input variables, the deviations between accepted bid and actual charging were computed for each β value and the value that leads to its lowest value was selected. The result was a β equal to 1.0 and 0.8 for fleets A and B correspondingly (section 4.7 presents sensitivity analysis of the β value).

The optimization problems are solved with IBM ILOG CPLEX 12.2 optimizer [210] using the Python API. The execution time of the *global* approach for a time horizon (H) of 72 half-hour time intervals was 0.041 seconds. For the *divided* approach, it was 0.639 seconds for 1500 EV and, for the operational algorithm, the maximum execution time was 0.475 seconds.

The comparison between the *global* and *divided* approaches, in terms of deviation between accepted bid and actual charging values and costs from participating in the market, is conducted in the 100 samples generated with the sampling process described in section 4.5.5. Though, first, an illustrative example of the optimization output and results is presented.

4.6.1 Illustrative Example of the Optimization Models Output and Results

Figure 4.7 depicts an illustrative example of the day-ahead optimization output (i.e., accepted energy bid) from the two approaches for one day of the evaluation dataset. The plot shows a dissimilarity between the two approaches in all time intervals. The *global* approach has time intervals with no purchased energy in both days (in particular during the last seven hours), while the *divided* approach purchased energy in all time intervals.

This suggests that the energy purchased by the *global* approach is more concentrated, which may create difficulties in avoiding deviations. Conversely, the energy purchased by the *divided* approach is more dispersed, which may facilitate the operational management algorithm. As expected, the hours with higher energy purchased are during the night, where the forecasted prices have low values.

The estimated cost from energy purchasing (i.e., the value of the objective function) for the next day was 303.9 € with the *global* approach and 324.8 € with the *divided* approach.

During the operating day, the aggregator uses the operational management algorithm to coordinate the EV charging and minimize the imbalance costs. The output of the operational

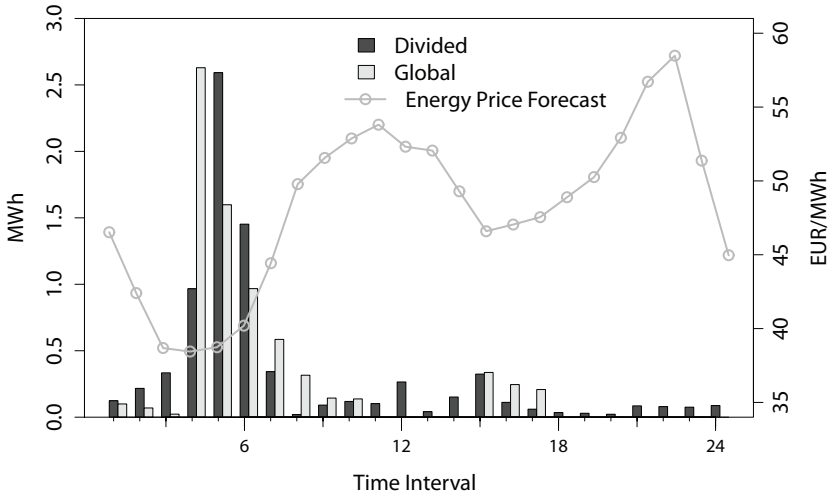

Figure 4.7: *Accepted bids of the global and divided approaches and day-ahead energy price forecast for one illustrative day.*

algorithm are the actual charging values by EV and the sum of the individual charging values is depicted together with the accepted bid in Figure 4.8a for the *global* approach and 4.8b for the *divided* approach. The energy price forecast and realized value are also presented.

Due to the imbalance costs and the mismatch between forecasted and realized energy price, the actual cost of energy purchasing will be different from the estimated one. In this illustrative day, the actual cost was 292 € for the *global* approach (280.5 € for $E_t^{cons} \cdot p_t$ and 11.5 € for the imbalance costs) and 277.4 € for the *divided* approach (276.1 € for $E_t^{cons} \cdot p_t$ and 1.3 € for the imbalance costs). In this case, the true cost was lower than the estimated cost, because the forecast overestimated the energy prices. A comparison between the costs obtained with both bidding approaches for the three months evaluation dataset of the 100 samples will be presented in section 4.6.3.

Figure 4.8 also shows that the *global* approach, for the period between the 19th and 24th time intervals (where the energy bids were zero), presented negative deviations between accepted bid and actual charging values (energy shortage) with a total of -0.48 MWh, while in the *divided* approach the deviations were only -0.09 MWh. In other periods, such as between the 4th and 7th time intervals, the deviations were positive in the *global* approach (0.3 MWh) and zero in the *divided* approach. The next section compares the absolute value of the deviations obtained with both approaches for the three months evaluation dataset of the 100 samples.

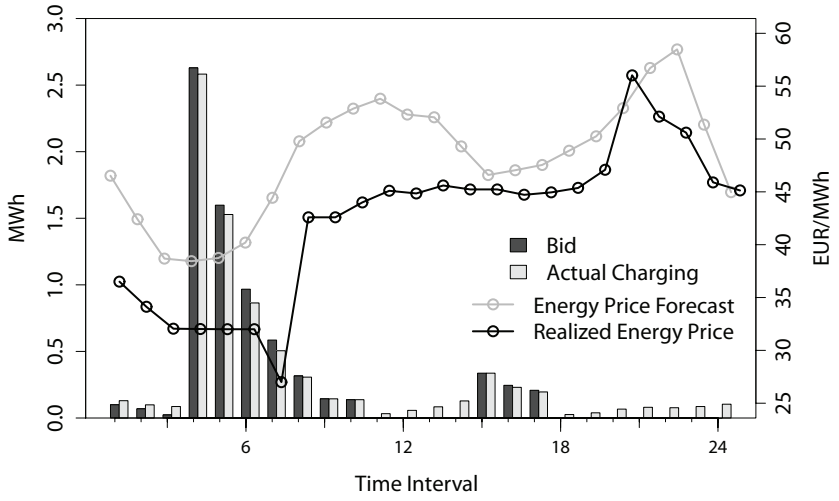

(a) *Global.*

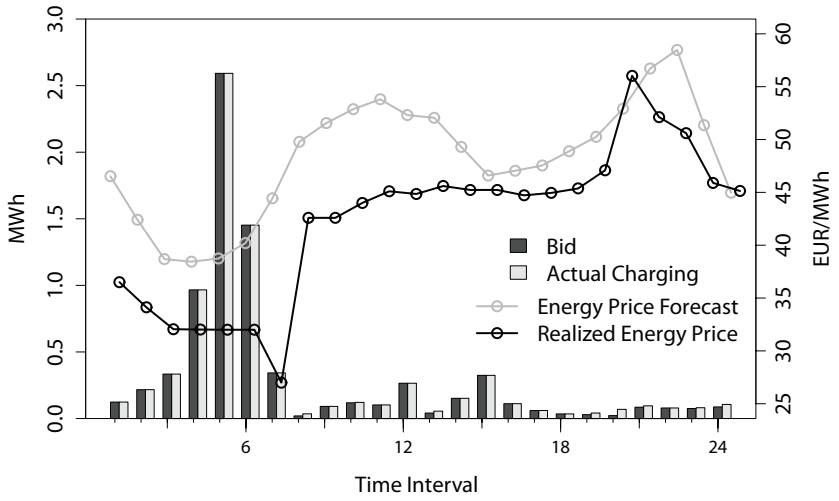

(b) *Divided.*

Figure 4.8: *Accepted bids and actual charging (from the operational algorithm), day-ahead energy price forecast and realized values for one illustrative day.*

4.6.2 Comparison of the Deviations Between Accepted Bid and Actual Charging Values

The *divided* and *global* approaches use different forecasts for the EV variables and a merely evaluation of their forecast error (results presented in appendix B) does not give complete information about the algorithms' performance. Conversely, the deviation between accepted bid (output of the day-ahead optimization) and actual charging values (output of the operational algorithm) impacts the imbalance costs of the aggregator. Therefore, this section compares the Mean Absolute Percentage value of the Deviations (MAPD) between bid (E_t) and actual

charging $\left(\sum_{j=1}^{M_t}\left(E^*_{t,j}\right)\right)$, calculated for each market time interval t (i.e., one hour):

$$MAPD = \frac{\sum_t \left(\left|\sum_{j=1}^{M_t}\left(E^*_{t,j}\right) - E_t\right|\right)}{\sum_t \left(\sum_{j=1}^{M_t}\left(E^*_{t,j}\right)\right)} \cdot 100 \tag{4.34}$$

The Deviations Bias (DBIAS), that measures whether there is an overall surplus or shortage of energy in the accepted bid, is also used:

$$DBIAS = \frac{\sum_t \left(\sum_{j=1}^{M_t}\left(E^*_{t,j}\right) - E_t\right)}{\sum_t \left(\sum_{j=1}^{M_t}\left(E^*_{t,j}\right)\right)} \cdot 100 \tag{4.35}$$

Figure 4.9 depicts boxplots[7] with the two metrics for the *divided* approach with forecasted information and for the two fleets. The deviation between accepted bid and actual charging values is 9.4% on average in fleet A and 10.7% in fleet B. As shown in appendix B, the forecast error of the individual variables (availability and charging requirement) in fleet B is slightly worse than in fleet A, which explains the higher MAPD.

Since the EV dataset is always the same in each random sample, the variation in MAPD from sample to sample is only due to different energy and imbalance prices. In other words, these deviations occur because the energy is purchased in different time intervals according to the forecasted prices. The small variation in both metrics indicates that the *divided* approach is robust to the electricity market conditions (i.e. energy price ranking).
The values of the DBIAS show that in fleet A the accepted bids underestimate (positive bias) the actual charging (shortage of purchased energy), while in fleet B the bids overestimate the actual charging (surplus of purchased energy).

Figures 4.10 and 4.11 depict the two metrics for the *global* approach using two different sets of inputs for the day-ahead *global* optimization model: (a) forecasts for the EV variables and market prices; (b) realized values of the EV variables and market prices (the realized value of the imbalance prices is also used in the operational algorithm).

Note that in the *global* approach, using the realized values of the EV variables (total charging requirement and maximum power) is different from using the actual charging values that

[7] The boxplot has five statistics: lowest datum (within 1.5 IQR) of the lower quartile, lower quartile, median, upper quartile, and the highest datum (within 1.5 IQR) of the upper quartile. The outliers are also identified on the boxplot.

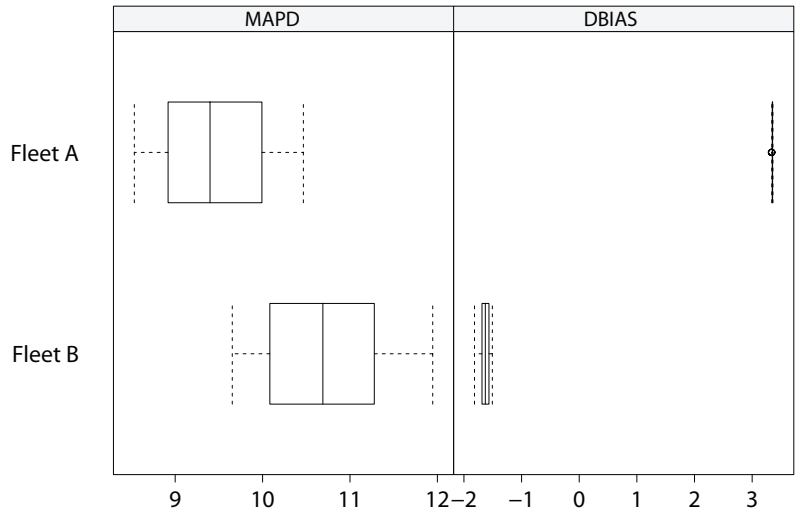

Figure 4.9: *MAPD of the divided approach with forecasted information for fleets A and B.*

result from the operational algorithm, because the operational algorithm uses individual information from the EV and the *global* approach does not. Therefore, and as demonstrated in section 4.2.2, the *global* approach with the realized values as input presents deviations that are not due to forecast errors, but are related to information loss when only aggregated values are used for computing the optimal bid.

The MAPD in this bidding approach, in contrast to the *divided* approach, has a more widespread variation for different market conditions. For instance, the boxplot for fleet A with forecasted information varies between 19% and 29%.
The average values of the MAPD are also higher compared to the *divided* approach: 24.4% with forecasted and 25.5% with realized values in fleet A; 19.6% with forecasted and 19.3% with realized values in fleet B. In the case of fleet A, the MAPD with forecasted values is lower on average than the one obtained when using realized values. This means that these deviations are originated by the loss of information from using aggregated information, which is difficult to detach from the influence of forecast errors.

The results for DBIAS show that for fleet A the accepted bids underestimate the actual charging values, while in fleet B the bids obtained with forecasted values overestimate the actual charging and the bids obtained with realized values are underestimating.

4.6.3 Comparison of Costs from Participating in the Electricity Market

The previous section compared the deviations of the two optimization models and these deviations result in imbalance costs for the aggregator that are added to the cost from purchasing energy in the market. This comparison gave an indication of the algorithms' performance, but

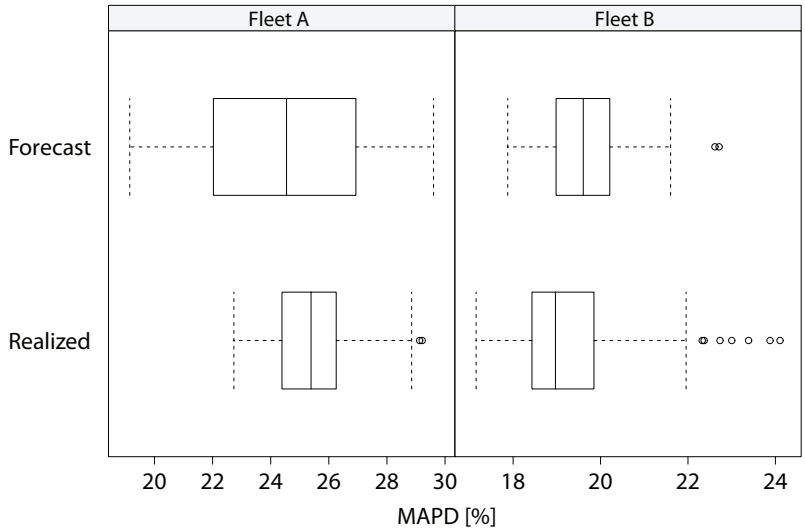

Figure 4.10: *MAPD of the global approach (for fleets A and B) with forecasted and realized values of the EV variables and market prices used as input.*

the total wholesale cost [computed with equation (4.18) from section 4.4] incurred by the aggregator is what affects its business activity and should be used to measure the performance and robustness of the proposed optimization models.

Figure 4.12 depicts the total cost increase obtained by the *divided* approach with forecasted values of the EV variables and market prices as inputs, compared to the results obtained when realized values of these variables are used as input in the day-ahead optimization.

In both fleets, the total cost increase, compared to the use of realized values, is low on average. The average cost increase in fleet A is 3.9% and 2.8% in fleet B. Nevertheless, there are some outliers in fleet A and its maximum cost increase is 10.3%. These results for fleet A contrast with the MAPD results from the previous section, since fleet A obtained the lowest MAPD on average. This emphasizes the importance of comparing the algorithms' performance in terms of total cost since different imbalance prices in positive and negative directions and price forecast errors affect the final results.

This small cost increase suggests that more advanced optimization models, including stochastic information, can only improve over this small percentage.

Figure 4.13 depicts the total cost increase of the *global* approach with realized and forecasted values as input. The average total cost difference is 2.9% in fleet A and 1.5% in fleet B. Note that, in fleet A, some samples present a negative cost increase, meaning that the result obtained with the forecasted values is better than the one obtained with realized values. This was an expected result since the MAPD values from the previous section showed that the results obtained with forecasted values have lower deviations on average.

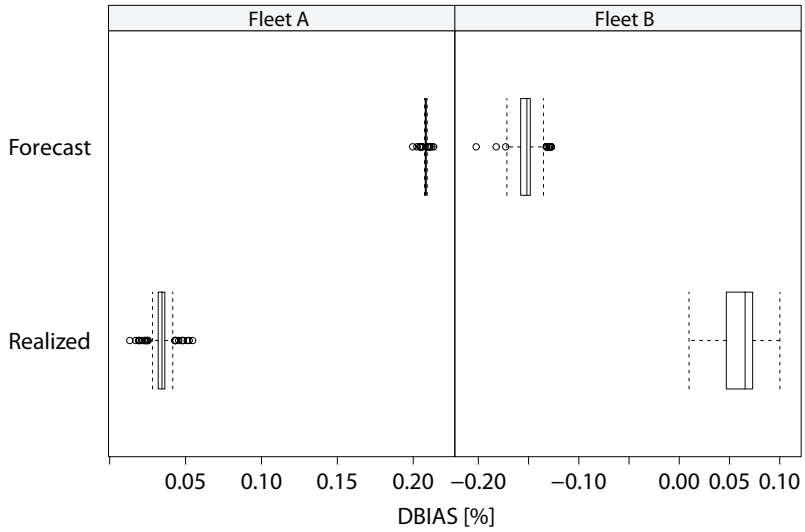

Figure 4.11: *DBIAS of the global approach (for fleets A and B) with forecasted and realized values of the EV variables and market prices used as input.*

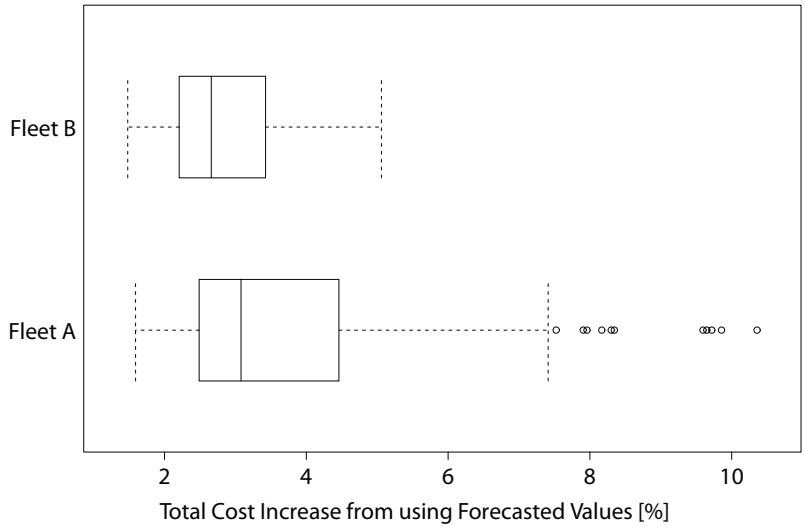

Figure 4.12: *Total cost increase obtained by the divided approach, for fleets A and B, when using forecasted values as input compared to the use of realized values in the day-ahead optimization.*

These low values in cost increase indicate that the forecast errors have a low impact on results. As shown in the appendix B, the forecast error for the aggregated variables is lower than the ones obtained for individual variables. This low impact of forecast errors is traded-off with imbalance costs originated from modeling the EV fleet only with aggregated information.

In both optimization approaches, the cost increase in fleet A is higher compared to B. Since the same forecasts for the EV variables are used in all 100 samples, this wide variation of the cost increase in fleet A is mainly due to forecast errors in the energy and imbalance prices which affect more fleet A than fleet B.

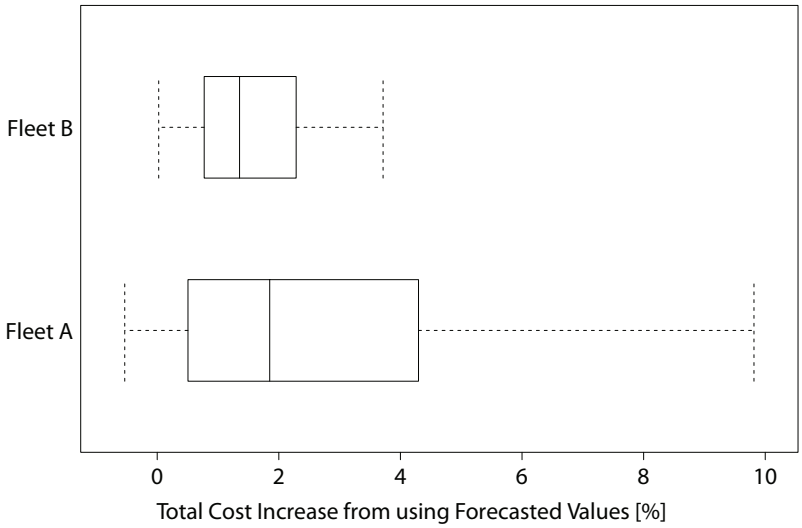

Figure 4.13: *Total cost increase obtained by the global approach, for fleets A and B, when using forecasted values as input compared to the use of realized values in the day-ahead optimization.*

Figure 4.14 depicts the reduction of the total cost and its three components compared to the *inflexible* approach (i.e., all EV are inflexible loads): cost of energy purchased in the day-ahead market $[E_t^{bid} \cdot p_t$ in equation (4.17)], cost of positive imbalances or surplus cost $[\pi_t^+ \cdot \left[E_t^{bid} - E_t^{cons}\right]$ in equation (4.18)], and cost of negative imbalances or shortage cost $[\pi_t^- \cdot \left[E_t^{cons} - E_t^{bid}\right]$ in equation (4.18)].

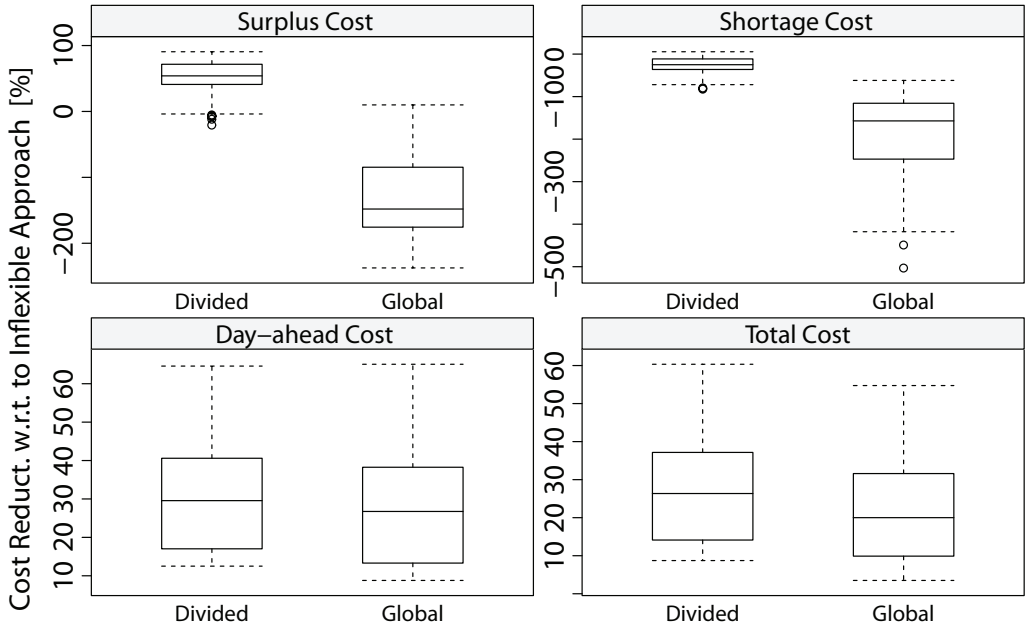

Figure 4.14: *Costs reduction of the divided and global approaches in fleet A compared to the inflexible EV load approach and using forecasts for all the variables.*

The *global* approach has the highest imbalance costs (both shortage and surplus) since it also has the highest deviation values. The *divided* one reduces the surplus imbalance cost

compared to the *inflexible* approach but the shortage cost is higher. The *inflexible* approach presents a lower forecast error (as shown in appendix B), which justifies the lowest imbalance cost compared to the other two approaches. Note that negative values mean that the surplus and shortage cost of the *inflexible* approach are lower than the imbalances costs of the *divided* or *global* approach and these negative values can be greater than -100%. For example, in one test sample of fleet A the surplus cost was 0.46 k€ in the *inflexible* approach and 1.57 k€ in the *global* approach, which represents a negative cost reduction of -241%.

The *divided* approach presents the highest day-ahead and total cost reduction. The average reduction of the day-ahead cost is 31.2% compared to 28.5% from the *global* approach and, in the total cost, the reduction is 27.7% compared to 22.5% from the *global* approach.
The main contribution to reduce the total cost compared to the *inflexible* approach is from the day-ahead cost, since the inflexible EV charge in more expensive time intervals. Moreover, the main contribution to the difference between *divided* and *global* approaches comes from the imbalance costs, since the day-ahead costs of both approaches are rather similar.

Figure 4.15 depicts the costs reduction for fleet B. The conclusions for the imbalance costs are analogous to fleet A.

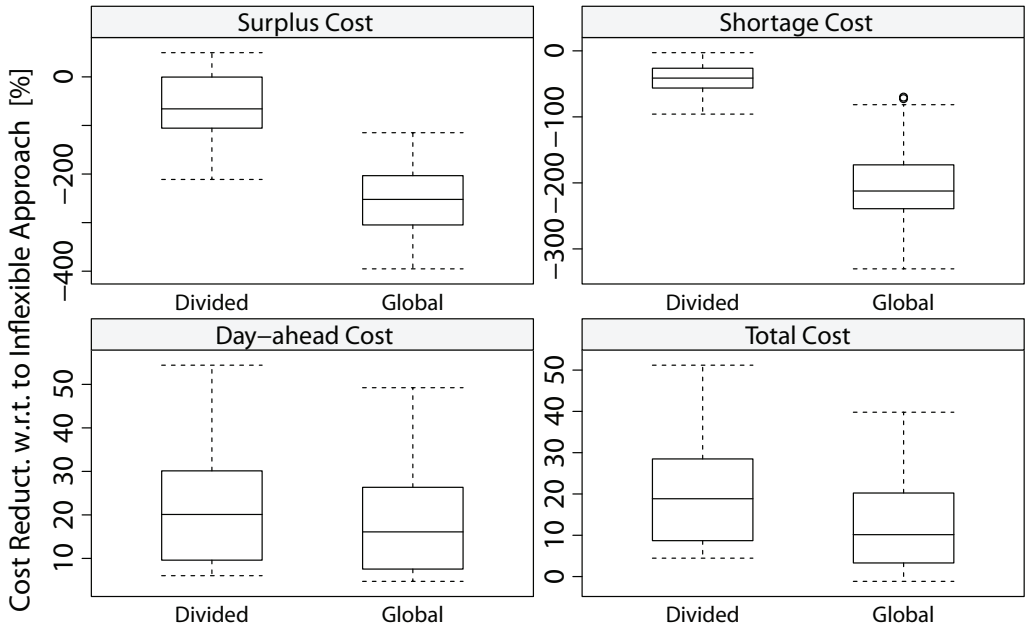

Figure 4.15: *Costs reduction of the divided and global approaches in fleet B compared to the inflexible EV load approach and using forecasts for all the variables.*

Similarly to fleet A, the *divided* approach achieved the highest day-ahead cost reduction: 22.1% on average against 18.7% of the *global* approach. In terms of total cost reduction, on average, it was 20.6% in the *divided* approach and 12.9% in the *global*.
The total cost decrease with fleet B is lower and this occurs because the EV of this fleet have

less flexibility (depicted in Figure A.7 of appendix A), compared to fleet A. The average plug-in time (or duration of the availability period) is rather similar in both fleets, as well as the availability pattern of both fleets. Thus, the higher charging requirement of fleet B in periods with similar length (on average) decreases its flexibility to charge in intervals with lower price.

4.7 Sensitivity Analysis of the *Global* Approach

Since the *global* approach has a parameter (β), it is important to conduct sensitivity analysis to evaluate the impact of its value on the deviation between accepted bid and actual charging values (measured by the MAPD) and also on the imbalance costs. The analysis is conducted for fleets A and B, being the first 9 months of 2010 used to fit the forecasting models and the last three months of the same year used to produce forecasts and test the optimization model. The β value was changed between 0 and 1 for different sizes of the EV fleet.

Figure 4.16 depicts a scatter plot relating different β values (ranging from 0 to 1 with 0.05 increments) to the deviation between bid and actual charging (MAPD) for four different aggregation sizes. As depicted for fleet A, when the value of β approximates 1 the MAPD decreases. The impact of β in the MAPD is significant. For example, in the case with 1500 EV, β equal to 0 (which means no adjustment in the maximum charging power) leads to a MAPD of 60.43%, while β equal to 1 leads to a MAPD of 32.21%. The value of the MAPD decreases with the aggregation size, so for 75 EV, MAPD is 62.26% (β=1), while for 1500 EV it is 32.21% (β=1).

The behavior for fleet B is depicted in Figure 4.17. In this fleet, the β that leads to the lowest MAPD is 0.7 for 150 EV, 0.75 for 75 EV and 500 EV, and 0.8 for 1500 EV. The value of MAPD decreases until 20.04% when the aggregation size increases. For this fleet, β values greater than 0.8 lead to high MAPD values. This happens because high β values in this fleet are very restrictive, and for this reason in some time intervals, it is necessary to present bids with high values for satisfying charging requirements that were delayed because of the high β value. This makes bids more concentrated in some time intervals (not necessarily the intervals with the lowest prices), and the highest deviation values occur exactly in these time intervals.

These two plots suggest that the MAPD of the *global* approach may change with the group of EV. In this test case, the MAPD value is different for each fleet, as well as the variation with different values of β.

Figure 4.18 depicts the total cost, day-ahead cost, shortage and surplus costs for the *global*

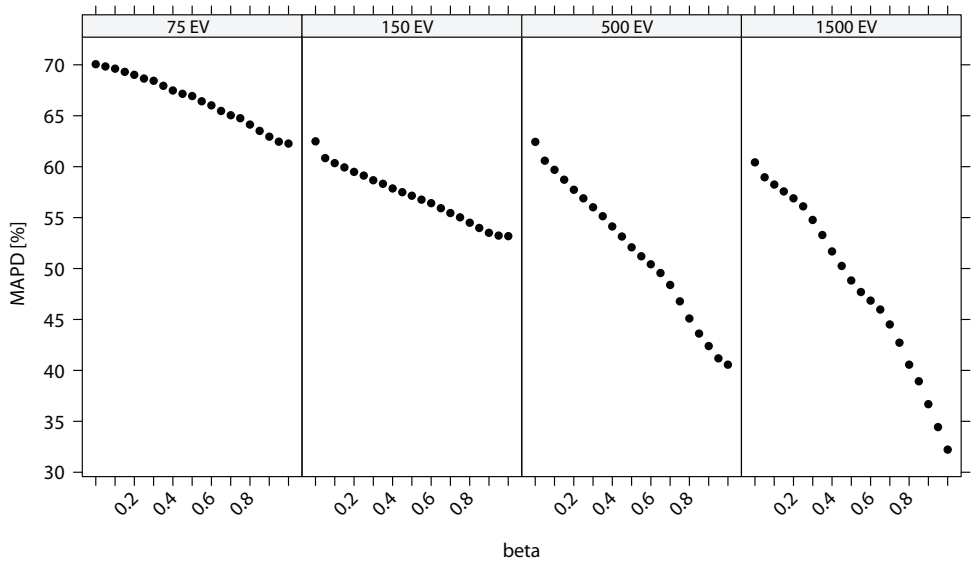

Figure 4.16: *β (from 0 to 1 with 0.05 increments) against MAPD for different aggregation sizes and fleet A.*

approach with different values of β and for fleet A with 1500 EV.

The plot shows that the day-ahead cost increases with β. This means that a lower β gives more "freedom" to the optimization algorithm for placing the bids in the time intervals with the lowest price. Conversely, this "freedom" results in an increase of the deviation between accepted bid and actual charging (i.e., MAPD increases), and consequently in an increase of shortage and surplus costs. The addition of these three components results in a total cost increase when β decreases.

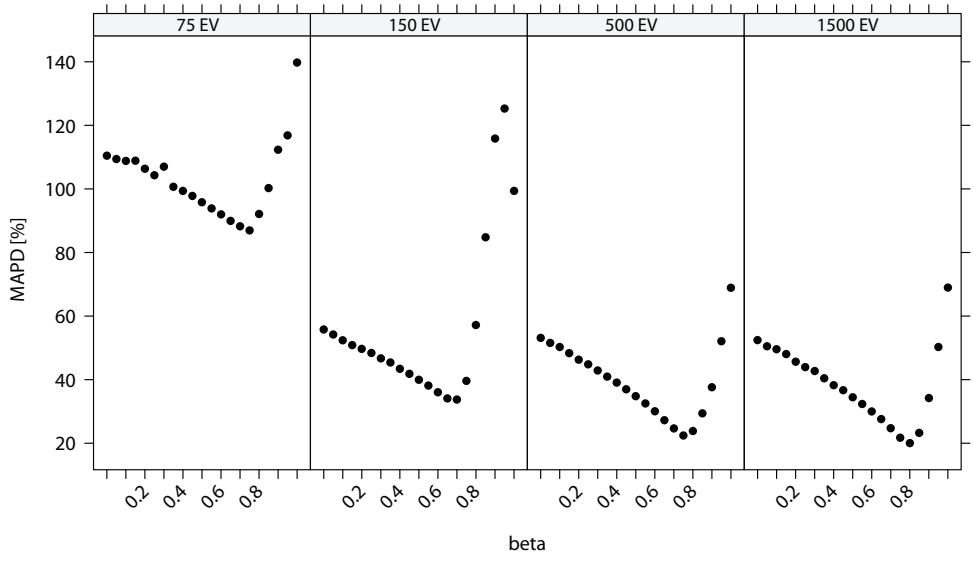

Figure 4.17: *β (from 0 to 1 with 0.05 increments) against MAPD of different aggregation sizes and fleet B.*

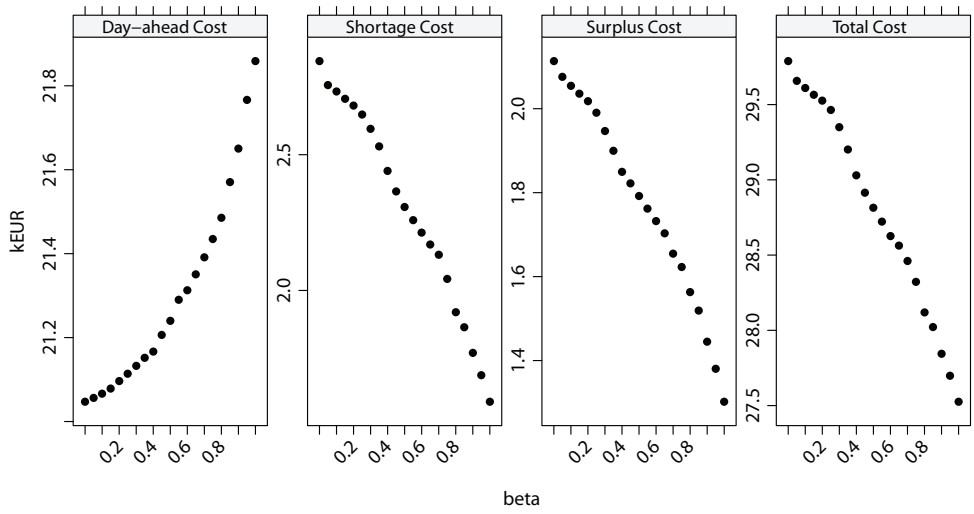

Figure 4.18: *The impact of β in the components of the total cost for fleet A with 1500 EV.*

Due to this cost divergence, it may happen that the β value with the lowest MAPD does not match the point with the lowest total cost. Figure 4.19 depicts this situation for fleet B. In this case, the β with the lowest MAPD was 0.8, while the one with the lowest total cost is 0.6. The day-ahead cost decreases with β, but the surplus and shortage costs start to increase when β is greater than 0.8.

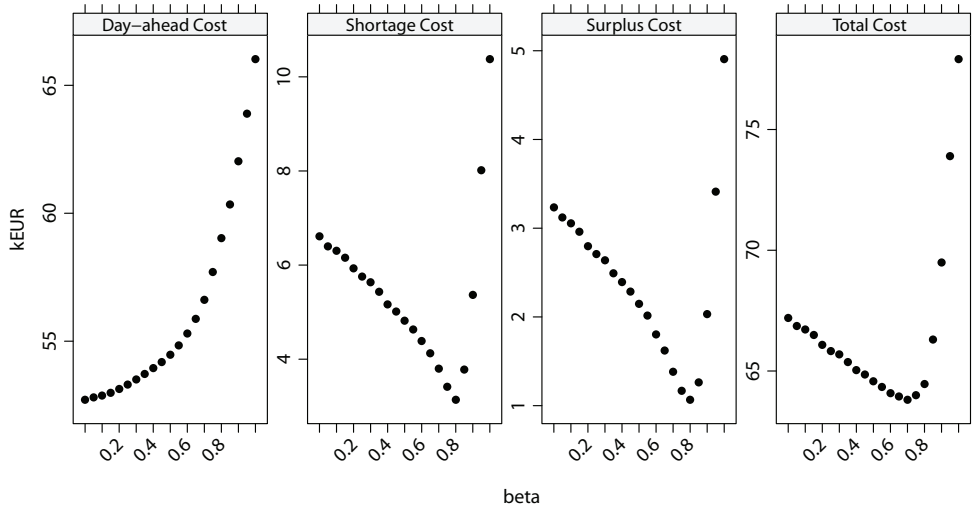

Figure 4.19: *The impact of β in the components of the total cost for fleet B with 1500 EV.*

4.8 Performance of the Operational Management Algorithm

4.8.1 Comparison with State of the Art Operational Algorithms

This section compares the operational algorithm proposed in this thesis (named *optimized*) with two algorithms from the literature: (a) the heuristic method with maximum charge rate that is based on a priority function from Amoroso and Cappuccino [164] (named *priority-based*); (b) the heuristic algorithm based on the energy price ranking from Wu et al. [165] (named *price-ranking-based*). These algorithms were modified by Lima [30] and a description can be found in appendix C. Note that the operational algorithm is independent of the algorithm or procedure used to make the bids and, in this section, the input bids are from the *divided* approach.
Furthermore, in order to stress the importance of coordinating EV charging, results from an uncoordinated strategy are also presented. The *uncoordinated* strategy means no coordination between the EV charging and the aggregator only aggregates (or sums) the EV individual charging values. In this case, each EV minimizes its own imbalances.

Figure 4.20 depicts the MAPD as a function of different fleet sizes (between 15 EV and 1500 EV) for each operational management algorithm and for the two fleets. Since all the algorithms use the same energy bids as input, the dissimilar values of MAPD are only due to a different distribution of the actual charging inside the EV fleet.

In both fleets, the MAPD decreases as the number of EV increases (i.e., aggregation size). Both plots show a high MAPD reduction for small aggregation sizes and a small reduction for sizes greater than 150 EV. This highlights the importance of aggregating EV to mitigate forecast errors. However, when the EV charging is uncoordinated, the value of MAPD is much higher compared to the other three algorithms; in the case with 1500 EV, it is around 39% in fleet A and 32% in fleet B. These results stress the importance of coordinating the individual charging of the EV for decreasing the final deviations.

The *optimized* algorithm outperformed all the other operational algorithms in terms of MAPD. With this algorithm, in fleet A, the MAPD decreases from 38.23% (with 15 EV) to 10.23% (with 1500 EV) and in fleet B, from 32.76% to 10.80%. With the *priority-based* algorithm, the MAPD decreased from 39.60% to 13.07% in fleet A, and from 33.66% to 12.22% in fleet B, and with the *price-ranking-based* algorithm it decreases from 41.54% to 14.51% in fleet A, and from 36.82% to 12.00% in fleet B.

The surplus and shortage costs obtained with the *optimized*, *priority-based* and *price-ranking-based* algorithms are depicted in Figure 4.21. The average costs of the *uncoordinated* strategy

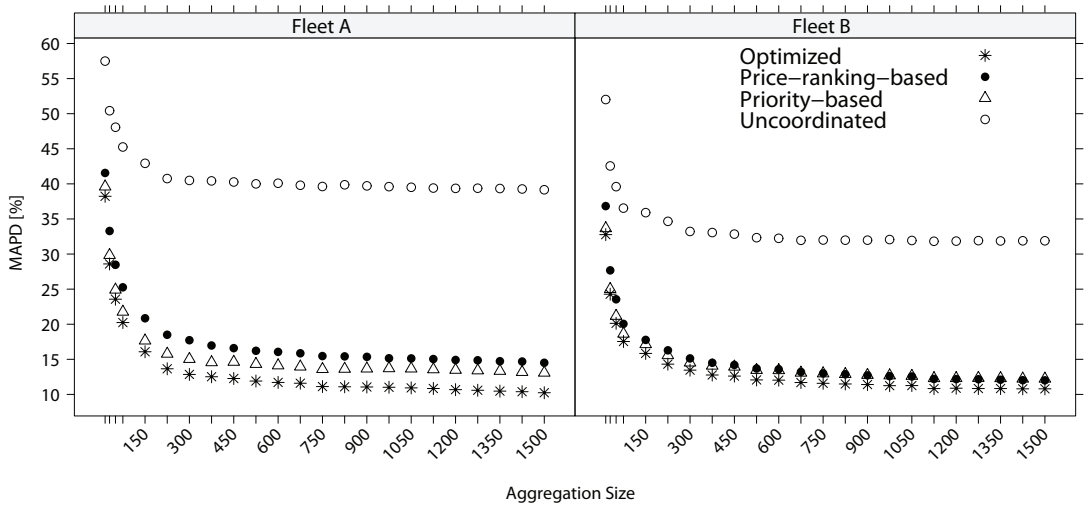

Figure 4.20: *Aggregation size against MAPD for fleets A and B obtained with four different operational management algorithms. The fleet size is 15, 30, 50, and from 75 to 1500 EV with 75 increments.*

are: 1.45 *k*€ of shortage cost and 1.42 *k*€ of surplus cost in fleet A; 2.25 *k*€ of shortage cost and 3.05 *k*€ of surplus cost in fleet B.

Since the fleet size is only 1500 EV and the test period is 3 months, the imbalance costs are considerably low in all three operational algorithms (but much higher in the *uncoordinated* strategy). In relative terms, the cost difference between the imbalance costs of the three operational algorithms is significant. In fleet A, the *optimized* algorithm reduces, on average, the surplus cost in 27.58% compared to the *priority-based* approach, and 48.3% compared to the *price-ranking-based*; the cost reduction in the shortage cost is 23.79% and 40.10%, correspondingly.
The reduction in fleet B is lower: in the surplus costs is 7.41% and 16.08% correspondingly and in the shortage cost is 17.90% and 22.36%.

4.8.2 The Impact of Very Short-term Forecasts

The *optimized* algorithm for operational management only uses information from the plugged-in EV and it does not use very short-term forecasts for the EV not plugged-in in time interval t_0. In order to quantify the impact from not using these forecasts in the algorithm, the *divided* optimization is solved using the realized values of all variables (energy price and EV), and two strategies are considered: (a) the individual optimization, that results from the *divided* approach, is followed in the next day and it results in a perfect match between market bid and actual charging; (b) the operational management algorithm without very short-term forecasts is used to minimize the absolute difference between actual charging and market bid (obtained with realized values).

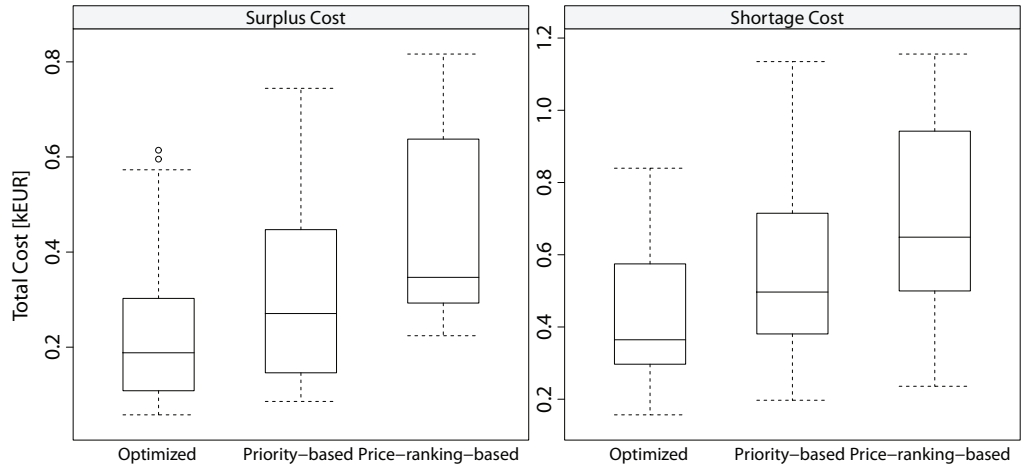

(a) *Fleet A.*

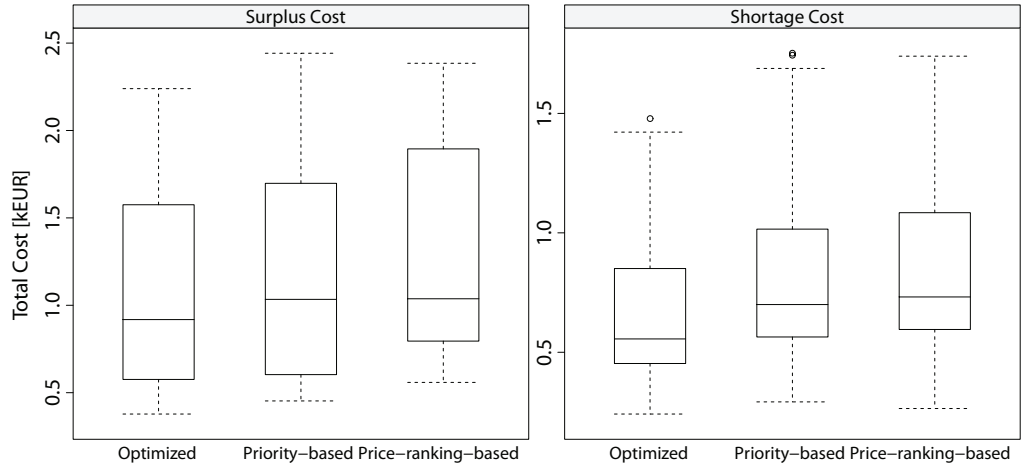

(b) *Fleet B.*

Figure 4.21: *Surplus and shortage costs for fleets A and B obtained with three different operational management algorithms.*

These two strategies exclude the forecast errors influence in the day-ahead optimization and their comparison gives an upper bound for the improvement that can be obtained with very short-term forecasts.

Table 4.5 presents the average, minimum and maximum values in the 100 samples of the following variables: MAPD obtained with strategy (b); total cost increase of strategy (b) compared to strategy (a). These two variables measure the impact in deviations and costs from not using very short-term forecasts in the operational management algorithm.

The results show that the impact is low and, since this is only an upper bound, the inclusion of very short-term forecasts is likely to accomplish an improvement below the values in Table 4.5. Therefore, it can be concluded that very short-term forecasts in the operational management algorithm have a marginal impact in the final result.

Table 4.5: *Total cost increase and deviations (measured with MAPD) obtained from not including very short-term forecasts in the operational management algorithm (average [minimum,maximum]).*

	MAPD [%]	Total Cost Increase [%]
Fleet A	1.98% [1.52%,2.61%]	4.73% [2.16%,9.32%]
Fleet B	2.73% [1.99%,4.12%]	3.89% [1.93%,7.19%]

4.9 Discussion

In this chapter, two alternative optimization approaches (with different representation of the EV information) for supporting an EV aggregator participating in the day-ahead energy market were presented and compared. For each approach, statistical models were proposed to forecast the required information about EV availability and consumption. Moreover, an operational management algorithm that extracts benefits from aggregating EV is described to minimize the imbalance costs related to deviations between purchased and consumed electrical energy. These three phases (forecast>day-ahead optimization>operational management) of the model chain are crucial for the aggregator business activity.

The major difference between the two proposed optimization approaches, *global* and *divided*, lies in the representation of the forecasted information for the EV fleet. In fact, the *divided* approach essentially consists in dispatching the EV individually based on the forecasted prices, and does not use the capability of combining the EV individual charging. Conversely, the *global* approach takes advantage of the aggregation capacity since it uses the aggregated variables related to the EV availability and consumption. Nevertheless, using the output of the *divided* approach, the operational management algorithm explores the aggregation capacity (i.e., coordinates the EV individual charging) for minimizing the imbalance costs.

The forecasting results show that the algorithms provide acceptable quality to be used as input for optimizing the day-ahead bids. Nevertheless, it is important to stress that these algorithms were a first approach to the problem and have a high potential of improvement in future works. The error of the aggregated variables used in the *global* approach is low and the evaluation of the total cost indicated that advanced forecasting algorithms can only accomplish improvements over a small percentage. The forecast errors for the individual EV variables are high, but lead to a low deviation in the *divided* approach, which suggests an acceptable quality.

The results showed that the operational management algorithm is crucial for decreasing deviation costs by combining the EV individual charging. This was particularly significant in the *divided* approach where a forecast error of around 30% for charging requirement resulted in

a final deviation around 9.5%. The comparison between *global*, *divided* and inflexible bidding approaches lead to the following conclusions:

- the *global* approach has a higher deviation value compared to the *divided* one, which results in a higher total cost. For instance, in one EV fleet the *divided* approach reduced the total cost around 27.7% compared to an *inflexible* approach, while the *global* approach reduced 22.5%;
- the *divided* approach is more robust to different EV fleets and energy price patterns. For the two EV fleets and a sampling process with 100 samples, the deviation in the *divided* approach ranged from 8.5 to 12%, while in the *global* approach ranged from 18 to 30%;
- the *inflexible* approach also benefits from aggregating EV, which leads to low forecast error, but its total cost is high because the EV are charged during high price periods;
- the algorithms presented a computational performance acceptable for practical applications.

The forecasting and optimization models were tested with EV synthetic data anticipating a future scenario. Nevertheless, the conclusions about the model's performance can be generalized to case-studies with real EV data and the algorithms can be applied without any change.

As an overall conclusion, the *divided* approach outperformed the *global* approach. Therefore, this approach is enhanced in the following chapters to include the possibility of offering secondary and balancing reserve bids.

Chapter 5

Optimization Models for the Secondary Reserve Market

Abstract

This chapter formulates a day-ahead optimization problem for energy and secondary reserve bids, and an operational management algorithm that coordinates EV charging in order to minimize differences between contracted and realized values of energy, and supply secondary reserve with acceptable reliability. Forecasts for EV and market variables are included in the model. A market settlement scheme that includes a penalty term for reserve shortage situations is proposed. The algorithms are evaluated in a test case constructed with synthetic time series for EV and data from the Iberian electricity market.

5.1 Introduction

The participation of loads in ancillary services markets has gained relevance in the recent years, in particular with the deployment of the Smart Grid concept. The EV, when aggregated, is a suitable candidate for offering secondary reserve in the electricity market.

The work in this chapter explores a solution where the EV aggregator controls directly the charging of EV plugged-in in slow charging points and sells secondary reserve power in the electricity market. The *divided* approach described in chapter 4 is extended to include the possibility of offering secondary reserve power in both upward and downward directions, and using forecasts for the EV variables (produced by the statistical models described in chapter 4). Moreover, an operational management algorithm is proposed to coordinate EV charging

and minimize the difference between contracted and realized values of energy and reserve. An important characteristic of the proposed approach is that the formulation of the optimization problem takes into account the specific characteristics of secondary reserve.

This chapter starts by describing the problem, with particular emphasis to the characteristics of secondary reserve (section 5.2). Then, the formulation of the day-ahead and operational management optimization problems is presented (sections 5.3 and 5.4). After the operational phase, it is necessary to calculate the total cost, which includes the income from having available secondary reserve, but also a penalty for reserve shortage situations. For this purpose, two alternative market settlement schemes are proposed in section 5.5. The robustness of the proposed models is examined in section 5.6 using the test case of chapter 4. Finally, a discussion of the main results and modeling assumptions is presented in section 5.7.

5.2 Problem Description

5.2.1 Participation in the Electricity Market

In this chapter, a sequential market-clearing mechanism (i.e., the secondary reserve market is cleared after the energy market) is assumed to take place since the Iberian electricity market is used as test case. This is the most common situation in Europe. Nevertheless, the same algorithms could be applied to a market with a joint clearing of energy and reserve bids.

The aggregator participates in the day-ahead energy market with bids for purchasing energy, with a gate closure at hour 10h00, and a day-ahead session for secondary reserve takes place at 14h00. The TSO defines the secondary reserve requirements for each hour of the next day and purchases the corresponding quantity in the secondary reserve market.

The secondary reserve market is assumed to have a common price for upward and downward directions. An illustration of the market clearing process with a common reserve capacity price is depicted in Figure 5.1. This is the case of Portugal, where 1/3 of the reserve power is in the downward direction and 2/3 in upward direction [46]. In Spain, there is also a common capacity price, and the agents offer reserve bids in both directions[1]. In the USA, four out of seven ISO have a single price for each megawatt of secondary reserve regardless of direction [63]. For instance, the regulation band in PJM, for demand response, is divided

[1] According to the market-clearing results in e-sios platform (http://www.esios.ree.es), accessed in January 2013, the market agents must present reserve power bids in both directions but the ratio changes with the hour of the day and from unit to unit.

into equal shares for both directions [211]. Another possibility is to allow separated reserve bids in each direction.
This chapter covers these two possibilities: one where the upward and downward reserve power must respect a predefined ratio, and another where the market agents can offer separated reserve power in both directions (without the loss of generality, it is assumed a single capacity price for both directions).

In general, the electricity markets have hourly or half-hourly time steps. For the secondary reserve market, the power in the reserve bid is assumed to be constant during the market interval. For example, a conventional generator can operate at 50 MW and supply additional 50 MW as upward reserve at constant power during one hour. In contrast, an EV aggregator may not be able to offer constant power during a complete hour because several EV can depart and arrive during that interval. For example, the aggregator can have 1000 EV plugged-in during a half-hour and 800 EV during the second half-hour. If all EV are charging at 2 kW (but with a maximum charging power of 3 kW), the aggregator can offer 1MW of downward reserve in the first half-hour and 0.8 MW in the second. However, in an hourly time interval, the average power would be 0.9 MW, which can only be attained during the first half-hour.

Therefore, in this thesis a change in the current market rules is proposed to promote the participation of EV in secondary reserve. The market time interval remains one hour, which means that from the market-clearing it results an hourly price, but the secondary reserve bid submitted by the EV aggregator is decomposed in sub-hourly intervals of predefined length Δt and with constant power. In the aforementioned example, assuming Δt=0.5 hr, the downward reserve bid would be: 1 MW for the first half-hour and 0.8 MW for the second. This information is used by the AGC, when defining the regulation signals for each reserve resource and the aggregator is penalized if it does not comply with the constant power in each time step of length Δt. The time length Δt is a predefined value and should be defined in accordance to the average trip duration time.

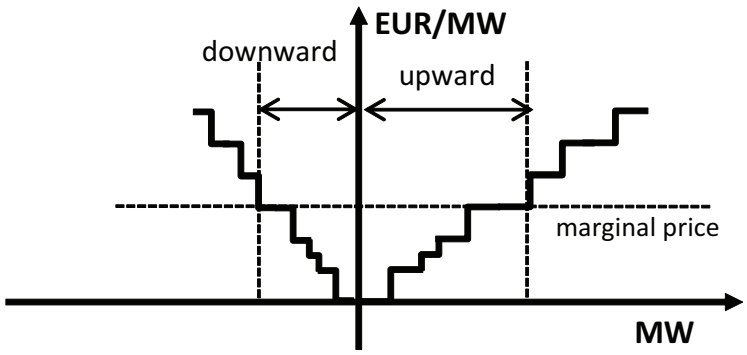

Figure 5.1: *Market clearing of the secondary reserve bids.*

Note that most of the electricity markets created complex bids to accommodate specific characteristics of conventional generation units, such as minimum run times or minimum revenues. Thus, this can be seen as an additional complex bid designed for EV aggregators (and also for other types of flexible loads). This change demands a new market-clearing algorithm that takes into account complex bids from the EV aggregator.
The alternative for the aggregator would be to submit the minimum reserve power in the market interval, but this would decrease the aggregator's income and would not create incentives for having EV supplying secondary reserve.

Figure 5.2 depicts the sequence of tasks for the participation in the day-ahead energy and secondary reserve markets. Firstly, the aggregator, at day D, forecasts the EV charging requirement and availability, as well as the energy and reserve prices. This forecasted information is the input of a day-ahead optimization model (for next day D+1) that computes the bids for the energy and secondary reserve markets. The bid submitted by the aggregator contains the secondary reserve band divided into upward and downward power, and since the aggregator is considered a "price-taker", the price for available reserve capacity is assumed lower enough to have the bid accepted.

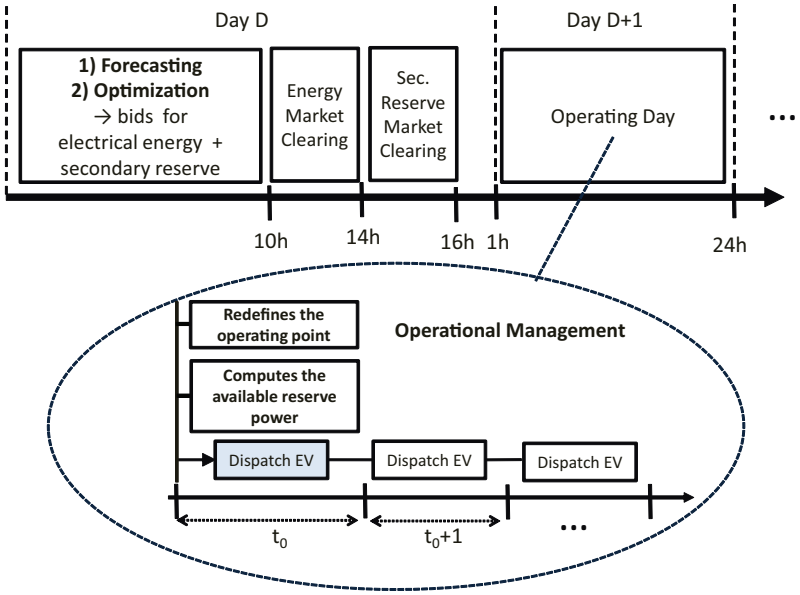

Figure 5.2: *Sequence of tasks for participating in the day-ahead energy and secondary reserve markets.*

During the operating day (day D+1), before the beginning of each time interval t_0 (with length Δt), the aggregator redefines the EV fleet operating point, computes the available upward and downward reserve power and communicates this information to the TSO. The aggregator dispatches the EV for meeting the fleet's operating point for each time interval (t_0, $t_0 + 1$,...), and places the plugged-in EV on standby to supply upward and downward reserve power in response to an AGC request. An operational management algorithm is used

to coordinate the EV charging. A penalty term is applied for cases with reserve shortage.

The physical interaction between aggregator and EV (i.e., communication) can be performed with the standardized technology reviewed in section 2.5 of chapter 2.

5.2.2 Characteristics of the Secondary Reserve

In the absence of perturbations, the events handled by secondary reserve are usually minute-to-minute random fluctuations inside the operating period (as illustrated by Figure 5.3), but in some cases, this reserve can also be used to handle large deviations between load and generation (e.g., unplanned outage or loss of synchronism from a generator) [34]. Secondary reserve must only be used to correct the ACE, and not for other purposes such as to minimize unintentional energy imbalances[2] [33].

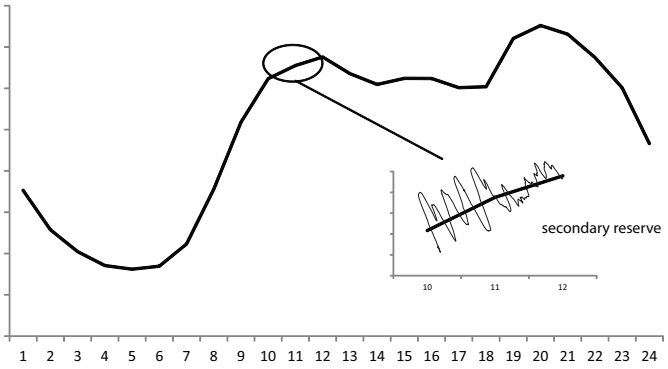

Figure 5.3: *Secondary reserve.*

Figure 5.4 depicts the AGC regulation signal of PJM (secondary reserve is called *regulation reserve* in PJM) for 6 hours, in 2 seconds time steps and normalized between -1 (upward) and 1 (downward) of the available reserve power in each hourly period[3]

This signal is the output of the AGC model and it is sent by PJM for each resource owner assigned to supply secondary reserve. For instance, in the first 6 seconds, the reserve resource receives a signal that goes between -1 to 1, while in some time instants, the resource receives a signal of 0, which means to work at its predefined operating point (i.e., no reserve provision). In other periods, such as between 4000 and 6000 seconds, the requested reserve power is within 0.5 and -0.5.

[2] Defined by ENTSO-E as the difference between the scheduled and the actual values of power deliveries [212].

[3] Data collected from: PJM Regulation Performance Senior Task Force, http://www.pjm.com/committees-and-groups/task-forces/rpstf.aspx (accessed in December 2012). Note that the original signal was for generators, with a negative value for downward reserve and a positive one for upward reserve. Here the signal is inverted since EV is a load.

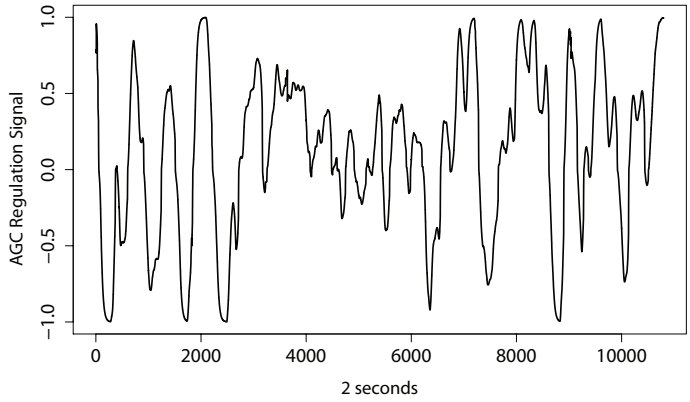

Figure 5.4: *PJM AGC regulation signal for 6 hours with 2 seconds time steps.*

This reserve encloses specific characteristics, reviewed in the remaining of this section, which must be considered when developing optimization models for an EV aggregator. These characteristics are generally neglected in the formulation of the optimization problems described in the literature for the participation of EV aggregators in the secondary reserve (see section 2.6.1 of chapter 2).

The first characteristic is that, despite being contracted on an hourly basis, secondary reserve is normally not dispatched in the same direction during the complete hour. In an hourly period, the reserve can be dispatched in one direction during a period below one hour (e.g., upward reserve during 40 minutes), while in other cases, it can be dispatched in both directions (e.g., 10 minutes of upward and 50 minutes of downward reserve).

Figure 5.5 depicts the histograms for the number of equivalent minutes of secondary upward reserve dispatch of an hydro and a thermal power plant in Portugal[4]. The number of equivalent minutes corresponds to the ratio between the dispatched reserve power (electrical energy in MWh) and its available reserve power (in MW).

The two histograms show a wide variation of the number of equivalent minutes. This means that, when making a reserve power bid, the aggregator does not know, with certainty, the reserve dispatch duration. For a downward reserve bid of 1 MW, a value of 20 minutes in the histogram corresponds to activate this reserve at full power only during 20 minutes (in a one hour interval) and, in this case, the EV fleet charges 0.2 MWh of electrical energy, instead of the expected 1 MWh. In contrast to generation units, this creates a problem for EV since their charging requirements must be satisfied and the aggregator does not know beforehand, with certainty, the quantity of electrical energy that will be charged as downward reserve. The same is valid for upward reserve.

[4] Data collected from: http://www.mercado.ren.pt/ (accessed in December 2012).

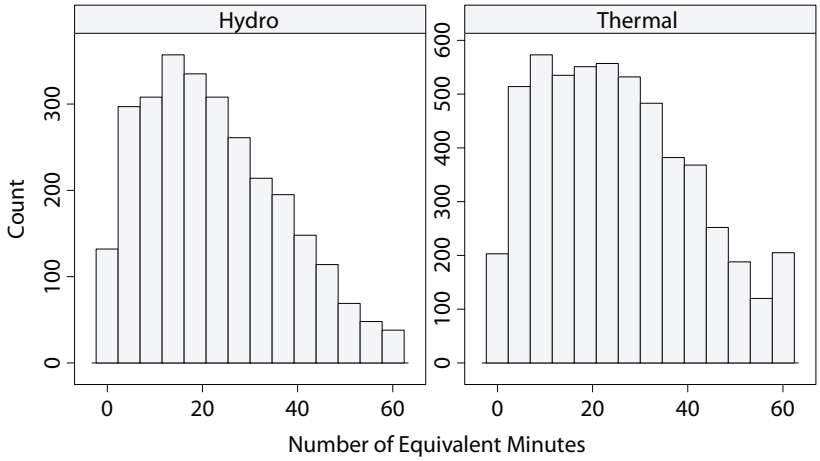

Figure 5.5: *Histograms for the number of equivalent minutes of the upward secondary reserve of a hydro (Alqueva) and thermal (Lares) power plants in Portugal for the year 2011.*

The number of equivalent minutes of dispatched secondary reserve is generally low. For instance, the annual average of the hydropower plant is 22 minutes for upward and 24 minutes for downward reserve.

A second characteristic is that the net electrical energy (i.e., dispatched downward reserve minus dispatched upward reserve in the same hourly interval) from the reserve provision is different from zero in each hour.

Figure 5.6a depicts the histogram of the net electrical energy of secondary reserve in Portugal, during the year 2011. Note that these values are from the total dispatched reserve power in Portugal, and not from an individual generator, since the AGC signal used in Portugal is not publicly available. As shown in the histogram, the net electrical energy is frequently different from zero.

The same conclusion is valid for Figure 5.6b, where the histogram of the hourly AGC regulation signal transmitted by PJM for each reserve resource is depicted. This hourly signal is obtained from the 2 seconds regulation signal of Figure 5.4 as follows:

$$AGC_h = \sum_{t \in h} \left(AGC_t^{''} \cdot \frac{2}{3600} \right) \tag{5.1}$$

where $AGC_t^{''}$ is the 2 seconds signal.

Each one of these hourly values, multiplied by the available reserve power in the corresponding hour (which is the same for both directions), gives the net electrical energy of the secondary reserve provision. For example, for an EV with POP equal to 2 kW, upward reserve equal to 1 kW, downward equal to 1 kW, and an hourly AGC signal equal to -0.5 means that the net electrical energy from reserve provision is -0.5 kWh, which shows that the battery SoC,

by the end of the hourly period, is incremented by 1.5 kWh (i.e., 2 kWh from the POP minus the 0.5 kWh from the net energy). An hourly value equal to zero means that the reserve is dispatched in both directions during the same time. In this case, the battery SoC is incremented by the electrical energy corresponding to the POP value (2 kWh in the example), which is certain and known in advance. However, also in the PJM signal, there is a high frequency of values different from zero, which adds uncertainty to the EV battery SoC by the end of each hourly period.

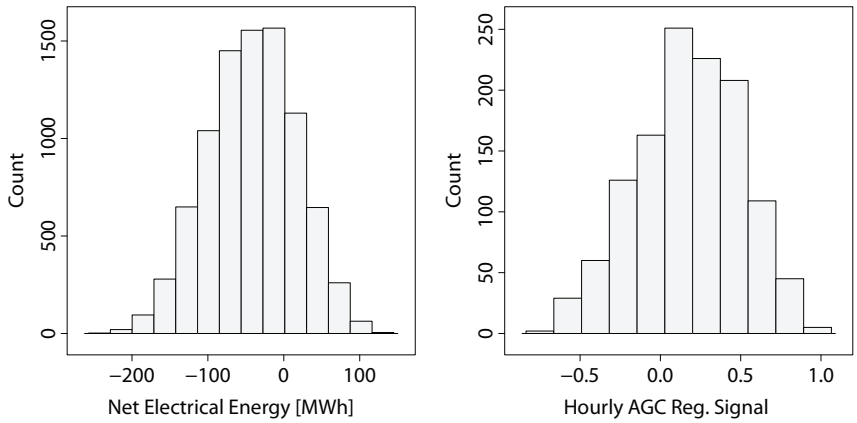

(a) *Histogram of the net electrical energy of secondary reserve in Portugal for the year 2011.*

(b) *Histogram of the hourly AGC regulation signal from PJM for 51 days.*

Figure 5.6: *Histograms of the secondary reserve in Portugal and PJM.*

A third characteristic, and linked to the second one, is that producing forecasts with acceptable accuracy for the net electrical energy related to the reserve provision is challenging. Figure 5.7a depicts the autocorrelation plot of the total net electrical energy of secondary reserve in Portugal (i.e., the variable in the histogram of Figure 5.6a), during the year 2011.

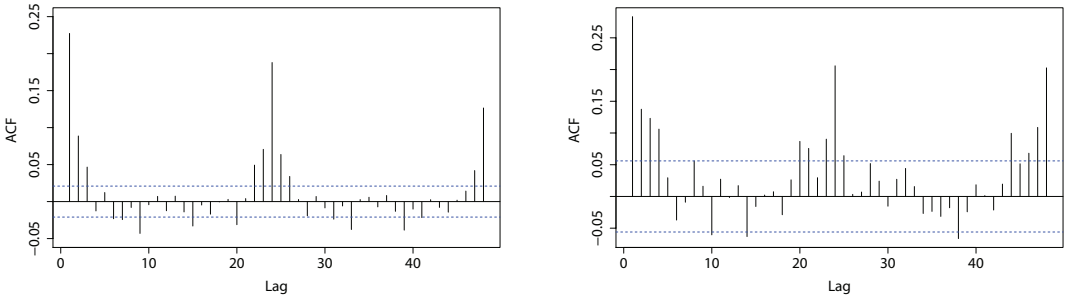

(a) *Autocorrelation function of the net electrical energy of secondary reserve in Portugal for the year 2011.*

(b) *Autocorrelation function of the hourly AGC regulation signal from PJM for 51 days.*

Figure 5.7: *Autocorrelation plots of the secondary reserve in Portugal and PJM.*

This plot shows an autocorrelation below 0.25 for all time lags, and the value for $t-1$ is only around 0.25. This low value of serial dependency suggests that there is a low amount of information in the past values of the time series [213], which makes challenging to produce forecasts with acceptable accuracy. This is consistent with the expected random nature of the secondary reserve dispatch.

Figure 5.7b depicts the autocorrelation diagram of the hourly PJM regulation signal time series during the 51 days. Similar to the Portuguese case, this diagram presents a "weak" autocorrelation.

To conclude, the analyses conducted in this section showed the following:

- the duration period of the dispatched secondary reserve is variable, and in general, lower than one hour;
- the net electrical energy from the reserve dispatch is frequently different from zero, and it is difficult to forecast its value with acceptable accuracy.

Therefore, the formulation of the day-ahead optimization problem, which will be described in the next section, should include constraints that allow a degree of flexibility in handling situations where the available reserve in the previous intervals was not dispatched in one direction (on the contrary to what was planned by the aggregator) or was dispatched only for a limited period of time in one direction.
This is illustrated in Table 5.1, where the bids from one EV plugged-in during four hours and with a charging requirement of 4 kWh are presented. The net electrical energy from the reserve provision is unknown in advance and different values can lead to reserve shortage situations.

For instance, if the net energy in interval H1 is 0.3 kWh and -0.8 in H2 [hypothesis (a)], the EV in interval H3 can only operate at 0.5 kWh since the EV has already charged 3.5 kWh in intervals H1-H2 and the charging requirement is 4 kWh. In this case, it is unable to supply downward reserve in interval H3 and the available upward reserve power is only 0.5 kW. On the other hand, if the net energy in interval H1 is -1.5 kW and -1.8 kW in H2 [hypothesis (b)], the aggregator is able to supply 1 kW of downward reserve in interval H3, but if downward reserve is not dispatched in that interval, the EV must charge 3 kWh in interval H4 (instead of the planned 1 kWh) and it is unable to guarantee a constant upward reserve power of 2 kW during the complete hour, otherwise the charging requirement of 4 kWh is not satisfied during the availability period.

Table 5.1: *Secondary reserve bids from one EV plugged-in during four hours (with a charging requirement of 4 kWh) and net electrical energy that results from the reserve provision during the first two hours.*

	H1	H2	H3	H4
E_k [kWh]	2	2	2	1
P_k^{up} [kW]	2	2	2	0
P_k^{down} [kW]	1	1	1	0
(a) net energy [kWh]	0.3	-0.8		
(b) net energy [kWh]	-1.5	-1.6		

5.3 Day-ahead Energy and Reserve Optimization

The previous section discussed the characteristics of secondary reserve and concluded that it is not possible to produce forecasts with acceptable quality for the hourly AGC regulation signal. Thus, the formulation of the day-ahead optimization problem described in this section disregards this information, and the goal is to obtain robust solutions that assure an acceptable reliability of the secondary reserve provision as well as an attractive income to the aggregator and the EV in its portfolio.
First, the input variables and corresponding forecasting algorithms are described, followed by the day-ahead optimization model.

Input Variables and Forecasts

The day-ahead optimization model uses the following forecasts as inputs: (a) charging requirement and availability forecast of each EV; (b) day-ahead electrical energy price; (c) day-ahead price for available and dispatched secondary reserve.

The EV variables and energy price are forecasted with the statistical algorithms described in chapter 4.

The price for available reserve capacity is common for each direction and it is forecasted with a seasonal ARIMA model selected by the function *auto.arima* from R package *forecast* [214]. Figure 5.8 depicts a day-ahead forecast of the capacity price for one day from the test case described in chapter 4. The forecast shows an acceptable fit with the realized value. Note that the capacity price shows a rather stable variation along the day, but with peaks in some hours. This price forecast has an important impact on the results since the majority of the income from selling secondary reserve comes from having available reserve power. Appendix A presents a statistical analysis of the market price data and appendix B the forecast error results for the reserve capacity price.

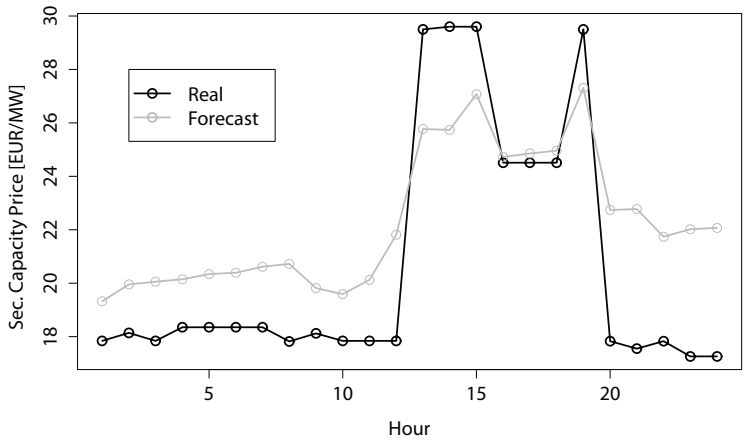

Figure 5.8: *Day-ahead forecast of the secondary reserve capacity price in Portugal.*

In contrast to the energy and reserve capacity price time series, the time series of the price for dispatched reserve is irregular because the price only exists when the reserve is used in that direction. The forecasting literature about algorithms for irregular time series is scarce, in particular for seasonal time series. The only work about irregular seasonal time series is the modified Holt-Winters algorithm [215]. In this chapter, this algorithm is used to forecast the dispatched reserve price.
The model's parameters are estimated to minimize the root mean square error of one step-ahead forecasts, using the limited-memory modification of the BFGS quasi-Newton method [216] (implemented in function *optim* of the R base distribution).

Figure 5.9 depicts a one step-ahead forecast and realized values of the upward tertiary reserve price for two illustrative days (48 hours) from the test case described in chapter 4. Note that in Portugal and Spain the energy delivered as secondary reserve is priced at the tertiary reserve price and in some time intervals the upward reserve was not dispatched, thus there is no price for those intervals. Moreover, the price forecast is produced for a complete day, but here the forecasted values are only depicted for the intervals with realized values.
The forecast shows a good fit to the realized value, but in the second day (around hour 40) there is a large deviation between forecast and realized values. This price is less relevant for the optimization results, since the percentage of dispatched secondary reserve power is generally low. Appendix B presents the forecast error results.

Formulation of the Optimization Problem

The decision variables of the day-ahead optimization problem are illustrated in Figure 5.10: optimized energy ($E_{t,j}$) for charging the j$^{\text{th}}$ EV in time interval t (i.e., the preferred operating point - POP), upward and downward secondary reserve power ($P_{t,j}^{down}$ and $P_{t,j}^{up}$) of the j$^{\text{th}}$ EV

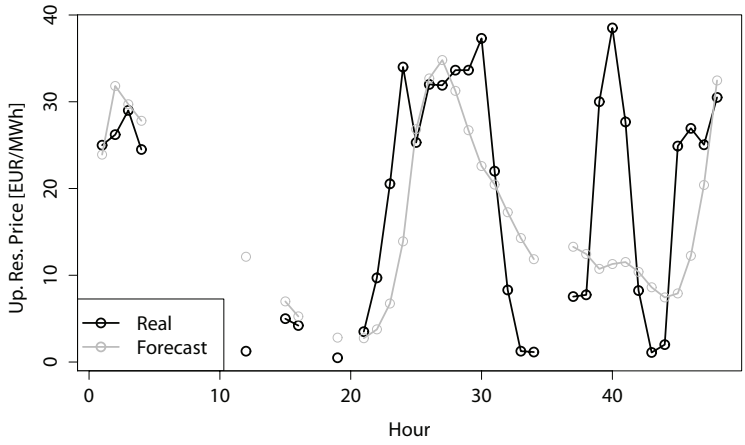

Figure 5.9: *One step-ahead forecast for the upward tertiary reserve price in Portugal.*

for time interval t. In this example, the EV operates at 1 kW and offers a secondary reserve power of 3 kW (2 kW for downward reserve and 1 kW for upward reserve). The energy and reserve bids are the sum of the individual values of each EV. Similarly to the *divided* approach from the previous chapter, this optimization problem can also be solved individually for each EV.

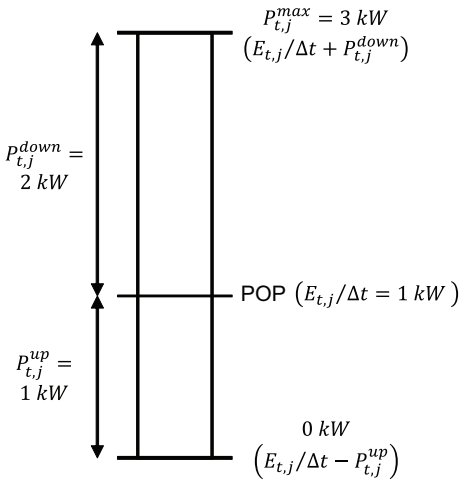

Figure 5.10: *POP, upward and downward reserve power of one EV.*

The optimization problem is formulated assuming that there is a single reserve capacity price. For markets with separated sessions for upward and downward secondary reserve, the modification would be a different capacity price for each direction.

The objective function is the minimization of the total cost, divided into the following components: (a) cost of purchasing electrical energy; (b) income from reducing EV charging (dispatched upward reserve); (c) cost from charging EV as dispatched downward reserve; (d)

income from having available secondary reserve power. It can be written as:

$$\min \sum_{t \in H} \left(\begin{array}{c} \hat{p}_t \cdot \sum_{j=1}^{M_t} \left(E_{t,j} \right) - \hat{p}_t^{up} \cdot \sum_{j=1}^{M_t} \left(P_{t,j}^{up} \cdot \Delta t \right) + \hat{p}_t^{down} \cdot \sum_{j=1}^{M_t} \left(P_{t,j}^{down} \cdot \Delta t \right) - \\ \hat{p}_t^{cap} \cdot \sum_{j=1}^{M_t} \left(P_{t,j}^{up} + P_{t,j}^{down} \right) \end{array} \right) \tag{5.2}$$

where $\hat{p}_t$ is the forecasted day-ahead energy price, $\hat{p}_t^{up}$ the forecasted price for dispatched upward reserve, $\hat{p}_t^{down}$ the forecasted price for dispatched downward reserve, $\hat{p}_t^{cap}$ the forecasted price for reserve capacity, M_t the number of EV plugged-in at time interval t, Δt the length of time interval t, H a set of time intervals from the optimization horizon (e.g., for one day with $\Delta t = 30$ minutes, H ranges between 1 and 48).

The constraints of the optimization problem are described in the following paragraphs.

The method for computing the reserve band is as follows: first, the charging requirements are satisfied considering the purchased energy and the upward reserve power, and then, the downward reserve power is the remaining capacity (below the maximum charging power, P_t^{max}) in each time interval t.

The first point leads to the following constraint:

$$\sum_{t \in \hat{H}_j^{plug}[i]} \left(E_{t,j} - P_{t,j}^{up} \cdot \Delta t \right) = \hat{R}_{j,i}, \quad \forall j \in \{1, \cdots, M_t\}, \forall i \in \{1, \cdots, L_j\} \tag{5.3}$$

where $\hat{H}_j^{plug}[i]$ is the i$^{\text{th}}$ forecasted availability period (from a set with L_j availability periods) of the j$^{\text{th}}$ EV, and $\hat{R}_{j,i}$ the forecasted charging requirement for the i$^{\text{th}}$ availability period of the j$^{\text{th}}$ EV.

The second point leads to the following constraint for downward reserve:

$$E_{t,j} \big/ \Delta t + P_{t,j}^{down} \leq P_j^{\max}, \forall j \in \{1, \cdots, M_t\}, \forall t \in H \tag{5.4}$$

The upward reserve band is limited by the energy bid in each time interval:

$$P_{t,j}^{up} \leq \left(E_{t,j} \big/ \Delta t \right), \forall j \in \{1, \cdots, M_t\}, \forall t \in H \tag{5.5}$$

and its total is limited by the charging requirement in each availability period:

$$\sum_{t \in \hat{H}_j^{plug}[i]} \left(P_{t,j}^{up} \cdot \Delta t \right) \leq \hat{R}_{j,i}, \quad \forall j \in \{1, \cdots, M_t\}, \forall i \in \{1, \cdots, L_j\} \tag{5.6}$$

Constraint (5.6) is included to avoid the aggregator from offering a total upward reserve greater than the total energy that the EV fleet can consume (i.e., the charging requirement).

The total downward reserve is also constrained by the charging requirement:

$$\sum_{t \in \hat{H}_j^{plug}[i]} \left(P_{t,j}^{down} \cdot \Delta t \right) \leq \hat{R}_{j,i}, \quad \forall j \in \{1, \cdots, M_t\}, \forall i \in \{1, \cdots, L_j\} \tag{5.7}$$

With the constraint (5.8), the aggregator can only offer upward reserve in a specific interval if the EV is able to consume the corresponding quantity both in the same and subsequent time intervals. This increases the robustness of the bidding optimization since it forces the EV to be capable of consuming the quantity that is offered as upward reserve. Otherwise, considerable penalization (topic discussed in section 5.5) could be incurred if upward reserve cannot be supplied. This constraint consists in postponing EV charging by offering upward reserve:

$$\sum_{k=t}^{k=t_{final} \in \hat{H}_j^{plug}[i]} \left(P_{k,j}^{up} \cdot \Delta t \right) \leq \frac{\sum_{k=t}^{k=t_{final} \in \hat{H}_j^{plug}[i]} (E_{k,j})}{2}, \tag{5.8}$$
$$\forall j \in \{1, \cdots, M_t\}, \forall t \in H, \forall i \in \{1, \cdots, L_j\}$$

where t_{final} is the last time interval of the ith availability period.

In (5.8), the total consumption reduction between t and t_{final} must be below or equal to half of the energy consumed in the same period.

In order to illustrate this constraint, Table 5.2 presents three candidate solutions for offering upward reserve with an EV plugged-in during six hours and with a charging requirement of 9 kWh and maximum charging power of 3 kW.
Solution (a), with constraint (5.8), is unfeasible because the charging requirement is already satisfied after interval H3, and the aggregator makes an upward reserve offer in intervals H5 and H6 where it is not able to supply if requested by the TSO.
In the case of solution (b), after interval H2 there are 3 kWh of charging requirement that remains to be satisfied, and so the EV has flexibility to offer upward reserve. However, the upward reserve offer in interval H4 is only feasible if the upward reserve is supplied at 100% in interval H3, and in interval H5 is only feasible if it is dispatched at 100% in intervals H3 and H4 (note that this is highly improbable in the secondary reserve framework).
Finally, solution (c) is feasible. For instance, in interval H3 the EV offers 3 kW of upward reserve, and it consumes additional 3 kW in the remaining time intervals (H4 in this case).

It is important to stress that, with constraints (5.8) and (5.3), the upward reserve power is limited by the fleet's ability to postpone charging. Both constraints assumed that 100% of the upward power is dispatched by the AGC (a similar assumption was made in [151]), which is conservative since it limits the available reserve power (e.g., if a mobilization of 20% was assumed, the upward power bid could be higher). However, it also offers robustness since the available reserve power in the current interval is not affected even if the upward reserve is

Table 5.2: *Set of charging solutions of an EV offering upward reserve power in a six hours availability period with a charging requirement of 9 kWh.*

(a) *Unfeasible solution 1.*

	H1	H2	H3	H4	H5	H6
E_k [kWh]	3	3	3	0	3	3
P_k^{up} [kW]	0	0	0	0	3	3

(b) *Unfeasible solution 2.*

	H1	H2	H3	H4	H5	H6
E_k [kWh]	3	3	3	3	3	3
P_k^{up} [kW]	0	0	3	3	3	0

(c) *Feasible solution.*

	H1	H2	H3	H4	H5	H6
E_k [kWh]	3	3	3	3	3	3
P_k^{up} [kW]	3	0	3	0	3	0

dispatched in lower quantities during previous intervals. For instance, if the reserve in interval H1 of solution (c) is not fully dispatched, there would be a surplus of consumed electrical energy compared to what was planned, but the aggregator can consume less in interval H2 (if necessary) to compensate this surplus at a cost of an energy imbalance penalty.

For electricity markets (like in Portugal), that requires a predefined ratio between upward and downward reserve power, the reserve band is divided into upward and downward directions with the following equality:

$$P_{t,j}^{up} = \mu \cdot P_{t,j}^{down}, \forall j \in \{1, \cdots, M_t\}, \forall t \in H \tag{5.9}$$

where μ is the ratio between upward and downward secondary reserve.

In Portugal, the reserve band is divided into 2/3 for upward and 1/3 for downward, so the value of μ is 2.

After solving the LP problem, a post-processing phase is applied to the downward reserve. In order to create sufficient flexibility to supply upward reserve, the purchased energy is higher than the charging requirement [due to equation (5.3)]. Thus, this post-processing phase eliminates downward reserve bids from the time intervals where the total purchased energy is above the charging requirement. This is performed with the values of $E_{t,j}$ calculated by

solving the LP problem and with the following equation:

$$P_{t,j}^{down} = \begin{cases} \min\left(\hat{R}_{j,i} - \sum_{k=t_{initial}}^{t}\left(E_{k,j}\right), P_{t,j}^{down}\right) & , if\ P_{t,j}^{down}\cdot\Delta t + \sum_{k=t_{initial}}^{t}\left(E_{k,j}\right) \leq \hat{R}_{j,i} \\ 0 & , if\ P_{t,j}^{down}\cdot\Delta t + \sum_{k=t_{initial}}^{t}\left(E_{k,j}\right) > \hat{R}_{j,i} \end{cases} \tag{5.10}$$

where $t_{initial}$ is the first time interval of the ith forecasted availability period, i.e. $t_{initial} \in \hat{H}_j^{plug}[i]$.

If the aggregator, according to the market rules, must guarantee a certain ratio between upward and downward reserve power, equality (5.9) is used to adjust upward reserve power in order to maintain the ratio.

Equation 5.10 increases the robustness of the downward reserve bid, since, even in cases where the upward reserve from the previous intervals is not dispatched, the aggregator is able to supply the downward power in the subsequent intervals regardless of the dispatched upward reserve.

Table 5.3 presents a potential solution for energy and reserve bids of one EV with charging requirement of 9 kWh. In this example, the downward reserve power bid in interval H5 is removed in the post-processing phase, since the sum of E_k between intervals H1 and H4 is already equal to the charging requirement. Therefore, there is a risk of the EV not being able to make available a downward reserve power of 1 kW in interval H5. For instance, if in interval H2 only 0.5 kWh is dispatched as upward reserve and in interval H3 only 0.2 kWh, the total electrical energy after interval H4 would be 8.3 kWh, and, since it can only charge additional 0.7 kWh, the EV is unable to guarantee a downward reserve power of 1 kW in interval H5. In this case, because of constraint 5.10, the aggregator can only offer downward reserve during the first four intervals.

Table 5.3: *Example of a charging solution of an EV offering upward and downward reserve power in a six-hour availability period with a charging requirement of 9 kWh.*

	H1	H2	H3	H4	H5	H6
E_k [kWh]	2	2	2	3	2	2
P_k^{up} [kW]	0	1	1	0	2	0
P_k^{down} [kW]	0	0.5	0.5	0	1	0

Figure 5.11a depicts the output of the day-ahead optimization model for one day (with hourly intervals) from the test case described in chapter 4 and for fleet A. The forecasts of the energy and secondary reserve capacity prices are depicted in Figure 5.11b. The reserve power is divided into 1/3 for downward and 2/3 for upward reserve.

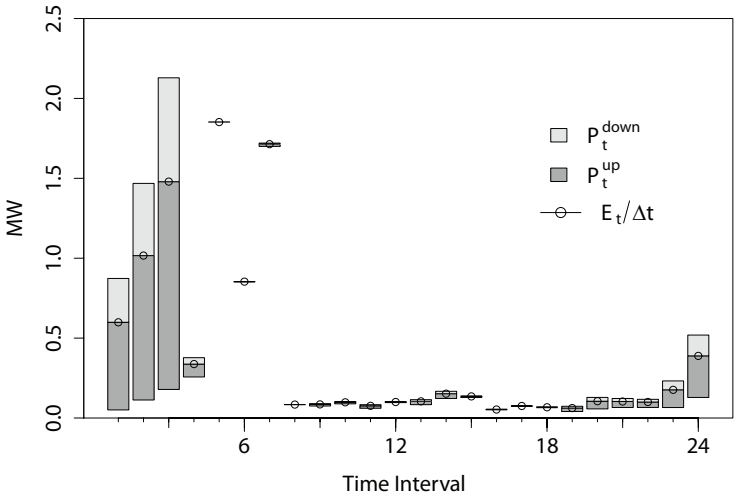

(a) *Energy and secondary reserve power bids.*

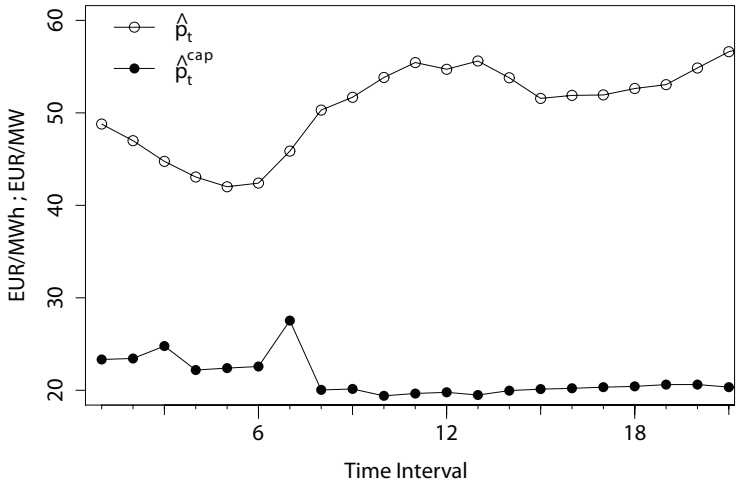

(b) *Forecasted secondary reserve capacity price and energy price.*

Figure 5.11: *Output of the day-ahead optimization (energy and secondary reserve power bids) for one illustrative day of the test case (fleet A).*

The aggregator mostly presents reserve power bids in the period between hourly intervals 1 and 4, and intervals 20 and 24, while during the remaining intervals the offered reserve is rather low. Note that, in order to offer secondary reserve power, the aggregator must offer an energy bid that is the reference operating point from which supplies upward and downward reserve. For instance, in interval 2, the energy bid is 1.01 MW, from which a reserve of 0.9 MW is offered in upward direction (upward band is between 1.01 MW and 0.11 MW) and half of this value is offered in the downward direction (reserve band is between 1.01 MW and 1.46 MW).

This bids' pattern is consistent with the drivers' behavior. The available power for secondary reserve is higher when the number of plugged-in EV is high and also when the charging requirements are not yet fully satisfied. For instance, in intervals 5 and 6, the secondary reserve bid is zero, since either the charging requirement of the EV is almost satisfied or there is no

flexibility to postpone charging, as the EV will depart in the next intervals. The aggregator also makes secondary reserve offers in intervals where the forecasted energy price is high (e.g., intervals 21 and 22), mainly because the reserve capacity price offsets this price increase and the reserve bids are constrained by the availability and charging requirement of each EV (e.g., a high reserve capacity price in interval 7 does not necessarily result in a high secondary reserve power bid).
Because of constraints (5.5)-(5.8), the aggregator offers upward power earlier (between intervals 19 and 24 and between 1 and 4) to consume the necessary energy after those intervals and meet the charging requirement.

The estimated total cost, calculated from the objective function (5.2), and assuming that the upward and downward reserve is 100% dispatched, is 182.7 €. This cost is just an estimate and only after the operational phase is it possible to calculate the real wholesale total cost.

Figure 5.12a depicts the output of the day-ahead optimization model for one day of fleet B, and the corresponding price forecasts are depicted in Figure 5.11b.

The main difference to the previous example is that this fleet, in this illustrative day, offered secondary reserve in the period between 12 and 19 hours. Furthermore, the price forecasts show that in some hours the reserve capacity price is above the energy price (note that this situation also occurred in the realized values). In this case, offering reserve is very attractive, but, as explained before, the reserve bids are constrained by the EV availability and charging requirement. Therefore, in hour 6, the difference between capacity and energy price is the highest, but there is no available flexibility to offer more reserve.
The estimated total cost of this illustrative day is -42.1 €.

These two days will be revisited during the next section to illustrate the output of the operational management algorithm.

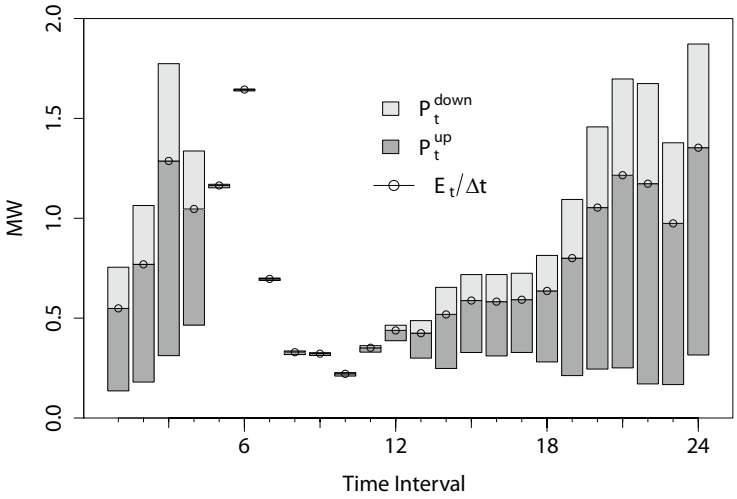

(a) *Energy and secondary reserve power bids.*

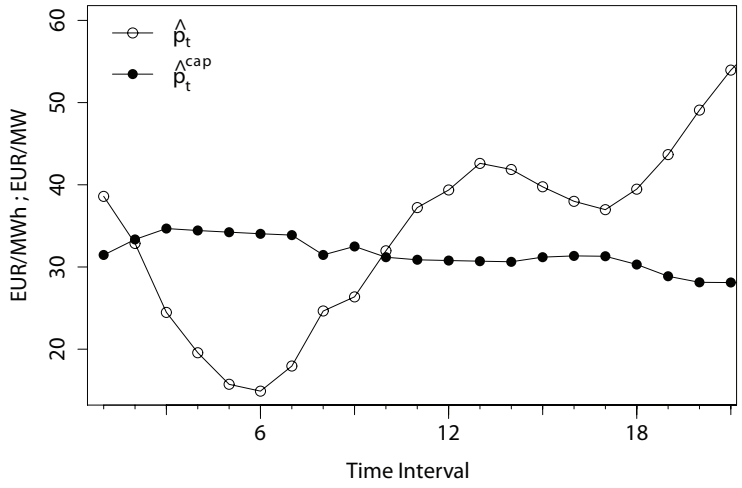

(b) *Forecasted secondary reserve capacity price and energy price.*

Figure 5.12: *Output of the day-ahead optimization (energy and secondary reserve power bids) for one illustrative day of the test case (fleet B).*

5.4 Operational Management Algorithm

The previous section described the day-ahead optimization model for deriving the energy and secondary reserve bids. During the operating day, the aggregator coordinates the EV charging to comply with the AGC signal and deliver secondary reserve with acceptable reliability. This section describes an operational management algorithm to meet this goal.

The operational algorithm uses two types of information: (a) accepted bids from the electricity market (E_t, P_t^{down}, P_t^{up}, depicted in Figure 5.13) for time intervals t with length Δt (the same used in the day-ahead optimization); (b) updated available reserve power in the beginning of each interval of the operating day. Note that the quantities in the accepted bids, as explained in section 5.2.1, are divided by time intervals with length Δt (which are contained inside the

market time interval).

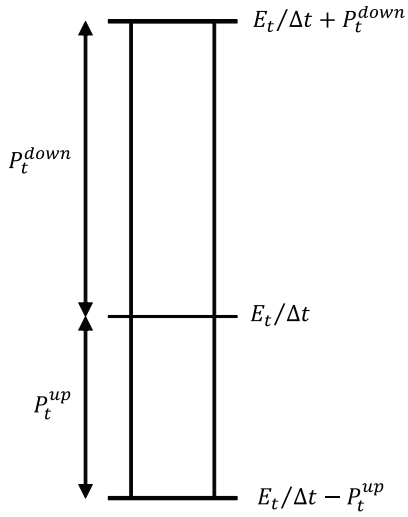

Figure 5.13: *Outputs of the day-ahead optimization for energy and secondary reserve bids.*

The second point means that the aggregator informs the TSO, before the beginning of t_0, about the available secondary reserve. For instance, this is a common practice in PJM [211].

The operational management algorithm is divided into two phases that are described in the following subsections: first, the redefinition of the EV fleet operating point and calculation of the available reserve power, and then, the coordination of the EV charging to comply with the AGC requests.

5.4.1 EV Fleet Operating Point and Calculation of the Available Reserve

The aggregator, 15 minutes before the beginning of time interval t_0 (e.g., necessary time to activate tertiary or balancing reserve if necessary) and using the information from the plugged-in EV, calculates the available reserve power in both directions for that interval and communicates this information to the TSO.

These values are updated during the operation hour (e.g. every minute for the next 5 minutes), since the available reserve power can be reduced if the reserve is dispatched in one direction during a long period. For instance, an EV with a residual charging requirement of 1.5 kWh is able to supply 3 kW, but only during 30 minutes. Therefore, the aggregator must update these values in a continuous basis and for a time horizon of at least 5 minutes. The AGC modifies its control signal based on the available power communicated by the aggregator. Financial penalization schemes for reserve shortage situations are discussed in section 5.5.

The first step for computing the available reserve power, consists in determining the operating point P'_{t_0} (i.e., the actual POP for time interval t_0). The operating point is a constant charging level that the aggregator can sustain during the complete interval t by coordinating the EV fleet charging, and from which the upward and downward reserves are supplied. Note that this is the operating point of the EV fleet and not of each EV. In the operational phase, the aggregator combines the EV individual charging to attain the contracted reserve levels, and it may happen that a specific EV only supplies reserve in one direction. For instance, an EV with an operating point of zero can contribute to the provision of the downward reserve power. The operating point is also used to calculate energy imbalances (deviation to the accepted energy bid) and corresponding penalties in the market settlement phase.

Without the presence of uncertainty, the operating point would be equal to the accepted energy bid. However, because of forecast errors, the operating point will deviate from the energy bid, which creates energy imbalances and decreases the availability of secondary reserve. Therefore, the aggregator should define an operating point during the operational phase that guarantees the contracted reserve at a cost of increasing the energy imbalances. The following paragraphs describe a procedure that re-calculates (using the energy bid as reference) the operating point in order to maximize the availability of secondary reserve power.

It is important to note that changing the operating point in order to increase the available secondary reserve is a standard practice in power system operation. Figure 5.14 illustrates how ENTSO-E (former UCTE) recommends the use of tertiary reserve to free up secondary reserve. In this example, generators M1 and M2 decrease their operating points in order to increase the available upward secondary reserve, and the energy imbalance originated by this change in the operating points is covered by starting generator M3 as upward tertiary reserve.

First, the aggregator, before the beginning of time interval t_0, and using the information of all plugged-in EV, computes two variables:

- $\bar{P}^{\min}_{t_0}$: minimum, constant and feasible charging power of the EV fleet in time interval t_0;
- $\bar{P}^{\max}_{t_0}$: maximum, constant and feasible charging power of the EV fleet in time interval t_0;

The $\bar{P}^{\min}_{t_0}$ is computed by solving the following optimization problem:

$$\min \left[\varphi \left(\sum_{j=1}^{M_{t_0}} \left(E^*_{t_0,j} \right) - 0 \right) + \sum_{k=t_0+1}^{T} \left(\varphi \left(E_k - \sum_{j=1}^{M_k} \left(E^*_{k,j} \right) \right) \right) \right] \tag{5.11}$$

where the decision variable $E^*_{k,j}$ is the electrical energy to be consumed by the j$^{\text{th}}$ EV, E_k the

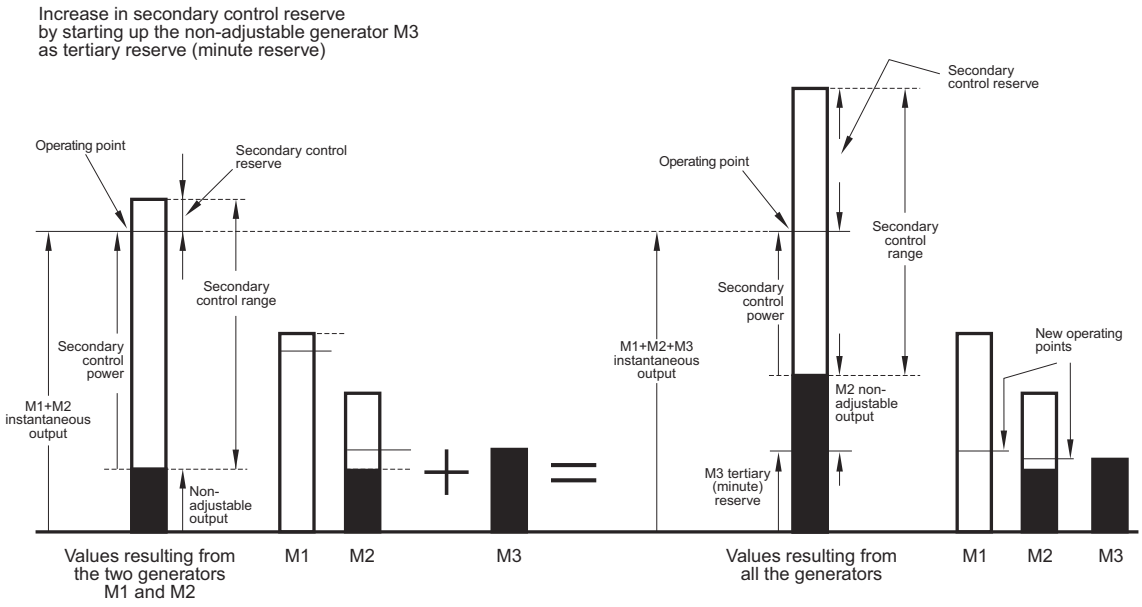

Figure 5.14: *Increase in secondary reserve by starting the non-adjustable generator M3 as tertiary reserve [34].*

result (or accepted bid) from the day-ahead optimization model, t_0 the first time interval of the optimization period, T the time interval of the last plugged-in EV to depart and φ a convex loss function given by:

$$\varphi(u) = \begin{cases} u \cdot \hat{\pi}_k^+, u \geq 0 \\ -u \cdot \hat{\pi}_k^-, u < 0 \end{cases} \tag{5.12}$$

where $\pi_{t_0}^+$ and $\pi_{t_0}^-$ are made equal to a large number, and $k > t_0$ are made equal to the forecasted imbalance prices.

The optimization problem consists in charging the EV fleet as close as possible to zero in time interval t_0, respecting the maximum charging power (5.13) and charging requirement (5.14) constraints. Note that $\bar{P}_{t_0}^{\min} = \sum_{j=1}^{M_{t_0}} \left(\frac{E_{t_0,j}^*}{\Delta t} \right)$.

$$\frac{E_{k,j}^*}{\Delta t} \leq P_j^{\max}, \quad \forall j \in \{1, \cdots, M_k\}, \forall k \in H_j^{plug}[i], \forall i \in \{1, \cdots, L_j\} \tag{5.13}$$

$$\sum_{k \in H_j^{plug}[i]} \left(E_{k,j}^* \right) = R_{t_0,j,i}, \quad \forall j \in \{1, \cdots, M_k\}, \forall i \in \{1, \cdots, L_j\} \tag{5.14}$$

The value of $\bar{P}_{t_0}^{\max}$ is calculated with:

$$\bar{P}_{t_0}^{\max} = \sum_{j=1}^{M_{t_0}} \left(\min \left(\frac{R_{t_0,j}}{\Delta t}, P_j^{\max} \right) \right) \tag{5.15}$$

which means that it is equal the maximum charging power constrained by the residual charging requirement. For instance, an EV with residual charging requirement equal to 1 kWh in a half-hour period and with a maximum charging power of 3 kW, can only charge at constant 2 kW ($=\bar{P}_{t_0}^{\max}$) during that interval.

These two variables, together with the accepted energy bid (E_{t_0}), are used to define the operating point. Figure 5.15 depicts three situations that may occur in terms of energy bid value and the variables required to calculate the EV fleet operating point.

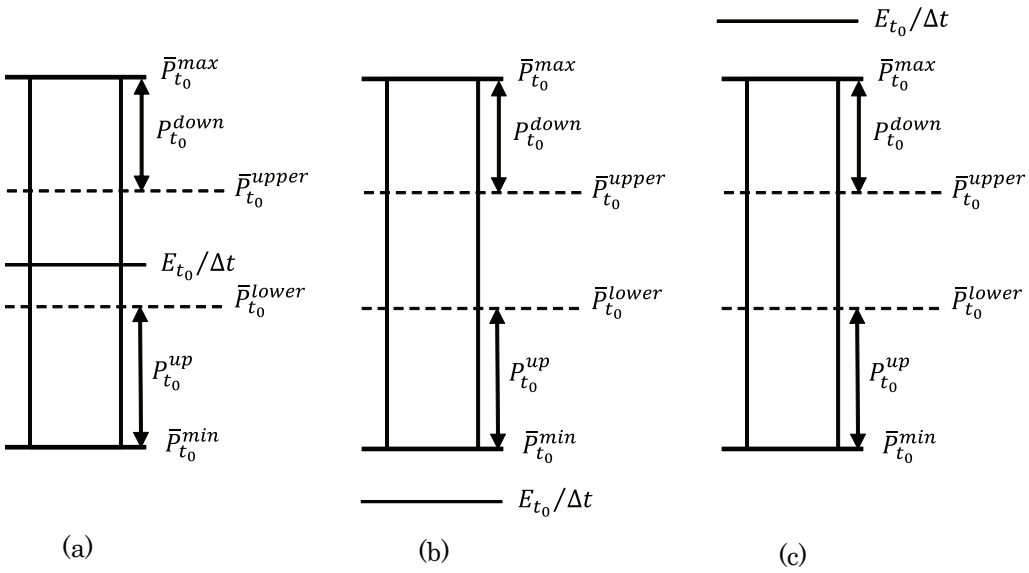

Figure 5.15: *Variables required to redefine the operating point of the EV fleet.*

In situation (a), the accepted energy bid is within the minimum and maximum consumption power limits. In order to guarantee full availability of the reserve power, the operating point should be within two limits: upper power limit that guarantees full availability of downward reserve power in time interval t_0 ($\bar{P}_{t_0}^{upper} = \bar{P}_{t_0}^{\max} - P_{t_0}^{down}$), and lower power limit that guarantees full availability of upward reserve power ($\bar{P}_{t_0}^{lower} = \bar{P}_{t_0}^{\min} + P_{t_0}^{up}$).

Depending on the accepted energy bid value, the following can occur:

- **if** $\bar{P}_{t_0}^{upper} \geq \bar{P}_{t_0}^{lower}$ (any operating point between $\bar{P}_{t_0}^{upper}$ and $\bar{P}_{t_0}^{lower}$ allows full availability of the reserve, thus it is selected the closest point to the energy bid)
  - **if** $E_{t_0}/\Delta t \in \left[\bar{P}_{t_0}^{lower}, \bar{P}_{t_0}^{upper}\right] \Rightarrow P'_{t_0} = E_{t_0}/\Delta t$
  - **if** $\bar{P}_{t_0}^{lower} > E_{t_0}/\Delta t \Rightarrow P'_{t_0} = \bar{P}_{t_0}^{lower}$ (the operating point is made equal to $\bar{P}_{t_0}^{lower}$ since it is the closest point to the energy bid)
  - **if** $\bar{P}_{t_0}^{upper} < E_{t_0}/\Delta t \Rightarrow P'_{t_0} = \bar{P}_{t_0}^{upper}$ (the operating point is made equal to $\bar{P}_{t_0}^{upper}$ since it is the closest point to the energy bid)

- **if** $\bar{P}_{t_0}^{upper} < \bar{P}_{t_0}^{lower}$, $P'_{t_0} = E_{t_0} \big/ \Delta t$ (any change in the operating point value would increase the reserve availability in one direction, at the cost of the other direction; the choice is to maintain the operating point equal to the energy bid value)

In situation (b), the accepted energy bid is below the minimum consumption power level. The operating point is defined as follows:

- **if** $\bar{P}_{t_0}^{upper} \geq \bar{P}_{t_0}^{lower} \Rightarrow P'_{t_0} = \bar{P}_{t_0}^{lower}$ (the operating point should be within $\bar{P}_{t_0}^{lower}$ and $\bar{P}_{t_0}^{upper}$, and it is made equal to $\bar{P}_{t_0}^{lower}$ since it is the closest point to the energy bid)

- **if** $\bar{P}_{t_0}^{upper} < \bar{P}_{t_0}^{lower}$, $P'_{t_0} = \min\left(\bar{P}_{t_0}^{upper}, \bar{P}_{t_0}^{\min}\right)$ (it is not possible to offer the full contracted reserve in both directions; if $\bar{P}_{t_0}^{upper}$ is greater than $\bar{P}_{t_0}^{\min}$, it is not possible to offer upward reserve and the operating point is made equal to $\bar{P}_{t_0}^{\min}$; if it is lower, the operating point is made equal to $\bar{P}_{t_0}^{upper}$ and it is possible to offer upward reserve between this point and $\bar{P}_{t_0}^{\min}$)

In situation (c), the accepted energy bid is greater than the maximum consumption power level. The operating point is defined as follows:

- **if** $\bar{P}_{t_0}^{upper} \geq \bar{P}_{t_0}^{lower} \Rightarrow P'_{t_0} = \bar{P}_{t_0}^{upper}$ (the operating point should be within $\bar{P}_{t_0}^{lower}$ and $\bar{P}_{t_0}^{upper}$, and it is made equal to $\bar{P}_{t_0}^{upper}$ since it is the closest point to the energy bid)

- **if** $\bar{P}_{t_0}^{upper} < \bar{P}_{t_0}^{lower}$, $P'_{t_0} = \min\left(\bar{P}_{t_0}^{lower}, \bar{P}_{t_0}^{\max}\right)$ (it is not possible to offer the full contracted reserve in both directions; if $\bar{P}_{t_0}^{lower}$ is greater than $\bar{P}_{t_0}^{\max}$, it is not possible to offer downward reserve and the operating point is made equal to $\bar{P}_{t_0}^{\max}$; if it is lower, the operating point is made equal to $\bar{P}_{t_0}^{lower}$ and it is possible to offer downward reserve between this point and $\bar{P}_{t_0}^{\max}$)

The goal of this approach was to change the operating point in order to comply with the contracted reserve power, while at the same time, it tries to avoid a significant increase of energy imbalances.

This change in the operating point creates an energy imbalance, which the TSO solves by calling balancing or tertiary reserve, and the aggregator pays a financial penalty for this energy imbalance. The aggregator can trade this operating point change in intraday or real-time markets, which results in a decrease of the energy imbalances. However, the participation in these markets is not addressed in this thesis.

The operating point is used to calculate the available upward and downward reserve power. The available upward reserve power ($P_{t_0}^{'up}$) is given by:

$$P_{t_0}^{'up} = \min\left(P'_{t_0}, P_{t_0}^{up}\right) \tag{5.16}$$

This equation means that the aggregator can only decrease a charging rate that is attainable. For instance, if the upward reserve bid is 5 MW and the operating point is only 3 MW, then the available reserve capacity should be 3 MW.

The available downward reserve power ($P'^{down}_{t_0}$) is given by:

$$P'^{down}_{t_0} = \min\left(P^{down}_{t_0}, \sum_{j \in K}\left(P^{\max}_{j}\right) - P'_{t_0}\right) \tag{5.17}$$

where K is the set of plugged-in EV in t_0 with $R_{t_0} > 0$ (i.e., the charging requirement is not fully satisfied), and $\sum_{j \in K}\left(P^{\max}_{j}\right)$ the maximum instantaneous charging power of the EV fleet in time interval t_0. The available reserve power is the minimum between accepted bid and the difference between the maximum instantaneous charging power of the EV fleet and the operating point.

Figure 5.16a depicts the redefinition of the operating point for the illustrative example of Figure 5.11 (output of the day-ahead optimization). The accepted energy bid, the consumption limits, and the redefined operating point are depicted for each hour. The first grey area is the interval between $\bar{P}^{min}_{t_0}$ and $\bar{P}^{max}_{t_0}$, which defines the range of feasible values for the EV fleet charging power taking into account its constraints. The dark grey area is the interval between $\bar{P}^{lower}_{t_0}$ and $\bar{P}^{upper}_{t_0}$, which defines the range of charging power values that assure a compliance with the contracted secondary reserve levels.

All the operating points are within the bands $\left[\bar{P}^{min}_{t_0} : \bar{P}^{max}_{t_0}\right]$ and $\left[\bar{P}^{lower}_{t_0} : \bar{P}^{upper}_{t_0}\right]$ (which means no reserve power shortage), while the accepted bids in intervals 6, 7 and 12 are above the limit $\bar{P}^{max}_{t_0}$. Thus, in those three intervals the operating point cannot be equal to the accepted energy bid (i.e., it must be lower). In interval 1, the accepted energy bid (that corresponds to 0.6 MW) is below the limit $\bar{P}^{lower}_{t_0}$ (0.655 MW), thus the operating point is made equal to the lower limit.

Figure 5.16b depicts the operating point redefinition for the illustrative example of Figure 5.12 (output of the day-ahead optimization). In interval 18 of this example, the lower limit is greater than the upper limit ($\bar{P}^{lower}_{t_0}$=0.52 MW and $\bar{P}^{lower}_{t_0}$=0.49 MW), and since the energy bid (0.8 MW) is within the maximum and minimum limits (0.14 MW and 0.9 MW), the operating point is made equal to the bid value. In interval 17, the accepted energy bid (0.59 MW) was above the limit $\bar{P}^{max}_{t_0}$ (0.56 MW) and the operating point is made equal to the upper limit (0.43 MW). Note that, in several intervals (such as 3 and 24), the operating point is made equal to the accepted energy bid, that is, within the upper and lower limits.

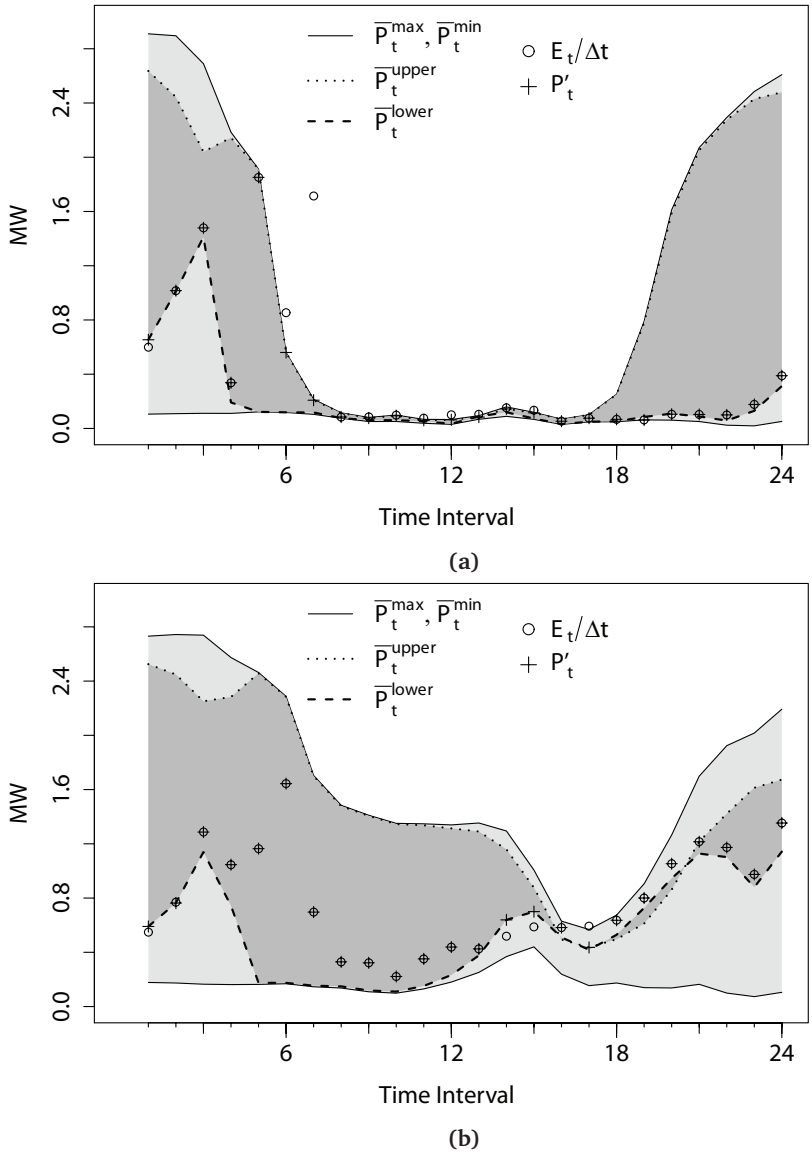

Figure 5.16: *Illustrative examples for the calculation of the redefined operating point.*

5.4.2 Operational Management

During the operating day and when the AGC signal is zero, the aggregator dispatches the EV to consume the operating point (P'_{t_0}) in t_0 and minimize the deviations to the accepted energy bids (in $k > t_0$). This is accomplished with the following objective function:

$$\min \left[\varphi \left(P'_{t_0} - \sum_{j=1}^{M_{t_0}} \left(\frac{E^*_{t_0,j}}{\Delta t} \right) \right) + \sum_{k=t_0+1}^{T} \left(\varphi \left(E_k - \sum_{j=1}^{M_k} \left(E^*_{k,j} \right) \right) \right) \right] \tag{5.18}$$

The two constraints (5.13) and (5.14) are also considered.

When upward reserve is needed, the AGC sends a signal to the aggregator, and the aggregator

dispatches the EV to supply the requested reserve using the following objective function:

$$\min \left[\varphi \left(\left(P'_{t_0} - P'^{up}_{t_0} \right) - \sum_{j=1}^{M_{t_0}} \left(\frac{E^*_{t_0,j}}{\Delta t'} \right) \right) + \sum_{k=t_0+1}^{T} \left(\varphi \left(E_k - \sum_{j=1}^{M_k} \left(E^*_{k,j} \right) \right) \right) \right] \tag{5.19}$$

where $\Delta t'$ ($\leq \Delta t$) is the length of the period where the secondary reserve was activated.

When the AGC sends a signal requesting downward reserve, the following objective function is used:

$$\min \left[\varphi \left(\left(P'_{t_0} + P'^{down}_{t_0} \right) - \sum_{j=1}^{M_{t_0}} \left(\frac{E^*_{t_0,j}}{\Delta t'} \right) \right) + \sum_{k=t_0+1}^{T} \left(\varphi \left(E_k - \sum_{j=1}^{M_k} \left(E^*_{k,j} \right) \right) \right) \right] \tag{5.20}$$

The constraints (5.13) and (5.14) are also considered for these two objective functions. Because of constraint (5.14), it may happen that that both $P'^{down}_{t_0}$ and $P'^{up}_{t_0}$ become depleted after some time ($< \Delta t$). This occurs for the upward reserve, since the main priority is to satisfy the charging requirement of the EV drivers, and it may not be possible to reduce the charging rate for a long period of time. For the downward reserve, this occurs when the batteries of some EV become full during Δt or the charging requirement becomes fully satisfied.

In this case, the aggregator communicates the new available reserve power to the TSO, which can mobilize tertiary reserve to free up additional secondary reserve or dispatch additional reserve power from other resources. The aggregator pays a high penalty for not being able to supply the required reserve (topic discussed in section 5.5).

The operational management algorithm is sequential and can be summarized as follows:

1. new information is available from the recently plugged-in EV (i.e., that connected for charging between $t_0 - 1$ and t_0) and is included in equation (5.14) of the optimization model;

2. using this information, the aggregator computes the operating point, available upward and downward reserve power: P'_{t_0}, $P'^{down}_{t_0}$, $P'^{up}_{t_0}$. This information is communicated to the TSO;

3. during time interval t_0:

   - the AGC sends signals requesting upward or downward reserve. The aggregator solves the optimization problem from (5.19)-(5.20) and sends set points to the EV fleet. The prices $\hat{\pi}^+_{t_0}$ and $\hat{\pi}^-_{t_0}$ are made equal to a large number (e.g., 103);

   - the aggregator updates the charging requirement of each EV based on the operating point plus dispatched reserve. Moreover, updates and communicates the new

values of available reserve to the TSO;

4. this process is repeated for the next time interval $t_0 + 1$ with the recently arrived EV.

This operational algorithm concludes the management process of the EV fleet charging. The aggregator starts with the day-ahead optimization (Figures 5.11 and 5.12), before the beginning of the operating hour redefines the operating point (Figure 5.16), and during the operating hour, coordinates the EV charging to comply with the contracted levels. The output (or result) of this last phase is the electrical energy consumed by the EV fleet in each hour, which is depicted in Figure 5.17a for the illustrative example of Figure 5.11. Together with the EV fleet actual consumption, the operating point and the available upward and downward reserve power are also depicted. Figure 5.17b depicts the number of equivalent minutes for the illustrative day.

For example, in hour 1, the number of equivalent minutes of dispatched reserve was 42.24 min for downward and 17.76 min for upward, and the electrical energy consumed by the EV fleet by the end of that interval was 0.68 MWh, which corresponded to increasing the charging level from 0.65 MW (P'_{t_0}) to 0.68 MW by supplying more downward than upward reserve power (i.e., $E^{down}_{t_0} = 0.27 \cdot 42.24/60 = 0.19$ MWh against $E^{up}_{t_0} = 0.55 \cdot 42.24/60 = 0.16$ MWh). In hour 24, the secondary reserve was also activated in both directions (46 min for upward and 8.5 min for downward reserve) and the consumed electrical energy was below the operating point.

Figure 5.18a depicts the output of the operational management algorithm for the illustrative day of Figure 5.12. Figure 5.18b depicts the number of equivalent minutes. The conclusions are rather similar to the previous day. In some hours, the consumed electrical energy deviates from the operating point since reserve was mainly dispatched in one direction. Only in hour 23, are the operating point and consumed electrical energy similar. This happens because the downward reserve was dispatched by around 39 min (but it is half of the upward reserve power), and the upward reserve was dispatched by half of this time (21 min) but with twice the reserve power. The net electrical energy from the reserve provision was approximately zero: $-0.8 \cdot (21/60) + 0.4 \cdot (39/60) = -0.02$ MWh.

The market settlement phase, which will be described in the next section, is applied *a posteriori* and gives the "true" cost of the aggregator. In the two illustrative examples, the total cost, after the operational management phase, was 204.9 € (in contrast to 182.7 € estimated in the day before) and 119.3 € (in contrast to -42.1 €) correspondingly. This cost difference is explained by a dispatched reserve power below 100%, price forecast errors, and imbalance costs. Note that there are no reserve shortage situations in these two days.

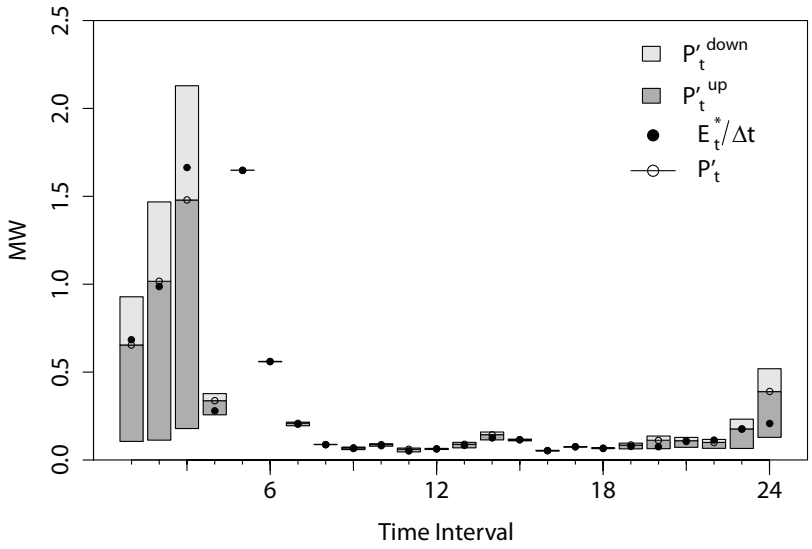

(a) *Operating point, available upward and downward reserve power, and electrical energy consumed by the EV fleet during the operating interval.*

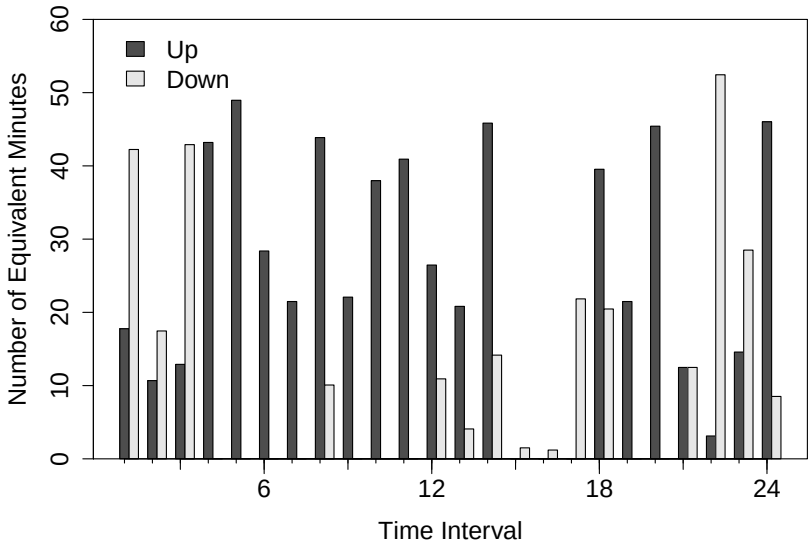

(b) *Number of equivalent minutes of upward and downward secondary reserve .*

Figure 5.17: *Illustrative example of the operational management algorithm output for secondary reserve and fleet A.*

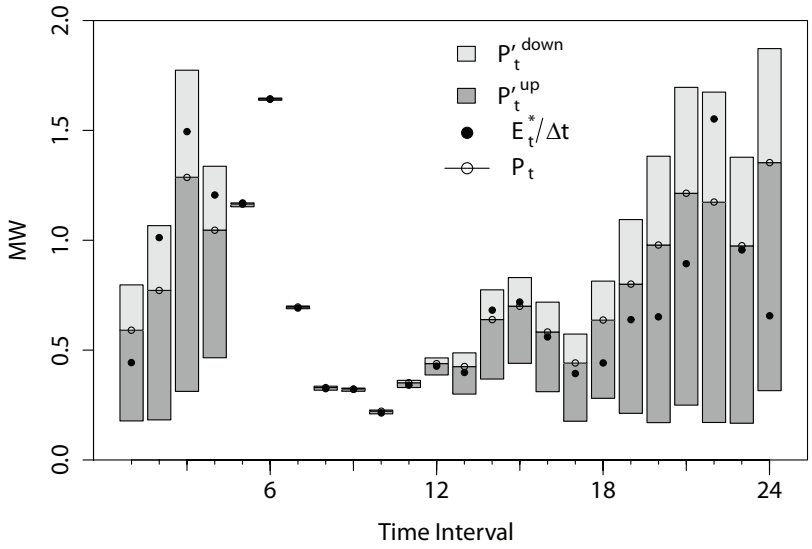

(a) *Operating point, available upward and downward reserve power, and electrical energy consumed by the EV fleet during the operating interval.*

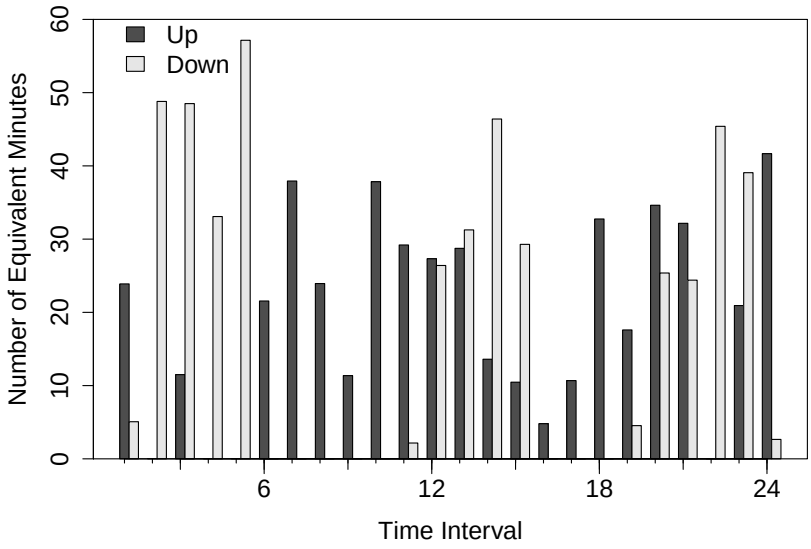

(b) *Number of equivalent minutes of upward and downward secondary reserve.*

Figure 5.18: *Illustrative example of the operational management algorithm output for secondary reserve and fleet B.*

5.5 Market Settlement

A settlement phase takes place after the operating day, where the costs related to energy imbalances and reserve shortage are added to the cost from purchasing energy and to the income from having available secondary reserve.

In this paper, two alternative penalization schemes for reserve shortage are considered: (a) the aggregator is penalized when it is unable to supply the constant reserve power during the complete interval Δt (based on the scheme adopted in Portugal [57]); (b) the aggregator is only penalized when it fails to respond with adequate reserve power to a signal from the AGC (inspired by [157] and also by the PJM regulation reserve remuneration scheme [77]).

For settlement scheme (a), in each direction of reserve, the aggregator is penalized by the difference between the accepted reserve bid and the reserve power that can be sustained during the complete interval t. The downward reserve power that can be sustained ($\bar{P}_t^{down}$) is given by:

$$\bar{P}_t^{down} = \min\left(P_t^{down}, \bar{P}_t^{\max} - P_t'\right) \tag{5.21}$$

For the upward reserve, the $\bar{P}_t^{up}$ is given by:

$$\bar{P}_t^{up} = \min\left(P_t^{up}, P_t' - \bar{P}_t^{\min}\right) \tag{5.22}$$

The TSO and Energy Regulator may audit these values to avoid fraud. In fact, ERCOT defines similar variables [150][217]: the High Sustained Limit (HSL), that is the maximum sustained power consumption of the load resource, which is computed from the real-time averaged MW during the 30 minutes of constant output, and Low Sustained Limit (LSL) which is the equivalent for downward reserve.

The total cost is computed with the intervals of length Δt and is given by:

$$Total\ Cost = \sum_t \begin{pmatrix} P_t' \cdot \Delta t \cdot p_t + E_t^{down} \cdot p_t^{down} - \\ E_t^{up} \cdot p_t^{up} - p_t^{cap} \cdot \left(\bar{P}_t^{down} + \bar{P}_t^{up}\right) + \\ \Psi\left(P_t' \cdot \Delta t, E_t\right) + \Phi\left(P_t^{down}, P_t^{up}, \bar{P}_t^{down}, \bar{P}_t^{up}\right) \end{pmatrix} \tag{5.23}$$

where $P_t' \cdot \Delta t$ is the consumed electrical energy that corresponds to the operating point (paid at the energy price, p_t), E_t^{down} the consumption corresponding to the dispatched downward secondary reserve (paid at the downward tertiary reserve price, p_t^{down}), E_t^{up} the dispatched upward secondary reserve (paid at the upward tertiary reserve price, p_t^{up}), $p_t^{cap} \cdot \left(\bar{P}_t^{down} + \bar{P}_t^{up}\right)$ the income from having available reserve capacity, Ψ the costs associated to deviations from the purchased energy (i.e., deviation between $P_t' \cdot \Delta t$ and accepted energy bid E_t), Φ the costs associated to reserve shortage.

For the reserve capacity income, the aggregator is remunerated by the values of reserve power that can be sustained during interval t, and a penalty term proportional to the deviation between P_t^{up} and $\bar{P}_t^{up}$ (and between P_t^{down} and $\bar{P}_t^{down}$) is imposed.

In a real situation, the values of E_t^{up} and E_t^{down} are metered, but here they are calculated as follows:

$$E_t^{up} = P_t'^{up} \cdot \lambda_t^{up} - RNS_t^{up} \tag{5.24}$$

where λ_t^{up} is the number of equivalent minutes of dispatched upward reserve, and RNS^{up} is the upward reserve not supplied.

The RNS_t^{up} is also metered, but here is calculated as the difference between the actual charging value (the output of the operational management algorithm, E_t^*) and the charging value that would be obtained in case of no reserve shortage ($\tilde{E}_t = P_t' - P_t'^{up} \cdot \lambda_t^{up} + P_t'^{down} \cdot \lambda_t^{down}$):

$$RNS_t^{up} = \begin{cases} \min\left(E_t^* - \tilde{E}_t, P_t'^{up} \cdot \lambda_t^{up}\right) & , if\ E_t^* > \tilde{E}_t \\ 0 & , if\ E_t^* \leq \tilde{E}_t \end{cases} \tag{5.25}$$

The calculation of E_t^{down} is analogous:

$$E_t^{down} = P_t'^{down} \cdot \lambda_t^{down} - RNS_t^{down}$$

$$RNS_t^{down} = \begin{cases} \min\left(\tilde{E}_t - E_t^*, P_t'^{down} \cdot \lambda_t^{down}\right) & , if\ E_t^* < \tilde{E}_t \\ 0 & , if\ E_t^* \geq \tilde{E}_t \end{cases} \tag{5.26}$$

where λ_t^{down} is the number of equivalent minutes of dispatched downward reserve.

The cost term Ψ penalizes energy imbalances as follows:

$$\Psi = \begin{cases} \left(E_t - P_t' \cdot \Delta t\right) \cdot \left(p_t - p_t^{surplus}\right) & , E_t > P_t' \cdot \Delta t \\ \left(P_t' \cdot \Delta t - E_t\right) \cdot \left(p_t^{shortage} - p_t\right) & , E_t \leq P_t' \cdot \Delta t \end{cases} \tag{5.27}$$

The penalization term for reserve shortage, Φ, is as follows:

$$\Phi = \begin{cases} \gamma \cdot p_t^{cap} \cdot \left(P_t^{down} - \bar{P}_t^{down}\right) & , P_t^{down} > \bar{P}_t^{down} \\ \gamma \cdot p_t^{cap} \cdot \left(P_t^{up} - \bar{P}_t^{up}\right) & , P_t^{up} > \bar{P}_t^{up} \end{cases} \tag{5.28}$$

where γ is a penalization coefficient that can take any positive value. The value used in Portugal and Spain is 1.5 (which is also adopted in this chapter) [54].

Note that the terms RNS_t^{up} and RNS_t^{down} are not included in (5.28) because the difference between P_t^{up} and $\bar{P}_t^{up}$ (and between P_t^{down} and $\bar{P}_t^{down}$) is an upper bound for their value.

In settlement scheme (b), the total cost is given by:

$$TotalCost = \sum_t \left(\begin{array}{c} P'_t \cdot \Delta t \cdot p_t + E_t^{down} \cdot p_t^{down} - \\ E_t^{up} \cdot p_t^{up} - p_t^{cap} \cdot \left(P_t'^{down} + P_t'^{up} \right) + \\ \Psi \left(P'_t \cdot \Delta t, E_t \right) + \Phi \left(P_t^{down}, P_t^{up}, P_t'^{down}, P_t'^{up}, RNS_t^{up}, RNS_t^{down} \right) \end{array} \right) \tag{5.29}$$

Note that in this case, the reserve capacity payment is a function of $P_t'^{down}$ and $P_t'^{up}$. Furthermore, the reserve shortage penalty Ψ has two components: one that penalizes the unavailable reserve power using equation (5.28), but for the deviation between $P_t'^{up}$ and P_t^{up} (and between $P_t'^{down}$ and P_t^{down}); and another that penalizes the reserve not supplied (i.e., depleted reserve) - RNS_t^{up} and RNS_t^{down}. It is given by:

$$\begin{aligned} \Phi = & \begin{cases} \gamma \cdot p_t^{cap} \cdot \left(P_t^{down} - P_t'^{down} \right) & , P_t^{down} > P_t'^{down} \\ \gamma \cdot p_t^{cap} \cdot \left(P_t^{up} - P_t'^{up} \right) & , P_t^{up} > P_t'^{up} \end{cases} \\ & + \rho \cdot p_t^{up} \cdot RNS_t^{up} + \left(p_t - p_t^{down} \right) \cdot RNS_t^{down} \end{aligned} \tag{5.30}$$

where ρ is a penalization coefficient similar to γ.

Inspired by the Demand Response Reserves Pilot Program at ISO New England [218], in this thesis the value of ρ is made equal to one. For upward reserve, this means that the aggregator must supply more than 50% of the contracted reserve. Otherwise, the penalty term is greater than the payment for partially supplying the reserve. For the downward reserve, the penalization term is different. It is equal to the difference between p_t^{down} and p_t, otherwise hours with p_t^{down} equal to zero (i.e., the most expensive reserve hours) would not be penalized.

5.6 Test Case Results

The previous sections described the optimization framework (day-ahead optimization > redefinition of the operating point > operational management), and the total wholesale cost can be calculated with the market settlement scheme described in the preceding section.
In this section, the optimization framework is applied to the test case of chapter 4 and evaluated from the aggregator (i.e., total wholesale cost) and TSO's (i.e., reserve shortage magnitude) viewpoints.

The optimization framework is tested in a set of test samples with different market prices and number of equivalent minutes of dispatched reserve, using the sampling process described in chapter 4 with the adaptations described in section 5.6.1. One outcome of this evaluation is the robustness of the optimization problems, measured by the variation of the total cost and percentage of reserve shortage under different conditions (or test samples).

The optimization problems are solved with IBM ILOG CPLEX 12.5 optimizer [219] using the Python API (64 bits). The average execution time of the day-ahead algorithm was 13.3 seconds on a laptop computer with an Intel Core i5 CPU M450 @ 2.40 GHz processor and 4 GB of RAM. For the operational algorithm, it was 0.61 seconds.

5.6.1 Sampling Process

The sampling process described in chapter 4 is used to create 30 test samples (9 months for training and 3 months of evaluation) from different periods of two years of data[5] (2010 and 2011). This allows tests with different energy and reserve price data.

The following sampling process, based on the binary time series of the direction of dispatched secondary reserve in Portugal, is used to create different realizations of the number of equivalent minutes of dispatched secondary reserve:

- if upward secondary reserve is activated (i.e., the binary time series for upward reserve has value 1), a sample is taken from the distribution of the number of equivalent minutes from the histogram of Figure 5.5 (thermal power plant). This gives the value of $\Delta t'$ in equation (5.19) and λ_t^{up} in (5.24);
- if downward secondary is activated, a sample is taken from the histogram for downward secondary reserve, and it gives the value of $\Delta t'$ in equation (5.20) and λ_t^{down} in (5.26);
- when the reserve is not dispatched in one direction, the values of $\Delta t'$ and λ are zero in that direction.

5.6.2 Aggregator's Viewpoint: Total Cost

The EV aggregator's viewpoint is mainly related to the total wholesale cost, and the goal is to reduce this cost by offering secondary reserve. Therefore, in this section, the total cost calculated with settlement schemes (a) and (b) for the 30 test samples is compared with the divided approach from chapter 4. Note that the reserve shortage events also affect the total cost (penalty cost terms are included in its calculation), but are more related to the TSO's goals and therefore are quantified in section 5.6.3.

Figure 5.19a depicts the total cost reduction of fleets A and B for each test sample, using

[5] The market data of Portugal was downloaded from http://www.mercado.ren.pt (accessed in December 2012), but data from the year 2009 were not used because of some inconsistencies in the secondary reserve data.

as reference the cost obtained with the divided approach (i.e., only electrical energy bids). The results are also divided in the case with a ratio between reserve bids and the case with separated bids.

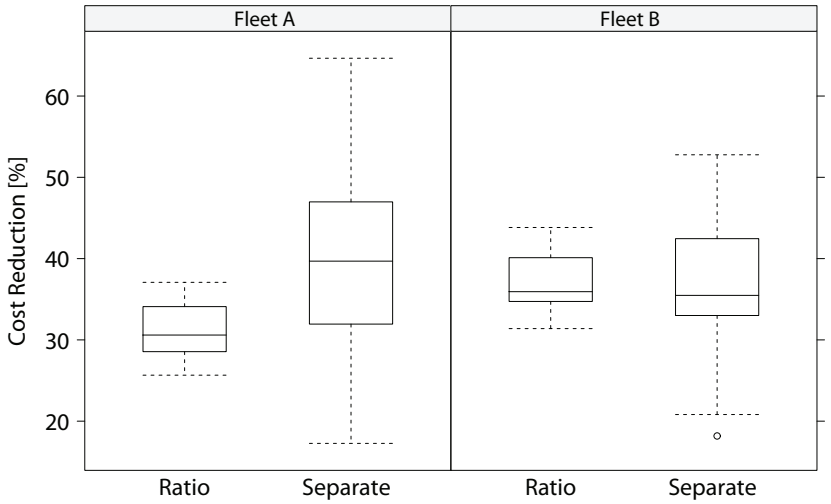

(a) *Total cost reduction regarding the divided algorithm that only optimizes and submits energy bids.*

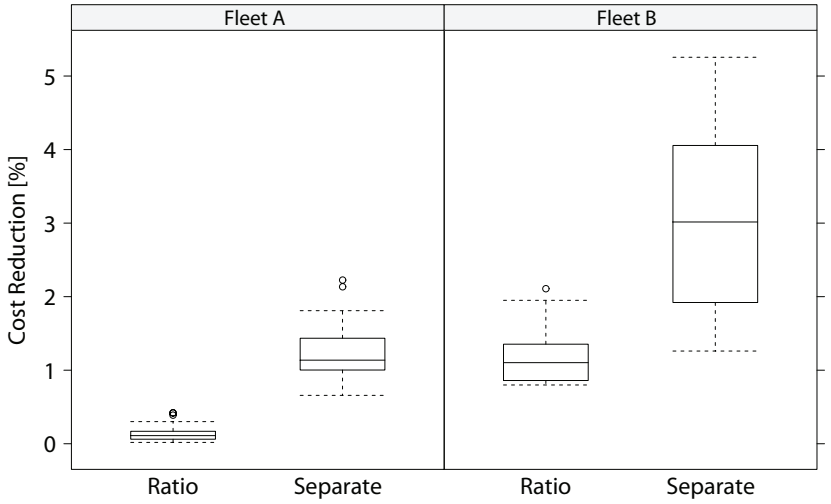

(b) *Total cost reduction of scheme (b) compared to scheme (a).*

Figure 5.19: *Total cost reduction in fleets A and B from selling secondary reserve.*

The results show that the participation in secondary reserve market decreases the total cost in: 31% (fleet A) and 37.1% (fleet B) on average with reserve ratio bids; 38.7% (fleet A) and 36% (fleet B) on average with separated reserve bids.

In some test samples, the cost reduction with separated bids is lower than the one obtained with a reserve ratio. This occurs in 9 out of 30 samples in fleet A and 17 out of 30 samples in fleet B. Table 5.4 presents the value of the total cost's components [using settlement scheme (a) from equation (5.23)] for one test sample (3 months of evaluation) of fleet B where the

cost reduction was 36.8% in the ratio case and 32.9% in the separated case.

Table 5.4: *Total cost's components of settlement scheme (a) for a test sample of fleet B.*

Total cost's components [k€]	Ratio	Separated
(+) Cons. Elect. Energy $\left(P'_t \cdot \Delta t \cdot p_t\right)$	73.55	80.64
(+) Down. Res. Cost $\left(E_t^{down} \cdot p_t^{down}\right)$	1.83	1.05
(-) Up. Res. Income $\left(E_t^{up} \cdot p_t^{up}\right)$	15.67	20.2
(-) Income Available Res. $\left(p_t^{cap} \cdot \left(\bar{P}_t^{down}, \bar{P}_t^{up}\right)\right)$	24.44	25.00
(+) Imb. Cost (Ψ)	2.38	3.24
(+) Res. Shortage Cost (Φ)	0.39	0.72
Total Cost	38.04	40.45

This lower cost reduction obtained with separated bids occurs because the cost with the operating point $\left(P'_t \cdot \Delta t \cdot p_t\right)$ is higher, which means that the EV fleet operates at a higher power level (or in intervals with higher prices) in order to guarantee an acceptable reliability for the upward reserve. The income from having available reserve power $\left(-p_t^{cap} \cdot \left(\bar{P}_t^{down}, \bar{P}_t^{up}\right)\right)$ and dispatched upward reserve $\left(-E_t^{up} \cdot p_t^{up}\right)$ is higher with separated bids but it is not sufficient to offset the cost increase related to the operating point. Note that the goal was to increase the available reserve power in order to meet the contracted bids and not to minimize the energy imbalances costs or the costs related to the operating point.

Another characteristic is that, in some test samples, the total of upward and downward reserve power is lower in the separated bids compared to the case with a predefined ratio, which leads to a lower income from available reserve power. This suggests that the use of a ratio between upward and downward reserve bids gives to the EV aggregator a more balanced and uniform distribution of the reserve power by the EV, which also explains a narrow variation of the cost reduction compared to the separated case. It was also observed that the post-processing phase for the downward reserve power reduces much more the reserve power when separated bids are calculated.

Figure 5.19b compares the total cost reduction of settlement scheme (b) compared to the total cost calculated with scheme (a). Scheme (b) penalizes less the situations with reserve shortage, since the aggregator only loses part of the income when it is not able to follow the AGC regulation signal. In Figure 5.19b, the cost reduction is higher in the separated case of fleet B, which, as will be presented in section 5.6.3, is the case with the highest reserve shortage magnitude. Therefore, settlement scheme (b) is financially more attractive to the EV aggregator and creates more incentives for the EV participation since it takes into account the stochastic nature of the EV supplying secondary reserve. Scheme (a), from the TSO's viewpoint, is more attractive since it demands a higher compliance is terms of reserve provision (or penalizes more reserve shortage events). Nevertheless, since EV is a cheap

and fast-responding reserve resource compared to the conventional ones, the TSO can adopt scheme (b) to better account for its specific characteristics. Note that scheme (b) is also attractive to other demand-side resources, such as small size storage units and thermoelectric loads.

Figure 5.20 depicts the cost reduction for two cases: perfect forecast for the EV variables used in the day-ahead optimization; perfect forecast for all variables. The reference for computing the cost reduction is the energy and secondary reserve bids obtained with forecasts for all the variables [i.e., the result from Figure 5.19 using scheme (b)].

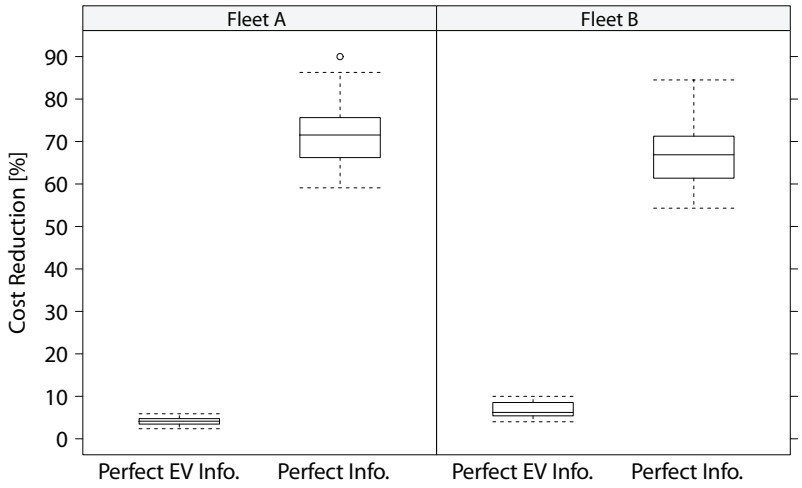

Figure 5.20: *Reduction in the total cost for both fleets and with two different sets of available information: perfect forecast for the EV variables; perfect forecast for all the variables. The reference is the result obtained with forecasts for all the variables.*

The use of perfect forecasts for the EV variables only accomplishes a cost reduction of 4.1% in fleet A and 6.7% in fleet B on average. This suggests that the uncertainty of the EV variables has a small impact in the total cost. The impact on cost reduction is substantial when perfect forecasts are used for all the variables (e.g., market prices, dispatched reserve): 71.5% in fleet A and 67.1% in fleet B. Nevertheless, this "perfect forecast" assumption is only theoretical since variables, such as the reserve direction, cannot be forecasted with acceptable accuracy (as discussed in section 5.2.2). This also shows that neglecting this uncertainty may lead to very optimistic results.

The following section addresses the TSO's viewpoint, which is related to the reliability of the secondary reserve supplied by the EV aggregator. This reliability is mainly measured by the magnitude of the reserve shortage events, which also influences the aggregator's total cost.

5.6.3 TSO's Viewpoint: Reserve Shortage

Traditionally, the TSO contracts resources that supply reserve with high reliability standards and, in general, only unplanned outages can create reserve shortage events. Reserve resources such as flexible loads or storage units, can become depleted during an hourly interval, mainly due to electrical energy constraints such as storage capacity. In this case, the TSO faces a scenario with uncertainty associated to the available reserve.
Therefore, evaluating the magnitude of reserve shortage events that result from using the proposed optimization framework indicates, from the TSO's viewpoint, the degree of reliance on this reserve resource.

In this section, different metrics are used to measure the magnitude and number of reserve shortage events associated to the EV aggregator and corresponding optimization models. The variation of these metrics in the 30 test samples gives an indication of the algorithm's robustness to different realizations of market prices and number of equivalent minutes for dispatched reserve.

The first metric is the Percentage of Reserve Power Shortage (pRPS), given by:

$$pRPS^{up} = \frac{\sum_t \left(P_t^{up} - P_t'^{up}\right)}{\sum_t \left(P_t^{up}\right)} \cdot 100\% \tag{5.31}$$

pRPS measures the difference between the accepted reserve power bid (P_t^{up}) and the available reserve power ($P_t'^{up}$) communicated by the EV to the aggregator before the beginning of time interval t_0. A similar metric is used for downward reserve.

Table 5.5a presents the results (average, minimum and maximum values) of the pRPS for upward and downward reserve in fleets A and B and for a situation where the secondary reserve power is divided into 2/3 for upward and 1/3 for downward.

With the exception of downward reserve in fleet B, all cases show a low pRPS meaning that the deviation between available and contracted reserve power is low.

The higher values of $pRPS^{down}$ in fleet B can be explained by the negative bias (overestimation) of the charging requirement forecast (see Table B.3 in appendix B) which is translated to an overestimation of the actual charging values as shown in chapter 4. An overestimation of the charging requirement contributes to an overestimation of the downward reserve power and consequently to an increase of the reserve shortage due to forecast errors.

Moreover, the test samples with high $pRPS^{down}$ also exhibit a high total of offered upward reserve power. In order to offer this high upward reserve power, the aggregator needs to pur-

Table 5.5: *Percentage of upward and downward reserve power shortage (pRPS) for fleets A and B (average [minimum,maximum]).*

(a) *Upward and downward bids with a predefined ratio.*

	$pRPS^{up}$	$pRPS^{down}$
Fleet A	0.005% [0.00%,0.03%]	0.17% [0.00%,0.59%]
Fleet B	0.00% [0.00%,0.002%]	2.42% [0.94%,5.36%]

(b) *Separated upward and downward bids.*

	$pRPS^{up}$	$pRPS^{down}$
Fleet A	0.26% [0.007%,0.80%]	0.096% [0.00%,0.63%]
Fleet B	0.22% [0.01%,0.68%]	3.37% [0.07%,11.60%]

chase more electrical energy in the market, and if the upward reserve is not fully dispatched, this surplus can decrease the downward reserve availability. Note that this is more critical if the flexibility of the EV is lower, which is the case of fleet B (see appendix A).

Table 5.5b presents the pRPS results for a situation where the upward and downward reserve bids are separated (i.e., there is no predefined ratio). Like in the previous table, higher pRPS values occur for downward reserve and fleet B. The reasons are the same, but in this case, it is clearer that high $pRPS^{down}$ occurs for test samples where the total of upward reserve power is much higher than the total of downward reserve power.

For instance, the maximum value of $pRPS^{down}$ (11.60%) occurs for a test sample where a total of 27.2 MW (in a three month evaluation period) was offered as downward reserve and a total of 1056.2 MW was offered as upward reserve. This low downward reserve power occurs because the post-processing phase of equation (5.10) removes most of the downward bids (without the post-processing, the total downward reserve power would be 225.3 MW). This significant decrease of the downward reserve bids in the post-processing phase suggests that, due to the high amount of offered upward reserve power (and consequently a higher purchased electrical energy), the aggregator may have problems in supplying the downward reserve power in this test sample.

Nevertheless, note that the average value of $pRPS^{down}$ in the 30 test samples of fleet B was 3.37%, which seems to be an acceptable value for the aggregator's performance.

The previous metric pRPS only measures the shortage of the available reserve power in the beginning of each interval. In this case, the TSO is informed beforehand (e.g., 15 minutes before the operating hour) about this reserve shortage and can take preventive measures, such as activate a secondary reserve bid not dispatched by the market-clearing, to maintain

the same level of the contracted secondary reserve.

However, during each interval, if the reserve is dispatched for a long period in one direction, it may happen that the reserve becomes depleted and the aggregator is unable to supply more secondary reserve (i.e., the available reserve power becomes zero). The Percentage of Constant Reserve Power Shortage (pCRPS) between $[\bar{P}_t^{up}$ and $P_t^{up}]$ is used to measure these reserve shortage events and is given by:

$$pCRPS^{up} = \frac{\sum_t \left(P_t^{up} - \bar{P}_t^{up}\right)}{\sum_t \left(P_t^{up}\right)} \cdot 100\% \tag{5.32}$$

A similar metric is also used for downward reserve.

Another metric is the Percentage of Intervals with Constant Reserve Power Shortage (pICRPS), which is given by the number of intervals with reserve power shortage divided by the number of intervals with reserve bids. This metric is also calculated separately for each reserve direction.

The metrics pCRPS and pICRPS measure reserve shortage events by assuming that the accepted reserve bid is activated in the same direction, at full power, during the complete interval t. Therefore, both give an upper bound (calculated *a priori*) to the reserve shortage magnitude and are related to market settlement scheme (a). In this case, the aggregator, 15 minutes before the operating interval, can send this information to the TSO (or update this information during the operating interval), and the TSO takes preventing measures if necessary.

Figure 5.21 depicts the pCRPS and pICRPS for upward and downward reserve bids of fleets A and B. The results are divided by a case with a ratio between the two reserve directions and a case with separated bids.

The pCRPS results are consistent with Table 5.5, but they are higher since this metric encompasses the available reserve power shortage in the beginning of each time interval (measured by the pRPS) plus the reserve power shortage during the operating interval if constant full reserve power is requested in the same direction during the complete interval. The pCRPS is low for fleet A on average (higher values are for separated bids) and it is higher in fleet B, in both reserve directions.

The pICRPS is high in both fleets and reserve directions, but particularly in the case with separated reserve bids. Note that what is more important for the TSO (and also for the aggregator) is the reserve shortage magnitude and not the number of intervals with shortage. Since the average pCRPS is lower in both fleets, it indicates that the magnitude of the reserve

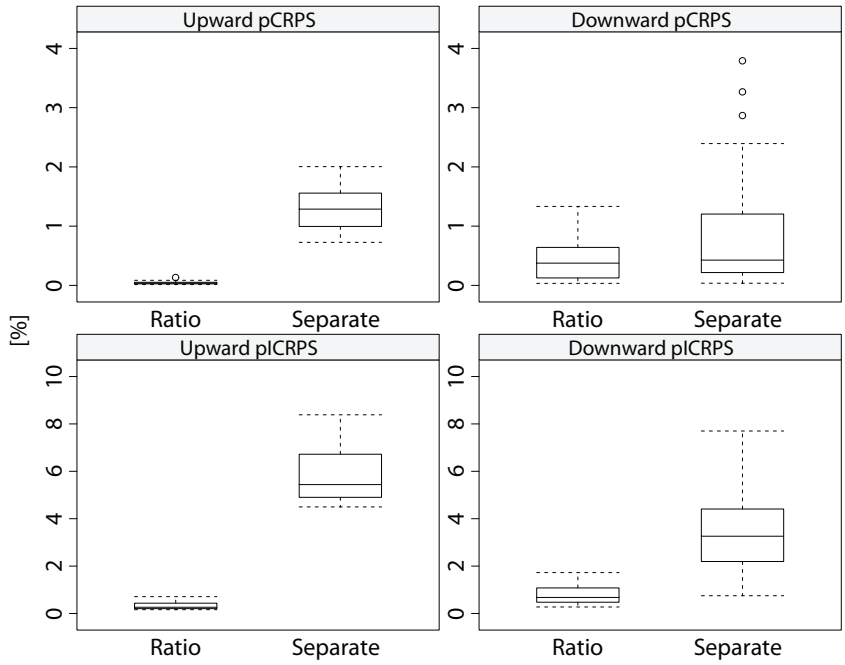

(a) *Fleet A.*

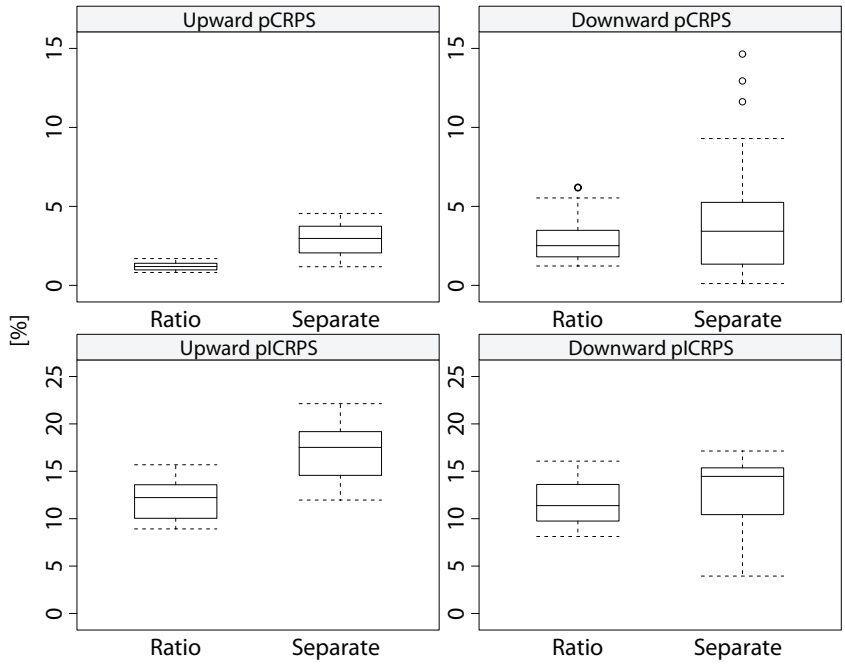

(b) *Fleet B.*

Figure 5.21: *pCRPS and pICRPS for upward and downward reserve directions.*

shortage events is minimal in each time interval, which is desired by a TSO.

These results for upward and downward reserve can be improved by assuming that, in the contract between the EV driver and aggregator, a degree of flexibility for the target SoC is established. The aggregator only guarantees 95% or 90% of the target SoC (instead of 100%)

when there is a risk of upward reserve shortage. Figure 5.22 depicts the pCRPS^{up} results for both fleets assuming separated bids for each reserve direction and for two target SoC tolerance levels (in addition to 100%): 95% and 90%.

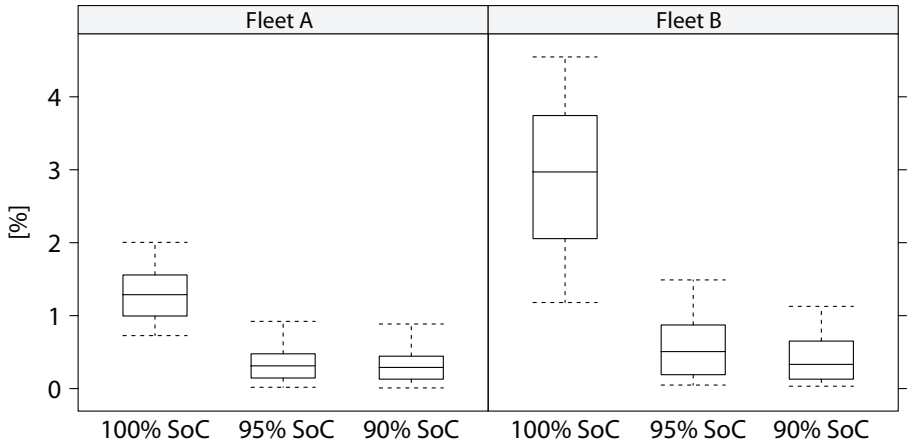

(a) *Percentage of Constant Reserve Power Shortage (pCRPS).*

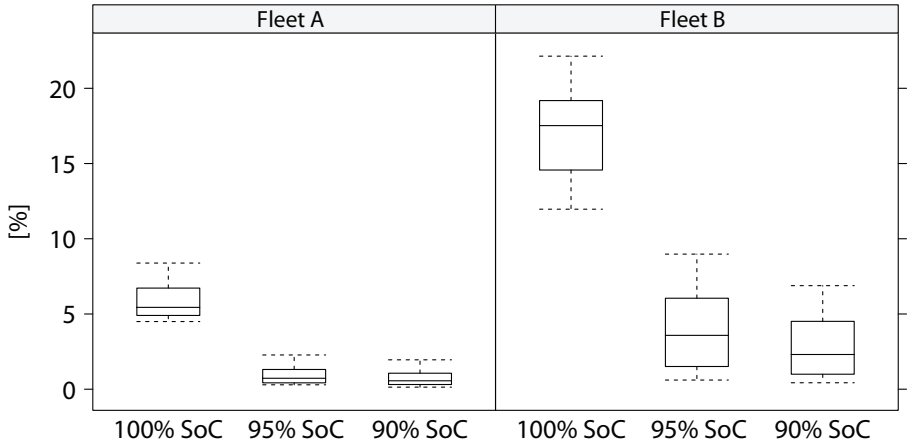

(b) *Percentage of Intervals with Constant Reserve Power Shortage (pICRPS).*

Figure 5.22: *pCRPS and pICRPS for upward reserve direction (separated bids) as a function of two different tolerances for the target SoC.*

With a 100% target SoC, the average pCRPS^{up} is 1.26% in fleet A and 2.86% in fleet B. When the SoC tolerance is 90%, the pCRPS^{up} presents a significant decrease, showing an average value of 0.3% (fleet A) and 0.4% (fleet B). Therefore, during the operating day, the aggregator can use this additional flexibility from the EV to mitigate reserve shortage situations. The same is valid for pICRPS^{up}. For fleet A, it decreased from 5.84% to 0.71%, and for fleet B it decreased from 16.8% to 2.85%.

The same tolerance can be applied to downward reserve, and in this case, it means consuming additional 5% or 10% of the target SoC (note that this is only possible in EV with a target SoC below 100%).

Two additional metrics for measuring the reserve reliability are the Percentage of Reserve Not

Supplied (pRNS) and Percentage of Intervals with Reserve Not Supplied (pIRNS). The pRNS is given by:

$$pRNS^{up} = \frac{\sum_t \left(RNS_t^{up}\right)}{\sum_t \left(P_t^{up}\right)} \tag{5.33}$$

pIRNS is given by the number of intervals with RNS divided by the number of intervals with reserve bids.

Note that pRNS and pIRNS, in contrast to pCRPS and pICRPS, only measures the situations where the EV aggregator is unable to supply the contracted reserve power when requested by the AGC during the operating interval. These two metrics are less severe and are related to market settlement scheme (b). Both metrics quantify reserve shortage events inside the operating interval. In this situation, the TSO activates tertiary reserve bids to free up additional secondary reserve (operation depicted in Figure 5.14).

Figure 5.23 depicts the pRNS and pIRNS for upward and downward directions.

Compared to the pCRPS values, and for both reserve directions, the reserve shortage from not responding with adequate power to an AGC signal is much lower and its average value is below 1% in both fleets (the exception is the upward reserve in fleet B with a value close to 1.5%). Only in the upward reserve of fleet B is the $pIRNS^{up}$ higher, but the $pRNS^{up}$ is lower, which indicates reserve shortage events with low magnitude.

The comparison between the pCRPS and pRNS results indicates that the settlement scheme (b) discussed in the previous section might be more favorable to the aggregator, since in this scheme the aggregator is only penalized by the pRPS and pRNS, and the sum of these two metrics is lower compared to an *a priori* calculation of the reserve shortage using the pCRPS metric.

The combination of the upward and downward results shows that if the aggregator agrees on a tolerance for the SoC with the EV driver, it is possible to offer day-ahead secondary reserve to the TSO with very low magnitude of reserve shortage events using the optimization models described in this chapter. Note that, even without considering the SoC tolerance, the algorithms already exhibited an acceptable reliability, which is appealing to the TSO.
In general, these reserve shortage events do not jeopardize the power system security since the TSO can replace this depleted reserve with tertiary reserve, but it is translated to an increasing use of tertiary reserve. The cost of using more tertiary reserve, as described in the market settlement phase, should be passed to the EV aggregators by imposing penalty terms.

Finally, it is important to underline that the different results obtained for each test sample are exclusively because of different realizations (or test samples) of the number of equivalent min-

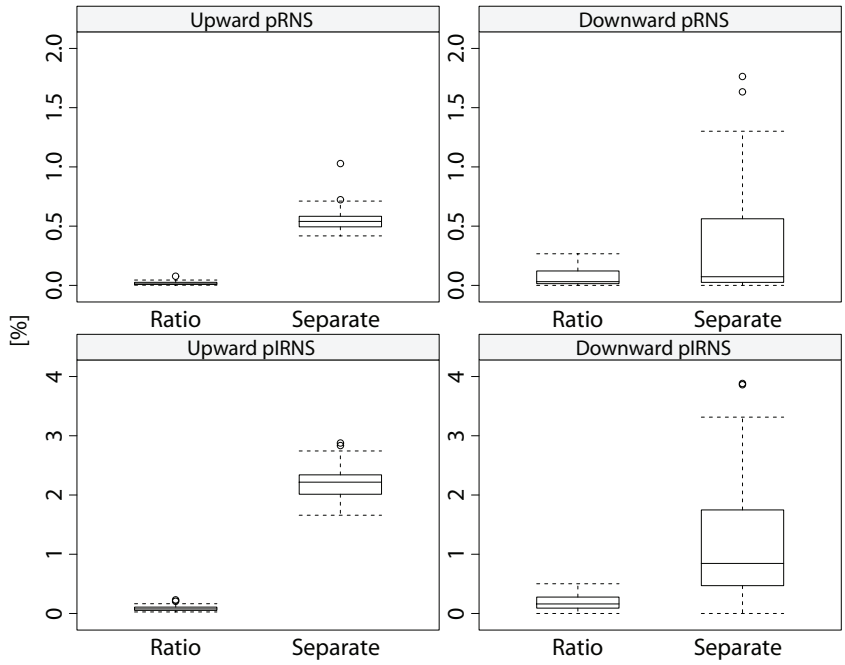

(a) *Fleet A.*

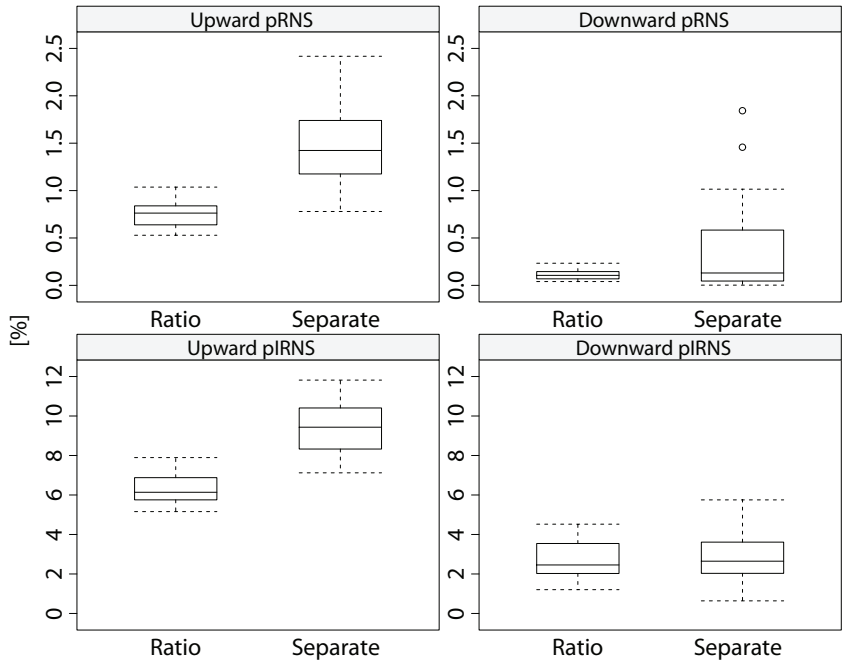

(b) *Fleet B.*

Figure 5.23: *pRNS and pIRNS of upward and downward reserve in fleets A and B.*

utes of dispatched reserve, and because of the forecasted and realized market prices. These different realizations lead to distinct energy and secondary reserve bids, which ultimately lead to distinct results in terms of reserve shortage.

5.6.4 Different Quality of the EV Variables Forecasts

The previous tests were conducted using the same forecasts for the EV variables. In this section, the optimization framework is tested for charging requirement and availability forecasts with increasing error by introducing additional noise into the initial forecasts (i.e., forecasts used in the previous section, called "base case"). The objective is to assess the evolution of pCRPS and pRNS for forecasts with different quality.

This exercise is conducted for one test sample (i.e., 3 months of evaluation), and using the following approach:

- *charging requirement forecast*: a truncated Gaussian distribution is centered (i.e., the mean value) on the forecasted value of the base case. The standard deviation is equal to a percentage of the mean value (values in Table 5.6). The minimum value is zero and the maximum value is the maximum electrical energy that can be consumed in the forecasted availability period. A sample is taken from the truncated distribution and generates an altered charging requirement forecast;

- *availability forecast*: a truncated Gaussian distribution is centered on the forecasted departure and arrival time instants of each availability period, and the standard deviation values are presented in Table 5.6. For the arrival time instant, the minimum and maximum values are within the departure time instant of the previous availability period and the last interval of the time horizon. For the departure time instant, the minimum and maximum values are within the arrival time instant of the same period and the last interval of the time horizon. A sample (rounded to an integer number) is taken from the truncated distribution and generates an altered availability forecast.

Table 5.6 presents the standard deviation values used in the creation of eight different charging requirement and availability forecasts with increasing error compared to the base case. The forecast error analysis of these eight forecasts is presented in appendix B.2.1 for the aggregated values of the individual forecasts.

Figure 5.24 depicts the pCRPS and pRNS for upward and downward reserve in fleets A and B, as a function of the different forecasts from Table 5.6. A ratio between upward and downward reserve bids is considered.

In both fleets, the increasing standard deviation of the charging requirement forecast (cases 1-4) does not create a significant variation in the reserve shortage metrics. The proposed day-ahead and operational algorithms seem to be robust to forecast errors in the charging requirement. In fleet B, there is a peculiar behavior. In cases 1-4, the pCRPS^{down} and pRNS^{down},

Table 5.6: *Standard deviation values used in the truncated Gaussian distributions for the charging requirement and availability forecasts.*

Case	St. Dev. of Charg. Req. [%]	St. Dev. of Availability [half-hour]
0 (base case)	0%	0
1	20%	1
2	30%	1
3	60%	1
4	80%	1
5	10%	3
6	10%	5
7	10%	6
8	100%	8

for downward reserve decrease, compared to the base case when the standard deviation increases, and for upward reserve, it is the opposite. This behavior can be partially explained by the bias of the charging requirement forecast. As mentioned before, the base case has a negative bias (overestimation) of the charging requirement forecast, which results in an increase of the reserve shortage due to the forecast errors. The forecasts of cases 1-4 still with a negative bias, but lower compared to the base case. Nevertheless, the differences between these cases are negligible. Note that the charging requirement error of cases 1-4 increased, compared to the base case, but even in these cases, the pCRPS and pRNS values of both reserve directions remained almost the same, which shows the robustness of the proposed algorithms.

Cases 5-7 are characterized by the increasing standard deviation in the departure and arrival time instants of each EV. For both fleets and reserve directions, the pRNS and pCRPS values increase significantly when the standard deviation increases. The impact is more severe in the downward reserve power of both fleets. This change in the availability forecast means an increase of the phase error in the arrival and departure time instants. As showed in the forecast error analysis of appendix B.2.1, this increases particularly the forecast error of the aggregated charging requirement forecast.
The increasing magnitude of the reserve shortage situations, suggests that the proposed algorithms are less robust to phase errors in the availability forecast. In fact, phase errors in the arrival and departure time instants influence the available reserve. For instance, an EV arriving later than the forecasted value means that its contribution to the available reserve power is zero while it is not plugged-in, and a departure instant earlier than the forecasted value means that the EV is less flexible than what was forecasted and its contribution to the available reserve power ends sooner than what was expected.

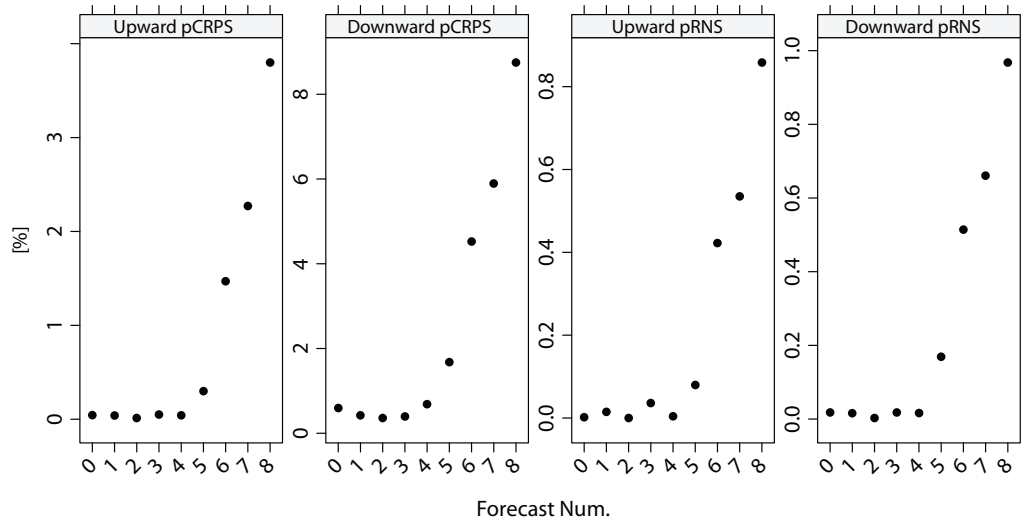

(a) *Fleet A.*

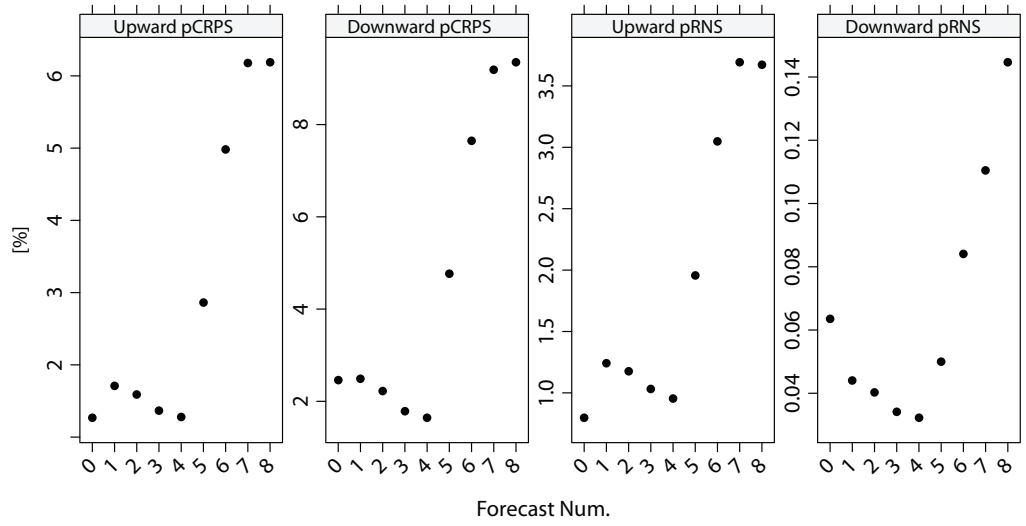

(b) *Fleet B.*

Figure 5.24: *pCRPS and pRNS of upward and downward reserve in fleets A and B for different qualities of charging requirement and availability forecast (with a ratio between upward and downward reserve bids).*

For extreme values of standard deviation (case 8), the values of pRNS and pCRPS, for both reserve directions, increase significantly. The values of pRNS still low in this case, but the values of pCRPS increase to values up to 9% in downward reserve and up to 4% and 6% for upward reserve.

Figure 5.25 presents the results for the optimization with separated bids, and the conclusions are quite similar. The main difference to Figure 5.24 is that the pCRPS^{down} (and pRNS^{down}) for cases 5-8 is lower and the pCRPS^{up} (and pRNS^{up}) is higher in both fleets.

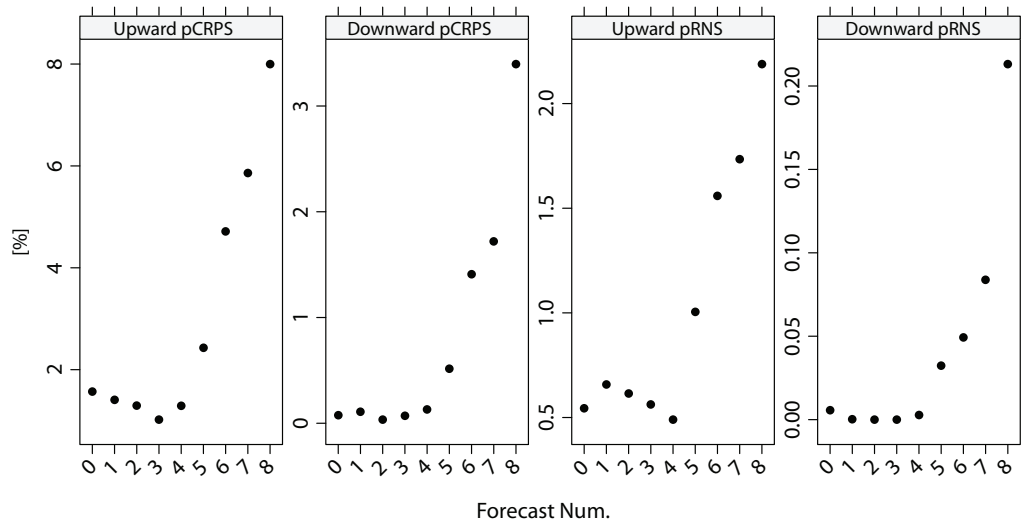

(a) *Fleet A.*

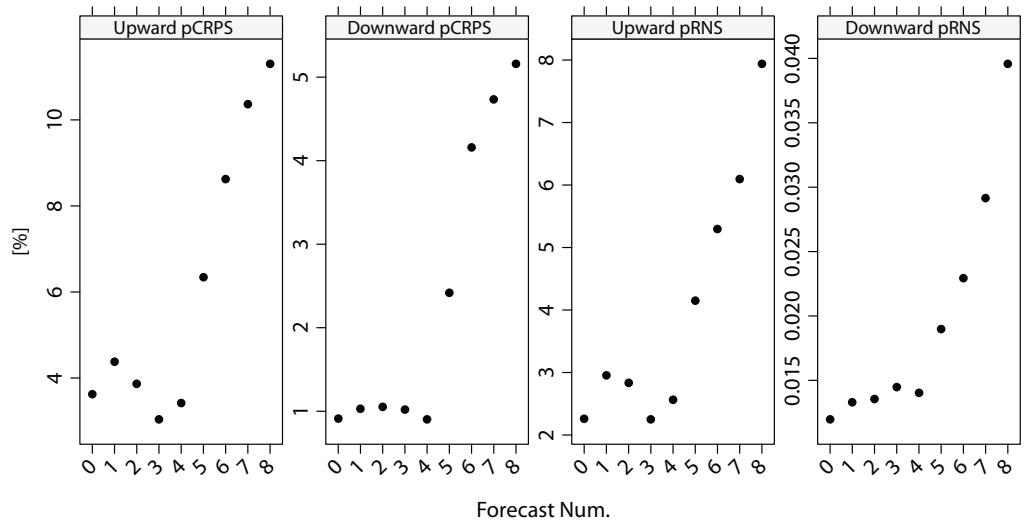

(b) *Fleet B.*

Figure 5.25: *pCRPS and pRNS of upward and downward reserve in fleets A and B for different qualities of charging requirement and availability forecast (with separated upward and downward reserve bids).*

5.7 Final Remarks

This chapter covers two different types of algorithms for an EV aggregator participating in the secondary reserve market: (a) day-ahead optimization based on forecasted values to determine the electrical energy bid and secondary reserve power bid; (b) operational management algorithm that redefines the EV fleet operating point and coordinates the EV individual charging to guarantee the full contracted reserve power.

Using the day-ahead and operational algorithm, the total wholesale cost of the EV aggregator decreased on average between 30% and 40%, compared to a strategy that only optimizes

the energy bids. The algorithms are also capable of assuring the contracted reserve with acceptable reliability (e.g., considering both reserve directions, the percentage of reserve power shortage ranges between 0.3% and 4% on average). This high reliability is important from the TSO's viewpoint.

The algorithms' robustness was tested and the results showed that the proposed algorithms are robust to an increase in the forecast errors of the EV variables. Nevertheless, the phase errors in the availability forecast can increase significantly the magnitude of the reserve shortage situations and represent the most critical source of error for the secondary reserve provision.

The results also show that the role of the price and the EV variables forecast errors cannot be neglected when evaluating the algorithms, mainly because they create energy imbalances between purchased and consumed energy, which affects the reliability of the reserve provision. The assumption of perfect forecast, or the incorrect evaluation of the algorithm performance (e.g., neglecting the need to calculate the true available reserve power), might lead to excessively optimistic results. Moreover, the reserve shortage results differ for different realizations of the market prices and dispatched reserve values and for different EV fleets. For example, the algorithms' test in different time periods (with different prices and number of equivalent minutes of dispatched reserve), and using the same EV fleet, showed that the percentage of downward reserve power shortage could range between 0.1% and 15%.

It was also showed that the use of a ratio between upward and downward reserve power contributes to a more balanced distribution of the reserve power by each EV and consequently to a higher reliability, compared to a case without any ratio (i.e., separated bids for upward and downward reserve power).

The integration of EV aggregators in the secondary reserve market demands the definition of new market rules and protocols. This chapter identified three new changes in the market protocols:

- the aggregator should be allowed to present bids in the market step (e.g., one hour) decomposed in sub time-slots (e.g., 10 minutes) in order to better capture the variation of the available reserve power due to arrivals and departures of EV;

- a penalty term for reserve shortage should be introduced. Nevertheless, at the same time, the market settlement scheme should take into account the stochastic nature of the EV behavior. For example, it is more adequate a settlement scheme that only penalizes situations where the EV is not able to respond with sufficient reserve power to an AGC signal;

- during the operating day, the EV aggregator should inform the TSO, e.g. every 5 min-

utes, about any change in its available reserve power and the TSO can take preventive measures based on this information.

This chapter was not intended to conduct a full economic analysis about the economic viability of EV supplying secondary reserve. However, it shows that the proposed algorithms contribute to decreasing the wholesale costs of an EV aggregator, which consequently provides a margin to offer lower retailing tariffs to EV drivers. Moreover, the proposed algorithms ensure an acceptable reliability of the supplied reserve (i.e., low amount of reserve shortage) which is important to increase the confidence of the TSO in these new reserve resources. Like in the previous chapter, although the models were tested in synthetic time series, the algorithms can be applied to cases with real EV data.

From the TSO's perspective, the participation of EV in the reserve market can potentially decrease the system costs and provide fast-responding reserve to handle RES-E variability. Another advantage, and in contrast to storage units and conventional power plants that have a high investment cost, EV does not require any significant investment (excluding the smart grid infrastructure). Nevertheless, the TSO, in order to use this resource to maintain the same reliability level at a lower cost, should create conditions for a fair competition between EV (and other flexible loads) and conventional reserve resources by adopting the abovementioned changes in the market protocols. Furthermore, these changes to integrate reserve resources that are affected by uncertainty and variability also contribute to the integration of RES-E power plants in the reserve market (e.g., wind turbines participating in secondary reserve provision [220]), which can lead to the decommissioning of GHG intensive reserve power plants.

Chapter 6

Optimization Models for the Balancing Reserve Market

Abstract

This chapter formulates a day-ahead optimization model for the electrical energy and balancing reserve bids. Two operational management algorithms covering alternative gate closures (i.e., day-ahead and hour-ahead) are also described to coordinate EV individual charging and mitigate forecast errors. In hour-ahead balancing reserve markets it is possible to update the reserve bids 45 minutes before physical delivery. A case-study with data from the Iberian electricity market and synthetic EV time series is used to evaluate the optimization models.

6.1 Introduction

The increasing penetration of renewable generation in power systems is motivating changes in the operational procedures and electricity market rules. The use of power systems reserves to handle renewable generation uncertainty is currently a topic of discussion and research [41][221], and some TSO are already considering a new reserve category for handling imbalances due to renewable energy forecast errors. In this scenario, it is essential to promote the efficient use of all the flexible resources from the generation and demand-side.

The EV has sufficient flexibility to increase/decrease their consumption level in response to energy imbalances between realized and scheduled values. Therefore, an EV aggregator can contribute with additional flexibility to the power system and is a potential provider of balancing reserve. This chapter explores a scenario where the EV aggregator controls directly

the charging process of EV plugged-in to residential/work charging points and sells balancing reserve in the electricity market.

The *divided* approach described in chapter 4 is extended to include the possibility of offering bids for upward and downward balancing reserve (as an alternative to offering secondary reserve). Two operational management algorithms are also proposed: one that assumes binding day-ahead bids and coordinates the EV charging to reduce deviation costs and ensures a reliable delivery of balancing reserve, and another designed for electricity markets that allows an update of the balancing reserve bids 45 minutes before physical delivery.

A market settlement scheme is also proposed to calculate the total cost of the aggregator's wholesale activity, including a penalty term for reserve shortage situations.

This chapter starts by describing the problem, with particular emphasis on the balancing reserve characteristics. Then, the day-ahead and operational management algorithms are described. A market settlement scheme is described to calculate the aggregator's total cost. The optimization models' robustness is examined in a test case with data from the Iberian electricity market and synthetic EV time series. Finally, the concluding remarks are presented.

6.2 Problem Description

6.2.1 Characteristics of the Balancing Reserve

The balancing reserve is dispatched by the TSO to solve energy imbalances between scheduled (i.e., result of the electricity market) and realized values. Non-marginal energy imbalances are expected in power systems with high penetration of wind and solar-based generation. Figure 6.1 illustrates how balancing reserve is used by the TSO to solve imbalances. In cases (a) and (b), the conventional generation from the power system was scheduled by the electricity market (or by a unit commitment model) to meet the load bids considering the price of purchasing and selling bids. Excluding forecast errors and unplanned outages, there would be a perfect match between generation and load in each market time interval (e.g., one hour). Note that the fluctuations and deviations inside each time interval are handled by primary, secondary and tertiary reserves.

However, due to forecast errors in different market agents (e.g., a wind or solar farm) it is necessary to call balancing reserve in order to maintain the load-generation balance and reduce the need to use primary, secondary and tertiary reserves. In case (a), 15 minutes before the operating hour, the TSO generates a forecast for the total system load and total

renewable generation. In case of a large negative imbalance between forecasted total load and generation (due to renewable energy forecast errors), the TSO calls upward balancing reserve to cover this imbalance. In case (b), the imbalance is positive and the TSO calls downward balancing reserve.

The balancing reserve is supplied by online and offline units with response time generally less than 10/15 min for full delivery. In general, the balancing reserve when mobilized, supplies the full power during a long period (e.g., one hour).

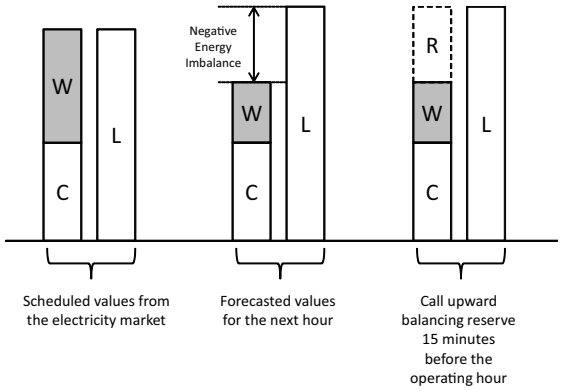

(a) *Upward balancing reserve.*

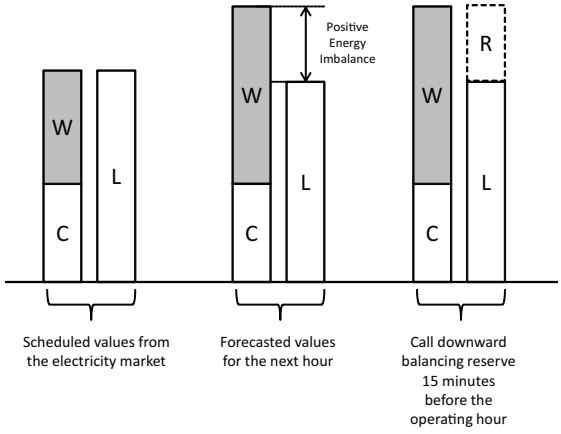

(b) *Downward balancing reserve.*

Figure 6.1: *Balancing reserve (C: conventional generation; W: wind generation; L: load; R: balancing reserve).*

In Portugal, the TSO is using tertiary reserve (which, in fact, is called *reserva de regulação*) to solve large imbalances between load and generation. In the draft version of the ENTSO-E "Network Code on Load-Frequency Control and Reserves", it is also mentioned that the reserve category *replacement reserve* (which replaces tertiary reserve) can also be used to anticipate expected imbalances [222]. In order to avoid different interpretations, hereafter the Portuguese *reserva de regulação* is simply referred to as balancing reserve.

Table 6.1 shows two hours from the year 2011 to illustrate how this balancing reserve is used

by the TSO[1].

In hour 17h00 of 7 September 2011, the dispatched upward reserve was 540 MWh (in an hourly total load of around 6,500 MW) and two market agents together contributed to the negative energy imbalance with 440 MWh. Table 6.1a shows the reserve power bids of the market agents and their dispatched values. Note that all the market agents supply their full reserve power during that hour (totalizing 540 MWh), but units U9-U11 did not participate in the reserve. These three units are from the same power plant, and since the bid price is lower than units U12-U15, the reason for not dispatching this reserve was probably network constraints (but this information is not confirmed by the TSO). Unit U15 defines the marginal price of the upward reserve service, 87.2 €/MWh.

In hour 3h00 of 17 May 2011, the dispatched downward reserve was 493.2 MWh (in an hourly total load of around 4,500 MW) and one market agent contributed with 499 MWh for the positive energy imbalance. Table 6.1b shows the reserve bids of the market agents and their dispatched values. Like in the previous example, the dispatched units supplied full reserve power during the whole hour. The last dispatched unit (U8, which defines the reserve price) delivered 13.2 MWh of electrical energy during that hour (from a reserve power of 71 MW) and defined the reserve price (i.e., 15 €/MWh). Note that for downward reserve, a lower reserve price means more expensive reserve.

The units that provide this reserve are activated to supply the service 15 minutes before the beginning of the operating hour if the imbalance is estimated to be high. For instance, U7 in Table 6.1a was scheduled by the market (i.e., after intraday sessions) to generate 0 MWh, and 15 minutes before the operating hour it was rescheduled to produce 160 MWh as upward reserve; U2 in Table 6.1b was scheduled to generate 500 MWh, and it was rescheduled to produce 475 MWh (15 minutes before the operating hour) in order to supply downward reserve. Nevertheless, the reserve units can also be called during the operating hour to cover unexpected large imbalances or to solve technical problems such as branches' overload [46]. The manual reserve in the Nordic countries is operated in a similar mode and it is purchased by the TSO in the regulation power market [223].

According to [224], balancing reserve (called *load-following* by the author) differs from secondary (called *regulation* by the author) in two important aspects: (a) it is used over long periods of time compared to secondary reserve; (b) the changes in reserve direction are frequently predictable and have similar daily patterns. This second aspect will be discussed with more detail in section 6.3.1 when forecasting the reserve direction variable.

[1] The Portuguese TSO makes publicly available (in http://www.mercado.ren.pt) the reserve bids and how much reserve power was dispatched by each physical unit.

Table 6.1: *Illustrative example of the upward and downward balancing (called "reserva de regulação") reserve dispatch in Portugal.*

(a) *Upward reserve: 17h00, 7 September 2011*

Unit	Power [MW]	Price [€/MWh]	Dispatched Reserve [MWh]
U1	30	68.50	30
U2	40	71.20	40
U3	30	78.15	30
U4	30	78.17	30
U5	40	78.20	40
U6	30	79.05	30
U7	160	80.00	160
U8	40	80.20	40
U9	235	82.50	0
U10	60	83.00	0
U11	60	83.20	0
U12	30	85.15	30
U13	30	86.15	30
U14	40	86.20	40
U15	40	87.20	40
		...	

(b) *Downward reserve: 3h00, 17 May 2011*

Unit	Power [MW]	Price [€/MWh]	Dispatched Reserve [MWh]
U1	30	42.00	30
U2	25	41.00	25
U3	40	40.00	40
U4	5	36.25	5
U5	115	25.75	115
U6	115	21.75	115
U7	150	20.00	150
U8	72	15.00	13.2
		...	

6.2.2 Participation in the Electricity Market

The EV aggregator participates in the day-ahead electrical energy market with bids for purchasing energy and is paid at a single marginal price. The gate closure is at 10h00.

Furthermore, a market for balancing reserve is also considered. In this market, the loads offer bids to increase (downward reserve) or decrease (upward reserve) their power consumption

and the TSO is the buyer. Figure 6.2 depicts the clearing of the balancing market, with a different marginal price for each reserve direction. The reserve bids consist in a quantity (in MW) and a price for dispatched energy (in €/MWh). Note that some balancing reserve markets may also have a capacity price (in €/MW), but it is more common to find this in secondary reserve markets.
In general, the marginal price of upward reserve is greater or equal to the energy price, while the downward reserve price is lower or equal.

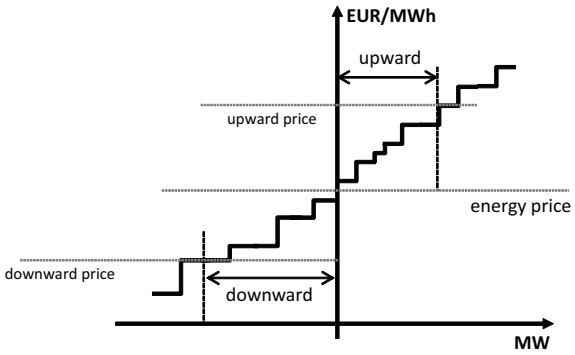

Figure 6.2: *Market clearing of the balancing reserve bids.*

This chapter covers two alternative gate closures for the balancing market: (a) the reserve market opens right after the energy market closure, and the submitted bids for the next day are binding; (b) the submission of bids starts on the day prior to the operating day, can continue during the operating day and closes one hour before the operating hour (i.e., the aggregator is allowed to update or remove the reserve bid 45 minutes before physical delivery).

In the day-ahead bidding [situation (a)], the TSO defines the reserve requirements for the next day (using for example a probabilistic algorithm [225]) and purchases the corresponding quantity in the day-ahead balancing market. In the course of the operating day, 15 minutes before and during the operating hour, the TSO calls the reserve purchased in the previous day. In the hour-ahead bidding [situation (b)], 15 minutes before and during the operating hour, the TSO selects the balancing reserve bids following a price merit order (as depicted in Figure 6.2). The reserve price is the bid's price of the last dispatched unit during the operating hour.

Figure 6.3 depicts a diagram with the sequence of tasks for an EV aggregator participating in the energy and balancing reserve market.

The time intervals are based on the Iberian electricity market. Before hour 10h00 of day D, the aggregator forecasts the market prices and the EV variables, it optimizes the energy and balancing reserve bids, and then submits bids in the (a) energy and reserve market or (b) energy market. The market settlement process takes place between hours 11h00 and 14h00 of day D.

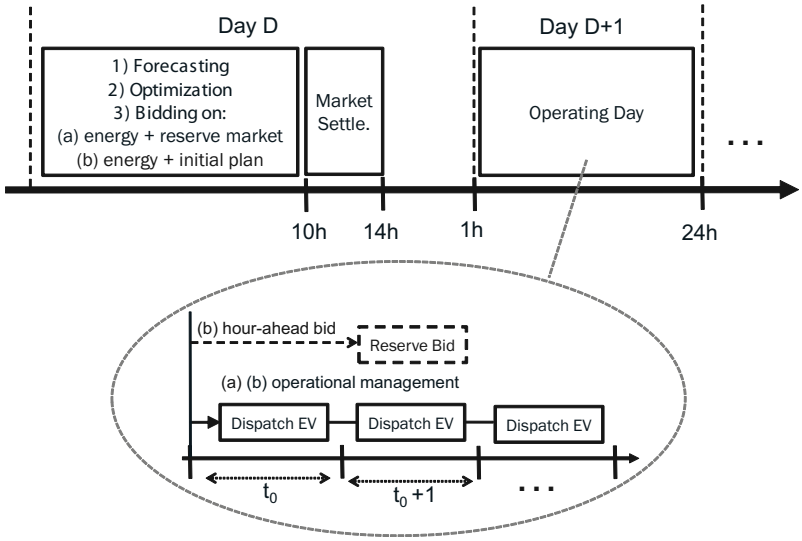

Figure 6.3: *Sequence of tasks for participating in the energy and balancing reserve market sessions.*

Afterwards the aggregator, during the operating day and using an operational management algorithm, coordinates the EV charging to fulfill the market commitments. If hour-ahead reserve bids are allowed, the operational algorithm also calculates, before the beginning of hour t_0, the reserve bid for the next hour t_0+1 . The EV are dispatched for each time interval until departure, and the charging power for hour t_0 is transmitted and followed by each EV.

There is also the possibility of balancing reserve shortage, and in this case, the aggregator communicates, 15 minutes before the operating interval, any shortage reserve power to the TSO. This does not jeopardize the system security since the TSO can activate balancing reserve bids with a price higher than the aggregator's price. The aggregator pays a high penalty for this reserve shortage.

Similarly to the secondary reserve market of chapter 5, the balancing reserve bids are submitted with an hourly time-step but the EV aggregator's bids are disaggregated by sub time-intervals with length Δt (e.g., half-hour).

6.3 Day-Ahead Energy and Reserve Optimization

6.3.1 Input Variables and Forecasts

The day-ahead optimization model takes the following forecasts as inputs: (a) charging requirement and availability forecast of each EV; (b) day-ahead electrical energy price; (c) price for upward and downward balancing reserve; (d) direction of the balancing reserve.

The EV variables and energy price are forecasted with the statistical algorithms described in chapter 4. The price for upward and downward balancing reserve is forecasted with the Holt-Winters algorithm for irregular time series [215].

The balancing reserve direction indicates whether the reserve was dispatched in upward or in downward direction. For modeling the reserve direction, two binary variables are used, one for upward and another for downward reserve. For instance, the upward variable takes value "1" if reserve is dispatched in that direction and "0" if not.

Figure 6.4 depicts the autocorrelation plots of the upward secondary and balancing reserve direction time series. The autocorrelation is calculated with the formula from [226] and ranges between -0.25 and 0.25. The autocorrelation for secondary reserve is very low (i.e., below 0.02) which suggests that the binary time series is almost random and the past values of the time series do not have sufficient information to produce a forecast with acceptable quality. In [227], it is shown that different statistical learning algorithms used to forecast the secondary reserve direction have a performance similar to a random predictor (e.g., flip of a coin).

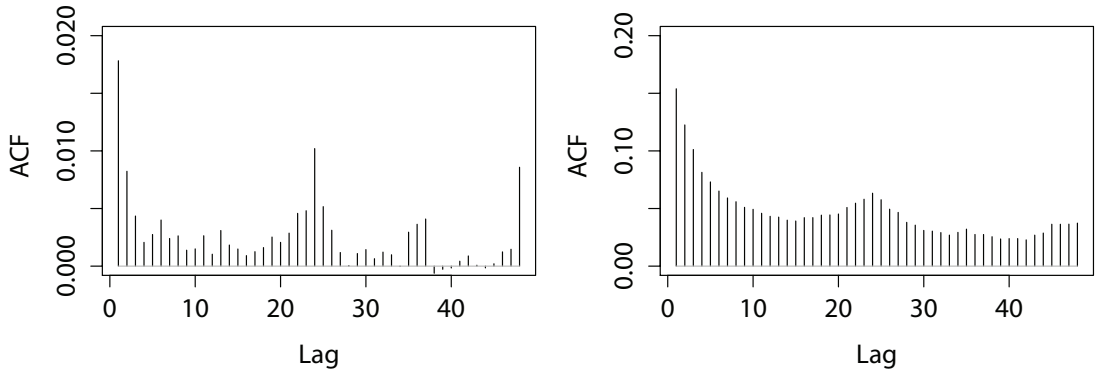

(a) *Secondary reserve.* **(b)** *Balancing reserve.*

Figure 6.4: *Autocorrelation diagrams of the binary variable that indicates if the secondary and balancing reserve was dispatched in the upward direction (Portugal, year 2011).*

The autocorrelation plot for balancing reserve presents higher autocorrelation values. The first lag presents an autocorrelation of around 0.15, and the time lag that corresponds to the previous day ($t - 24$) presents a value above 0.05. This suggests that the past values of the time series have useful information to forecast this time series. Moreover, since this reserve is used to handle renewable generation forecast errors, and based on the model described in [228], the forecasts of energy price and wind power penetration are also used as candidate covariates in a feature selection algorithm.

The following set of covariates were used in the feature selection process: lagged variables of

the response variable, forecasted energy price for Portugal, forecasted wind power penetration of the Iberian Peninsula, periodic function for the hour of the day and weekday.

The covariates were selected using the recursive (or backward) feature selection algorithm from R package *caret* [229]. The backward selection starts with all the candidate covariates, and each covariate is ranked using the accuracy of classification problems as the performance metric to select the "best" model. At each iteration, the top ranked covariates are retained and the model's performance is assessed. The subset of covariates with higher accuracy is determined after this iterative process. In order to avoid overfitting, 10-fold cross-validation over the training dataset is used. More details about the algorithm can be found in [230].

Four different statistical learning algorithms [231] suitable for binary outcomes are considered: GLM (Generalized Linear Model) with the response variable following a binomial distribution, naive Bayes, multilayer perceptron neural networks and support vector machines. The feature selection is applied in the GLM and the selected variables are also used as inputs in the other three algorithms.

A different learning model is fitted for the upward and downward reserve direction. For instance, a possible GLM that forecasts the day-ahead upward balancing reserve binary variable τ_t^- would be:

$$prob\left(\tau_t^- = 1|x\right) = 1\Big/\left(1+\exp\left(-\left(\begin{array}{c}\phi_0+\phi_1\cdot\tau_{t-24}^-+\phi_2\cdot\tau_{t-48}^- \\ +\phi_3\cdot\tau_{t-96}^-+\phi_4\cdot\tau_{t-120}^-+\phi_5\cdot\tau_{t-168}^- \\ +\phi_6\cdot wp_t+\phi_7\cdot\hat{p}_t+D_t+h_t\end{array}\right)\right)\right) \tag{6.1}$$

where τ_{t-l}^- are lagged variables of the response variable, $\hat{p}_t$ is the day-ahead energy price forecast, wp_t is the day-ahead forecast of the wind power penetration, x the set of covariates (i.e., τ_{t-l}^-, wp_t, etc.), D_t and h_t are periodic functions for the weekday and hour of the day. The model for day-ahead downward reserve binary variable (τ_t^+) is analogous.

A possible GLM for hour-ahead forecast of the variable τ_t^- is as follows:

$$prob\left(\tau_t^{-(ha)} = 1|x\right) = 1\Big/\left(1+\exp\left(-\left(\begin{array}{c}\phi_0+\phi_1\cdot\tau_{t-1}^-+\phi_2\cdot\tau_{t-2}^- \\ +\phi_3\cdot\tau_{t-3}^-+\phi_4\cdot\tau_{t-24}^-+\phi_5\cdot\tau_{t-48}^-+ \\ \phi_6\cdot\tau_{t-168}^-\end{array}\right)\right)\right) \tag{6.2}$$

The model for hour-ahead forecast of variable τ_t^+ is analogous.

The outputs are the *posterior* probabilities $prob\left(\tau_t^- = 1|\cdot\right)$ and $prob\left(\tau_t^+ = 1|\cdot\right)$. The decision rule for transforming the *posterior* probabilities into binary values consists in setting to "1" the most probable direction: $\hat{\tau}_t^- = 1$ if $prob\left(\tau_t^- = 1|\cdot\right) > prob\left(\tau_t^+ = 1|\cdot\right)$; $\hat{\tau}_t^+ = 1$ if

$prob\left(\tau_t^- = 1|\cdot\right) < prob\left(\tau_t^+ = 1|\cdot\right)$

For the test case of chapter 4, the GLM algorithm compared to the other three learning algorithms, achieved the best performance, as shown in appendix B. Therefore, it is used to produce day-ahead and hour-ahead forecasts for the reserve direction. On average, the accuracy (or hit-rate) of the day-ahead forecasts is 60% for upward and 64% for downward. For hour-ahead forecasts, the accuracy increases to 76% and 77%, correspondingly. In [228], it is reported an accuracy of 71% for both directions (obtained with an SVM) for the manual reserve in one control area of Denmark.

6.3.2 Formulation of the Optimization Problem

The decision variables of the day-ahead optimization are: energy purchased by the aggregator in the energy market for the j$^{\text{th}}$ vehicle and time interval t ($E_{t,j}$); downward reserve ($P_{t,j}^{down}$); upward reserve ($P_{t,j}^{up}$). The bid is the aggregation of the individual contribution from each EV for the same time interval t.

The objective function is the minimization of the total cost divided into three components: (a) cost of purchasing electrical energy in the energy market; (b) cost from charging EV with downward reserve (i.e., cheap charging); (c) income from reducing the consumption (upward reserve) using the energy bid as baseline value. It is written as:

$$\min \sum_{t \in H} \left(\begin{array}{c} \hat{p}_t \cdot \sum_{j=1}^{M_t} \left(E_{t,j}\right) + \hat{p}_t^{down} \cdot \sum_{j=1}^{M_t} \left(P_{t,j}^{down} \cdot \Delta t\right) - \\ \hat{p}_t^{up} \cdot \sum_{j=1}^{M_t} \left(P_{t,j}^{up} \cdot \Delta t\right) \end{array} \right) \tag{6.3}$$

where $\hat{p}_t$ is the forecasted energy price for time interval t, $\hat{p}_t^{down}$ the forecasted price of dispatched downward balancing reserve, $\hat{p}_t^{up}$ the forecasted price of dispatched upward balancing reserve, Δt the length of time interval t, H the set of time intervals from the optimization horizon, M_t the number of EV plugged-in.

This optimization problem can also be solved individually for each EV

The constraints are described in the following paragraphs.

The energy purchased in the market for charging during Δt plus the downward reserve power must be below or equal to the maximum charging power of the j$^{\text{th}}$ EV in each time interval t:

$$E_{t,j} \Big/ \Delta t + P_{t,j}^{down} \leq P_j^{\max}, \quad \forall j \in \{1, \cdots, M_t\}, \forall t \in H \tag{6.4}$$

The upward reserve power should be lower or equal to the energy purchased in the market

for charging during Δt in each time interval t:

$$P_{t,j}^{up} \leq \left(E_{t,j} \middle/ \Delta t\right) \cdot \hat{\tau}_t^-, \quad \forall j \in \{1, \cdots, M_t\}, \forall t \in H \tag{6.5}$$

where τ_t^- is the binary variable representing the upward reserve direction; when its value is "0", the upward reserve power must be zero. The downward reserve power should be zero when the forecasted binary variable for the downward reserve direction (τ_t^+) is "0":

$$P_{t,j}^{down} \leq P_t^{\max} \cdot \hat{\tau}_t^+, \quad \forall j \in \{1, \cdots, M_t\}, \forall t \in H \tag{6.6}$$

Similarly to chapter 5, the constraint of (6.7) is included to allow only upward balancing reserve bids in intervals where it is possible to consume the corresponding quantity both in the same and subsequent time intervals. Otherwise, the aggregator could incur in a considerable penalty (topic that will be discussed in section 6.5) if the upward reserve cannot be supplied. The constraint for postponing EV charging by offering upward reserve power is as follows:

$$\sum_{k=t}^{k=t_{final} \in \hat{H}_j^{plug}[i]} \left(P_{k,j}^{up} \cdot \Delta t\right) \leq \frac{\sum_{k=t}^{k=t_{final} \in \hat{H}_j^{plug}[i]} \left(E_{k,j} + P_{k,j}^{down} \cdot \Delta t\right)}{2}, \tag{6.7}$$
$$\forall j \in \{1, \cdots, M_t\}, \forall t \in H, \forall i \in \{1, \cdots, L_j\}$$

The balance between energy and reserve bids should be equal to the charging requirement of the jth EV in the ith availability period:

$$\sum_{t \in \hat{H}_j^{plug}[i]} \left(E_{t,j} + P_{t,j}^{down} \cdot \Delta t - P_{t,j}^{up} \cdot \Delta t\right) = \hat{R}_{j,i}, \quad \forall j \in \{1, \cdots, M_t\}, \forall i \in \{1, \cdots, L_j\} \tag{6.8}$$

Finally, the total upward reserve power in the ith availability period is limited by the charging requirement:

$$\sum_{t \in \hat{H}_j^{plug}[i]} \left(P_{t,j}^{up} \cdot \Delta t\right) \leq \hat{R}_{j,i}, \quad \forall j \in \{1, \cdots, M_t\}, \forall i \in \{1, \cdots, L_j\} \tag{6.9}$$

Not including (6.9) would lead to a risky bidding strategy (i.e., high penalization costs for reserve shortage), because the aggregator could offer a total upward reserve greater than the total of electrical energy that the EV fleet can consume.

This day-ahead optimization model is based on the possibility of forecasting the balancing reserve direction and uses that information for defining the energy and balancing reserve bids. Figure 6.5a depicts an illustrative result for one day (in hourly intervals) of the test case described in chapter 4, in which the day-ahead balancing reserve and energy bids and corresponding prices are presented.

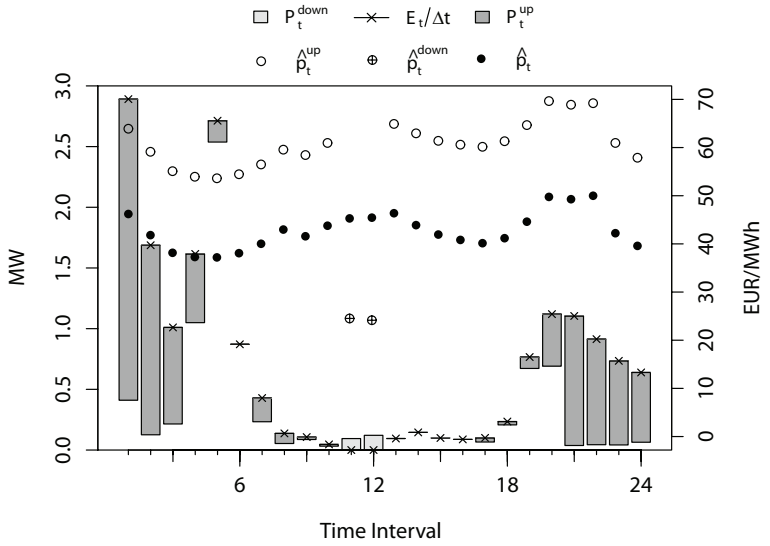

(a)

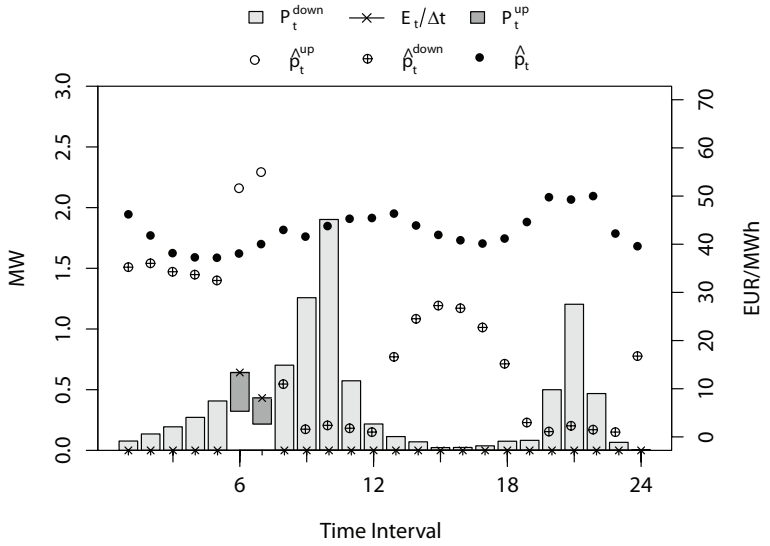

(b)

Figure 6.5: *Illustrative examples of the day-ahead energy and balancing reserve optimization.*

Note that there is only an upward reserve price and bid when $\hat{\tau}_t^- = 1$, and downward reserve price and bid when $\hat{\tau}_t^+ = 1$. For instance, in interval 1, the EV fleet is charging 2.89 MW, and a consumption reduction of 2.81 MW is offered by the aggregator as upward reserve. The hours with downward reserve bids are only intervals 11 and 12 (where $\hat{\tau}^+ = 1$). In intervals 4, 5 and 6, $\hat{\tau}_t^-$ is equal to 1, but there is not an upward bid because there is no flexibility for offering consumption reduction and meeting the charging requirement at the same time. The available flexibility was used in the previous hours (between 1 and 3), which also corresponds to the period with the highest upward reserve price. For this day, the strategy of the aggregator was to postpone the EV charging (i.e., offer upward reserve) as much as possible.

Figure 6.5b depicts a second illustrative day in which the majority of the reserve bids were submitted in the downward direction. There are only upward reserve bids in intervals 6 and 7. In the other intervals, the value of $\hat{\tau}^+$ was equal to 1 and the aggregator did not present any bid in the energy market and offered downward reserve bids in order to charge its EV at a price below the energy price. For instance, in interval 9 the downward reserve price was forecasted to be 1.6 €/MWh and the aggregator offered 1.25 MW as downward reserve. The strategy of the aggregator, in this day, was to charge the EV with cheap electrical energy (at the downward reserve price).

6.4 Operational Management Algorithms

The previous section described the day-ahead optimization model for energy and balancing reserve bids. This section presents two sequential optimization models that cover the two alternative gate closures. Note that, when hour-ahead reserve bids are allowed, the result from the day-ahead optimization is only an initial plan that can be updated during the operating day. Similarly to the operational algorithms from chapters 4 and 5, these two algorithms are independent from the formulation of the day-ahead optimization.

In contrast to the operational management algorithm for secondary reserve, for the balancing reserve, it is not possible to change the operating point because this reserve is precisely used to solve energy imbalances. In this case, the operating point should always be equal to the accepted energy bid (note that this energy bid can be updated in intraday or real-time markets).

6.4.1 Operational Management for Day-Ahead Reserve Bids

The central idea of the operational management algorithm consists in scheduling the EV charging independently of the realized τ^+ and τ^- values, which are unknown at the beginning of each time interval.

The aggregator follows the strategy from the day-ahead optimization model by minimizing the difference between the total charging and day-ahead plan (E_t, P_t^{down},P_t^{up}). This guarantees lower penalty costs due to reserve shortage and energy imbalances.

The objective function is convex and can be formulated for a period between t_0 and T (i.e.,

interval of the last EV to depart) with time intervals of length Δt as follows:

$$\min \sum_{k=t_0}^{T} \left(\varphi \left(E_k + P_k^{down} \cdot \Delta t - P_k^{up} \cdot \Delta t - \sum_{j=1}^{M_t} \left(E_{k,j}^{*} \right) \right) \right) \tag{6.10}$$

where $E_{k,j}^{*}$ is the actual charging of the j$^{\text{th}}$ EV, t_0 the first time interval of the optimization period, Δt the same interval length of the day-ahead optimization model and φ a piecewise loss function given by:

$$\varphi(u) = \begin{cases} u \cdot \theta_k^{+}, u \geq 0 \\ -u \cdot \theta_k^{-}, u < 0 \end{cases} \tag{6.11}$$

where θ_k^{+} and θ_k^{-} are constants that penalize situations with positive and negative deviations correspondingly. For example, in time intervals with downward reserve bids, θ_k^{+} must be higher than θ_k^{-}, because negative deviation ($u < 0$) means that the offered downward reserve is fully dispatched. In intervals with upward reserve bids, θ_k^{-} must be higher than θ_k^{+} in order to penalize more positive deviations. The ideal is to have $u = 0$, and there is no penalty for this case.

Like in the previous chapters (see section 4.4 in chapter 4), this convex function can be expressed in its epigraph form.

The operational algorithm has two constraints. The consumed energy in each time interval must be below or equal to the maximum available power for charging:

$$\frac{E_{k,j}^{*}}{\Delta t} \leq P_j^{\max}, \quad \forall j \in \{1, \cdots, M_k\}, \forall k \in H_j^{plug}[i], \forall i \in \{1, \cdots, L_j\} \tag{6.12}$$

The total consumed energy during the availability period must be equal to the charging requirement of the i$^{\text{th}}$ availability period :

$$\sum_{k \in H_j^{plug}[i]} \left(E_{k,j}^{*} \right) = R_{t_0,j,i}, \quad \forall j \in \{1, \cdots, M_k\}, \forall i \in \{1, \cdots, L_j\} \tag{6.13}$$

This optimization problem is applied sequentially for each time step of length Δt and as new EV arrive for charging:

1. the expected departure time instant and target SoC of the recently plugged-in EV (i.e., that connected for charging between $t_0 - 1$ and t_0) are included in equation (6.13) of the optimization model;

2. using this information, the aggregator solves the optimization problem for a period between t_0 and the maximum departure time interval of all the EV plugged-in in time interval (this maximum is updated every time step). The values of θ_k^{+} and θ_k^{-} are

defined as follows: for the time intervals with $P_k^{down} \cdot \Delta t > 0$, θ_k^+ is made equal to a large number (10^6) and θ_k^- to small number (10), and when $P_k^{up} \cdot \Delta t > 0$ is the opposite ($\theta_k^+ = 10$ and $\theta_k^- = 10^6$); in time interval t_0, and since the dispatch will be actually followed by the EV and cannot be modified, the value of $\theta_{t_0}^+$ is made equal to an even higher number (10^9) if $P_k^{down} \cdot \Delta t > 0$, and $\theta_{t_0}^-$ equal to 10^3, and if $P_k^{up} \cdot \Delta t > 0$, $\theta_{t_0}^-$ is made equal to 10^9 and $\theta_{t_0}^+$ equal to 10^3;

3. set points corresponding to the charging levels for time interval t_0 are transmitted to the plugged-in EV; only the dispatch for time interval t_0 remains unchanged, but the charging levels for the subsequent time intervals can be modified in the next iteration (next time interval, $t_0 + 1$); the residual charging requirement is updated for the next period, $R_{t_0+1,j} = R_{t_0,j} - E^*_{t_0,j}$;

4. this process is repeated for the next time interval $t_0 + 1$ (go back to step 1).

In this operational algorithm, during the operating day, the aggregator can only coordinate the EV charging to minimize the differences to the day-ahead plan. The next subsection describes an operational algorithm that modifies the day-ahead balancing reserve bids during the operating day, using information from the plugged-in EV. Note that intraday and real-time markets for electrical energy were not considered in this thesis, but the energy bids could also be updated during the operating day using those market sessions.

6.4.2 Operational Management for Hour-Ahead Reserve Bids

When hour-ahead reserve bids are allowed, the operational management algorithm is used to update the initial plan. In this case, the day-ahead plan is not firmly followed, and the aggregator can update the reserve bids (increase or decrease) or present new bids. The optimization model described in the following paragraphs is an adaptation of (6.10)-(6.13).

Without loss of generality, the time interval length Δt for this formulation is half-hour, and the market time interval is one hour. In the beginning of even intervals (with t_0 starting in zero), $t_0 \in \{2 \cdot \mathbb{Z}\}$, the aggregator defines the final reserve bid for half-hour intervals $t_0 + 2$ and $t_0 + 3$ (i.e., the next hour); in odd intervals ($t_0 \in \{2 \cdot \mathbb{Z} + 1\}$), the aggregator only defines the EV charging schedule to meet the accepted bids. The objective function is as follows:

$$\min \sum_{k=t_0}^{T} \left(\varphi \left(E_k^{DA} - \sum_{j=1}^{M_t} \left(E^*_{k,j} \right) \right) \right) \tag{6.14}$$

where E_k^{DA} is the initial plan from the day-ahead optimization that can take the following values:

- when $t_0 \in \{2\cdot\mathbb{Z}+1\}$ and $k \in \left[t_0, t_0+2\right]$, E_k^{DA} is equal to $E_k + P_k^{down}\cdot\Delta t + \Delta_k^{down} - P_k^{up}\cdot\Delta t + \Delta_k^{up}$, and for $k \in \left[t_0+3, 48\right]$ is equal to $E_k + P_k^{down}\cdot\Delta t - P_k^{up}\cdot\Delta t$;

- when $t_0 \in \{2\cdot\mathbb{Z}\}$, for $k \in \left[t_0, t_0+1\right]$ E_k^{DA} is equal to $E_k + P_k^{down}\cdot\Delta t + \Delta_k^{down} - P_k^{up}\cdot\Delta t + \Delta_k^{up}$, and for $k \in \left[t_0+2, 48\right]$ is equal to $E_k + P_k^{down}\cdot\Delta t - P_k^{up}\cdot\Delta t$.

The variables Δ_k^{up} and Δ_k^{down} are adjustments of the initial reserve bids that can take zero, negative and positive values. Both are calculated, with a sequential algorithm that will be explained in the remaining of this section [mostly related to equations (6.18)-(6.21)], in the following time intervals: for $t_0 \in \{2\cdot\mathbb{Z}\}$ and $k \in \left[t_0, t_0+1\right]$, Δ_k^{up} and Δ_k^{down} were estimated in t_0-2 (i.e., one hour before); for $t_0 \in \{2\cdot\mathbb{Z}+1\}$ and $k = t_0$, were estimated in t_0-3 (i.e., three half-hours before), and for $k \in \left[t_0+1, t_0+2\right]$, were estimated in t_0-1 (i.e., one half-hour before).

The penalty term of the convex loss function φ is selected in order to ensure a reliable provision of the contracted balancing reserve and update the reserve bids (e.g., decrease the reserve bid when it is not possible to supply the full reserve power).

When $t_0 \in \{2\cdot\mathbb{Z}+1\}$, the aggregator cannot present new balancing reserve bids, thus, the goal is to ensure a reliable prevision of the reserve service. The loss function φ becomes:

$$\varphi(u) = \begin{cases} u\cdot\hat{\pi}_k^{+} & ,u \geq 0 \wedge k \in \left[t_0+3, 48\right] \\ -u\cdot\hat{\pi}_k^{-} & ,u < 0 \wedge k \in \left[t_0+3, 48\right] \\ u\cdot M & ,u > 0 \wedge k \in \left[t_0, t_0+2\right] \wedge \left(P_k^{down} + \Delta_k^{down}\right) > 0 \\ u\cdot\hat{\pi}_k^{-} & ,u < 0 \wedge k \in \left[t_0, t_0+2\right] \wedge \left(P_k^{down} + \Delta_k^{down}\right) > 0 \\ u\cdot M & ,u < 0 \wedge k \in \left[t_0, t_0+2\right] \wedge \left(P_k^{up} - \Delta_k^{up}\right) > 0 \\ u\cdot\hat{\pi}_k^{+} & ,u > 0 \wedge k \in \left[t_0, t_0+2\right] \wedge \left(P_k^{up} - \Delta_k^{up}\right) > 0 \end{cases} \tag{6.15}$$

where M is a large number equal to 10^3, $\hat{\pi}_k^{+}$ and $\hat{\pi}_k^{-}$ are forecasted imbalance prices and $u = E_k^{DA} - \sum_{j=1}^{M_t}\left(E_{k,j}^{*}\right)$.

For the time intervals between t_0+3 and 48, the deviation u is penalized with the forecasted energy imbalance price; this corresponds to the first two rows of the loss function (6.15). The reserve bids in these intervals can be modified in the subsequent intervals.
The last four rows are for intervals between t_0 and t_0+2, in which hour-ahead balancing reserve bids were already submitted and cannot be modified. For these intervals, the penalties are defined as follows: a $u > 0$ means that the actual charging of the EV fleet is below E_k^{DA} which represents downward reserve shortage if $P_k^{down} + \Delta_k^{down} > 0$, and this situation should get a higher penalty M (in case of no downward reserve bid, the penalty term is the energy imbalance price); a $u < 0$ and $P_k^{up} + \Delta_k^{up} > 0$ means upward reserve shortage and the penalty should be high, while if $P_k^{down} + \Delta_k^{down} > 0$, it means that the full downward reserve is

dispatched, but there is a negative imbalance that is penalized at the corresponding imbalance price.

When $t_0 \in \{2 \cdot \mathbb{Z}\}$, the aggregator coordinates the EV charging in time intervals t_0 and t_0+1, since the reserve bids in these intervals cannot be modified, and it updates the reserve bids of intervals t_0+2 and t_0+3 (i.e., next hour). The loss function is as follows:

$$\varphi(u) = \begin{cases} u \cdot \hat{\pi}_t^+ & ,u \geq 0 \wedge k \in \left[t_0+4, 48\right] \\ -u \cdot \hat{\pi}_t^- & ,u < 0 \wedge k \in \left[t_0+4, 48\right] \\ u \cdot M & ,u > 0 \wedge k \in \left[t_0, t_0+1\right] \wedge \left(P_k^{down} + \Delta_k^{down}\right) > 0 \\ u \cdot \hat{\pi}_t^- & ,u < 0 \wedge k \in \left[t_0, t_0+1\right] \wedge \left(P_k^{down} + \Delta_k^{down}\right) > 0 \\ u \cdot M & ,u < 0 \wedge k \in \left[t_0, t_0+1\right] \wedge \left(P_k^{up} - \Delta_k^{up}\right) > 0 \\ u \cdot \hat{\pi}_t^+ & ,u > 0 \wedge k \in \left[t_0, t_0+1\right] \wedge \left(P_k^{up} - \Delta_k^{up}\right) > 0 \\ -u \cdot M & ,u > 0 \wedge k \in \left[t_0+2, t_0+3\right] \wedge P_k^{up} > 0 \wedge \hat{\tau}_k^{-(ha)} = 1 \\ u \cdot M & ,u < 0 \wedge k \in \left[t_0+2, t_0+3\right] \wedge P_k^{up} > 0 \wedge \hat{\tau}_k^{-(ha)} = 1 \\ -u \cdot M & ,u < 0 \wedge k \in \left[t_0+2, t_0+3\right] \wedge P_k^{down} > 0 \wedge \hat{\tau}_k^{+(ha)} = 1 \\ u \cdot M & ,u > 0 \wedge k \in \left[t_0+2, t_0+3\right] \wedge P_k^{down} > 0 \wedge \hat{\tau}_k^{+(ha)} = 1 \end{cases} \tag{6.16}$$

The first two rows are analogous to the rows of (6.15), but for the time intervals between t_0+4 and 48. The next four rows are also analogous to the last four rows of (6.15), but they correspond to time intervals t_0 and t_0+1, since in these two time intervals the aggregator cannot modify the balancing reserve bids.

The aggregator can update the balancing reserve bids for the next hour (i.e., time intervals t_0+2 and t_0+3), and the last four rows of (6.16) update the reserve bids based on hour-ahead forecasts for $\hat{\tau}_k^{+(ha)}$ and $\hat{\tau}_k^{-(ha)}$. The penalty terms for these two intervals are defined as follows: when $\hat{\tau}_k^{-(ha)} = 1$ and $P_k^{up} > 0$, a positive u means that the upward reserve power from the day-ahead optimization can be fully dispatched and can be increased, thus the penalty term is $-M$ in order to promote this reserve power increase; when u is negative it means an upward reserve shortage which should be avoided by placing a large penalty; when $\hat{\tau}_k^{+(ha)} = 1$ and $P_k^{down} > 0$ the idea is analogous, but in this case, a negative u means that the downward power from the day-ahead optimization can be fully dispatched and increased.

It is also possible to replace a downward bid by an upward one and vice-versa. This is attained by making E_k^{DA} equal to E_k for $k \in \left[t_0+2, t_0+3\right]$ and including the following additional rows in (6.16):

$$\begin{cases} -u \cdot M & ,u > 0 \wedge k \in \left[t_0+2, t_0+3\right] \wedge P_k^{up} = 0 \wedge \hat{\tau}_k^{-(ha)} = 1 \wedge \hat{\tau}_k^{+(ha)} = 0 \\ u \cdot M & ,u < 0 \wedge k \in \left[t_0+2, t_0+3\right] \wedge P_k^{up} = 0 \wedge \hat{\tau}_k^{-(ha)} = 1 \wedge \hat{\tau}_k^{+(ha)} = 0 \\ -u \cdot M & ,u < 0 \wedge k \in \left[t_0+2, t_0+3\right] \wedge P_k^{down} = 0 \wedge \hat{\tau}_k^{+(ha)} = 1 \wedge \hat{\tau}_k^{-(ha)} = 0 \\ u \cdot M & ,u > 0 \wedge k \in \left[t_0+2, t_0+3\right] \wedge P_k^{down} = 0 \wedge \hat{\tau}_k^{+(ha)} = 1 \wedge \hat{\tau}_k^{-(ha)} = 0 \end{cases} \tag{6.17}$$

These additional rows work as follows: if $\hat{\tau}_k^{-(ha)} = 1$ and $\hat{\tau}_k^{+(ha)} = 0$, and if the aggregator did not plan (i.e., output of the day-ahead optimization) an upward reserve bid (i.e., $P_k^{up} = 0$), the penalty term for positive deviation should be negative in order to create an opportunity to offer upward reserve (note that $E_k^{DA} = E_k$ for these two intervals), and the penalty for negative deviation should be equal to a large number M; the same reasoning is applied to the downward reserve when $\hat{\tau}_k^{+(ha)} = 1$ and $P_k^{down} = 0$.

Equations (6.14)-(6.17) define the loss function that is used to calculate the value of E_k^*. This loss function can be represented in its epigraph form, and the constraints of (6.12) and (6.13) are also considered. The operational management algorithm is sequentially solved in each time interval and the values of Δ_k^{down} and Δ_k^{up} are calculated in the process. The sequential process is as follows:

1. new information from the recently plugged-in EV (i.e., between $t_0 - 1$ and t_0) is available. Forecasts for a time horizon between t_0 and 48 are produced for π_k^+ and π_k^-, and one hour-ahead forecasts are produced for $\hat{\tau}^{+(ha)}$ and $\hat{\tau}^{-(ha)}$;

2. solving the optimization problem with the objective function of (6.15)-(6.17). The result is the $E_{k_j}^*$ for each EV;

3. after solving the optimization problem, if $t_0 \in \{2 \cdot \mathbb{Z}\}$, the reserve bids for the next hour (i.e., $k \in [t_0 + 2, t_0 + 3]$) are updated by calculating Δ_k^{up} and Δ_k^{down} as follows:

$$\begin{gathered} if \left(\sum_k \left(E_k^*\right) < \sum_k \left(E_k^{DA}\right)\right) \wedge \left(\sum_k \left(E_k^{down}\right) > 0 \wedge \sum_k \left(E_k^{up}\right) = 0\right), \\ \Rightarrow \Delta_k^{down} = E_k^* - E_k^{DA} \Rightarrow \Delta_k^{down} < 0 \\ if \left(\sum_k \left(E_k^*\right) > \sum_k \left(E_k^{DA}\right)\right) \Rightarrow \Delta_k^{down} > 0 \end{gathered} \tag{6.18}$$

   a negative Δ_k^{down} decreases the downward reserve bid (which is bounded by the P_k^{down} value), while a positive value increases the bid;

$$\begin{gathered} if \left(\sum_k \left(E_k^*\right) < \sum_k \left(E_k^{DA}\right)\right) \wedge \left(\sum_k \left(E_k^{down}\right) = 0 \wedge \sum_k \left(E_k^{up}\right) > 0\right), \\ \Rightarrow \Delta_k^{up} = E_k^* - E_k^{DA} \Rightarrow \Delta_k^{up} < 0 \\ if \left(\sum_k \left(E_k^*\right) > \sum_k \left(E_k^{DA}\right)\right) \Rightarrow \Delta_k^{up} > 0 \end{gathered} \tag{6.19}$$

   a negative Δ_k^{up} increases the upward reserve bid, while a positive value decreases the bid (which is bounded by the P_k^{up} value);

$$\begin{gathered} if \left(\sum_k \left(E_k^*\right) < \sum_k \left(E_k^{DA}\right)\right) \wedge \left(\hat{\tau}_k^{-(ha)} = 1 \wedge \hat{\tau}_k^{+(ha)} = 0 \wedge \sum_k \left(P_k^{up}\right) = 0\right), \\ \Rightarrow \Delta_k^{down} = -P_k^{down} \cdot \Delta t,\ \Delta_k^{up} = E_k^* - E_k^{DA} \\ if \left(\hat{\tau}_k^{-(ha)} = 0 \wedge \hat{\tau}_k^{+(ha)} = 1 \wedge \sum_k \left(P_k^{down}\right) = 0\right) \Rightarrow \Delta_k^{up} = P_k^{up} \cdot \Delta t \end{gathered} \tag{6.20}$$

   in the first condition, the downward bid is replaced by an upward bid, while the upward

reserve bid is removed in the second;

$$\begin{gathered} if\ \left(\sum_k \left(E_k^*\right) > \sum_k \left(E_k^{DA}\right)\right) \wedge \left(\hat{\tau}_k^{-(ha)} = 1 \wedge \hat{\tau}_k^{+(ha)} = 0 \wedge \sum_k \left(P_k^{up}\right) = 0\right), \\ \Rightarrow \Delta_k^{down} = -P_k^{down} \cdot \Delta t \\ if\ \left(\hat{\tau}_k^{-(ha)} = 0 \wedge \hat{\tau}_k^{+(ha)} = 1 \wedge \sum_k \left(P_k^{down}\right) = 0\right) \\ \Rightarrow \Delta_k^{up} = -P_k^{up} \cdot \Delta t,\ \Delta_k^{down} = E_k^* - E_k^{DA} \end{gathered} \tag{6.21}$$

in the first condition, the downward bid is removed, while in the second the upward bid is replaced by a downward bid;

4. set points corresponding to the charging levels for time interval t_0 are transmitted to the plugged-in EV, and if $t_0 \in \{2 \cdot \mathbb{Z}\}$, balancing reserve bids are submitted to intervals $t_0 + 2$ and $t_0 + 3$;

5. this process is repeated for the next time interval (go back to step 1).

For the same day of Figure 6.5a, Figure 6.6a compares the offered upward reserve power with the day-ahead and hour-ahead bidding. It is possible to see that the hour-ahead bidding adjusts the day-ahead (or initial) plan in several hours. In some intervals, such as 4 and 5, the hour-ahead algorithm presents a new upward bid, while in others (1 and 19, for example) it decreases the upward reserve value.

Figure 6.6b shows the percentage of upward reserve shortage obtained with the two bidding approaches. As expected, the hour-ahead bid results in a much lower percentage and time intervals with reserve shortage. Nevertheless, it is important to note that, even with hour-ahead bids, situations with reserve shortage can occur because during the hourly gap some EV without charging flexibility[2] might park for charging. For these time intervals, a possible solution is to establish in the contract between the driver and the aggregator, a degree of flexibility for the target SoC. The aggregator guarantees only 95% or 90% of target SoC (instead of 100%) when there is a risk of reserve shortage (this solution will be explored in section 6.6.3).

The results for downward reserve shortage are not presented here. However, in contrast to upward reserve, the hour-ahead bid guarantees that all the offered downward reserve is supplied. This is an expected result because in the hourly gap between the bid and physical delivery, the only event that can occur is the arrival of additional EV for charging, and this does not represent a negative impact on the downward reserve reliability.

Figure 6.6c shows the actual charging of the EV fleet (i.e., $E_t^* / \Delta t$), as well as the realized values of τ_t^- and τ_t^+, and the accepted energy and reserve bids. As shown in this plot, the

[2] EV that need to charge at maximum power in all the intervals of the availability period for meeting the defined target SoC.

balancing reserve was provided by the aggregator in almost all the intervals. For example, in interval 1, the system imbalance was in the two directions, and the aggregator reduced the EV charging from 2.89 MW (the accepted energy bid) to 0.41 MW (by supplying 2.48 MW of upward reserve). In interval 12, the system imbalance was in the downward direction and the aggregator supplied 0.12 MW of downward reserve (the energy bid was zero). The new upward reserve bids produced by hour-ahead bidding in intervals 4 and 5 were actually supplied by the aggregator.

The estimated total cost of the day-ahead optimization (i.e., associated to Figure 6.5a) for this day was 68 € [calculated with the objective function (6.3)]. After the operational management phase, the total cost (calculated with the settlement scheme described in the next section) was 185 € with day-ahead bids and 160 € with hour-ahead bids. Note that this total cost includes the cost from purchasing electrical energy, income from balancing reserve and reserve shortage penalty costs.

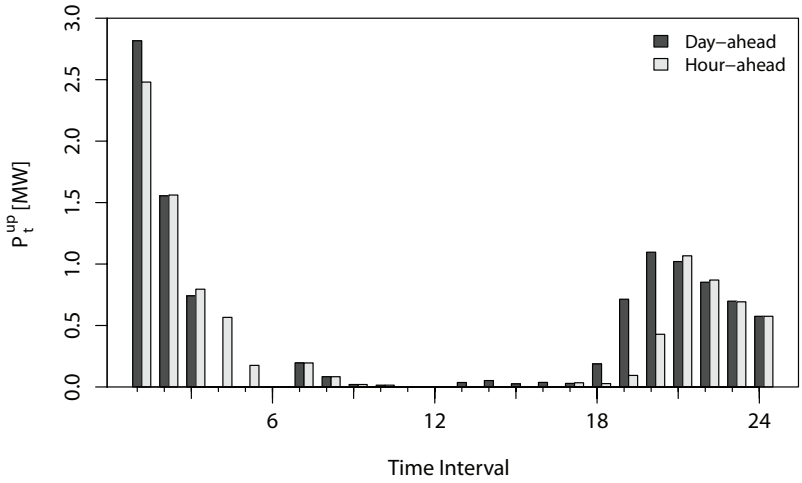

(a) *Upward reserve power of day-ahead and hour-ahead balancing reserve bids.*

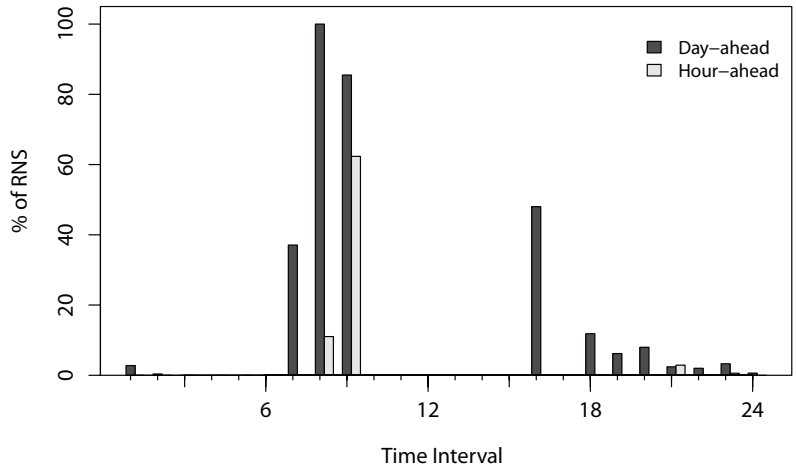

(b) *Percentage of reserve not supplied of the day-ahead and hour-ahead bids.*

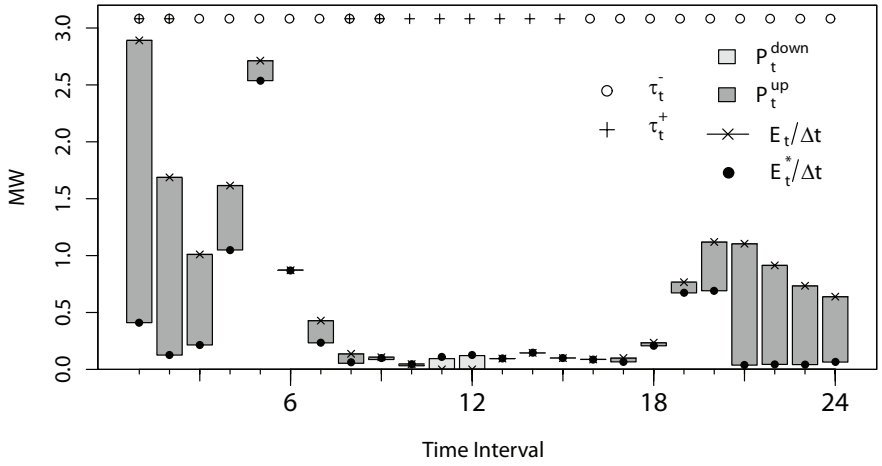

(c) *Actual charging of the EV fleet with hour-ahead bids.*

Figure 6.6: *Illustrative example of the day-ahead and hour-ahead operational management algorithms output for balancing reserve.*

6.5 Market Settlement

This section describes the market settlement phase of the energy and balancing reserve bids. The following variables are used to compute the total cost: E_t (total purchased electrical energy); P_t^{up} (total upward reserve bid); P_t^{down} (total downward reserve bid); E_t^* (total actual charging resulting from the operational management algorithm).

The upward reserve consists in reducing the consumption using E_t (i.e., the accepted energy bid) as baseline. However, as underlined by Bushnell et al. [232], any payment for consumption reduction of a load faces a challenge in measuring this reduction compared to the consumption level in the absence of a payment (called baseline). For instance, it can create an unwanted incentive to over-bid in the electrical energy market (i.e., inflate their baseline) in order to increase their level of reduction.

Regarding EV, an incorrect baseline might create a chance for gambling with the upward reserve and energy bid values. For example, if the aggregator forecasts a $prob\left(\tau_t^- = 1|x\right) > 0.9$ for a specific hour, one potential strategy will be to present an abnormally high E_t knowing that a consumption reduction (upward balancing reserve) will be requested by the TSO. If the reserve is used, it will represent a windfall profit, if not, the aggregator will incur in a financial penalization (but the probability is low).

Thus, in this thesis a baseline that places a cap on the paid upward reserve is introduced. The baseline E_t^{base} is given by:

$$E_t^{base} = \min\left(E_t, \sum_{j=1}^{M_t}\left(\min(R_{t,j}, P_j^{\max}\cdot\Delta t)\right)\right) \tag{6.22}$$

In words, the baseline is the minimum between accepted energy bid and the total energy that is possible to consume during that time interval (i.e., minimum between the maximum charging power and the residual charging requirement at time interval t). Consider 10 EV plugged-in and able to charge 3 kW during one hour. If the energy bid is equal to 40 kWh, the baseline would be equal to 30 kWh since the plugged-in EV can only consume this value, and not 40 kWh, during that hour.
This baseline guarantees that the reference for the upward reserve is actually the energy that can be consumed in that hour and not an inflated energy bid.

In a real situation, the TSO and the aggregator have metering values of the dispatched upward and downward balancing reserve. Here, and for conducting the robustness tests of section 6.6, the dispatched reserve values are calculated as follows:

- if $\tau_t^- = 1 \wedge P_t^{up} > 0 \Rightarrow E_t^{up*} = \max\left(0, E_t^{base} - E_t^*\right)$ where E_t^{up*} is the dispatched upward balancing reserve. It may occur that $E_t^{up*} > E_t^{up}$ (where E_t^{up} is given by $P_t^{up} \cdot \Delta t$), in this case, E_t^{up*} is made equal to E_t^{up} and the "additional reserve" is calculated as $\Delta E_t^{up*} = E_t^{up*} - E_t^{up}$;

- if $\tau_t^+ = 1 \wedge P_t^{down} > 0 \Rightarrow E_t^{down*} = \max\left(0, E_t^* - E_t^{base}\right)$ where E_t^{down*} is the dispatched downward balancing reserve. When $E_t^{down*} > E_t^{down}$ (where E_t^{down} is given by $P_t^{down} \cdot \Delta t$), the "additional reserve" ΔE_t^{down*} is calculated;

- the consumed electrical energy (after removing the dispatched reserve values) is given by $E_t^{cons} = E_t^* - E_t^{down*} + E_t^{up*}$.

After computing these variables, the total cost is given by:

$$TotalCost = \sum\nolimits_t \left(\begin{array}{l} E_t^{cons} \cdot p_t + E_t^{down*} \cdot p_t^{down} - E_t^{up*} \cdot p_t^{up} + \\ \Psi\left(E_t^{cons}, E_t\right) + \Phi\left(E_t^{up}, E_t^{up*}, E_t^{down}, E_t^{down*}\right) \end{array} \right) \tag{6.23}$$

where Ψ are the costs associated to deviations from the purchased energy (i.e., deviation between E_t^{cons} and E_t), and Φ are the costs associated to reserve shortage (deviation between E_t^{down} and E_t^{down*}, and between E_t^{up} and E_t^{up*}).

The term Ψ for energy imbalances is as follows:

$$\Psi = \begin{cases} \left(E_t - E_t^{cons}\right) \cdot \left(p_t - p_t^{surplus}\right) & , E_t > E_t^{cons} \wedge \Delta E_t^{up*} = 0 \\ 0 & , E_t > E_t^{cons} \wedge \Delta E_t^{up*} > 0 \\ \left(E_t^{cons} - E_t\right) \cdot \left(p_t^{shortage} - p_t\right) & , E_t < E_t^{cons} \wedge \Delta E_t^{down*} = 0 \\ 0 & , E_t < E_t^{cons} \wedge \Delta E_t^{down*} > 0 \end{cases} \tag{6.24}$$

Note that situations with "additional reserve" (ΔE_t^{up*} or ΔE_t^{down*}) help solving system deviation, thus the aggregator pays an imbalance price equal to the energy price (which means no penalty).

When the unit fails to deliver the contracted balancing reserve, it incurs in a penalty. The scheme proposed in this thesis is inspired by the penalty scheme of the ISO New England forward reserve market [218]. The aggregator is paid by the dispatched reserve (E_t^{down*} and E_t^{up*}) and a penalization term proportional to the deviation between E_t^{down*} and E_t^{down} (and between E_t^{up*} and E_t^{up}) is imposed. This gives the following:

$$\Phi = \begin{cases} \rho \cdot p_t^{up} \cdot \left(E_t^{up} - E_t^{up*}\right) & , E_t^{up} > E_t^{up*} \\ \left(p_t - p_t^{down}\right) \cdot \left(E_t^{down} - E_t^{down*}\right) & , E_t^{down} > E_t^{down*} \end{cases} \tag{6.25}$$

In the Demand Response Reserves Pilot Program of the ISO New England, ρ was made equal to one [218], and this value is also used in this chapter. As explained in the previous chapter,

for secondary reserve, a $\rho = 1$ means that the aggregator must supply at least half of the contracted upward reserve to get some income from supplying this service.

6.6 Test Case Results

The previous sections described optimization models for two alternative gate closures: (a) day-ahead optimization followed by an operational management algorithm that minimizes, during the operating day, the deviations to the accepted day-ahead bids; (b) day-ahead optimization followed by an operational algorithm that updates reserve bids until one hour before physical delivery. After the operational management phase, the total wholesale cost can be calculated with the market settlement scheme described in the preceding section.

In this section, these two optimization frameworks are applied to the test case of chapter 4 and evaluated from the aggregator and TSO's viewpoints. The following tests were conducted:

- the optimization models are evaluated from the aggregator and the TSO's viewpoints in 30 test samples characterized by different market prices and directions (i.e., upward or downward) of dispatched reserve. For each test sample, the total wholesale cost is calculated, as well as the magnitude and number of intervals with Reserve Not Supplied (RNS);
- the additional value from forecasting the reserve direction is assessed by comparing the forecasts produced by the GLM and four basic (or heuristic) forecasts;
- the error of the availability and charging requirement forecasts is increased by perturbing the initial forecasts, and the impact on the RNS is evaluated.

Appendix A presents a statistical analysis of the market price data.

The average execution time[3] of the day-ahead optimization model was 4.8 seconds, 0.64 seconds for the operational algorithm and 1.1 seconds for the hour-ahead operational algorithm.

6.6.1 Sampling Process

The same sampling process of chapter 4 is used to create 30 test samples from different periods of three years of data (2009-2011). Each test sample corresponds to a time period

[3] Laptop computer with an Intel Core i5 CPU M450 @ 2.40 GHz processor and 4 GB of RAM, IBM ILOG CPLEX 12.5.

with different energy and balancing reserve prices, and also different direction of dispatched balancing reserve[4]. Each test sample is divided into 9 months for the training dataset and 3 months for the evaluation dataset.

The direction of dispatched balancing reserve (i.e., *reserva de regulação*) in Portugal for the same three year period is used as the realized values of τ_t^+ and τ_t^- and also as historical data to fit the GLM.

6.6.2 Aggregator's Viewpoint: Total Cost

For the EV aggregator, the total wholesale cost is the main criterion for assessing the quality of the proposed optimization models. Therefore, this section compares the total of the proposed optimization models, for both day-ahead and hour-ahead gate closures, with the divided approach from chapter 4. This total cost already includes the costs related to reserve shortage and section 6.6.3 will quantify the reserve shortage magnitude, which covers the TSO's viewpoint.

In this section, it is assumed that the available reserve power from the EV aggregator is fully dispatched during each time interval t. In general, this is applicable since balancing reserve is activated to cover an energy imbalance in a specific market interval (e.g., one hour), as illustrated in Table 6.1 of section 6.2.1. Nevertheless, in some cases the reserve might be activated during the operating interval, which means that it is partly dispatched in that interval. The impact of this partial activation will be evaluated in terms of RNS in section 6.6.3. In terms of total cost, this partial activation means a lower income from reserve provision since only part of the reserve is dispatched.

Figure 6.7 depicts the total cost reduction of day-ahead (section 6.4.1) and hour-ahead (section 6.4.2) balancing reserve bidding algorithms, using as reference the total cost from the divided approach of chapter 4 (i.e., only energy bids).

The hour-ahead reserve bid attains a higher cost reduction (using the divided approach as reference) compared to the day-ahead reserve bid in both EV fleets. Nevertheless, the difference is not significant: for the hour-ahead reserve bidding, the average cost reduction is 25.08% in fleet A and 21.87% in fleet B; for the day-ahead reserve bidding, it is 20.9% in fleet A and 14.04% in fleet B.

The main contribution to this difference comes from the reserve shortage penalty. The op-

[4] The market data of Portugal was downloaded from http://www.mercado.ren.pt/ (accessed in December 2012)

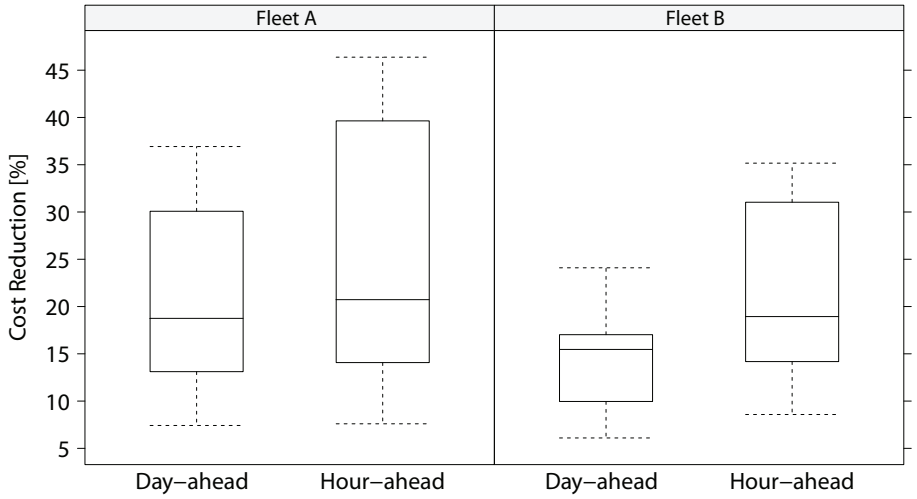

Figure 6.7: *Reduction in the total cost compared to optimizing only the energy bids.*

erational algorithm for the hour-ahead bids is mainly used to correct reserve bids (increase or decrease the power) and avoid reserve shortage, and there is no sufficient flexibility left by the day-ahead optimization for turning a downward into an upward bid (and vice-versa). For instance, the intervals with downward reserve bids normally have no energy bid, thus, in these hours, it is not possible to offer consumption reduction (upward reserve). This might change if intraday trading is considered.

The range of cost reduction in the 30 samples is wide, e.g., in fleet A (hour-ahead) the maximum is 46.4% and the minimum is 7.6%. This difference is mainly explained by the reserve prices: the minimum cost reduction is achieved by a price difference between dispatched upward reserve and energy of 6.2 €/MWh and 9.5 €/MWh for the downward reserve; in the maximum reduction, the price differences are 15.9 €/MWh for upward reserve and 12.7 €/MWh for downward reserve.

From the aggregator's viewpoint, these cost reduction results show that proposed optimization models, compared to an approach that only optimizes the energy bids, can create a significant reduction in the total cost depending on the reserve prices level.

So far, the tests were conducted with forecasts for all variables, including reserve prices and direction. An improvement in the forecasting accuracy leads to a decrease in the total cost, but as shown in the previous chapters, the cost reduction with better EV forecasts might not be high. Figure 6.8 depicts the cost reduction for three cases: hour-ahead reserve bids, perfect forecast for the EV variables, and perfect forecast for all the variables. The reference for the cost reduction is the day-ahead balancing reserve bidding (i.e., with the operational management of section 6.4.1). Note that a cost reduction greater than 100% means that the total cost obtained with perfect forecast for all variables is negative.

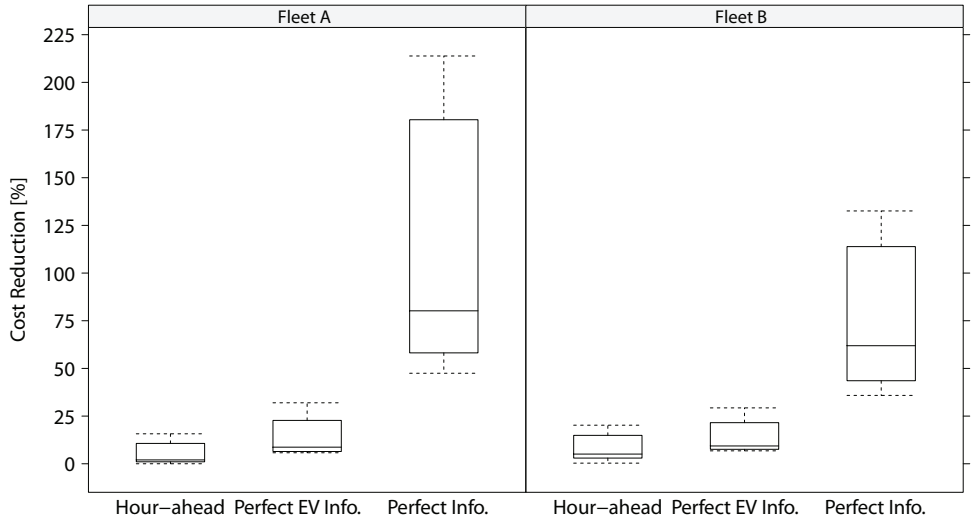

Figure 6.8: *Total cost reduction of three different sets of available information, using the day-ahead balancing reserve bidding as reference.*

The hour-ahead bidding only accomplishes a cost reduction (on average) of 5.46% in fleet A and 8.45% in fleet B. Furthermore, even when perfect forecasts are used for the EV variables, the cost reduction is of 13.75% for fleet A and 13.64% for fleet B. This shows that the uncertainty in the EV variables has a small impact in the cost, although the impact on the RNS is more significant (as it will be shown in the following section). Finally, when perfect forecasts are used for the reserve direction and price, the impact on cost reduction is very substantial. Note that these variables require day-ahead forecasts, and even with more advanced forecasting algorithms, it is difficult to accomplish an improvement close to the one with perfect forecasts.

In this figure, there is a significant difference between the cost reduction results of fleets A and B. The drivers of fleet B are characterized by having a lower flexibility compared to fleet A.

The analysis of the results for "perfect EV info" (i.e., without the influence of forecast errors) shows that fleet A offers more upward reserve power. For instance, on average 61.3% of the energy bid is offered as upward reserve [i.e., $P_t^{up} \Big/ \left(E_t \cdot \Delta t\right)$] in fleet A, while in fleet B, only 53.2% is offered. This has a direct influence in the income from upward reserve: in fleet A, it is 61.8% of the energy cost [i.e., $\left(E_t^{up*} \cdot p_t^{up}\right) \Big/ \left(E_t^{cons} \cdot p_t\right)$] on average, while in fleet B it is 51.% on average. The same conclusions are derived for downward reserve. This shows that the economic results cannot be generalized to other fleets (and markets), since they depend from several variables, such as market data, driver's behavior and traveled distance.

6.6.3 TSO's Viewpoint: Reserve Shortage

Since the balancing reserve is not remunerated by available reserve power, and when contracted by TSO it is activated to supply full power during a predefined time interval, the reserve shortage in each direction is measured in terms of reserve not supplied (RNS).

15 minutes before the operating interval, the aggregator can inform the TSO about reserve shortage values, and the TSO activates balancing reserve bids with a higher price to cover this shortage (this cost is passed to the aggregator by the penalty term in the market settlement). Therefore, RNS events do not jeopardize the system security, but assessing the variation of RNS in the 30 test samples gives an indication of the algorithm's robustness to different market prices and direction of dispatched reserve and, at the same time, measures the degree of reliance that the TSO can have on this resource.

For the upward reserve, the percentage of RNS (pRNS^{up}) is given by:

$$pRNS^{up} = \frac{\sum_t \left(E_t^{up} - E_t^{up*}\right)}{\sum_t \left(E_t^{up}\right)} \cdot 100\% \tag{6.26}$$

The calculation of pRNS^{down} is similar.

A second metric is the percentage of intervals with RNS (pIRNS), which is given by the number of intervals with RNS divided by the number of intervals with reserve bids. This metric is also calculated separately for each reserve direction.

Table 6.2 presents the pRNS^{down} and pIRNS^{down} (average, minimum and maximum values of the 30 samples). As previously mentioned, the hour-ahead bidding guarantees that all the offered downward reserve power is delivered. Conversely, the day-ahead bidding presents RNS in some intervals, which will increment the total cost with penalty costs due to reserve shortage.

Table 6.2: *Downward pRNS and pIRNS from fleets A and B (average [minimum,maximum]).*

	pRNS^{down}		pIRNS^{down}	
	Day-ahead	Hour-ahead	Day-ahead	Hour-ahead
Fleet A	2.41% [1.6%,3.35%]	0.0%	3.56% [1.79%,5.27%]	0.0%
Fleet B	3.74% [2.56%,4.71%]	0.0%	10.18% [5.55%,15.71%]	0.0%

The pIRNS^{down} is high in fleet B, but the shortage magnitude is low as shown by the low values of pRNS^{down} (below 4% on average). The worst performance of fleet B is explained by a higher forecast error compared to fleet A. The pIRNS in fleet B is 10% on average, but the

magnitude of the shortage events is low as indicated by the low pRNS^{down} values. From the TSO's standpoint, the reserve offered with hour-ahead bids is more reliable.

Figure 6.9 depicts the results for the upward reserve (i.e., pRNS^{up} and pIRNS^{up}) considering three tolerable target SoC levels (100%, 95% and 90%). The pRNS^{up} values are higher than the ones of the downward reserve, suggesting a lower reliability in this reserve direction.

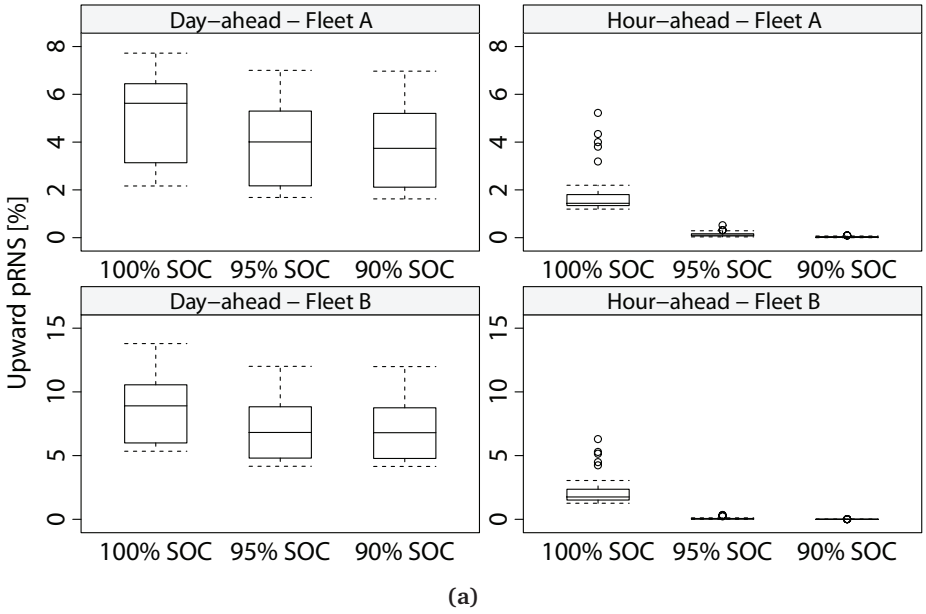

(a)

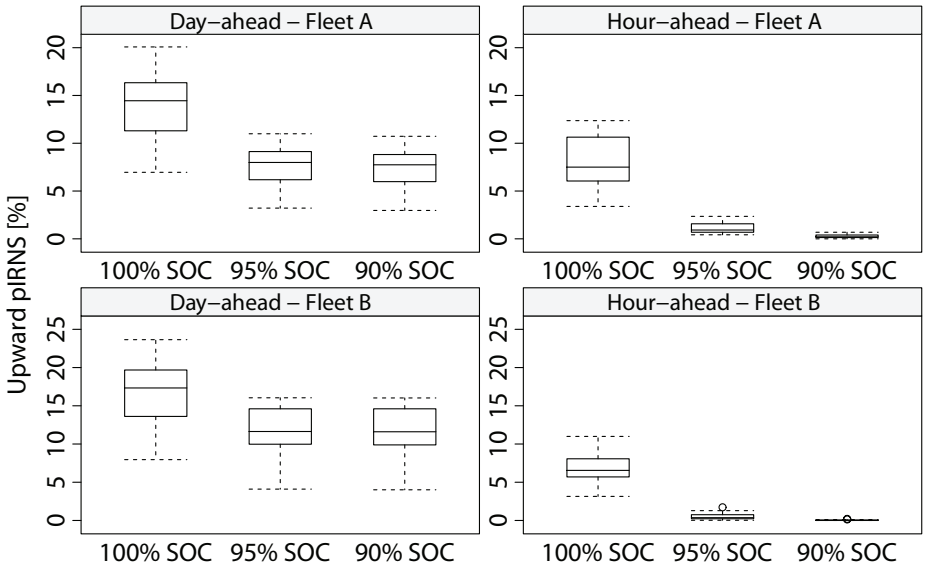

(b)

Figure 6.9: *Upward pRNS and pIRNS in fleets A and B.*

The day-ahead bids lead to a high pRNS^{up} on average in both fleets, but if a tolerance is used for the SoC, a reduction from 6% to 4% in fleet A and from 9% to 7% in fleet B is obtained. The hour-ahead bids also present intervals with pRNS^{up} (although a small average value),

and the $pRNS^{up}$ is decreased to almost zero when the SoC tolerance is used. The $pIRNS^{up}$ is also high, but it is reduced with hour-ahead bids and SoC tolerance.

These results show that hour-ahead bids combined with a degree of flexibility in the target SoC, allow the EV aggregator to supply downward and upward balancing reserve with acceptable reliability. Moreover, RNS values greater than zero result from forecast errors in the EV variables, which shows that this information cannot be neglected from an evaluation phase, since it can lead to non-marginal values of pRNS which influence the total wholesale cost of the aggregator.

Figure 6.10 presents the pRNS results for both upward and downward reserve assuming that the balancing reserve is only partially dispatched during each time interval (i.e., it is activated inside the operating interval). Note that this situation is less usual, but it can happen in some time intervals. Here, and for testing purposes, it is considered that this occurs in all time intervals and, in each interval, the dispatched reserve power is a sample taken from a uniform distribution (between 0.5 and 1) multiplied by the accepted reserve bid. Thus, it is assumed that at least 50% of the reserve power is actually dispatched (or the reserve is used during half of the time interval), but this value is different in each time interval.

The pRNS values are lower compared to Table 6.2 and Figure 6.9 (with 100% of target SoC) for both reserve directions and EV fleets. This is an expected result, since the EV aggregator is requested to supply less reserve than what was contracted, but it also shows that the optimization models are robust to this additional uncertainty (i.e., variable quantity of dispatched reserve power). Moreover, in this scenario, the $pRNS^{up}$ with hour-ahead bids is significantly improved compared to day-ahead bids, since a lower dispatched power of upward reserve has an affect similar to the SoC tolerance.

The results in this section show that, when hour-ahead bids are allowed, the TSO can have a higher reliance in the balancing reserve provided by the aggregator. With day-ahead bids, the pRNS is higher in both directions, but stills below 10% on average.

The next two subsections study the forecast errors' impact of the input variables in the total cost and pRNS values.

6.6.4 Impact of the Reserve Direction Forecast

Incorrect reserve direction forecasts require a change of the planned EV charging, which might result in higher pRNS and total cost for the aggregator. In order to understand whether or not the forecasts from the GLM represent additional value and the impact of erroneous fore-

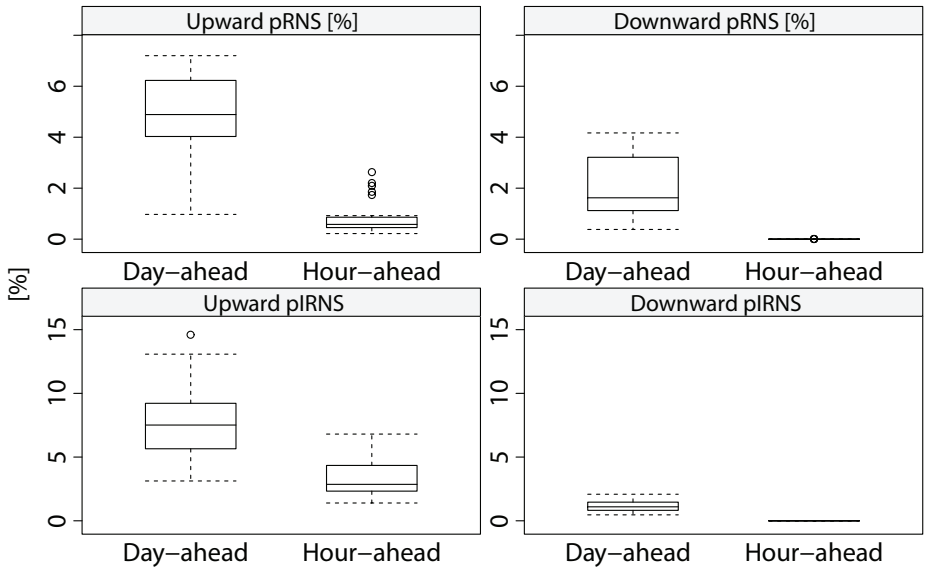

(a) *Fleet A.*

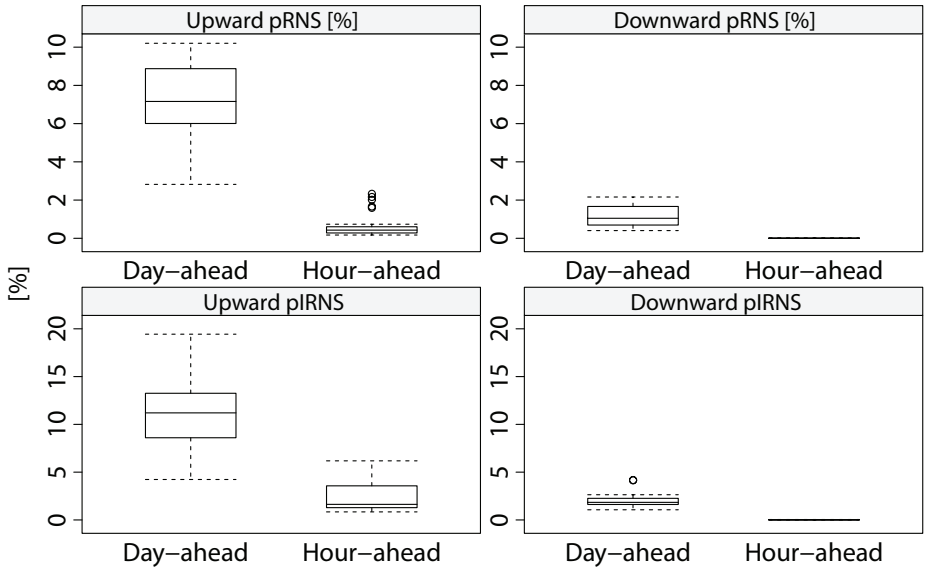

(b) *Fleet B.*

Figure 6.10: *Upward and downward pRNS and pIRNS of fleets A and B, assuming that the reserve is not fully dispatched during each time interval.*

casts in the total cost and pRNS, the reserve direction forecasts obtained with the following approaches are compared in terms of optimization results:

- *GLM forecast* (base case): forecast produced by the GLM and used in the previous sections;
- *naive predictor*: produces a forecast equal to the last observation from the same hour;
- *random predictor*: in classification problems, it is typical to compare the model's per-

formance with a random predictor (e.g., flip of a coin), and if the performance of both models is comparable, then it is concluded that the advanced model is not valuable [233]. In this case, the random predictor consists in sampling from a uniform distribution between 0 and 1; if the sample value is greater than 0.5, then $\hat{\tau}_t^- = 1$, if not, $\hat{\tau}_t^+ = 1$;

- *all upward*: the reserve direction is always upward and the aggregator offers upward reserve bids when possible;
- *all downward*: the reserve direction is always downward and the aggregator offers downward reserve bids when possible.

The forecast accuracy results of the these four algorithms can be found in appendix B.

Table 6.3 presents the average values of pRNS and cost increase (using the GLM forecast as reference) for the four different forecasts and obtained with day-ahead reserve bidding and operational management algorithm.

Table 6.3: *RNS of the upward and downward balancing reserve and total cost increase with different forecasts for the reserve direction (average [minimum,maximum]).*

(a) *Fleet A.*

	$pRNS^{up}$ [%]	$pRNS^{down}$ [%]	Cost Increase [%]
GLM forecast	4.95%	2.41%	ref.
Naive pred.	3.39%	2.88%	7.71% [-5.03%,26.88%]
Random pred.	3.17%	2.67%	37.70% [5.07%,106.07%]
All upward	4.48%	n.a.	29.95% [9.65%,65.35%]
All downward	n.a.	2.33%	39.28% [-7.18%,118%]

(b) *Fleet B.*

	$pRNS^{up}$ [%]	$pRNS^{down}$ [%]	Cost Increase [%]
GLM forecast	8.67%	3.74%	ref.
Naive pred.	7.39%	4.41%	8.01% [1.65%,16.76%]
Random pred.	8.13%	4.55%	33.35% [11.95%,73.60%]
All upward	7.58%	n.a.	35.21% [14.49%,71.11%]
All downward	n.a.	3.82%	20.28% [-7.13%,59.62%]

The pRNS results for both upward and downward reserves do not differ significantly with the reserve direction forecast, which indicates the optimization models' robustness. However, the results differ in terms of total cost increase. All four different forecasts present cost increase, compared to the results with GLM forecasts, in almost all the test samples. Only the *naive*

predictor in fleet A and the *all downward* forecast in both fleets present a negative cost increase (which means cost reduction) in some test samples, but on average, all the forecasts present a cost increase; in some test samples, the cost increase is greater than 60%. The *naive predictor* is the one that leads to the lowest cost increase.

In fleet A, the cost increase from the *random predictor* is higher than the *all upward* forecast, meaning that, in this case, a poor forecast in both directions leads to a higher cost compared to offering reserve only in one direction. The same is valid for fleet B, where the cost increase of the *all downward* forecast is lower than the one obtained by the *random predictor*.

An interesting observation is that the difference in the total cost between the different forecasts does not come from a lower income with upward reserve provision but from higher energy imbalance costs. Because of a low accuracy in forecasting the reserve direction, models, such as the *random predictor*, have a higher energy imbalances cost related to changes in the planned EV charging that must be performed when the realized reserve direction is not the same as the forecasted value. For example, if the downward reserve is not dispatched in one interval, the aggregator will need to consume this electrical energy in that interval anyway or in the subsequent intervals which creates an energy imbalance. The same is valid for upward reserve, if it is not dispatched in one hour, the aggregator has a surplus of electrical energy (compared to what was planned) and needs to reduce its consumption in this interval or in the next intervals, which also results in an energy imbalance. This leads to an increase of the aggregator's imbalance costs.

The analysis of the total cost's components for one test sample (i.e., 9 months of training dataset and 3 months of evaluation dataset) of fleet A is presented in Table 6.4a.

The *random* and *all upward* forecasts have a higher cost of consumed electrical energy, but also offer more upward reserve. Therefore, in these two cases, the income from the dispatched upward reserve is higher. Nevertheless, this high income does not result in a lower cost as in the GLM, since the imbalance costs are higher, and as shown in Table 6.4b, the ratio between dispatched and offered upward reserve is lower in these two cases. This occurs because of the lower accuracy of the *random* and *all upward* forecasts (see appendix B.4), which leads to an incorrect placement of upward and downward reserve bids in each time interval resulting in lower dispatched upward reserve and higher imbalance costs. Note that the aggregator must satisfy the driver's requirements even if reserve is not dispatched.

The *naive predictor* is characterized by a higher imbalance cost compared to the GLM forecast, as well as a higher cost with consumed electrical energy (but more upward reserve power is offered). In terms of consumed electrical energy, the higher value of 17.14 *k*€ (compared to 14.42 *k*€ of the GLM) is mitigated by a higher income from dispatched upward reserve

Table 6.4: *Total cost's components for one test sample (fleet A) with different forecasts for the reserve direction.*

(a) *Total cost's components.*

Total cost's components [k€]	GLM	Random Pred.	All Up.	All Down.	Naive Pred.
(+) Cons. Elect. Energy	14.42	17.72	21.15	8.16	17.14
(+) Down. Res. Cost	1.18	1.65	0.00	2.25	1.31
(-) Up. Res. Income	12.00	17.09	17.72	0.00	15.48
(+) Imb. Cost	3.35	11.11	4.99	7.30	6.07
(+) Res. Shortage Cost	1.32	1.12	2.13	0.36	1.16
Total Cost	8.29	14.52	10.55	18.08	10.20

(b) *Total dispatched and offered balancing reserve.*

	GLM	Random Pred.	All Up.	All Down.	Naive Pred.
Up. Res. [MW]	388	627	709	n.a.	540
Disp. Up. Res. [MWh]	248	352	371	n.a.	320
Ratio of Up. Res.	64.0%	56.2%	52.4%	n.a.	59.25%
Down. Res. [MW]	317	552	n.a.	676	399
Disp. Down. Res. [MWh]	196	268	n.a.	345	255
Ratio of Down. Res.	61.9%	48.5%	n.a.	51.08%	63.90%

(17.14-15.48=1.66 *k*€); note that, for the GLM forecast, this value is rather similar (i.e., 14.42-12.00=2.42 *k*€). The main difference is on the imbalance costs, mainly because in the upward reserve case the *naive predictor* has a lower percentage of dispatched reserve power compared to the GLM forecast, which ultimately results in higher energy imbalances.

The same is valid for the downward reserve. For instance, the *all downward* forecast leads to a higher total of downward reserve bids, but only 51.08% of this power is actually dispatched, which results in a high imbalance cost and also in a high cost with dispatched downward reserve.

As a concluding remark of this section, the presented results demonstrate that it is possible to produce forecasts for the reserve direction variable that represent additional value to the optimization problem, otherwise the cost increase values of the four forecasts would be close to zero or even negative compared to the GLM forecast. Furthermore, it should be underlined that both fleets use the same price and reserve direction forecasts, and the cost reduction results were different. This suggests that the value of the reserve direction forecast is not marginal and differs with the EV fleet characteristics and with the forecasted/realized market prices.

6.6.5 Different Quality of the EV Variables Forecasts

In this section, the optimization models' robustness is tested for charging requirement and availability forecasts with increasing error, using the same approach of section 5.6.4 in chapter 5. The standard deviations of the truncated Gaussian distribution are the same and are again presented in Table 6.5. Note that the same reserve direction forecast is used for each case.

Table 6.5: *Standard deviation values used in the truncated Gaussian distributions for the charging requirement and availability forecasts.*

Case	St. Dev. of Charg. Req. [%]	St. Dev. of Availability [half-hour]
0 (base case)	0%	0
1	20%	1
2	30%	1
3	60%	1
4	80%	1
5	10%	3
6	10%	5
7	10%	6
8	100%	8

Figure 6.11 depicts the pRNS for upward and downward balancing reserve in fleets A and B as a function of the different cases. In the upward reserve of fleet A, and similarly to the secondary reserve problem, the cases 5-8 present an increase of the pRNS^{up} value. However, for the downward reserve, the behavior is different and pRNS^{down} varies between 1% and 2% for cases 0-7, with case 8 showing a pRNS^{down} of around 4%.

Case 8 is characterized by higher amounts of offered downward and upward reserve power compared to the other cases. For instance, the total of offered downward reserve is 428 MW (in a three month evaluation dataset) in case 8, against 362 MW in case 0, and 395 MW in case 4. This higher amount could lead to more situations with reserve shortage. The difference between the base case and cases 1-4 is minor in this fleet.

In the downward reserve of fleet B, the cases 5-8 do not show increasing values of pRNS^{down} like in the case of secondary reserve. In fact, the base case presents the highest pRNS^{down}, although the pRNS^{down} values of all the cases are within 0.8% and 2.5%. In upward reserve, cases 5-8 show again an increasing value of pRNS^{up} and cases 2-4 a decreasing value compared to the base case. The main difference from cases 1-4 to the base case is a lower amount of offered upward and downward reserve, which could decrease the magnitude of the reserve

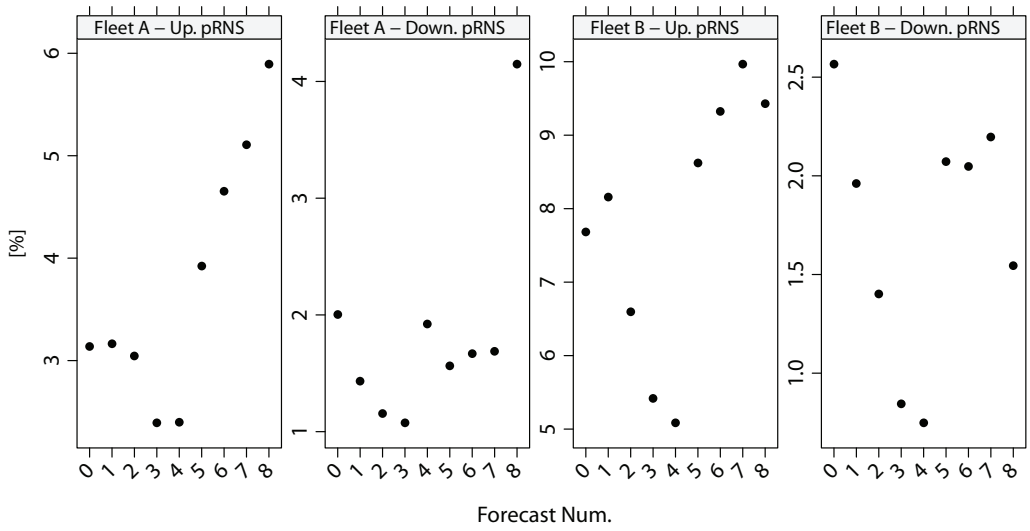

Figure 6.11: *pRNS of upward and downward balancing reserve in fleets A and B for different qualities of the charging requirement and availability forecast.*

shortage situations.

These results show that the optimization models for the balancing reserve exhibit a higher robustness to the individual forecast errors in each EV, when compared with the results obtained for secondary reserve. Moreover, this also shows that the individual forecast errors of each EV are important, since they result in different pRNS values, but are not central when aggregated, since the obtained pRNS values were of the same magnitude (even better in some cases) when the individual forecast error increases.

6.7 Final Remarks

In this section, a day-ahead optimization model and two operational management algorithms are described for supporting the participation of an EV aggregator in the energy and balancing reserve market sessions.

The operational algorithms cover two different gate closures for the balancing reserve: day-ahead and hour-ahead. The quality of the reserve provision was measured by the reserve not supplied (RNS), and the results show that an hour-ahead gate closure leads to a balancing reserve service with a percentage RNS (pRNS) lower than day-ahead bids. For instance, for upward reserve of one fleet, the day-ahead bidding leads to an average pRNS^{up} (in the 30 test samples) of around 5.5% with day-ahead bidding, while with hour-ahead is 1.5%. If the aggregator agrees with the EV driver a certain degree of tolerance to meet the target SoC (e.g.,

meeting only 90% of the target SoC), the $pRNS^{up}$ value can be improved, e.g. a reduction from 5.5% to 4% in the day-ahead bidding and a reduction from 1.5% to 0% in the hour-ahead bidding. Therefore, hour-ahead bidding, combined with a tolerance level for the SoC, can lead to reserve provision without RNS, which is desired from a TSO's viewpoint.

The analysis of the total cost results showed that an aggregator participating in the balancing reserve market could achieve a substantial reduction of its wholesale costs. For instance, in both fleets, the average cost reduction is around 20% compared to an algorithm that optimizes only energy bids, but in some test samples the cost reduction is between 25% and 45%. This cost reduction is lower compared to secondary reserve, but note that balancing reserve is not remunerated by available reserve capacity, which considerably decreases the reserve's income.

The robustness tests conducted over the algorithms showed the following conclusions:

- the market prices, the direction of dispatched balancing reserve and the EV fleet's characteristics have a high influence in the pRNS. For instance, the same forecast for the EV variables can lead to $pRNS^{up}$ ranging between 2% and 8% when the optimization models are tested in different time periods (or test samples);

- the reserve direction forecast errors do not have a high influence in the RNS values, but their influence in the total cost is significant. A poor forecast can result in a lower percentage of dispatched reserve power and in higher energy imbalance costs;

- the optimization models are robust to increasing error in the charging requirement and availability forecasts. Tests for forecasts with different accuracies showed that the pRNS value remains rather stable when the forecast accuracy decreases, and in some cases the pRNS is even lower.

Finally, although the topic of this chapter was balancing reserve, the proposed algorithms can also be adapted for other types of reserves, such as replacement reserves that are dispatched for a long period and have a predictable pattern in terms of dispatched direction.

Chapter 7

General Conclusions and Future Work

Abstract

This chapter summarizes the main contributions and findings from this thesis for the formulation of optimization models intended to support an EV aggregator participating in electricity markets. The topics for future work are also identified, covering extensions to other market sessions and possible enhancements of the optimization models formulation.

7.1 Contributions and Main Findings

7.1.1 Contributions

The first contribution from this PhD thesis is a complete framework that integrates optimization and forecasting models in each electricity market session and in the EV aggregator wholesale business activity. Within the proposed framework, optimization models were developed for the electrical energy, secondary and balancing reserve market sessions. This framework and corresponding forecasting/optimization models can be extended to aggregators of other types of flexible loads, such as thermoelectric loads.

For the participation in the day-ahead electrical energy market, two alternative formulations, called *global* (forecasts for aggregated EV variables) and *divided* (forecasts by each EV), were proposed. The main contributions from this work were a chain of models that integrates optimization and forecasting algorithms, and a comparison between the two alternative approaches for modeling the EV variables.

A day-ahead and operational management algorithms were proposed for an EV aggregator

participating in the day-ahead energy and secondary (or regulation reserve) market sessions. The main contributions were:

- formulation of a new and robust day-ahead optimization problem that takes into account the random characteristics of secondary reserve and uses forecasts for the market prices and EV variables as input;
- an operational management algorithm that coordinates the EV individual charging to meet the TSO reserve requests and redefines the operating point in order to maximize the available reserve power;
- a market settlement scheme and evaluation methodology of the total cost and reserve reliability (e.g., reserve power shortage) that can be used to compare different formulations of the optimization problem;

The participation of the EV aggregator in a balancing reserve market intended to handle imbalances between schedule and realized values (e.g., cover RES-E forecast errors) was also addressed in this thesis. The main contributions were:

- formulation of an optimization problem for day-ahead energy and balancing reserve bids, which includes forecasts for the EV variables and balancing reserve direction;
- an operational management algorithm for a market where day-ahead reserve bids are binding, and another for a market with hour-ahead reserve bids;
- a settlement scheme that includes reserve shortage costs and can be used to compare different algorithms.

Finally, another contribution is an estimation of the forecast errors impact in the optimization model's results and consequently in the total cost and reserve shortage magnitude.

7.1.2 Main Findings

The evaluation of the proposed day-ahead optimization models and operational management algorithms resulted in a set of conclusions divided by market session.

For the participation in the day-ahead electrical energy market, the following conclusions were obtained:

- the use of forecasts for aggregated EV variables (i.e., *global* approach) leads to a high deviation between the accepted energy bids and actual charging of the EV fleet, despite

its lower forecast error compared to individual forecasts mainly because it is unable to capture the temporal dynamics of the total maximum charging power. Therefore, it is recommended the use of forecasts by EV. This conclusion can be generalized for the optimization models that support the participation in the secondary and balancing reserve markets;

- an operational management algorithm that coordinates EV individual charging during the operating day is essential to minimize the difference between accepted bid and actual charging. For example, the individual forecasts are characterized by high forecast errors both in the EV availability and charging requirement, but after using the operational algorithm, the overall deviation is rather low (around 10% for the two EV fleets used as test-cases);

- the proposed optimization-based operational algorithm outperformed two heuristic algorithms from the state-of-the-art and can be extended to include secondary and balancing reserve bids.

Regarding the participation in the secondary reserve market, the following conclusions were derived:

- the proposed formulation for the day-ahead optimization problem showed a low magnitude of reserve shortage events and an interesting reduction in the total cost. Two aspects were essential for this performance: inclusion of constraints that increase the flexibility in dealing with situations where secondary reserve is not dispatched in the expected amount and direction; the operational management algorithm redefines the EV fleet operating point in order to increase the available secondary reserve power;

- forecast errors in the EV variables are a source of uncertainty, but the temporal pattern of market prices (both energy and reserve prices) is also relevant. For instance, the same EV fleet and with the same EV forecasts can obtain different values in terms of reserve shortage due to different market prices and corresponding forecasts. Note that, even with perfect price forecasts, the secondary reserve power bids are placed in different time intervals in response to different price patterns and, combined with forecast errors in the EV variables, lead to distinct reserve shortage results;

- phase errors in the EV availability forecast of each EV (i.e., departure and arrival time instants) can impact significantly the optimization results, but the proposed algorithms were found to be robust to the charging requirement forecast error of each EV;

- neglecting the forecast errors, temporal variation of the price values and EV fleets with different characteristics might lead to very optimistic results in terms of the aggregator's

cost and reserve shortage magnitude.

The following conclusions were obtained for the participation in the balancing reserve market:

- hour-ahead bids can help to improve considerably the balancing reserve reliability (i.e., results in a low reserve shortage magnitude), since it allows the use of information from recently plugged-in EV in the optimization and forecasting algorithms;
- the proposed formulation of the day-ahead optimization problem is based on the assumption that it is possible to forecast the balancing reserve direction with acceptable accuracy. The results showed that a GLM with binomial target variable is capable of obtaining a higher cost reduction compared to heuristic forecasting methods. This also shows the additional value in forecasting this variable;
- the proposed optimization models were found to be robust for different realizations of market prices and reserve direction (i.e., the tests were conducted in different time periods). Moreover, they also presented robustness to charging requirement and availability forecast errors;
- similarly to the conclusions for secondary reserve, the reserve shortage results differ with different market price patterns. Therefore, it is recommended the test and model comparison in different time periods.

The proposed framework and optimization algorithms enable the participation of EV aggregators in power system ancillary services. The results show that EV aggregators can supply reserve services with acceptable reliability and economically attractive under the current price levels (i.e., without the influence of EV).

Nevertheless, the electricity market rules and protocols should evolve with the integration of flexible loads, create conditions for a symmetric competition between supply and demand sides and take full use of the smart grid infrastructure. Based on the previous conclusions, the following recommendations are made to design future electricity markets that better accommodate EV aggregators:

- due to the stochastic nature of the EV driver's behavior, the possibility of updating the energy and reserve bids one hour before physical delivery contributes to a higher reliability of this service and promotes the participation of EV aggregators and other flexible loads in the electricity market;
- in order to enable the provision of reserve services from EV with acceptable reliability, sub-hourly secondary and balancing reserve bids should be allowed in the electricity

market in order to capture intra-hour variations (e.g., departure of several EV during one hour) of the available reserve power. This is an extension of the classical complex bids that were developed to accommodate the specific characteristics of conventional power plants;

- in order to promote a higher reliability of the reserve service, reserve markets should impose penalty prices in cases with reserve shortage, but at the same time they should take into account that an EV is a fast-responding reserve resource that offers a higher flexibility compared to other reserve resources (such as conventional power plants). The remuneration scheme that is being adopted in PJM and CAISO [77], which includes a term that penalizes reserve shortage and another that rewards fast-response time, creates incentives for the participation of EV since the reserve shortage penalty is balanced by a premium for fast-response to an AGC signal.

Note that enabling the operation of EV aggregators contributes to increasing the power system flexibility in dealing with RES-E increasing penetration, postpones investments in flexible resources that increase GHG emissions, increases market efficiency (e.g., competition and liquidity of the market) and demand elasticity.

7.2 Perspectives for Future Work

The following topics, related to the electricity market sessions, were identified for future work:

- *intraday and real-time markets*: extending the day-ahead optimization algorithms to include trading sessions between the daily market and operating hour. These trading sessions are useful to correct the bids by using updated forecasts for the EV variables and to obtain profit from price arbitrage between day-ahead and intraday/real-time trading sessions. Moreover, they can also be used to change the operating points for the secondary and balancing reserve provision;

- *bilateral contracts*: the aggregator can establish bilateral contracts with generators/loads to hedge against high market prices (i.e., mid-term planning) or to guarantee back-up support when supplying the reserve levels contracted in the market. A model can be developed to combine the participation in the spot market with bilateral contracts;

- *develop optimization models that consider a new type of AGC regulation signal*: different ISO in the USA are developing new AGC control signals in order to improve the participation of fast responding resources (e.g., flywheels, batteries) [211] [234]. The goal is to develop a regulation signal where its direction changes rapidly in order to ensure

a net energy around zero after a short period (e.g., 5 minutes). This new signal only handles fluctuations in load and generation and does not solve major perturbations in the system, such as unplanned outages of generation units. For the EV, this signal means that the net energy from the charging process will be approximately equal to the operating point, and the EV can supply upward and downward reserve power during each operating period without energy constraints related to the depth of discharge or maximum storage capacity.

The following aspects, related to the formulation of the optimization problems, were identified for future work:

- *stochastic optimization*: includes the uncertainties of the input variables in the optimization problem. It is important to underline that this task is challenging for two main reasons. Firstly, some variables, such as the dispatched secondary reserve, have a "weak" serial correlation, and thus, it is difficult to include reliable and sharp probabilistic forecasts in the optimization models. Secondly, the deviation between the bids and the total actual consumption is more important than the individual forecast errors of each EV because the operational coordination of EV charging mitigates most of these forecast errors. Therefore, in this case uncertainty modeling is complex and has a hierarchical structure (i.e., uncertainty by EV, by groups of EV and by complete EV fleet);

- *V2G mode*: the V2G mode was not considered in this thesis and requires some changes in the optimization problems formulation. For the electrical energy market, it is possible to explore price arbitrage using V2G, while for the secondary and balancing reserve markets, the possibility of injecting power as upward reserve must be included. In terms of forecasted variables, in addition to the EV availability and charging requirements, it is also necessary to forecast the SoC when the EV arrives for charging. Moreover, it is also necessary to include battery degradation costs related to bidirectional power injections;

- *non price-taker market agent*: in this thesis, the aggregator was assumed to be a price-taker. This is a reasonable assumption if there is sufficient competition in the market or if the aggregator is a small market agent. The alternative is to assume that the bids submitted by the aggregator have an impact on the market-clearing price. This alternative does not require major changes in the optimization models formulation, but in this case, it is not possible to decouple the price forecast from the buying/selling bids computed with the optimization model. Future research should consist in modeling the relation between bids value and price forecasts and include this information in the optimization models;

- *advanced forecasting algorithms for the EV variables*: developing forecasting algorithms

for the very short-term horizon (i.e., a few hours ahead) using recent information and including this information in the operational management algorithm; Moreover, the statistical forecasting models proposed in this thesis were primarily developed to supply the optimization algorithms with "real" forecasts, thus, these algorithms can be improved with new statistical algorithms, or combined with road traffic flow simulators and weather forecasts [235];

- *more detailed model for the EV battery*: in the literature it is reported that the maximum charging power decreases when the battery SoC approaches 100% [181]. It is relevant to evaluate the impact of this relation in the optimization results of a large EV fleet, which may require the development of a more detailed battery model for the optimization models.

Finally, another topic for future work is the definition of the retailing tariff value. The tariff should be established to ensure an attractive profit to the aggregator and, at the same time, capable of attracting new EV owners. This comprises different features, such as long-term optimization, marketing and consumer choice theory, which are related to the aggregator's business model.

For instance, the aggregator when defining the tariff value for a marketing campaign needs to evaluate complex relations between variables, such as how the tariff value affects its profit or the risk of losing the clients under contract. Moreover, the success of the marketing campaign also influences its ability to attract new clients. This problem demands an algorithm that performs long-term analysis/optimization based on market simulation (of both wholesale and retailing markets), modeling EV owners' reaction to tariff changes and expected retailing profit of the aggregator. In this context, the optimization models proposed in this PhD thesis give us the short-term strategy of the aggregator and the necessary input for a long-term optimization that should be developed as future work.

Bibliography

[1] *The Report of the Brundtland Commission, Our Common Future*. World Commission on Environment and Development, England: Oxford University Press, 1987.

[2] *Energy 2020. A strategy for competitive, sustainable and secure energy*, COM(2010) 639, European Commission, Brussels, November 2010. [Online]. Available: http://eur-lex.europa.eu/LexUriServ/LexUriServ.do?uri=COM:2010:0639:FIN:EN:PDF

[3] G. Brauner, W. D'Haeseleer, W. Gehrer, W. Glaunsinger, T. Krause, H. Kaul, and et al., "Electrical power vision. 2050 for Europe," Convention of National Associations of Electrical Engineers of Europe (EUREL), Brussels, Tech. Rep., February 2013. [Online]. Available: http://www.eurel.org/home/TaskForces/Documents/EUREL-PV2040-Full_Version_Web.pdf

[4] *Towards sustainable transportation. The Vancouver conference*, OECD proceedings ed., Organization for Economic Co-operation and Development (OECD), March 1996. [Online]. Available: http://www.oecd.org/greengrowth/greening-transport/2396815.pdf

[5] "EU transport in figures. Statistical pocketbook 2012," European Comission, Tech. Rep., 2012. [Online]. Available: http://ec.europa.eu/transport/facts-fundings/statistics/doc/2012/pocketbook2012.pdf

[6] M. Finley, "The oil market to 2030 - Implications for investment and policy," *Economics of Energy & Environmental Policy*, vol. 1, no. 1, pp. 25–36, 2012.

[7] "World energy outlook 2011. Executive summary," International Energy Agency, Tech. Rep., November 2011. [Online]. Available: http://www.worldenergyoutlook.org/media/weowebsite/2011/executive_summary.pdf

[8] "Directive 2009/28/EC on the promotion of the use of energy from renewable sources,"

Official Journal of the European Union, April 2009.

[9] *Clean power for transport: a European alternative fuels strategy*, COM(2013) 17, European Commission, Brussels, January 2013.

[10] R. Salter, S. Dhar, and P. Newman, "Technologies for climate change mitigation. Transport sector," UNEP Risø Centre, Tech. Rep., March 2011. [Online]. Available: http://tech-action.org/Guidebooks/TNA_Guidebook_MitigationTransport.pdf

[11] A. Schroten, H. van Essen, G. Warringa, M. Bolech, R. Smokers, and F. Fraga, "Cost effectiveness of policies and options for decarbonising transport," Task 8 paper produced as part of a contract between European Commission Directorate-General Climate Action and AEA Technology plc, Tech. Rep., February 2011. [Online]. Available: http://www.eutransportghg2050.eu/cms/assets/Uploads/Meeting-Documents/EU-Transport-GHG-2050-II-Task-8draftfinal21Nov11.pdf

[12] *Proposal for a directive of the European Parliament and of the Council on the deployment of alternative fuels infrastructure*, COM(2013) 18, European Commission, Brussels, January 2013.

[13] C. C. Chan, A. Bouscayrol, and K. Chen, "Electric, hybrid, and fuel-cell vehicles: architectures and modeling," *IEEE Transactions on Vehicular Technology*, vol. 59, no. 2, pp. 589–598, February 2010.

[14] "BP energy outlook 2030," January 2012. [Online]. Available: http://www.bp.com/liveassets/bp_internet/globalbp/STAGING/global_assets/downloads/O/2012_2030_energy_outlook_booklet.pdf

[15] T. Kerr, K. Breen, A. Gawel, P. Tepes, and et al., "Clean energy. Progress report," International Energy Agency, Tech. Rep., June 2011. [Online]. Available: http://www.cleanenergyministerial.org/Portals/2/pdfs/IEA_Clean_Energy_progress_report.pdf

[16] P. Taylor, T. Kerr, L. Fulton, J. Ward, P. Cazzola, F. Cuenot, and et al., "Technology roadmap. Electric and plug-in hybrid electric vehicles," International Energy Agency, Tech. Rep., June 2011. [Online]. Available: http://www.iea.org/publications/freepublications/publication/EV_PHEV_Roadmap.pdf

[17] T. Boßmann, W. Eichhammer, R. Elsland, S. Karcher, and M. Schäfer, "Policy report. Contribution of energy efficiency measures to climate protection within the European Union until 2050," Federal Ministry for the Environment, Nature Conservation and Nuclear Safety (BMU), Tech. Rep., June 2012. [Online]. Available: http://www.isi.

fraunhofer.de/isi-media/docs/e/de/publikationen/BMU_Policy_Paper_20121022.pdf

[18] P. Crist, "Electric vehicles revisited - costs, subsidies and prospects," May 2012, Background Paper for the 2012 Summit of the International Transport Forum, Leipzig, Germany. [Online]. Available: http://www.internationaltransportforum.org/jtrc/DiscussionPapers/DP201203.pdf

[19] R. T. Doucette and M. D. McCulloch, "Modeling the CO2 emissions from battery electric vehicles given the power generation mixes of different countries," *Energy Policy*, vol. 39, no. 2, pp. 803–811, February 2011.

[20] C. Samaras and K. Meisterling, "Life cycle assessment of greenhouse gas emissions from plug-in hybrid vehicles: Implications for policy," *Environmental Science & Technology*, vol. 42, no. 9, p. 3170–3176, April 2008.

[21] L. Göransson, S. Karlsson, and F. Johnsson, "Integration of plug-in hybrid electric vehicles in a regional wind-thermal power system," *Energy Policy*, vol. 38, no. 10, pp. 5482–5492, October 2010.

[22] F. J. Soares, "Impact of the deployment of electric vehicles in grid operation and expansion," Ph.D. dissertation, Faculdade de Engenharia, Universidade do Porto, December 2011.

[23] J. A. P. Lopes, F. Soares, and P. M. R. Almeida, "Integration of electric vehicles in the electric power system," *Proceedings of the IEEE*, vol. 99, no. 1, pp. 168–183, January 2011.

[24] A. Brooks, E. Lu, D. Reicher, C. Spirakis, and B. Weihl, "Demand dispatch," *IEEE Power and Energy Magazine*, vol. 8, no. 3, pp. 20–29, May-June 2010.

[25] V. Giordano, F. Gangale, G. Fulli, M. S. Jiménez, I. Onyeji, A. Colta, and et al., "Smart Grid projects in Europe: lessons learned and current developments," European Commission - Joint Research Centre, Tech. Rep. EUR 24856, 2011. [Online]. Available: http://ses.jrc.ec.europa.eu/sites/ses/files/documents/smart_grid_projects_in_europe_lessons_learned_and_current_developments.pdf

[26] A. Brooks and T. Gage, "Integration of electric drive vehicles with the electric power grid - a new value stream," in *Proceedings of the 18th International Electric Vehicle Symposium and Exhibition*, Berlin, Germany, October 2001.

[27] D. Raytchev and et al., "Quarterly report on European electricity markets," Market Observatory for Energy of the European Commission, Tech. Rep. Volume 1 Issue 5,

January-March 2012. [Online]. Available: http://ec.europa.eu/energy/observatory/electricity/doc/qreem_2012_quarter1.pdf

[28] D. H. Fisher, "Computing and AI for a sustainable future," *IEEE Intelligent Systems*, vol. 26, no. 6, pp. 14–18, November-December 2011.

[29] C. P. Gomes, "Computational sustainability: computational methods for a sustainable environment, economy, and society," *The Bridge - Frontiers of Engineering*, vol. 39, no. 4, pp. 5–13, 2009.

[30] N. Lima, "Comparação de estratégias de carregamento de veículos elétricos. Comparison of charging strategies for electric vehicles," Master's thesis, Faculdade de Engenharia, Universidade do Porto, September 2012. [Online]. Available: http://paginas.fe.up.pt/~ee07127/wp-content/uploads/2012/03/Dissertacao_NunoLima_ee07127.pdf

[31] B. Moselle and D. Harris, "Independent System Operators for EU energy markets," Brattle Group Newsletter, 2007. [Online]. Available: http://www.brattle.com/_documents/UploadLibrary/Newsletter30.pdf

[32] Y. G. Rebours, D. S. Kirschen, M. Trotignon, and S. Rossignol, "A survey of frequency and voltage control ancillary services - part I: technical features," *IEEE Transactions on Power Systems*, vol. 22, no. 1, pp. 350–357, February 2007.

[33] *Operational handbook. P1 – Policy 1: Load-Frequency Control and Performance*, ENTSO-E, March 2009. [Online]. Available: http://www.entsoe.eu/resources/publications/system-operations/operation-handbook/

[34] *Operational handbook. A1 – Appendix 1: Load-Frequency Control and Performance*, ENTSO-E, June 2004. [Online]. Available: http://www.entsoe.eu/resources/publications/system-operations/operation-handbook/

[35] *Harmonising the balancing market. Issues to be considered*, Nordic Energy Regulators (NordREG), May 2010. [Online]. Available: http://www.nordicenergyregulators.org/upload/Reports/NordREGreport5_2010_Balancing.pdf

[36] *Draft Network Code on Load-Frequency Control and Reserves*, ENTSO-E, January 2013 (under public consultation).

[37] H. F. Illian, "Frequency control performance measurement and requirements," Lawrence Berkeley National Laboratory, Tech. Rep. LBNL-4145E, December 2010. [Online]. Available: http://certs.lbl.gov/pdf/lbnl-4145e.pdf

[38] *Ancillary Service and Balancing Authority Area Solutions to Integrate Variable Generation*, North American Electric Reliability Corporation (NERC), March 2011. [Online]. Available: http://www.nerc.com/docs/oc/rs/NERC%20Balancing%20and%20Frequency%20Control%20040520111.pdf

[39] *NERC IVGTF Task 2.4 Report. Operating Practices, procedures and tools*, North American Electric Reliability Corporation (NERC), March 2011. [Online]. Available: http://www.nerc.com/docs/oc/rs/NERC%20Balancing%20and%20Frequency%20Control%20040520111.pdf

[40] B. J. Kirby, "Demand response for power system reliability: FAQ," Oak Ridge National Laboratory, Tech. Rep. ORNL/TM-2006/565, December 2006. [Online]. Available: http://www.consultkirby.com/files/TM_2006_565_Demand_Response_For_Power_System_Reliability_FAQ.pdf

[41] H. Holttinen, M. Milligan, E. Ela, N. Menemenlis, J. Dobschinski, B. Rawn, R. J. Bessa, D. Flynn, E. Gómez-Lázaro, and N. K. Detlefsen, "Methodologies to determine operating reserves due to increased wind power," *IEEE Transactions on Sustainable Energy*, vol. 3, no. 4, pp. 713–723, October 2012.

[42] E. Ela, M. Milligan, B. Kirby, E. Lannoye, D. Flynn, M. O'Malley, and B. Zavadil, "Evolution of operating reserve determination in wind power integration studies," in *Proceedings of the IEEE Power & Energy Society General Meeting*, Minneapolis, USA, July 2010.

[43] A. Robitaille, I. Kamwa, A. H. Oussedik, M. de Montigny, N. Menemenlis, M. Huneault, A. Forcione, R. Mailhot, J. Bourret, and L. Bernier, "Preliminary impacts of wind power integration in the Hydro-Quebec system," *Wind Engineering*, vol. 36, no. 1, pp. 35–52, February 2012.

[44] "Cross-border or reciprocal access to balancing markets," REN, REE, RTE - Action Plan for the South West Europe Electricity Regional Energy Market, Tech. Rep. Deliverable III.5, January 2008. [Online]. Available: http://www.energy-regulators.eu/portal/page/portal/EER_HOME/EER_ACTIVITIES/EER_INITIATIVES/ERI/South-West/Meetings1/IG_meetings/5supthsup%20SW%20IG/DD/SW%20ERI%20Deliverable%20III%205%20Part%20II%20-%20FINAL.pdf

[45] N. Navid, G. Rosenwald, and D. Chatterjee, "Ramp capability for load following in the MISO markets," Midwest ISO, Tech. Rep. Version No. 1.0, July 2011. [Online]. Available: https://www.midwestiso.org/Library/Repository/Communication%20Material/Key%20Presentations%20and%20Whitepapers/Ramp%20Capability%

20for%20Load%20Following%20in%20MISO%20Markets%20White%20Paper.pdf

[46] M. J. Clara, "Interconnections, congestion and market coupling. Market based provision of ancillary services," March 2010, presentation at the Market Simulation Course of the MIT Portugal Doctoral Program (FEUP).

[47] R. J. Bessa, M. A. Matos, I. C. Costa, L. Bremermann, I. G. Franchin, R. Pestana, N. Machado, H.-P. Waldl, and C. Wichmann, "Reserve setting and steady-state security assessment using wind power uncertainty forecast: a case study," *IEEE Transactions on Sustainable Energy*, vol. 3, no. 4, pp. 827–836, October 2012.

[48] *Methodologies for Determining Ancillary Service Requirements*, ERCOT, December 2011.

[49] R. S. Pindyck, "The dynamics of commodity spot and futures markets: a primer," *The Energy Journal*, vol. 22, no. 3, pp. 1–29, 2001.

[50] E. Tanlapco, J. Lawarrée, and C.-C. Liu, "Hedging with futures contracts in a deregulated electricity industry," *IEEE Transactions on Power Systems*, vol. 17, no. 3, pp. 577–582, August 2002.

[51] "Electricity market reform," House of Commons Energy and Climate Change Committee, Tech. Rep. Fourth Report of Session 2010-12, Volume I, May 2011. [Online]. Available: http://www.publications.parliament.uk/pa/cm201012/cmselect/cmenergy/742/742.pdf

[52] C. Weber, "Adequate intraday market design to enable the integration of wind energy into the European power systems," *Energy Policy*, vol. 38, no. 7, pp. 3155–3163, July 2010.

[53] E. L. Miguélez, I. E. Cortés, L. R. Rodríguez, and G. L. Camino, "An overview of ancillary services in Spain," *Electric Power Systems Research*, vol. 78, no. 3, pp. 515–523, March 2008.

[54] J. Barquín, L. Rouco, and E. Rivero, "Current designs and expected evolutions of day-ahead, intra-day and balancing market/mechanisms in Europe," OPTIMATE EU Project, Tech. Rep. D22, May 2011. [Online]. Available: http://www.optimate-platform.eu/downloads/

[55] Y. G. Rebours, D. S. Kirschen, M. Trotignon, and S. Rossignol, "A survey of frequency and voltage control ancillary services - part II: economic features," *IEEE Transactions on Power Systems*, vol. 22, no. 1, pp. 358–366, February 2007.

[56] D. J. Swider, "Efficient scoring-rule in multipart procurement auctions for power systems reserve," *IEEE Transactions on Power Systems*, vol. 22, no. 4, pp. 1717–1725, November 2007.

[57] *Manual de procedimentos do gestor do sistema*, REN, December 2008.

[58] "Boletín oficial del estado," vol.129 - Ministerio de Industria, Turismo Y Comercio, May 2009.

[59] *Italian power exchange*, Gestore Mercati Energetici (GME), November 2009. [Online]. Available: http://www.mercatoelettrico.org/En/MenuBiblioteca/documenti/20091112VademecumofIpex.pdf

[60] M. Rammerstorfer and C. Wagner, "Reforming minute reserve policy in Germany: a step towards efficient markets?" *Energy Policy*, vol. 37, no. 9, pp. 3513–3519, September 2009.

[61] L. Vandezande, L. Meeus, R. Belmans, M. Saguan, and J.-M. Glachant, "Well-functioning balancing markets: a prerequisite for wind power integration," *Energy Policy*, vol. 38, no. 7, pp. 3146–3154, July 2010.

[62] J. Rogers and K. Porter, "Wind power and electricity markets," Utility Wind Integration Group (UWIG), Tech. Rep., October 2011. [Online]. Available: http://www.uwig.org/windinmarketstableOct2011.pdf

[63] J. F. Ellison, L. S. Tesfatsion, V. W. Loose, and R. H. Byrne, "Survey of operating reserve markets in U.S. ISO/RTO-managed electric energy regions," Sandia National Laboratories, Tech. Rep. SAND2012-1000, September 2012. [Online]. Available: http://prod.sandia.gov/techlib/access-control.cgi/2012/121000.pdf

[64] A. Botterud, J. Wang, V. Miranda, and R. J. Bessa, "Wind power forecasting in U.S. electricity markets," *The Electricity Journal*, vol. 23, no. 3, pp. 71–82, April 2010.

[65] P. Wang, H. Zareipour, and W. D. Rosehart, "Characteristics of the prices of operating reserves and regulation services in competitive electricity markets," *Energy Journal*, vol. 39, no. 6, pp. 3210–3221, June 2011.

[66] G. W. Arnold, "Challenges and opportunities in Smart Grid: a position article," *Proceedings of the IEEE*, vol. 99, no. 6, pp. 922–927, June 2011.

[67] J. Torriti, M. G. Hassan, and M. Leach, "Demand response experience in Europe: policies, programmes and implementation," *Energy*, vol. 35, no. 4, pp. 1575–1583, April

2010.

[68] G. Heffner, C. Goldman, M. Kintner-Meyer, and B. Kirby, "Loads providing ancillary services: review of international experience. Technical appendix: Market descriptions," Lawrence Berkeley National Laboratory, Tech. Rep. LBNL-62701, May 2007. [Online]. Available: http://certs.lbl.gov/pdf/62701-app.pdf

[69] C. Søndergren, N. C. Bang, C. Hay, M. Togeby, and J. Østergaard, "Electric vehicles in future market models," EDISON Project, Tech. Rep. D2.3, June 2011. [Online]. Available: http://www.edison-net.dk/Dissemination/Reports.aspx

[70] J. Cochran, L. Bird, J. Heeter, and D. J. Arent, "Integrating variable renewable energy in electric power markets: best practices from international experience," National Renewable Energy Laboratory, Tech. Rep. NREL/TP-6A00-53732, April 2012. [Online]. Available: http://www.nrel.gov/docs/fy12osti/53732.pdf

[71] B. Kirby, M. O'Malley, O. Ma, P. Cappers, D. Corbus, S. Kiliccote, and et al., "Load participation in ancillary services. workshop report," U.S. Department of Energy, Tech. Rep., December 2011. [Online]. Available: http://www1.eere.energy.gov/analysis/pdfs/load_participation_in_ancillary_services_workshop_report.pdf

[72] J. W. Zarnikau, "Demand participation in the restructured Electric Reliability Council of Texas market," *Energy*, vol. 35, no. 4, pp. 1536–1543, April 2010.

[73] *PJM Manual 11: Energy & Ancillary Services Market Operations. Revision: 54*, PJM (Forward Market Operations), October 2012.

[74] P. L. Langbein, "Demand response participation in PJM wholesale markets," in *Proceedings of the 2012 IEEE PES Innovative Smart Grid Technologies (ISGT) Conference*, Washington, U.S.A., January 2012.

[75] J. H. Douglass and H. H. Shafferman, "Technical feasibility and value to the market of smaller demand-response resources providing ancillary services," ISO New England, Tech. Rep., October 2009. [Online]. Available: http://www.iso-ne.com/regulatory/ferc/filings/2009/oct/er10-___-000_10_29_09_order_719_compliance_report.pdf

[76] "2010 annual markets report," ISO New England - Internal Market Monitor, Tech. Rep., June 2011. [Online]. Available: http://www.iso-ne.com/markets/mkt_anlys_rpts/annl_mkt_rpts/2010/amr10_final_060311.pdf

[77] *Regulation Market Clearing for Performance and Mileage*, PJM (Regulation Performance Senior Task Force), August 2011. [Online].

Available: http://www.pjm.com/~/media/committees-groups/task-forces/rpstf/20110810/20110810-item-03-regulation-performance-evaluation-process.ashx

[78] *NYISO Tariffs: MST Section 15, Rate Schedules*, NYISO, November 2011.

[79] J. T. Salihi, "Energy requirements for electric cars and their impact on electric power generation and distribution systems," *IEEE Transactions on Industry Applications*, vol. IA-9, no. 5, pp. 516–532, September 1973.

[80] G. O. Murray and G. J. Ostrowski, "Powering the electric car," in *Proceedings of the 31st IEEE Vehicular Technology Conference*, vol. 31, April 1981, pp. 45–48.

[81] M. M. Collins and G. H. Mader, "The timing of EV recharging and its effect on utilities," *IEEE Transactions on Vehicular Technology*, vol. 32, no. 1, pp. 90–97, February 1983.

[82] S. Rahman and G. Shrestha, "An investigation into the impact of electric vehicle load on the electric utility distribution system," *IEEE Transactions on Power Delivery*, vol. 8, no. 2, pp. 591–597, April 1993.

[83] D. S. Callaway and I. A. Hiskens, "Achieving controllability of electric loads," *Proceedings of the IEEE*, vol. 99, no. 1, pp. 184–199, January 2011.

[84] W. Kempton and S. E. Letendre, "Electric vehicles as a new power source for electric utilities," *Transportation Research Part D-transport and Environment*, vol. 2, no. 3, pp. 157–175, September 1997.

[85] A. Brooks and S. Thesen, "PG&E and Tesla Motors: Vehicle to grid demonstration and evaluation program," in *Proceedings of the 23th International Battery, Hybrid and Fuel Cell Electric Vehicle Symposium & Exhibition (EVS23)*, Anaheim, USA, December 2007.

[86] L. P. Fernández, T. G. S. Román, R. Cossent, C. M. Domingo, and P. Frías, "Assessment of the impact of plug-in electric vehicles on distribution networks," *IEEE Transactions on Power Systems*, vol. 26, no. 1, pp. 206–213, February 2011.

[87] K. Clement-Nyns, E. Haesen, and J. Driesen, "The impact of charging plug-in hybrid electric vehicles on a residential distribution grid," *IEEE Transactions on Power Systems*, vol. 25, no. 1, pp. 371–380, February 2010.

[88] N. Hartmann and E. Özdemir, "Impact of different utilization scenarios of electric vehicles on the German grid in 2030," *Journal of Power Sources*, vol. 196, no. 4, pp. 2311–2318, February 2011.

[89] L. Bremermann, M. Rosa, M. Matos, J. A. P. Lopes, and J. Sumaili, "Operating reserve assessment incorporating a stochastic electric vehicle model," in *Proceedings of PMAPS 2012 - International Conference on Probabilistic Methods Applied to Power Systems*, Istanbul, Turkey, 2012.

[90] R. Sioshansi and P. Denholm, "Emissions impacts and benefits of plug-in hybrid electric vehicles and vehicle-to-grid services," *Environmental Science & Technology*, vol. 43, no. 4, pp. 1199–1204, February 2009.

[91] W.-P. Schill, "Electric vehicles in imperfect electricity markets: the case of Germany," *Energy Policy*, vol. 39, no. 10, pp. 6178–6189, October 2011.

[92] C. L. Moreira, "Identification and development of microgrids emergency control procedures," Ph.D. dissertation, Faculdade de Engenharia, Universidade do Porto, July 2008.

[93] P. M. R. Almeida, "Impact of vehicle to grid in the power system dynamic behaviour," Ph.D. dissertation, Faculdade de Engenharia, Universidade do Porto, November 2011. [Online]. Available: http://repositorio-aberto.up.pt/handle/10216/63462

[94] W.-P. Schill and C. Kemfert, "Modeling strategic electricity storage: the case of pumped hydro storage in Germany," *The Energy Journal*, vol. 32, no. 3, pp. 59–88, 2011.

[95] W. Kempton and T. Kubo, "Electric-drive vehicles for peak power in Japan," *Energy Policy*, vol. 28, no. 1, pp. 9–18, January 2000.

[96] W. Kempton, J. Tomic, S. Letendre, A. Brooks, and T. Lipman, "Vehicle to grid power: battery, hybrid, and fuel cell vehicles as resources for distributed electric power in California," Working Paper Series ECD-ITS-RR-01-03, UC Davis Institute for Transportation Studies, January 2001. [Online]. Available: http://escholarship.org/uc/item/5cc9g0jp

[97] W. Kempton and J. Tomic, "Vehicle-to-grid power fundamentals: calculating capacity and net revenue," *Journal of Power Sources*, vol. 144, no. 1, pp. 268–279, June 2005.

[98] B. D. Williams and K. S. Kurani, "Commercializing light-duty plug-in/plug-out hydrogen-fuel-cell vehicles: "Mobile Electricity" technologies and opportunities," *Journal of Power Sources*, vol. 166, no. 2, pp. 549–566, April 2007.

[99] S. B. Peterson, J. Whitacre, and J. Apt, "The economics of using plug-in hybrid electric vehicle battery packs for grid storage," *Journal of Power Sources*, vol. 195, no. 8, pp. 2377–2384, April 2010.

[100] S. B. Peterson, J. Apt, and J. Whitacre, "Lithium-ion battery cell degradation resulting from realistic vehicle and vehicle-to-grid utilization," *Journal of Power Sources*, vol. 195, no. 8, pp. 2385–2392, April 2010.

[101] D. Hawkins, "Vehicle to grid - a control area operators perspective," in *EVAA Electric Transportation Industry Conference*, 2001.

[102] S. L. Andersson, A. Elofsson, M. Galus, L. Göransson, S. Karlsson, F. Johnsson, and G. Andersson, "Plug-in hybrid electric vehicles as regulating power providers: case studies of Sweden and Germany," *Energy Policy*, vol. 38, no. 6, pp. 2751–2762, June 2010.

[103] W. Kempton, V. Udo, K. Huber, K. Komara, S. Letendre, S. Baker, D. Brunner, and N. Pearre, "A test of vehicle-to-grid (V2G) for energy storage and frequency regulation in the PJM system," MAGIC Consortium, Tech. Rep., January 2009. [Online]. Available: http://www.udel.edu/V2G/resources/test-v2g-in-pjm-jan09.pdf

[104] W. Kempton and J. Tomic, "Vehicle-to-grid power implementation: from stabilizing the grid to supporting large-scale renewable energy," *Journal of Power Sources*, vol. 144, no. 1, pp. 268–279, June 2005.

[105] T. Markel, M. Kuss, and P. Denholm, "Communication and control of electric vehicles supporting renewables," in *Proceedings of the 2009 IEEE Vehicle Power and Propulsion Systems Conference*, Michigan, USA, August 2009. [Online]. Available: http://www.nrel.gov/docs/fy09osti/46224.pdf

[106] C. K. Ekman, "On the synergy between large electric vehicle fleet and high wind penetration - an analysis of the Danish case," *Renewable Energy*, vol. 36, no. 2, pp. 546–553, February 2011.

[107] J. Kiviluoma and P. Meibom, "Influence of wind power, plug-in electric vehicles, and heat storages on power system investments," *Energy*, vol. 35, no. 3, pp. 1244–1255, March 2010.

[108] K. Fell, K. Huber, B. Zink, R. Kalisch, D. Forfia, D. Hazelwood, and et al., "Assessment of plug-in electric vehicle integration with ISO/RTO systems," ISO/RTO Council, Tech. Rep., March 2010. [Online]. Available: http://www.isorto.org/atf/cf/%7B5B4E85C6-7EAC-40A0-8DC3-003829518EBD%7D/IRC_Report_Assessment_of_Plug-in_Electric_Vehicle_Integration_with_ISO-RTO_Systems_03232010.pdf

[109] A. Brooks, "Vehicle-to-grid demonstration project: grid regulation ancillary service

with a battery electric vehicle," AC Propulsion Inc., Tech. Rep., December 2002. [Online]. Available: http://www.arb.ca.gov/research/apr/past/01-313.pdf

[110] C. Guille and G. Gross, "A conceptual framework for the vehicle-to-grid (V2G) implementation," *Energy Policy*, vol. 37, no. 11, pp. 4379–4390, November 2009.

[111] C. Quinn, D. Zimmerle, and T. H. Bradley, "The effect of communication architecture on the availability, reliability, and economics of plug-in hybrid electric vehicle-to-grid ancillary services," *Journal of Power Sources*, vol. 195, no. 5, pp. 1500–1509, March 2010.

[112] P. M. R. Almeida, J. A. P. Lopes, F. Soares, and M. H. Vasconcelos, "Automatic generation control operation with electric vehicles," in *Proceedings of the VIII (iREP) 2010 iREP Symposium Bulk Power System Dynamics and Control (iREP)*, Rio de Janeiro, Brazil, August 2010.

[113] J. Tomic and W. Kempton, "Using fleets of electric-drive vehicles for grid support," *Journal of Power Sources*, vol. 168, no. 2, pp. 459–468, June 2007.

[114] D. Dallinger, D. Krampe, and M. Wietschel, "Vehicle-to-grid regulation reserves based on a dynamic simulation of mobility behavior," *IEEE Transactions on Smart Grid*, vol. 2, no. 2, pp. 302–313, June 2011.

[115] T. Gómez, I. Momber, M. R. Abbad, and Álvaro Sánchez Miralles, "Regulatory framework and business models for charging plug-in electric vehicles: infrastructure, agents, and commercial relationships," *Energy Policy*, vol. 39, no. 10, pp. 6360–6375, October 2011.

[116] P. H. Andersen, J. A. Mathews, and M. Rask, "Integrating private transport into renewable energy policy: the strategy of creating intelligent recharging grids for electric vehicles," *Energy Policy*, vol. 37, no. 7, pp. 2481–2486, July 2009.

[117] "Decree law nº39/2010," Diário da Republica vol. 80 - Ministério da Economia, da Inovação e do Desenvolvimento, Ministério da Economia, da Inovação e do Desenvolvimento, pp. 1371–1386, April 2010.

[118] "Decree law nº647/2011," Boletín Oficial del Estado vol.122 - Ministerio de Industria, Turismo Y Comercio, May 2011.

[119] W. Kempton, "Aggregation server for grid-integrated vehicles," U.S. Patent 887 064, 09 21, 2010. [Online]. Available: http://appft1.uspto.gov/netacgi/nph-Parser?Sect1=PTO1&Sect2=HITOFF&d=PG01&p=

1&u=/netahtml/PTO/srchnum.html&r=1&f=G&l=50&s1=20110202192.PGNR.

[120] ——, "Electric vehicle equipment for grid-integrated vehicles," U.S. Patent 887 038, 09 21, 2010. [Online]. Available: http://appft1.uspto.gov/netacgi/nph-Parser?Sect1=PTO1&Sect2=HITOFF&d=PG01&p=1&u=/netahtml/PTO/srchnum.html&r=1&f=G&l=50&s1=20110202217.PGNR.

[121] J. R. Bryan, "An utility energy storage service provider," March 2011, presentation provided to the Rocky Mountain Clean Diesel Collaborative. [Online]. Available: http://www.epa.gov/region8/air/rmcdc/pdf/Grid_Supporting_Transportation.pdf

[122] C. Hay, M. Togeby, N. C. Bang, C. Søndergren, and L. H. Hansen, "Introducing electric vehicles into the current electricity markets," EDISON Project, Tech. Rep. D2.3, May 2010. [Online]. Available: http://www.edison-net.dk/Dissemination/Reports/Report_004.aspx

[123] W. Kempton and A. Dhanju, "Electric vehicles with V2G: storage for large-scale wind power," *Windtech International*, vol. 2, pp. 18–21, March 2006. [Online]. Available: http://www.udel.edu/V2G/docs/KemptonDhanju06-V2G-Wind.pdf

[124] B. K. Sovacool and R. F. Hirsh, "Beyond batteries: an examination of the benefits and barriers to plug-in hybrid electric vehicles (PHEVs) and a vehicle-to-grid (V2G) transition," *Energy Policy*, vol. 37, no. 3, pp. 1095–1103, March 2009.

[125] M. Hutton and T. Hutton, "Legal and regulatory impediments to vehicle-to-grid aggregation," *William & Mary Environmental Law and Policy Review*, vol. 36, no. 2, pp. 337–365, 2012.

[126] H. Bludszuweit and J. A. Domínguez-Navarro, "A probabilistic method for energy storage sizing based on wind power forecast uncertainty," *IEEE Transactions on Power Systems*, vol. 26, no. 3, pp. 1651–1658, August 2011.

[127] *Electric vehicle conductive charging system - Part 1: General requirements*, International Electrotechnical Commission Std. 61 851-1, 2010.

[128] *Guide to Electric Vehicle Infrastructure*, British Electrotechnical and Allied Manufacturers Association (BEAMA), May 2012.

[129] L. Dickerman and J. Harrison, "A new car, a new grid," *IEEE Power and Energy Magazine*, vol. 8, no. 2, pp. 55–61, March-April 2010.

[130] T. Theisen, R. Marques, J. Bagemihl, L. Bartsoen, S. Becker, G. Bernard,

and et al., “Facilitating e-mobility: EURELECTRIC views on charging infrastructure,” EURELECTRIC, Tech. Rep. D/2012/12.105/14, March 2012. [Online]. Available: http://www.eurelectric.org/media/27060/0322_facilitating_emobility_eurelectric_views_-_final-2012-030-0291-01-e.pdf

[131] *Electric Vehicles: Issues for the European Engineering Industries*, ORGALIME, February 2010. [Online]. Available: http://www.orgalime.org/Pdf/PP_electric_vehicles_Feb10.pdf

[132] *Standard-compliant charging controller for electric vehicle charging infrastructure*, Siemens AG, October 2011. [Online]. Available: http://www.automation.siemens.com/mcms/infocenter/dokumentencenter/ce/Documentsu20Brochures/6zb5131-0at02-0aa0.pdf

[133] C. Ricaud and P. Vollet, *Connection method for charging systems - a key element for electric vehicles*, Schneider Electric, 2010. [Online]. Available: http://www.schneider-electric.co.uk/documents/electrical-distribution/en/local/ev/Connection-method-for-charging-systems.pdf

[134] S. Bending, M. Ferdowsi, S. Channon, K. Strunz, E. Bower, A. Walsh, and et al., “Specifications for EV-grid interfacing, communication and smart metering technologies, including traffic patterns and human behavior descriptions,” MERGE EU Project, Tech. Rep. D1.1, August 2010. [Online]. Available: http://www.ev-merge.eu/

[135] D. P. Tuttle and R. Baldick, “The evolution of plug-in electric vehicle-grid interactions,” *IEEE Transactions on Smart Grid*, vol. 3, no. 1, pp. 500–505, March 2012.

[136] W. Su, H. Rahimi-Eichi, W. Zeng, and M.-Y. Chow, “A survey on the electrification of transportation in a smart grid environment,” *IEEE Transactions on Industrial Informatics*, vol. 8, no. 1, pp. 1–10, February 2012.

[137] V. C. Güngör, D. Sahin, T. Kocak, S. Ergüt, C. Buccella, C. Cecati, and G. P. Hancke, “Smart Grid technologies: communication technologies and standards,” *IEEE Transactions on Industrial Informatics*, vol. 7, no. 4, pp. 529–539, November 2011.

[138] S. Käbisch, A. Schmitt, M. Winter, and J. Heuer, “Interconnections and communications of electric vehicles and smart grids,” in *Proceedings of the First IEEE International Conference on Smart Grid Communications (SmartGridComm)*, Gaithersburg, USA, October 2010.

[139] D. Gantenbein, B. Jansen, D. Dykeman, P. B. Andersen, E. B. Hauksson, F. Marra, and

et al., "Distributed integration technology development," EDISON Project, Tech. Rep. D3.1, April 2011. [Online]. Available: http://www.edison-net.dk/Dissemination/Reports/D3.1.aspx

[140] E. Sortomme, M. M. Hindi, S. D. J. MacPherson, and S. S. Venkata, "Coordinated charging of plug-in hybrid electric vehicles to minimize distribution system losses," *IEEE Transactions on Smart Grid*, vol. 2, no. 1, pp. 186–193, March 2011.

[141] P. Richardson, D. Flynn, and A. Keane, "Optimal charging of electric vehicles in low-voltage distribution systems," *IEEE Transactions on Power Systems*, vol. 27, no. 1, pp. 268–279, February 2012.

[142] T. K. Kristoffersen, K. Capion, and P. Meibom, "Optimal charging of electric drive vehicles in a market environment," *Applied Energy*, vol. 88, no. 5, pp. 1940–1948, May 2011.

[143] S. Bashash, S. J. Moura, and H. K. Fathy, "On the aggregate grid load imposed by battery health-conscious charging of plug-in hybrid electric vehicles," *Journal of Power Sources*, vol. 196, no. 20, pp. 8747–8754, October 2011.

[144] S. Bashash, S. J. Moura, J. C. Forman, and H. K. Fathy, "Plug-in hybrid electric vehicle charge pattern optimization for energy cost and battery longevity," *Journal of Power Sources*, vol. 196, no. 1, pp. 541–549, January 2011.

[145] K. Deb, A. Pratap, S. Agarwal, and T. Meyarivan, "A fast and elitist multiobjective genetic algorithm: NSGA-II," *IEEE Transactions on Evolutionary Computation*, vol. 6, no. 2, pp. 182–197, April 2002.

[146] P. Sánchez-Martín, G. Sánchez, and G. Morales-España, "Direct load control decision model for aggregated EV charging points," *IEEE Transactions on Power Systems*, vol. 27, no. 3, pp. 1577–1584, August 2012.

[147] O. Sundström and C. Binding, "Charging service elements for an electric vehicle charging service provider," in *Proceedings of the IEEE Power and Energy Society (PES) General Meeting*, July 2011, pp. Detroit, USA.

[148] N. Rotering and M. Ilic, "Optimal charge control of plug-in hybrid electric vehicles in deregulated electricity markets," *IEEE Transactions on Power Systems*, vol. 26, no. 3, pp. 1021–1029, August 2011.

[149] S. Han, S. Han, and K. Sezaki, "Development of an optimal vehicle-to-grid aggregator for frequency regulation," *IEEE Transactions on Smart Grid*, vol. 1, no. 1, pp. 65–72,

June 2011.

[150] *Storage Participation in ERCOT*, Prepared by the Texas Energy Storage Alliance, January 2010. [Online]. Available: http://goodcompanyassociates.com/files/manager/ERCOT_Storage_Issues_Whitepaper-2-15-11.pdf

[151] J. J. Escudero-Garzás, A. García-Armada, and G. Seco-Granados, "Fair design of plug-in electric vehicles aggregator for V2G regulation," *IEEE Transactions on Vehicular Technology*, vol. 61, no. 8, pp. 3406–3419, October 2012.

[152] W. Yu, W. Rhee, S. Boyd, and J. M. Cioffi, "Iterative water-filling for Gaussian vector multiple-access channels," *IEEE Transactions on Information Theory*, vol. 50, no. 1, pp. 145–152, January 2004.

[153] E. Sortomme and M. El-Sharkawi, "Optimal charging strategies for unidirectional vehicle-to-grid," *IEEE Transactions on Smart Grid*, vol. 2, no. 1, pp. 131–138, March 2011.

[154] E. Sortomme and M. A. El-Sharkawi, "Optimal combined bidding of vehicle-to-grid ancillary services," *IEEE Transactions on Smart Grid*, vol. 3, no. 1, pp. 70–79, March 2012.

[155] ——, "Optimal combined bidding of vehicle-to-grid ancillary services," *IEEE Transactions on Power Systems*, vol. 3, no. 1, pp. 351–359, March 2012.

[156] C. Wu, H. Mohsenian-Rad, and J. Huang, "Vehicle-to-aggregator interaction game," *IEEE Transactions on Smart Grid*, vol. 3, no. 1, pp. 434–442, March 2012.

[157] S. Han, S. Han, and K. Sezaki, "Estimation of achievable power capacity from plug-in electric vehicles for V2G frequency regulation: case studies for market participation," *IEEE Transactions on Smart Grid*, vol. 2, no. 4, pp. 632–641, December 2011.

[158] M. Pantos, "Exploitation of electric-drive vehicles in electricity markets," *IEEE Transactions on Power Systems*, vol. 27, no. 2, pp. 682–694, May 2012.

[159] H. P. Hong, "An efficient point estimate method for probabilistic analysis," *Reliability Engineering & System Safety*, vol. 59, no. 3, pp. 261–267, March 1998.

[160] Y. Cao, S. Tang, C. Li, P. Zhang, Y. Tan, Z. Zhang, and J. Li, "An optimized ev charging model considering TOU price and SOC curve," *IEEE Transactions on Smart Grid*, vol. 3, no. 1, pp. 388–393, March 2012.

[161] W. Su and M.-Y. Chow, "Performance evaluation of an EDA-based large-scale plug-in hybrid electric vehicle charging algorithm," *IEEE Transactions on Smart Grid*, vol. 3, no. 1, pp. 308–315, March 2012.

[162] P. Larrañaga and J. A. Lozano, *Estimation of Distribution Algorithms: A New Tool for Evolutionary Computation*. Boston: Kluwer Academic, 2002.

[163] P. Kulshrestha, "An intelligent energy management system for charging of plug-in hybrid electric vehicles at a municipal parking deck," Master's thesis, Faculty of North Carolina State University, Raleigh, North Carolina, June 2009.

[164] F. A. Amoroso and G. Cappuccino, "Impact of charging efficiency variations on the effectiveness of variable-rate-based charging strategies for electric vehicles," *Journal of Power Sources*, vol. 196, no. 22, pp. 9574–9578, November 2011.

[165] D. Wu, D. C. Aliprantis, and L. Ying, "Load scheduling and dispatch for aggregators of plug-in electric vehicles," *IEEE Transactions on Smart Grid*, vol. 3, no. 1, pp. 368–376, March 2012.

[166] S. Bashash and H. K. Fathy, "Transport-based load modeling and sliding mode control of plug-in electric vehicles for robust renewable power tracking," *IEEE Transactions on Smart Grid*, vol. 3, no. 1, pp. 526–534, March 2012.

[167] D. S. Callaway, "Tapping the energy storage potential in electric loads to deliver load following and regulation, with application to wind energy," *Energy Conversion and Management*, vol. 50, no. 5, pp. 1389–1400, May 2009.

[168] V. Utkin, "Variable structure systems with sliding modes," *IEEE Transactions on Automatic Control*, vol. 22, no. 2, pp. 212–222, April 1977.

[169] M. D. Galus and G. Andersson, "Integration of plug-in hybrid electric vehicles into energy networks," in *Proceedings of the 2009 IEEE Bucharest Power Tech*, Bucharest, Romania, June/July 2009.

[170] M. Fahrioglu and F. L. Alvarado, "Designing incentive compatible contracts for effective demand management," *IEEE Transactions on Power Systems*, vol. 15, no. 4, pp. 1255–1260, November 2000.

[171] O. Sundström and C. Binding, "Flexible charging optimization for electric vehicles considering distribution grid constraints," *IEEE Transactions on Smart Grid*, vol. 3, no. 1, pp. 26–37, March 2012.

[172] N. O'Connell, Q. Wu, J. Østergaard, A. H. Nielsen, S. T. Cha, and Y. Ding, "Electric vehicle (EV) charging management with dynamic distribution system tariff," in *Proceedings of the 2nd IEEE PES International Conference and Exhibition on Innovative Smart Grid Technologies (ISGT Europe)*, Manchester, U.K., December 2011.

[173] S. Bae and A. Kwasinski, "Spatial and temporal model of electric vehicle charging demand," *IEEE Transactions on Smart Grid*, vol. 3, no. 1, pp. 394–403, March 2012.

[174] A. Ashtari, E. Bibeau, S. Shahidinejad, and T. Molinski, "PEV charging profile prediction and analysis based on vehicle usage data," *IEEE Transactions on Smart Grid*, vol. 3, no. 1, pp. 341–350, March 2012.

[175] A. Aabrandt, P. B. Andersen, A. B. Pedersen, S. You, B. Poulsen, N. O'Connell, and J. Østergaard, "Prediction and optimization methods for electric vehicle charging schedules in the EDISON project," in *Proceedings of the 2012 IEEE PES Innovative Smart Grid Technologies*, Washington, USA, January 2012.

[176] O. Sundström, O. Corradi, and C. Binding, "Toward electric vehicle trip prediction for a charging service provider," in *Proceedings of the 2012 IEEE International Electric Vehicle Conference (IEVC)*, Greenville, USA, March 2012.

[177] Y. Foucher, E. Mathieu, P. Saint-Pierre, J.-F. Durand, and J.-P. Daurès, "A semi-Markov model based on generalized Weibull distribution with an illustration for HIV disease," *Biometrical Journal*, vol. 47, no. 6, pp. 825–833, December 2005.

[178] A. Khotanzad, E. Zhou, and H. Elragal, "A neuro-fuzzy approach to short-term load forecasting in a price-sensitive environment," *IEEE Transactions on Power Systems*, vol. 17, no. 4, pp. 1273–1282, November 2002.

[179] O. Corradi, H. Ochsenfeld, H. Madsen, and P. Pinson, "Controlling electricity consumption by forecasting its response to varying prices," *IEEE Transactions on Power Systems*, vol. 28, no. 1, pp. 421–429, February 2013.

[180] O. Sundström and C. Binding, "Optimization methods to plan the charging of electric vehicle fleets," in *Proceedings of the International Conference on Control, Communication and Power Engineering (CCPE 2010)*, Chennai, India, July 2010, pp. 323–328.

[181] F. Marra, G. Y. Yang, C. Træholt, E. Larsen, C. N. Rasmussen, and S. You, "Demand profile study of battery electric vehicle under different charging options," in *Proceedings of the 2012 IEEE Power & Energy Society General Meeting*, San Diego, USA, July 2012.

[182] P. B. Andersen, R. Garcia-Valle, and W. Kempton, "A comparison of electric vehicle

integration projects," in *Proceedings of the 2011 IEEE Trondheim Power Tech*, Trondheim, Norway, June 2011.

[183] C. L. Moreira, D. Rua, E. Karfopoulos, E. Zountouridou, F. J. Soares, I. Bourithi, and et al., "Extended concepts of MG by identifying several EV smart control approaches to be embedded in the smart grid concept to manage ev individually or in clusters," MERGE EU Project, Tech. Rep. D1.2, June 2010. [Online]. Available: http://www.ev-merge.eu/

[184] C. Binding, D. Gantenbein, B. J. O. Sundstrom, P. B. Andersen, F. Marra, B. Poulsen, and C. Træholt, "Electric vehicle fleet integration in the Danish EDISON project - a virtual power plant on the island of Bornholm," in *Proceedings of the 2010 IEEE Power and Energy Society General Meeting*, Minneapolis, USA, July 2010.

[185] *Making the Connection. The Plug-In Vehicle Infrastructure Strategy*, Office for Low Emission Vehicles, June 2011. [Online]. Available: http://assets.dft.gov.uk/publications/making-the-connection-the-plug-in-vehicle-infrastructure-strategy/plug-in-vehicle-infrastructure-strategy.pdf

[186] S. Shah and S. M. Shahidehpour, "A heuristic approach to load shedding scheme," *IEEE Transactions on Power Systems*, vol. 4, no. 4, pp. 1421–1429, November 1989.

[187] R. Sioshansi and D. Hurlbut, "Market protocols in ERCOT and their effect on wind generation," *Energy Policy*, vol. 38, no. 7, pp. 3192–3197, July 2010.

[188] D. Rua, D. Issicaba, F. J. Soares, P. M. R. Almeida, R. J. Rei, and J. A. P. Lopes, "Advanced metering infrastructure functionalities for electric mobility," in *Proceedings of the 2010 IEEE PES Innovative Smart Grid Technologies Conference Europe (ISGT Europe)*, Gothenburg, Sweden, October 2010.

[189] A. Botterud, J. Wang, Z. Zhou, R. Bessa, H. Keko, J. Akilimali, and V. Miranda, "Wind power trading under uncertainty in LMP markets," *IEEE Transactions on Power Systems*, vol. 27, no. 2, pp. 894–903, May 2012.

[190] Álvaro Baíllo, S. Cerisola, J. M. Fernández-López, and R. Bellido, "Strategic bidding in electricity spot markets under uncertainty: a roadmap," in *Proceedings of the IEEE Power Engineering Society General Meeting*, Montreal, Canada, June 2006.

[191] S. Makridakis, S. Wheelwright, and R. Hyndman, *Forecasting: Methods and Applications*. New York: John Wiley and Sons, 1997.

[192] F. Soares, J. A. P. Lopes, P. Almeida, C. Moreira, and L. Seca, "A stochastic model to

simulate electric vehicles motion and quantify the energy required from the grid," in *Proceedings of the 17th Power Systems Computation Conference (PSCC) Conference*, Stockholm, Sweden, August 2011.

[193] M. Davidian and D. Giltinan, *Nonlinear Mixed Effects Models for Repeated Measurement Data*. London: Chapman and Hall, 1995.

[194] J. Pinheiro, D. Bates, S. DebRoy, and D. Sarkar, *nlme: Linear and Nonlinear Mixed Effects Models.*, R Package Version 3.1-102, 2011.

[195] H. Madsen, *Time Series Analysis*. London: Chapman and Hall/CRC, 2007.

[196] D. Kwiatkowski, P. C. Phillips, P. Schmidt, and Y. Shin, "Testing the null hypothesis of stationarity against the alternative of a unit root," *Journal of Econometrics*, vol. 54, no. 1-3, pp. 159–178, October-December 1992.

[197] M. Stone, "An asymptotic equivalence of choice of model by cross-validation and Akaike's criterion," *Journal of the Royal Statistical Society: Series B (Methodological)*, vol. 39, no. 1, pp. 44–47, 1977.

[198] T. Hastie and R. Tibshirani, *Generalized additive models*. London: Chapman & Hall/CRC, 1990.

[199] S. Wood, *Generalized Additive Models: an introduction with R*. London: Chapman and Hall/CRC, 2006.

[200] T. Jónsson, P. Pinson, and H. Madsen, "On the market impact of wind energy forecasts," *Energy Economics*, vol. 32, no. 2, pp. 313–320, March 2010.

[201] Y. Ji, J. Hao, N. Reyhani, and A. Lendasse, "Direct and recursive prediction of time series using mutual information selections," *Lecture Notes in Computer Science*, vol. 3512, pp. 1010–1017., 2005.

[202] T. R. Willemain, C. N. Smart, and H. F. Schwarz, "A new approach to forecasting intermittent demand for service parts inventories," *International Journal of Forecasting*, vol. 20, no. 3, pp. 375–387, July-September 2004.

[203] P. McCullagh and J. Nelder, *Generalized Linear Models*. London: Chapman & Hall/CRC, 1989.

[204] A. Gelman, Y. Su, M. Yajima, J. Hill, M. Pittau, J. Kerman, and T. Zheng, *rm: data analysis using regression and multilevel/hierarchical models*, R package version 1.4-13,

2011.

[205] B. Efron and R. Tibshirani, *An Introduction to the Bootstrap*. London: Chapman & Hall/CRC, 1994.

[206] P. Pinson, C. Chevallier, and G. Kariniotakis, "Trading wind generation with short-term probabilistic forecasts of wind power," *IEEE Transactions on Power Systems*, vol. 22, no. 3, pp. 148–1156, August 2007.

[207] S. Boyd and L. Vandenberghe, *Convex Optimization*. Cambridge: Cambridge University Press, 2004.

[208] "Inquérito à mobilidade da população residente (Questionnaire about the portuguese population mobility)," INE (Instituto Nacional de Estatística), Tech. Rep., 2000.

[209] M. Herrera, L. Torgo, J. Izquierdo, and R. Pérez-García, "Predictive models for forecasting hourly urban water demand," *Journal of Hydrology*, vol. 387, no. 1-2, pp. 141–150, June 2010.

[210] *ILOG CPLEX V12.2: User's Manual for CPLEX*, IBM, May 2010.

[211] *Demand Side Response in the Ancillary Service Markets*, PJM State & Member Training Department, October 2012. [Online]. Available: http://www.pjm.com/~/media/training/core-curriculum/ip-dsr/dsr-in-the-ancillary-service-markets.ashx

[212] *Operational handbook. A2 – Appendix 2: Scheduling and Accounting*, ENTSO-E, June 2004. [Online]. Available: http://www.entsoe.eu/resources/publications/system-operations/operation-handbook/

[213] C. Croarkin, W. Guthrie, and et al., *e-Handbook of Statistical Methods*. NIST/SEMATECH, April 2012. [Online]. Available: http://www.itl.nist.gov/div898/handbook/

[214] R. J. Hyndman, S. Razbash, and D. Schmidt, *forecast: Forecasting functions for time series and linear models*, R package version 3.19, 2012.

[215] T. Hanzák, "Holt-Winters method with general seasonality," *Kybernetika*, vol. 48, no. 1, pp. 1–15, 2012.

[216] R. H. Byrdand, P. Lu, J. Nocedal, and C. Zhu, "A limited memory algorithm for bound constrained optimization," *SIAM Journal on Scientific Computing*, vol. 16, no. 5, pp. 1190–1208, September 1995.

[217] *Limit Definitions for Real Time Operations*, ERCOT, 2010. [Online]. Available: http://nodal.ercot.com/about/index.html

[218] K. Agnew, R. Burke, and P. Ham-Su, "Participation of demand response resources in ISO New England's ancillary service markets," in *Proceedings of the International Energy Program Evaluation Conference (IEPEC)*, Chicago, USA, 2007.

[219] *IBM ILOG CPLEX Optimization Studio V12.5*, IBM, November 2012.

[220] R. G. de Almeida, E. D. Castronuovo, and J. A. P. Lopes, "Optimum generation control in wind parks when carrying out system operator requests," *IEEE Transactions on Power Systems*, vol. 21, no. 2, pp. 718–725, May 2006.

[221] R. Bessa, C. Moreira, B. Silva, and M. Matos, "Handling renewable energy variability and uncertainty in power systems operation," *Wiley Interdisciplinary Reviews: Energy and Environment*, 2013, in press (doi: 10.1002/wene.76).

[222] *Operational reserve ad-hoc team report*, ENTSO-E, May 2012.

[223] "Harmonisation of balance regulation in the Nordic countries," Nordel, Tech. Rep., December 2008.

[224] E. Hirst, "Integrating wind output with bulk power operations and wholesale electricity markets," *Wind Energy*, vol. 5, no. 1, pp. 19–36, January/March 2002.

[225] M. A. Matos and R. J. Bessa, "Setting the operating reserve using probabilistic wind power forecasts," *IEEE Transactions on Power Systems*, vol. 26, no. 2, pp. 594–603, May 2011.

[226] H. Herzel and I. Große, "Measuring correlations in symbol sequences," *Physica A: Statistical Mechanics and its Applications*, vol. 216, no. 4, pp. 518–542, July 1995.

[227] R. Bessa and M. Matos, "Forecasting issues for managing a portfolio of electric vehicles under a smart grid paradigm," in *Proceedings of the third IEEE PES Innovative Smart Grid Technologies Conference (ISGT 2012)*, Berlin, Germany, October 2012.

[228] T. Jónsson, "Forecasting of electricity prices accounting for wind power predictions," Master's thesis, Technical University of Denmark, Lyngby, Denmark, May 2008. [Online]. Available: http://pierrepinson.com/docs/Thesis_TryggviJonsson.pdf

[229] M. Kuhn, "Building predictive models in R using the caret package," *Journal of Statistical Software*, vol. 28, no. 5, pp. 1–26, November 2008.

[230] ——, "Variable selection using the caret package," Pfizer Global R&D, Tech. Rep., October 2012. [Online]. Available: http://cran.open-source-solution.org/web/packages/caret/vignettes/caretSelection.pdf

[231] T. Hastie, R. Tibshirani, and J. Friedman, *The Elements of Statistical Learning: Data Mining, Inference, and Prediction. 2nd edition*. New York: Springer-Verlag, 2008.

[232] J. Bushnell, B. F. Hobbs, and F. A. Wolak, "When it comes to demand response, is FERC its own worst enemy?" *The Electricity Journal*, vol. 22, no. 8, pp. 9–18, October 2009.

[233] T. Fawcett, "An introduction to ROC analysis," *Pattern Recognition Letters*, vol. 27, no. 8, pp. 861–874, June 2006.

[234] J. Hickey, "Limited energy storage resource (LESR) market integration update," in *Market Issues working Group*, November 2008.

[235] M. Kilpeläinen and H. Summala, "Effects of weather and weather forecasts on driver behaviour," *Transportation Research Part F: Traffic Psychology and Behaviour*, vol. 10, no. 4, pp. 288–299, July 2007.

[236] M. Gilliland, "Is forecasting a waste of time?" *Supply Chain Management Review*, vol. 6, pp. 16–23, 2002.

[237] M. Sokolova and G. Lapalme, "A systematic analysis of performance measures for classification tasks," *Information Processing & Management*, vol. 45, no. 4, pp. 427–437, July 2009.

Appendix A

Statistical Analyses of the Test Case Data

This appendix section presents statistical analyses of the synthetic EV time series and market data used in the test case. Two fleets with 1500 EV are analyzed by individual EV and aggregated time series. The energy and reserve (tertiary and secondary) prices from Portugal (Iberian electricity market) are also analyzed for a three year period (2009-2011).

A.1 Synthetic EV Time Series

Three different types of drivers' behavior can be found in the EV synthetic time series: (type 0) charge after the last trip of the day; (type 1) charge when parked; (type 2) charge when the battery SoC is below 40%.

A.1.1 Individual EV

Figure A.1 depicts the percentage of times, of each daily time interval (in half-hours), when the EV is plugged-in. Each line in the plot corresponds to one EV from fleet A and the availability pattern is divided by driver's type. Only the values for fleet A are depicted since the patterns of EV from fleet B are similar.

The type 0 drivers are normally plugged-in between the 36^{th} and 14^{th} intervals (i.e., between 18h00 and 7h00), however the spread between the curves is particularly high during the night, which indicates a very different behavior of these drivers. The type 1 drivers are plugged-in during the night and day-time and the patterns are more concentrated, but some EV show a distinct behavior. The type 2 drivers are less available during the whole day since

they only charge if the battery SoC is below 40%. These drivers show a preference for night charging and the spread between patterns is significant.

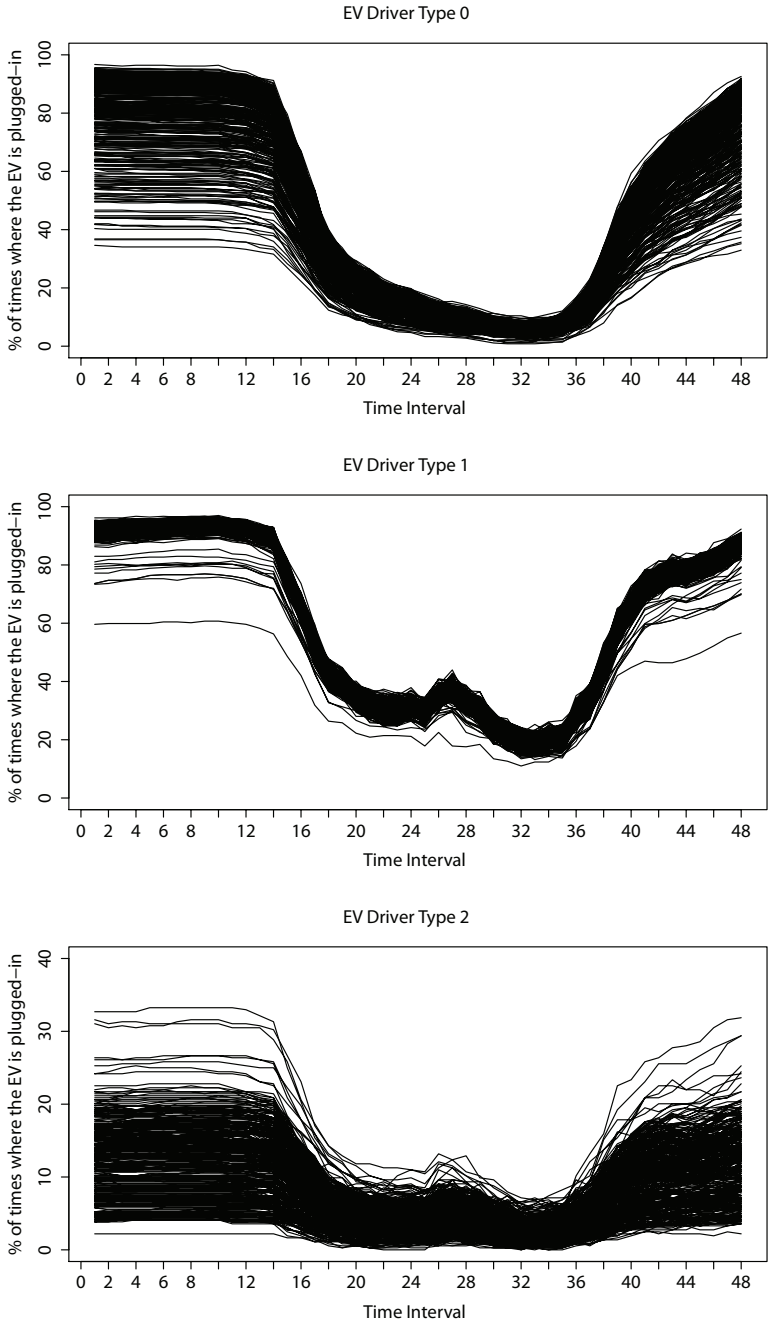

Figure A.1: *Availability daily pattern of each EV from fleet A divided by driver type.*

Figure A.2 depicts the frequency (counts) of arrivals and departures in each time interval from three EV (one from each driver's type) of fleet A. Consistent with the defined driver's behavior, the driver of type 0 frequently arrives by the end of the day for charging and departs before work schedule. A driver from type 1, in addition to a behavior similar to type 0, also arrives and departs from charging during day-time, with a peak at lunch time. The behavior of type

2 drivers is more erratic since the drivers charge when the battery SoC is below 40%.

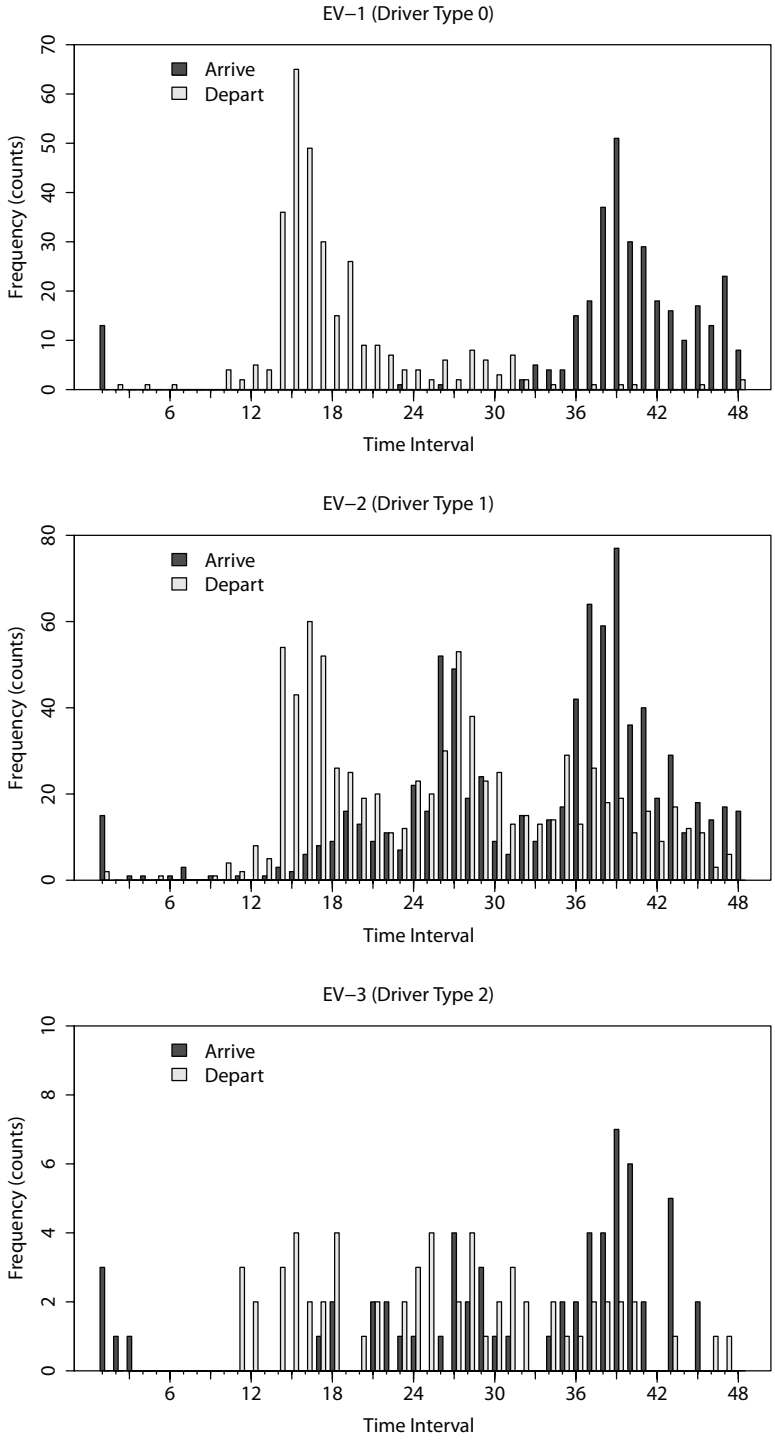

Figure A.2: *Frequency of arrivals and departures in each time intervals from three EV (one from a different driver type) from fleet A.*

Figure A.3 presents boxplots summarizing the distribution of the average and maximum plugged-in time of the 1500 EV from fleet A during one year. Figure A.4 depicts the results for fleet B. In both fleets, the types 0 and 1 drivers are plugged-in on average between

10 and 15 half-hours (i.e., 5 and 7.5 hours), while type 2 drivers are plugged-in between 25 and 30 half-hours (i.e., 12.5 and 15 hours). Regarding the maximum time, in both fleets there is a wide variation in each type and in some extremes cases the EV is plugged-in during more than two days.

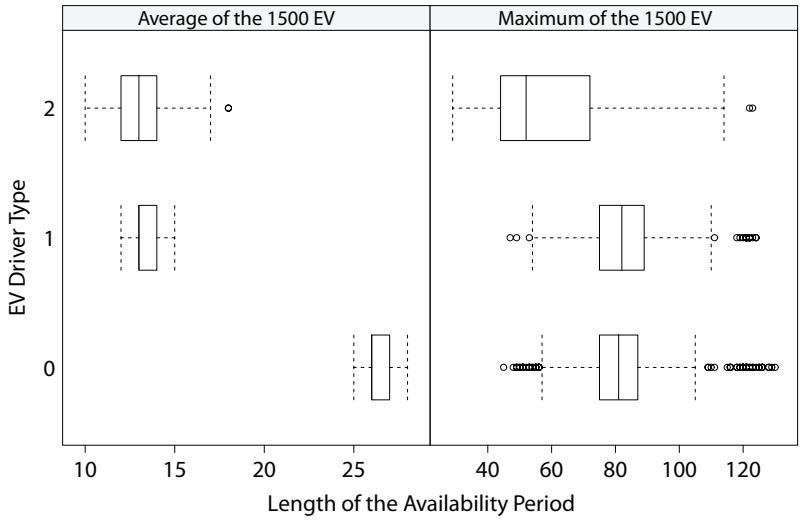

Figure A.3: *Boxplots summarizing the average and maximum plugged-in time (or duration of the availability period) of fleet A during one year.*

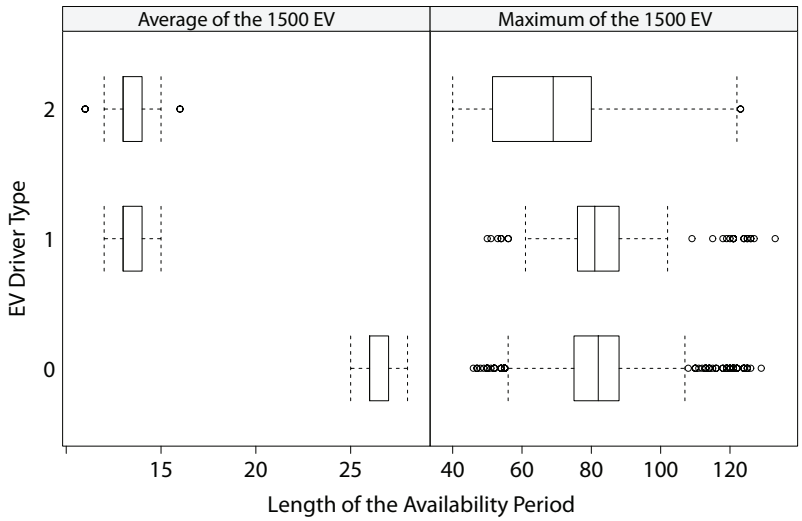

Figure A.4: *Boxplots summarizing the average and maximum plugged-in time (or duration of the availability period) of fleet B during one year.*

Figures A.5 and A.6 present boxplots summarizing the distribution of the average initial and target SoC of fleets A and B correspondingly, during one year. In the drivers of types 0 and 1, the two fleets present different values; the EV from fleet A has a higher initial and target SoC on average. It is also important to stress that target SoC is not always 100% and the type 2 drivers show a wide variation of the target SoC. Moreover, since type 1 drivers charge during the day, their initial SoC is higher compared to types 0 and 2.

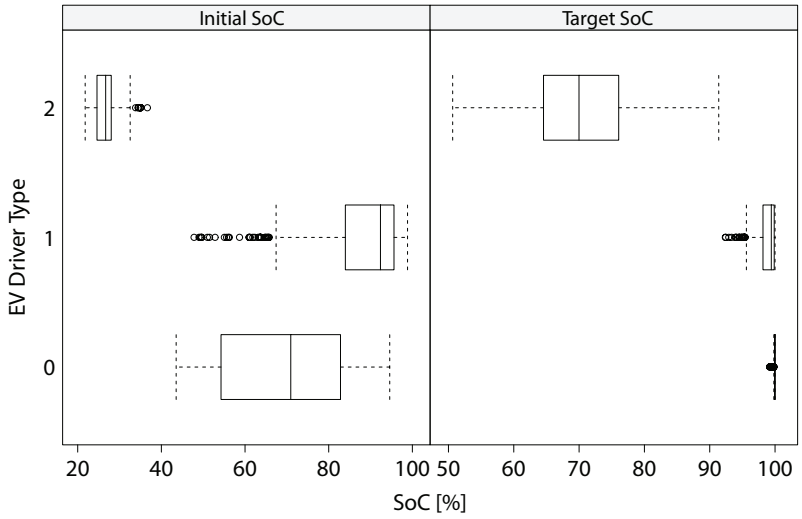

Figure A.5: *Boxplots summarizing the average initial and target SoC of fleet A during one year.*

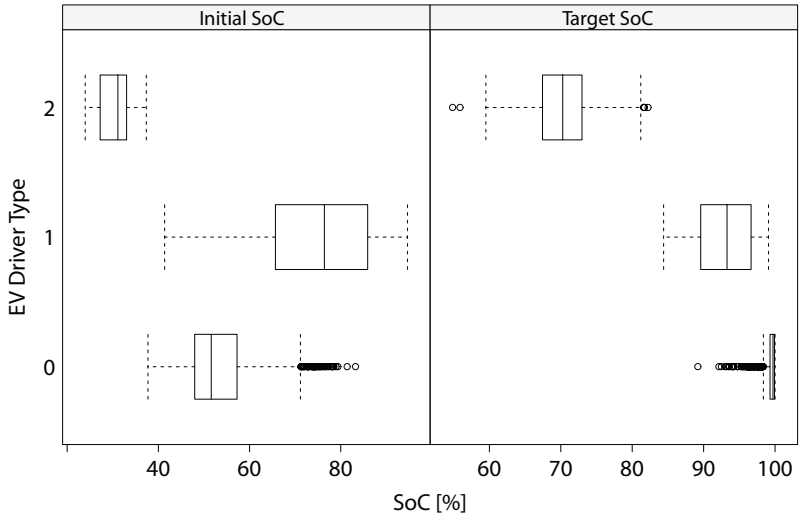

Figure A.6: *Boxplots summarizing the average initial and target SoC of fleet B during one year.*

Tables A.1 and A.2 present summary statistics of the average ratio (in percentage) between charging requirement and battery size during one year for fleets A and B correspondingly. The charging requirement of fleet B is higher, in particular for types 0 and 1 drivers.

This information, combined with the plugged-in time from Figures A.3 and A.4, can be used to measure the *flexibility* of each EV. For instance, an EV with a charging requirement of 5 kWh and plugged-in during 10 hours is more flexible than an EV with the same charging requirement but plugged-in only during 5 hours. In order to measure the *flexibility* of each EV, the following metric was adopted:

$$flexibility_j = \left(1 - \frac{R_{j,i} \Big/ \left(P_j^{\max} \cdot \Delta t\right)}{Tr_{j,i}}\right) \cdot 100, \quad \forall i \tag{A.1}$$

where $R_{j,i}$ is the charging requirement of j$^{\text{th}}$ EV for the availability period i, P_j^{max} is the maximum charging power, and $Tr_{j,i}$ is the length of the availability period i.

Table A.1: *Summary statistics of the average ratio (in percentage) between charging requirement and battery size for all vehicles from fleet A.*

	Min	1st Quartile	Mean	3rd Quartile	Max
Type 0	5.42	17.23	30.17	45.50	56.65
Type 1	1.14	4.15	11.17	13.87	46.17
Type 2	22.30	36.75	44.65	50.34	68.76

Table A.2: *Summary statistics of the average ratio (in percentage) between charging requirement and battery size for all vehicles from fleet B.*

	Min	1st Quartile	Mean	3rd Quartile	Max
Type 0	16.65	41.72	45.57	51.11	62.16
Type 1	4.44	10.79	18.96	24.07	45.83
Type 2	23.65	34.65	39.91	44.71	56.86

For each EV, Equation A.1 is used to compute the *flexibility* in each availability period and the average value from the complete year is computed. Figure A.7 depicts boxplots summarizing the average *flexibility* for each EV of fleets A and B. It can be concluded that the EV from fleet A are more *flexible* on average, in particular the types 0 and 1 drivers. Moreover, some type 2 drivers are *inflexible* during the whole year.

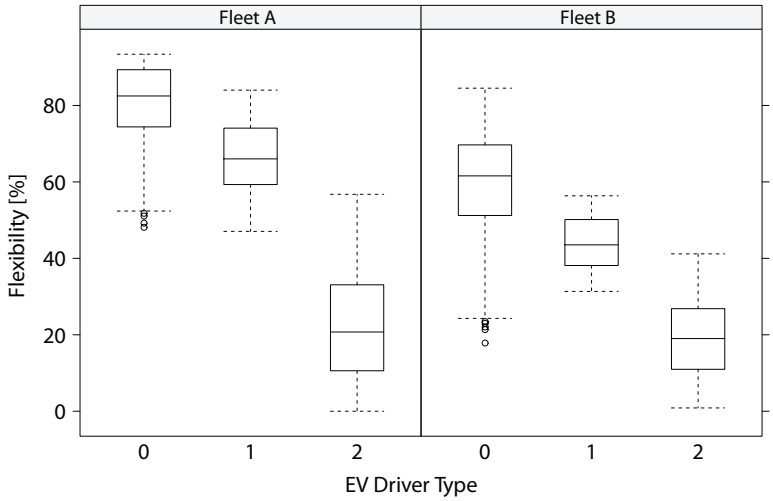

Figure A.7: *Boxplots summarizing the average flexibility of each EV in fleets A and B.*

Figure A.8 depicts the autocorrelation diagram[1] of the availability time series from three EV of each type from fleet A. The type 2 drivers show an autocorrelation diagram different from the types 0/1, while types 0 and 1 show a similar pattern. The EV drivers of types 0/1 have a clear double seasonal pattern (i.e. daily and weekly), while type 2 drivers' behavior does not have a seasonal cycle and the autocorrelation is lower compared to types 0/1. Note that autocorrelation diagrams of seasonal time series contain an oscillation at the same frequency (i.e., sinusoidal model).
The diagrams for the EV from fleet B are similar.

A.1.2 Aggregated EV

Tables A.3 and A.4 present summary statistics of the aggregated time series for fleets A and B correspondingly.

Table A.3: *Summary statistics of aggregated EV variables of fleet A.*

	Min	1st Quartile	Mean	3rd Quartile	Max
Max. Charg. Power [MW]	0.07	0.48	2.12	3.06	3.32
Charg. Req. [MWh]	0.00	0.02	0.15	0.148	1.62
Charg. Req. Dist. [MWh]	0.05	0.86	3.61	6.01	7.19
Inflexible Charg. [MWh]	0.0015	0.03	0.15	0.28	0.64

Figures A.9 and A.10 depict a seasonal plot [191] for one year of the aggregated variables of fleets A and B correspondingly. The plot shows the complete time series (one year of data) grouped by the individual seasons (daily pattern) in which the data were observed. Each line in the plot, with 48 half-hours, is one day from the whole time series; thus, each plot has 365 lines.

[1] The autocorrelation for binary time series is computed as follows [226]:

$$\rho_t = \frac{1}{n-t}\sum_{i=1}^{n-t}(y_i \cdot y_{i+t}) - \left(\frac{1}{n-t}\cdot\sum_{i=1}^{n-t}(y_i)\right)\cdot\left(\frac{1}{n-t}\cdot\sum_{i=1}^{n-t}(y_{i+t})\right) \tag{A.2}$$

where $\rho_t \in [-0.25, 0.25]$.

Table A.4: *Summary statistics of aggregated EV variables of fleet B.*

	Min	1st Quartile	Mean	3rd Quartile	Max
Max. Charg. Power [MW]	0.10	0.51	1.93	3.17	3.44
Charg. Req. [MWh]	0.00	0.04	0.09	0.34	3.40
Charg. Req. Dist. [MWh]	0.17	1.98	8.23	13.62	15.79
Inflexible Charg. [MWh]	0.02	0.08	0.34	0.62	1.06

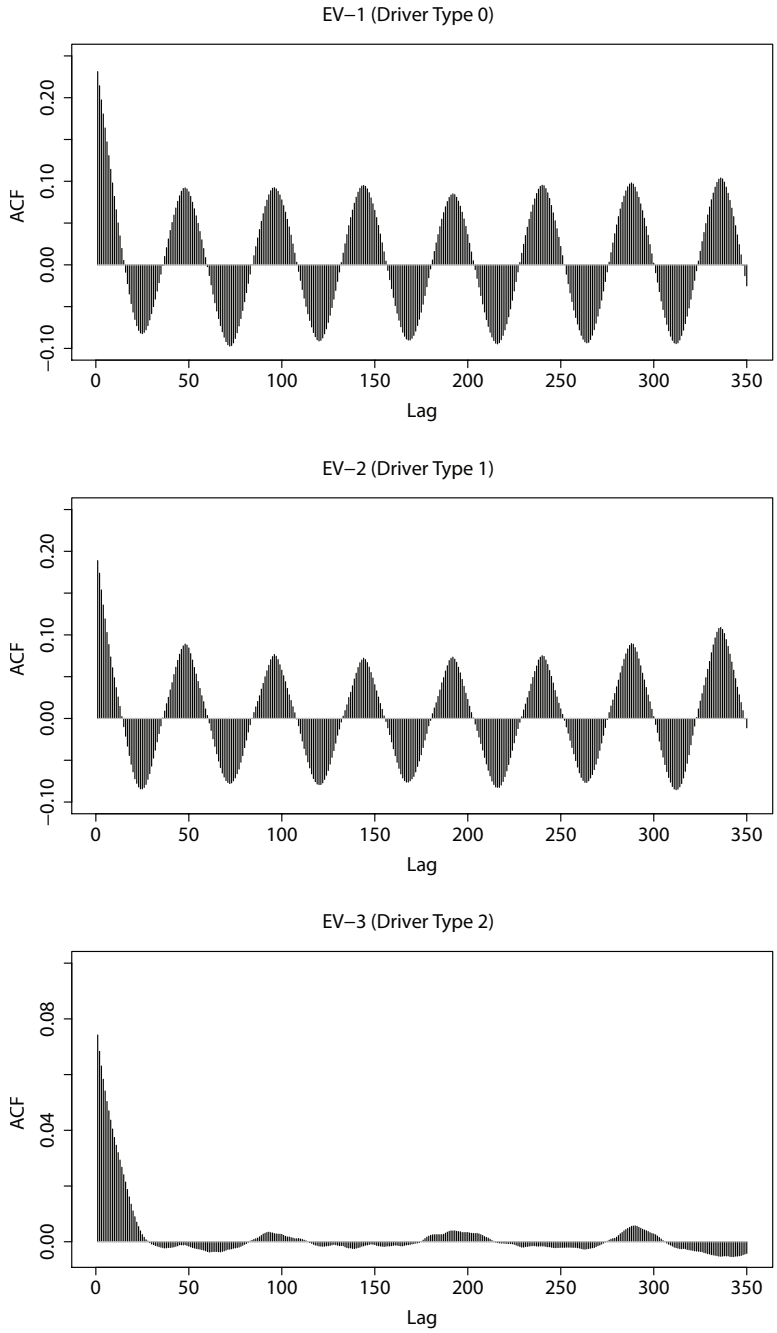

Figure A.8: *Autocorrelation diagram of the availability time series of one EV of each type (fleet A).*

The aggregated time series does not show a high daily variability and depicts two clear seasonal patterns: one for weekdays where the number of plugged-in EV in residential and office areas after 10h00 is low, and another for weekend days where the number of plugged-in EV is higher. Note that the shape of maximum charging power and charging requirement distribution is rather similar. Moreover, the charging requirement time series show a peak between 7h00 and 8h00 and the *inflexible* EV charging (i.e., all EV are *inflexible* clients) presents a high consumption after 19h00.

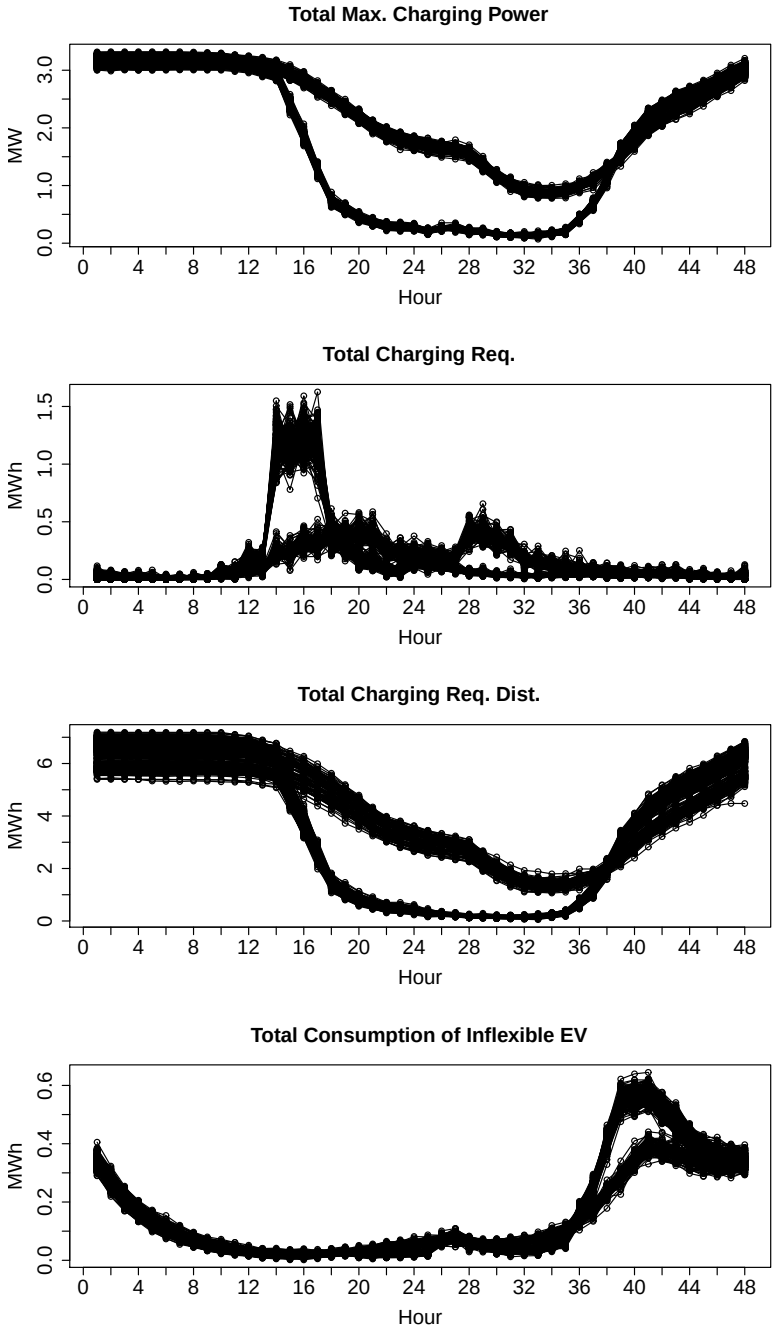

Figure A.9: *Seasonal plot of the aggregated variables from fleet A: maximum charging power, charging requirement, charging requirement distribution, consumption of inflexible EV.*

Figure A.11 depicts the autocorrelation diagram of the aggregated variables of fleet A. All the time series show a double seasonal cycle (daily and weekly) and the autocorrelation was considerably high, which is consistent with the seasonal plots from Figure A.9.

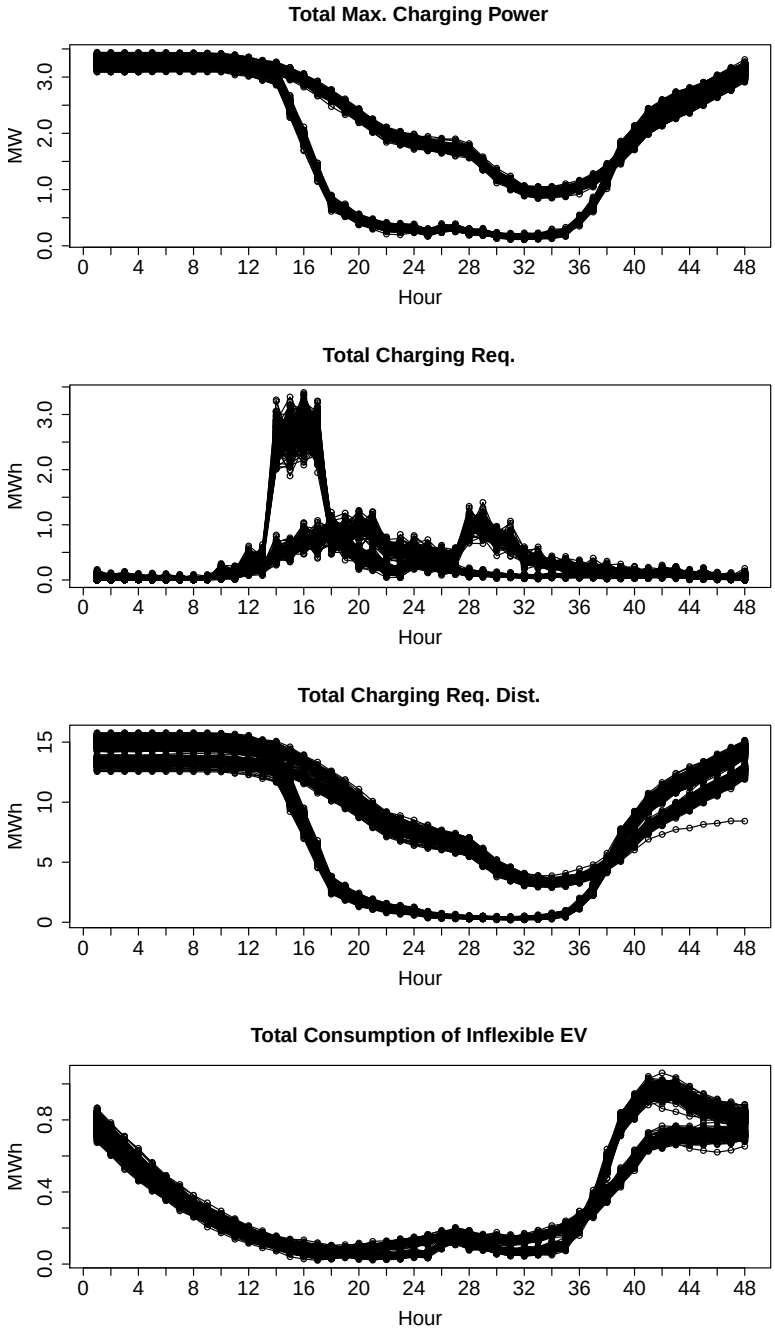

Figure A.10: *Seasonal plot of the aggregated variables from fleet B: maximum charging power, charging requirement, charging requirement distribution, consumption of inflexible EV.*

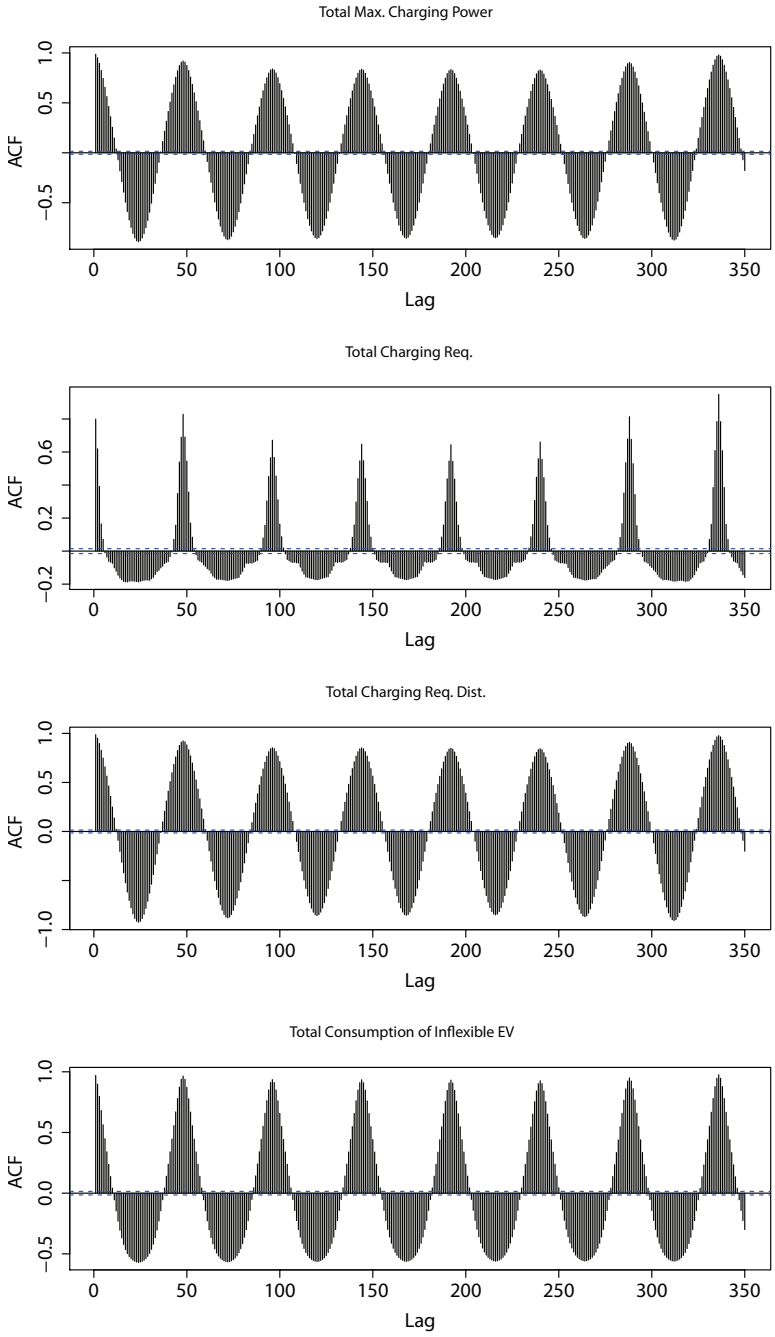

Figure A.11: *Autocorrelation diagram of the aggregated variables from fleet A: maximum charging power, charging requirement, charging requirement distribution, consumption of inflexible EV.*

A.2 Energy and Reserve Prices

Tables A.5-A.8 present summary statistics of the energy, tertiary and secondary reserve prices for the period between 2009 and 2011 in Portugal. The year with the highest average energy price was 2011, but the highest energy price (180 €/MWh) occurred in 2010. Hours with zero energy prices also occurred in these three years.

In terms of upward tertiary reserve price, 2011 was the year with the highest average upward price and the highest price (225 €/MWh). For downward reserve, the most expensive reserve is the one with the prices close to zero. In this case, the average price of the three years is rather similar, but years 2010 and 2011 have a 1st quartile close to zero.

These three years have a rather similar average and quartile values for secondary reserve price, but 2011 has an extreme price of 425 €/MW.

Table A.5: *Summary statistics of day-ahead electrical energy price (€/MWh) for years 2009, 2010 and 2011 in Portugal.*

	Min	1st Quartile	Mean	3rd Quartile	Max
2009	0.00	33.70	37.63	41.07	98.57
2010	0.00	30.50	37.32	46.82	180.30
2011	0.00	46.18	50.45	55.23	100.00

Table A.6: *Summary statistics of upward tertiary reserve price (€/MWh) for years 2009, 2010 and 2011 in Portugal.*

	Min	1st Quartile	Mean	3rd Quartile	Max
2009	0.00	36.30	41.50	47.00	140.00
2010	0.00	40.40	48.79	55.00	181.00
2011	0.10	53.50	65.34	72.00	225.00

Table A.7: *Summary statistics of downward tertiary reserve price (€/MWh) for years 2009, 2010 and 2011 in Portugal.*

	Min	1st Quartile	Mean	3rd Quartile	Max
2009	0.00	20.00	25.92	32.70	88.75
2010	0.00	0.10	23.00	36.00	100.00
2011	0.00	1.00	23.85	40.50	200.00

Figures A.12-A.14, depict for each year, a plot with a boxplot for the price in each hour (i.e., boxplot of the price conditioned to the hour of the day). In general, the pattern of the energy and tertiary reserve prices resembles the load pattern with low prices in valley hours and high prices in peak hours. Nevertheless, the upward tertiary reserve prices present a higher number

Table A.8: *Summary statistics of secondary reserve capacity price (€/MW) for years 2009, 2010 and 2011 in Portugal.*

	Min	1st Quartile	Mean	3rd Quartile	Max
2009	0.00	19.00	26.55	31.11	167.80
2010	10.05	18.93	27.59	32.60	180.30
2011	0.00	20.16	28.16	34.95	425.00

of outliers and variability compared to the energy price, while the downward reserve price is more concentrated in the range of low prices. Moreover, note that the period between 3h00 and 8h00 of year 2010 showed a frequently occurrence of zero energy prices, which with a significant penetration of EV may not occur.

The secondary reserve capacity price shows a completely different pattern, without a clear separation between peak and off-peak hours, with several outliers, and with some extreme price values (in particular during 2009) in off-peak hours. These high price values occur because there is a high concentration of market agents offering secondary reserve band.

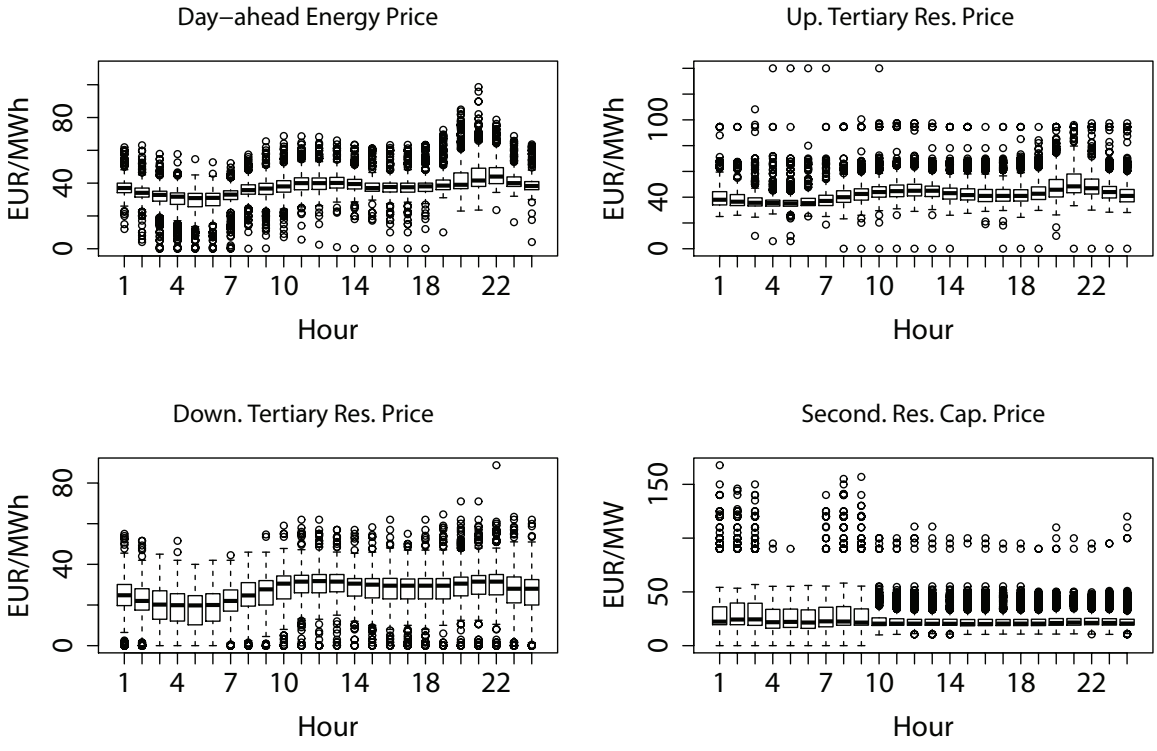

Figure A.12: *Boxplots conditioned to the hour of the day for the market prices of year 2009.*

Figure A.15 depicts the autocorrelation plot for the energy and secondary reserve capacity price for the year 2011 (the plots of the years 2009 and 2010 are similar). These plots show that both time series are non-stationary (since the autocorrelation is significant after lag 20)

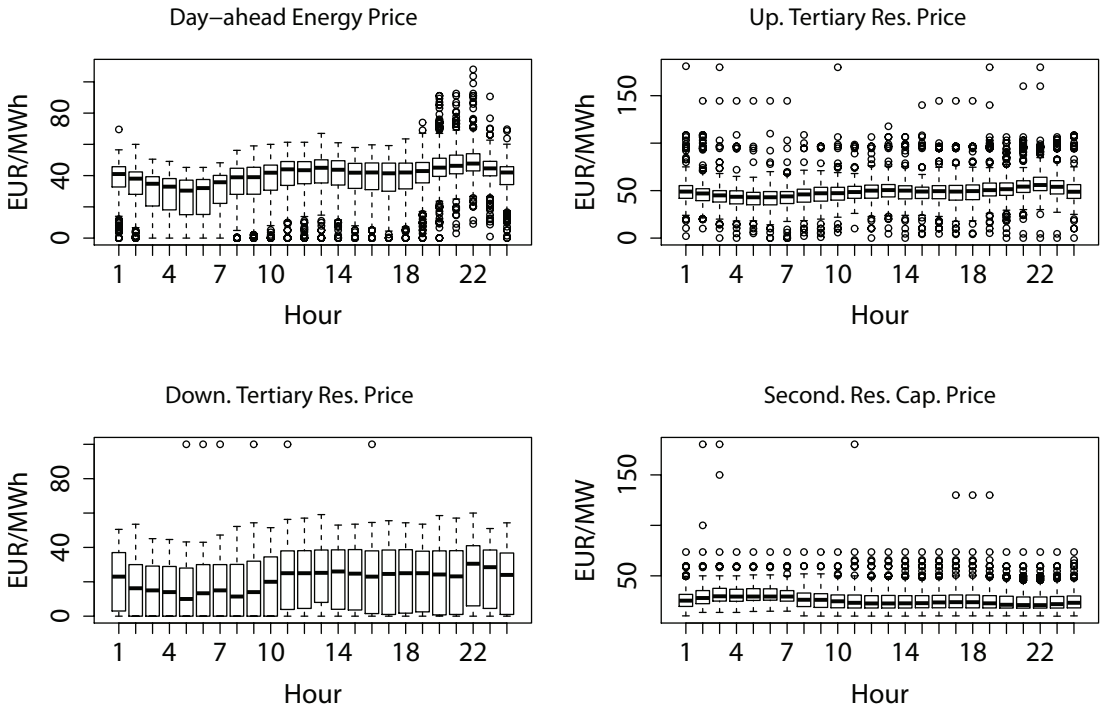

Figure A.13: *Boxplots conditioned to the hour of the day for the market prices of year 2010.*

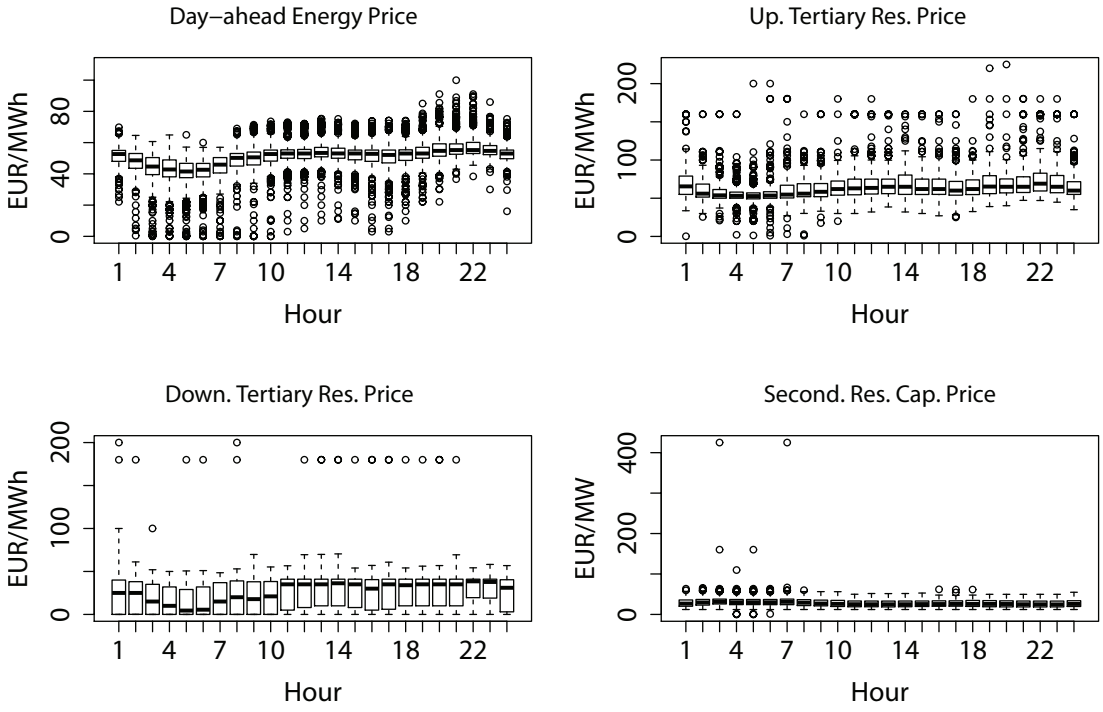

Figure A.14: *Boxplots conditioned to the hour of the day for the market prices of year 2011.*

and have a daily and weekly seasonal cycle.

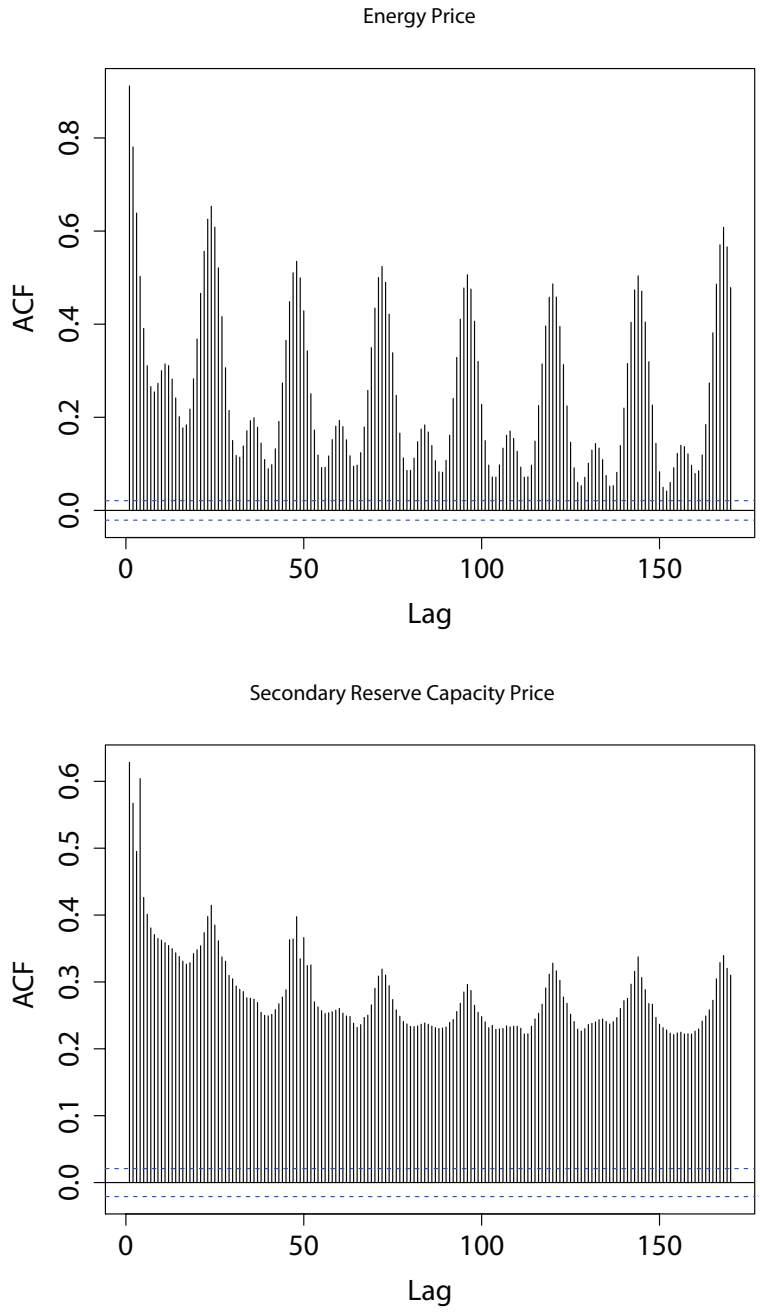

Figure A.15: *Autocorrelation plot of the energy and secondary reserve capacity prices for year 2011.*

Appendix B

Evaluation of the Forecast Performance

B.1 Aggregated EV Variables

This appendix section presents evaluation results for the three variables used in the *global* approach: total charging requirement, charging requirement distribution and total maximum charging power. Moreover, the results for a situation where all EV are *inflexible* loads are also presented.

The following metrics measure the forecast statistical quality. The classical Mean Absolute Percentage Error (MAPE), is given by:

$$MAPE = \frac{1}{N} \sum_{j=1}^{N} \left(\frac{\left| y_j - \hat{y}_j \right|}{y_j} \right) \cdot 100 \tag{B.1}$$

where y_j is the realized value, $\hat{y}_j$ the forecasted value and N the number of samples in the test dataset. The modified MAPE for time series with zero values (i.e., the charging requirement) [236]:

$$mMAPE = \frac{\sum_{j=1}^{N} \left(\left| y_j - \hat{y}_j \right| \right)}{\sum_{j=1}^{N} \left(y_j \right)} \cdot 100 \tag{B.2}$$

The Percentage Bias (PBIAS):

$$PBIAS = \frac{1}{N} \sum_{j=1}^{N} \left(\frac{\left(y_j - \hat{y}_j \right)}{y_j} \cdot \right) 100 \tag{B.3}$$

A modified percentage bias (mPBIAS) similar to Equation B.2 is used in variables with zero values.

Table B.1 presents the forecasting quality evaluation for the four EV variables of fleets A and B. The forecast time horizon is 100 look-ahead time steps (half-hour data).

The forecasts for the total charging power and charging requirement distribution show an acceptable quality, while the forecasts for the charging requirement present a higher MAPE in both fleets. Nevertheless, it is important to stress that these statistical performance metrics measure only the match between forecasted and realized value, and the true forecast value can only be assessed by comparing the costs that result from the bidding process. Moreover, the mMAPE metric for the charging requirement forecast is misleading. For instance, the forecast could indicate a 1 MWh of charging requirements that need to be satisfied until the 9^{th} hour, while the realized value is 1 MWh until the 12^{th} hour. This represents a high forecast error in the mMAPE sense, but, actually, it is only an anticipation of the charging requirement.

Table B.1: *Forecasting performance for the EV aggregated variables for fleets A and B; (*) the mMAPE and mPBIAS are used instead of MAPE and PBIAS.*

	Fleet A		Fleet B	
	MAPE [%]	PBIAS [%]	MAPE [%]	PBIAS [%]
Charg. power [MW]	5.46	-0.62	5.31	-0.76
Charg. req. [MWh] (*)	19.43	0.17	17.12	-0.24
Charg. req. dist. [MWh]	8.99	-1.89	7.53	-1.51
Inflexible load [MWh](*)	9.30	1.00	5.60	0.23

B.2 Individual EV Variables

This section presents evaluation results for the two variables used in the *divided* approach: availability and charging requirement of each EV.

The performance of the availability forecast is measured with a metric from the literature about evaluation in classification problems [237]:

$$Accuracy = \sqrt{\frac{TP}{TP+FP} \cdot \frac{TP}{TP+FN}} \cdot 100 \tag{B.4}$$

where TP is the number of correct plugged-in predictions (true positives), FN is the number of wrong zero predictions (false negative) and FP is the number of wrong plugged-in predictions (false positive).

Figure B.1 summarizes the availability forecast results divided by drivers' type with a boxplot for the two fleets and for a time horizon up to 100 time intervals ahead. Note that the boxplot is constructed with the forecast accuracy of each EV.

The availability forecast for type 2 drivers presents the lowest accuracy, suggesting that these availability patterns are difficult to forecast. Some forecasts for type 0 drivers also present a

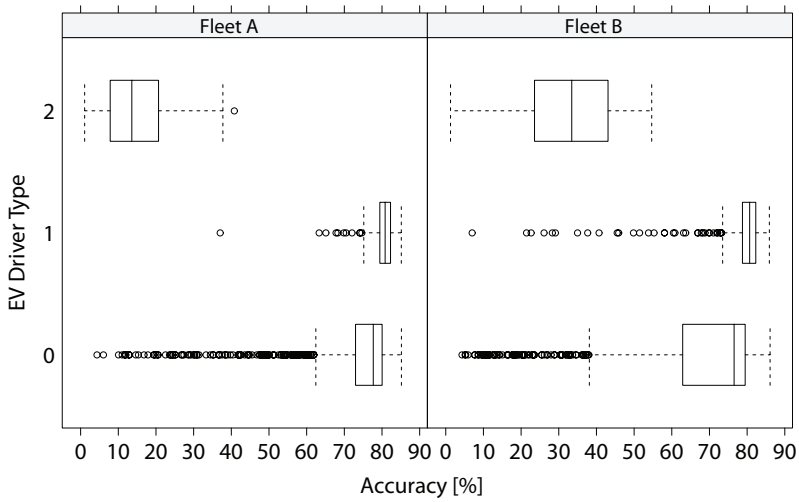

Figure B.1: *Boxplot with the accuracy of the availability forecast for fleets A and B.*

very low accuracy. The forecasts with low accuracy for types 0 and 2 drivers have in common a low number of time intervals in one year during which the EV is plugged-in for charging. For example, an EV of type 0 with accuracy equal to 4.31% is only plugged-in during 24.60% of one year time, and a type 2 driver with accuracy equal to 4.76% is only plugged-in during 12.37%. EV with better performance has a higher rate of plugged-in hours. For example, an EV with 80% of accuracy is plugged-in during 52.5% of the time.
These results suggest that the asymmetry in the number of plugged-in hours has a considerable impact on the model performance.

The evaluation of the charging requirement forecast quality should be made using perfect forecasts for the availability in order to remove its influence. Fig. B.2 depicts the boxplots for the mMAPE divided by fleet and EV driver type. Similar to the previous boxplots, each point is the forecast accuracy of each EV.

In fleets A and B, the drivers of types 0 and 1 present a mMAPE that ranges between 30% and 50%. On the other hand, the error for type 2 drivers is relatively low on average, and this happens because these clients only charge when the SoC is below a predefined threshold and this makes the charging requirement more predictable. The results for fleet B are rather similar with a slightly better performance of types 0 and 1 drivers.

It is important to stress that the individual errors by EV are high, but for an aggregator, what is important is the error after aggregating all the clients. Table B.2 presents the mMAPE for the total values of availability[1] and charging requirement. Table B.3 presents the PBIAS results.

These results show a good forecast quality for the aggregated availability and charging re-

[1] In this case, availability is a count variable with the number of EV plugged-in in each time interval.

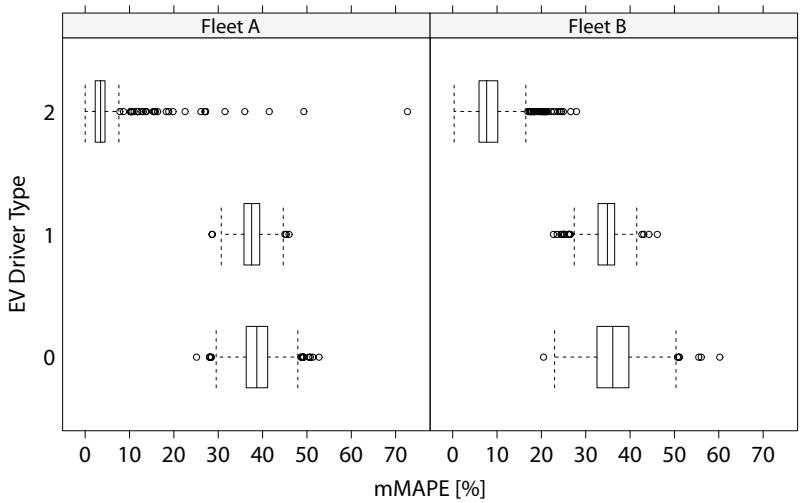

Figure B.2: *Boxplot with the mMAPE for the charging requirement of fleets A and B.*

Table B.2: *mMAPE of the aggregated availability and charging requirement forecast for fleets A and B with 1500 EV.*

	Availability Forecast	Charg. Req. w/ Perfect Forecast for Availability	Charg. Req. w/ Availability Forecast
Fleet A	6.99%	5.46%	29.93%
Fleet B	8.09%	4.71%	30.69%

quirement (with perfect availability forecast). The error increases when forecasts for the availability are used in the charging requirement forecast. Nevertheless, it is important to note that the individual errors in the availability forecast influence this result, and this high forecast error does not necessarily mean a poor performance. Since the availability forecast is different from the realized values, the charging requirements will also be different and placed in different departing hours. For example, the forecasts could indicate a 16 kWh of charging requirements that need to be satisfied until the 6^{th} hour, while the realized value is 16 kWh until the 8^{th} hour. This represents a high forecast error in the mMAPE sense, but, actually, it is only an anticipation of the charging requirement. These errors are higher than the ones of

Table B.3: *mPBIAS of the aggregated availability and charging requirement forecast for fleets A and B with 1500 EV.*

	Availability Forecast	Charg. Req. w/ Perfect Forecast for Availability	Charg. Req. w/ Availability Forecast
Fleet A	4.45%	0.01%	5.75%
Fleet B	-4.60%	0.24%	-5.86%

the aggregated variables from the previous section, but only the evaluation of the deviation between bid and actual consumption can give a true indication of the forecast error.

B.2.1 Forecast Error of the Changed Forecasts

The individual forecasts of charging requirement and availability analyzed in the previous section were changed by using a truncated Gaussian distribution to introduce additional noise in the forecasts and increase its error. Table B.4 presents the mMAPE and mPBIAS results for eight different aggregated forecasts of the charging requirement and availability in fleet A. Table B.4 presents the results for fleet B.

It is important to mention that the forecasts of cases 1-4 have a similar mMAPE but this does not mean that the forecasts are similar.

Table B.4: *mMAPE and mPBIAS of the modified aggregated availability and charging requirement forecast for fleet A.*

	mMAPE [%] Charg. Req.	mPBIAS [%] Charg. Req.	mMAPE [%] Availability	mPBIAS [%] Availability
0	29.93%	5.75%	6.99%	4.45%
1	37.48%	7.65%	7.31%	4.45%
2	37.70%	7.65%	7.32%	4.43%
3	36.50%	3.34%	7.31%	4.42%
4	35.72%	-3.49%	7.33%	4.45%
5	57.13%	7.67%	10.95%	5.20%
6	68.90%	8.04%	16.52%	6.68%
7	72.54%	8.34%	19.28%	7.38%
8	83.60%	-8.40%	24.50%	8.98%

Table B.5: *mMAPE and mPBIAS of the modified aggregated availability and charging requirement forecast for fleet B.*

	mMAPE [%] Charg. Req.	mPBIAS [%] Charg. Req.	mMAPE [%] Availability	mPBIAS [%] Availability
0	30.69%	-5.86%	8.09%	-4.60%
1	38.27%	-2.16%	8.61%	-4.60%
2	38.44%	-2.09%	8.61%	-4.59%
3	38.52%	-2.25%	8.62%	-4.60%
4	38.60%	-2.17%	8.63%	-4.61%
5	59.37%	-1.36%	11.52%	-3.81%
6	70.21%	0.25%	15.60%	-2.42%
7	73.63%	1.02%	18.05%	-1.79%
8	78.69%	2.57%	22.53%	-0.38%

B.3 Market Prices

To participate in the energy market with buying bids, the most important information is the ranking of the prices [165]. Therefore, in addition to the Mean Absolute Error (MAE), the Spearman rank correlation is used to measure the prices ranking quality. The Spearman correlation coefficient is computed for each pair of forecasted and realized values of a time horizon of 36 hours-ahead, and then averaged over the entire test period. Figure B.3 depicts boxplots summarizing the evaluation results in the 100 random samples for the energy price, positive and negative imbalance unit costs.

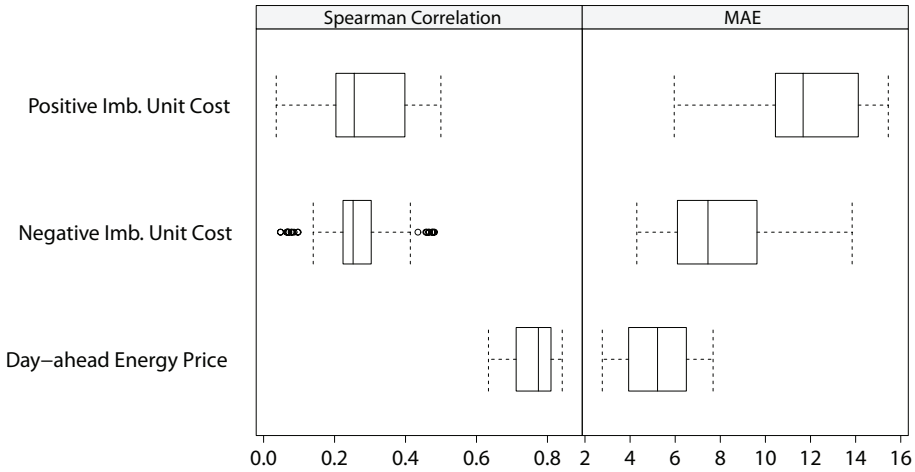

Figure B.3: *Spearman correlation and mean absolute error of the prices forecasts for 100 samples.*

The performance of the energy price is acceptable, the average for the rank correlation is 0.76 and MAE is 5.18 €/MWh. The forecasts for the imbalance unit costs present a low performance because their rank correlation is around 0.25 for both prices. The negative cost presents a low MAE (average of 7.78 €/MWh) when compared to the positive cost (average of 11.73 €/MWh). These results indicate that the forecasting approach for the imbalance unit costs has room for improvement.

Figure B.4 depicts the MAE of the day-ahead and hour-ahead forecasts for the tertiary reserve price (in €/MWh) and of the day-ahead forecast for the secondary reserve capacity price (in €/MW). The forecast error of the tertiary reserve prices is significantly high, in particular for the multi-step ahead forecasts. This shows that irregular time series with a high variability are difficult to forecast and new forecasting algorithms are needed for this type of series. Furthermore, it is conceivable that these prices are influenced by other variables, such as the load, wind power generation and electrical energy price. Thus, future work should consist in developing multivariate models for irregular time series.

The forecast error of the secondary reserve capacity price is lower compared to the results

for the tertiary reserve prices, and the forecast accuracy obtained with the ARIMA model is already satisfactory.

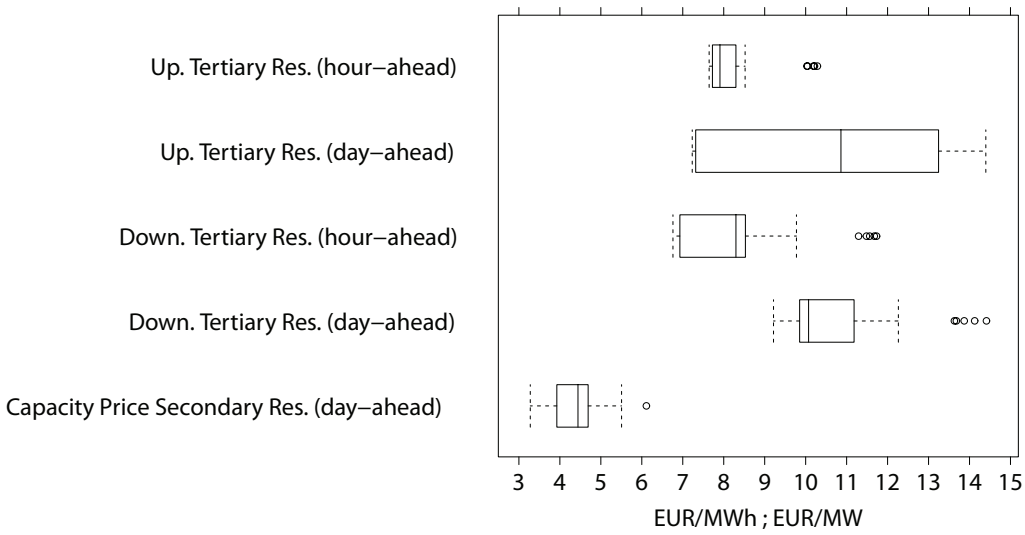

Figure B.4: *Mean absolute error of the forecasts for the tertiary and secondary reserve prices in Portugal.*

B.4 Reserve Direction

Four different statistical learning algorithms are compared in the task of forecasting the balancing reserve direction (tertiary reserve in Portugal) for the test case: GLM, support vector machines (SVM), multilayer perceptron neural networks (NN) and naive Bayes (NB). The parameters of the SVM and NN (including number of neurons in the hidden layers) were selected by using the tuning parameters function "train" of R package *caret* [229] and the covariates were selected using the feature selection algorithm from the same R package.

Table B.6 presents the performance results of the four algorithms in the 30 samples of the test case. The average results of the following performance metrics are presented:

- *accuracy*: calculated as follows:

$$accuracy = \frac{TP + TN}{TP + TN + FN + FP} \cdot 100\%$$

  where TP are the true positives, TN the true negatives, FN the false negatives and FP the false positives;

- *Area Under the ROC Curve* (AUC): measures the discriminating ability of a binary forecast model. The larger the AUC, the higher the likelihood that an actual positive case will be assigned a higher probability of being positive than an actual negative case [233].

The results show that the best performance is from the GLM, and only the SVM presents an accuracy much lower than 60%. The AUC of all the methods is above 0.5, which is the AUC attributed to a random predictor (e.g., flip of a coin). Note that a binary forecasting model very close to a random predictor (AUC with value 0.5), means that the model only extracts a small amount of information from the data.

Table B.6: *Accuracy and Area Under the ROC Curve (AUC) of the day-ahead forecasts for the balancing reserve direction in Portugal.*

(a) *Upward.*

Model	Accuracy	AUC
GLM	59.9%	0.64
NN	58.1%	0.61
NB	57.6%	0.64
SVM	52.1%	0.59

(b) *Downward*

Model	Accuracy	AUC
GLM	63.8%	0.66
NN	61.8%	0.62
NB	63.2%	0.65
SVM	55.8	0.6

Table B.7 presents the performance results of the GLM algorithm for hour-ahead forecasts in the 30 samples of the test case.

Table B.7: *Accuracy and Area Under the ROC Curve (AUC) of the hour-ahead forecasts for the balancing reserve direction in Portugal.*

GLM	Accuracy	AUC
Downward	75.7%	79.7
Upward	77.2%	80.3

Table B.8 presents the average accuracy of four basic (or heuristic) binary forecasting models in the 30 test samples.

Table B.8: *Accuracy of four different basic (or heuristic) binary forecast models.*

	Naive Predictor	Random Predictor	All Upward	All Downward
Up. Accuracy [%]	59.3%	49.9%	53.7%	n.a.
Down. Accuracy [%]	59.6%	49.9%	n.a.	58.9%

Appendix C

State of the Art Operational Algorithms

This appendix section describes two heuristic operational management algorithms from the literature. The first one is based on the priority order function described by Amoroso and Cappuccino [164] (named *priority-based*), and the other is described by Wu et al. [165] (named *price-ranking-based*). Lima [30] modified these two algorithms to allow an actual charging greater than the market bid in time intervals when some EV must charge, otherwise the charging requirement of these EV may not be fully satisfied.

C.1 Priority-based Algorithm

The first heuristic-based algorithm is based on the following priority function:

$$Q_{t,j} = \frac{R_{t,j}}{Tr_{r,j} \cdot P_j^{\max} \cdot \Delta t} \tag{C.1}$$

where $Q_{t,j}$ is the priority level of the j$^{\text{th}}$ EV in time interval t, $R_{t,j}$ is the residual charging requirement at time interval t, T_r is the remaining time until departure, and P_j^{max} is the maximum charging rate of the EV.
According to this function, an EV is as more important the more energy it requires and the less time it has until its departure.

The algorithm is sequential (i.e., solved in each time interval) and can be described as follows:

1. the aggregator receives the information (target SoC and expected departure time instant) from the recently plugged-in EV (i.e., connected for charging between $t_0 - 1$ and t_0) and computes the charging requirement $R_{t_0,j}$ for the j$^{\text{th}}$ EV;

2. the priority level $Q_{t_0,j}$ is computed for each plugged-in EV. The aggregator charges the EV by descending priority order until all EV are dispatched or until the purchased quantity (E_{t_0}) is depleted. The charge level of each EV is given by $E^*_{t_0,j} = \min\left(P^{max}_{t_0,j} \cdot \Delta t, R_{t_0,j}\right)$, where Δt is the length of the time interval. Two situations can occur:

   - $\sum_{j=1}^{M_{t_0}} \left(E^*_{t_0,j}\right) < E_{t_0}$, where all the EV plugged-in in time interval t_0 (represented by M_t), charging at $E_{t_0,j}$, are insufficient to fulfill the purchased electrical energy;

   - $\sum_{j=1}^{p} \left(E^*_{t_0,j}\right) = E^{bid}_{t_0}$ where the first p EV of the priority table are sufficient to fulfill the purchased electrical energy. However, in this case, it is necessary to check if the non-dispatched EV ($j > p$) are "flexible", i.e., if their charging requirement can be fulfilled within the time they have before departure (i.e., between $t_0 + 1$ and departure time instant). If not, these "inflexible" vehicles will charge in time interval t_0 and this leads to $\sum_{j=1}^{m} \left(E^*_{t_0,j}\right) > E^{bid}_{t_0}$, where $m > p$;

3. the value of $E^*_{t_0,j}$ is sent as a set-point for the j$^{\text{th}}$ EV, and the charging requirement is updated for the next period, $R_{t_0+1,j} = R_{t_0,j} - E^*_{t_0,j}$;

4. the process is repeated for the next time interval, $t_0 + 1$.

C.2 Price-ranking-based Algorithm

The second heuristic-based algorithm defines the EV charging strategy based on a ranking of the day-ahead energy price forecast and, in contrast to the previous algorithm, it defines the EV charging power during its complete availability period.

The algorithm is sequential (i.e., solved in each time interval), applied to each EV and can be described as follows:

1. the aggregator receives the arrival (t_0) and expected departure time instant (d_j) from the recently plugged-in EV (i.e., connected for charging between $t_0 - 1$ and t_0) and computes the charging requirement $R_{t_0,j}$ for the j$^{\text{th}}$ EV;

2. **for each EV** j:

   - the aggregator ranks the electrical energy prices used in the day-ahead optimization by ascending order. The ranking $rank_{k,j}\left(\hat{p}_k\right)$ is between the current time interval t_0 and the departure time instant[1] of the j$^{\text{th}}$ EV, and only for the k time

[1] If the departure time instant (d_j) is greater than the last time interval with associated price (K), then $d_j = K$.

intervals with purchased energy:
$\left\{k: \ t_0 \leq k \leq d_j \ \wedge \ E_k > 0\right\}$;

- then, it distributes the EV charging, $E^*_{k,j} = \min\left(P^{\max}_{k,j} \cdot \Delta t, R_{k,j}\right)$, according to $rank_j\left(\hat{p}_k\right)$, and updates the following variables: $E_k = E_k - E^*_{k,j}$ and $R_{k,j} = R_{k,j} - E^*_{k,j}$. Lima [30] introduced a modification to allow placing charging in intervals with $E_k = 0$ (i.e., the purchased energy in interval k has been depleted), when it is not possible to satisfy the charging requirement of the EV only with the intervals from $rank_{k,j}\left(\hat{p}_k\right)$. For these EV, a new price ranking is considered:
$\left\{k: \ t_0 \leq k \leq d_j \ \wedge \ E_k \geq 0\right\}$;

3. the value of $E^*_{t_0,j}$ is sent as a set-point for the j$^{\text{th}}$ EV, and the charging requirement is updated for the next period, $R_{t_0+1,j} = R_{t_0,j} - E_{t_0,j}$;

4. the process is repeated for the next time interval, $t_0 + 1$.